NEW APPROACHES TO ELEMENTAL SPECIATION

by

Azli Bin Sulaiman

Dip.Sc. & Ed., B.Sc. & Ed. (Hons.), M.Sc., CChem, MRSC

A Doctoral Thesis

submitted in partial fulfillment of the requirements

for the award of

the degree of Doctor of Philosophy

of the Loughborough University

September, 1996

Supervisor

Dr. B. L. Sharp, *B.Sc., Ph.D., DIC, CChem, FRSC*

Department of Chemistry, Loughborough University

G 9101808

Dedicated to

my wife Noor Sharidah

and our children

Hizaz Shahiela, Shakira Azeehan,

Izzat Fahmi and Adib Fikri

ABSTRACT

Elemental speciation has been one of the principal growth areas in analytical atomic spectrometry. This reflects the recognition that in the environmental and biological sciences, the transport, pool dynamics and toxicology of the elements are dependent on their chemical speciation. Significant progress has been made in elemental speciation by the direct coupling of separation techniques, notably the various forms of chromatography, to powerful elemental detectors such as ICP-MS. However, the strength of such hyphenated techniques, that they provide almost unambiguous identification of elemental associations, is often achieved at the expense of losing information about the ligands that are responsible for the speciation. The challenge must be to bring the two approaches to bear simultaneously so that quantitative and qualitative information on both the inorganic and organic components can be obtained simultaneously.

Capillary electrophoresis (CE) has developed into one of the most powerful separation techniques offering rapid separations with high resolution. However, these advantages are offset by low sensitivity which is a consequence of the very small (nl) samples that the technique can handle. These problems can be overcome by using high sensitivity detectors and hence the interest in coupling CE to ICP-MS. Coupling of CE to ICP-MS (CE-ICP-MS) has, therefore, the potential to provide rapid and quantitative elemental speciation information that is complementary to that provided by other techniques. This thesis describes an interface for coupling CE to ICP-MS and its applications to some common metal species. A particular interest in this work has been to investigate the potential of CE for studying metal complexes with humic and fulvic acids.

A technique that offers potential for determining both free element and complexed forms, without prior separation is electrospray/ion spray ionisation-mass spectrometry. Preliminary work is presented that investigates the applications of electrospray/ion spray ionisation-mass spectrometry to some common metal-ligand systems.

ACKNOWLEDGEMENTS

TABLE OF CONTENTS

Page No.

CHAPTER 3   INDUCTIVELY COUPLED PLASMA-MASS
               SPECTROMETRY

CHAPTER 8   COUPLING OF CAPILLARY ELECTROPHORESIS TO
INDUCTIVELY COUPLED PLASMA-MASS
SPECTROMETRY

LIST OF ABBREVIATIONS

CE	capillary electrophoresis
CE-ICP-MS	capillary electrophoresis- inductively coupled plasma-mass spectrometry
CGE	capillary gel electrophoresis
CIEF	capillary isoelectric focusing
CITP	capillary isotachophoresis
CZE	capillary zone electrophoresis
DAD	diode array detector
DIN	direct injection nebulisation
EOF	electroosmotic flow
FI	flow injection
GC	gas chromatography
GC-MS	gas chromatography-mass spectrometry
GPC	gel permeation chromatography
HEN	high efficiency nebuliser
HPLC	high performance liquid chromatography
HPSEC	high performance size exclusion chromatography
ICP-MS	inductively coupled plasma-mass spectrometry
i.d.	inner diameter
IR	infrared
LIF	laser induced fluorescence
MEKC	micellar electrokinetic chromatography
NMR	nuclear magnetic resonance
o.d.	outer diameter
rf	radiofrequency
RMM	relative molecular mass
RSD	relative standard deviation
SFC	supercritical fluid chromatography
UV	ultraviolet
UV/VIS	ultraviolet-visible

PUBLICATIONS AND PRESENTATIONS

"Capillary Electrophoresis ICP-MS: Preliminary Experiences", B. L. Sharp and A. B. Sulaiman, Atomic Spectroscopy Group RSC, Bristol, UK, March, 1995.

"Preliminary Experiences with Capillary Column Electrophoresis ICP-MS", B. L. Sharp and A. B. Sulaiman, Colloquium Spectroscopicum Internationale XXIX, Leipzig, Germany, August - September, 1995.

"Experiences with Capillary Column Electrophoresis ICP-MS", B. L. Sharp and A. B. Sulaiman, Federation of Analytical Chemistry and Spectroscopy Societies XXII, Ohio, USA, October, 1995.

"Coupling Capillary Electrophoresis to ICP-MS", B. L. Sharp and A. B. Sulaiman, 1996 Winter Conference on Plasma Spectrochemistry, Florida, USA, January, 1996.

"Capillary Electrophoresis-Inductively Coupled Plasma-Mass Spectrometry for Metal Chelates Studies", B. L. Sharp and A. B. Sulaiman, 8th Biennial National Atomic Spectroscopy Symposium, Norwich, UK, July, 1996.

"New Approaches in Elemental Speciation", B. L. Sharp and A. B. Sulaiman, 8th Biennial National Atomic Spectroscopy Symposium, Norwich, UK, July, 1996.

Chapter 1

CHAPTER ONE

INTRODUCTION

1.1   INTRODUCTION TO CHAPTER

This chapter deals with the background and rationale of the research and the scope and objectives. A summary of each chapter in the thesis is also included.

1.2   RESEARCH BACKGROUND AND RATIONALE

The term speciation has been used to designate the assembly of trace element compounds in a sample (static sense), to express the idea that trace element compounds react and are transformed (kinetic sense), and to refer to the process of determining trace element compounds (operational sense).   Speciation in the operational sense appears to be most useful [1].

Coupling analytical techniques for metal speciation studies has been a major interest of many researchers. One of the most successful approaches has been to couple the separation power of chromatography with the element specific detection of atomic spectroscopy [2, 3].   For instance, the coupling of high performance liquid chromatography with inductively coupled plasma-mass spectrometry (HPLC-ICP-MS) has outstanding capability mainly because of the advantages of ICP-MS such as low limits of detection, a wide linear dynamic range and the capability for isotopic analysis. However, this approach suffers from various deficiencies:

- Identification of species is by retention behaviour only, therefore it is dependent on *a priori* information and the availability of standards.

- No information is provided on the nature (type or strength) of the bonding and it is also not possible to positively identify the associated ligand.

- There is a problem of the degradation of labile complexes where the free and associated forms have different affinities for the column packing. It is not therefore possible to determine equilibrium constants in these circumstances.

- It may only be able to process one chemical form, for example polar, non-polar or ionic species; other species may pass straight through or be retained on the column which causes lack of recovery.

- Slowness of separation and poor resolution, for example with size exclusion chromatography.

- Gradient elution is normally employed to speed up analyses, but this may lead to changing spectral background.

- Mobile phases with a high salt content can erode the sampler and skimmer orifices. This causes a change in the aperture configuration which influences the ion beam and thereby the sensitivity.

- Mobile phases containing a large content of organic solvent can cause plasma instability and may quench it. Organic solvents also cause a deposition of carbon on the sampling cone leading to a change in the signal.

An alternative to conventional column chromatography is capillary electrophoresis (CE) which is relatively a new separation technique offering numerous advantages [4]:

- High separation efficiency ($N > 10^5$ to 10^6).

- Selective for charged species, both hydrophilic and hydrophobic materials may be determined.

- Short analysis times.

- Small samples volume (1 - 50 nl injected).

- Minimum buffer flow (20 μl min^{-1}).

- Simple relatively cheap columns.

- Operates in aqueous media.

- Numerous modes to vary selectivity and applications.

- Better resolution for high relative molecular mass molecules.

One of the major drawbacks with CE is its poor concentration sensitivity and the lack of a universal detection system [5]. Coupling of CE to ICP-MS has the advantages of fast separation and sensitive and selective detection. Therefore, this combination promises to be a powerful tool for metal speciation.

The search for a technique to carry out elemental speciation analysis without dependence on prior separation is gaining attention. The use of conventional atomic spectrometry as a detector always destroys molecular information and the instruments tend to be expensive with high running costs. A technique that offers the potential to provide simultaneous qualitative and quantitative information on both free element and complexed forms is electrospray/ion spray ionisation-mass spectrometry. However, it is yet to be demonstrated that this can provide both qualitative and quantitative information on trace species in complex samples.

1.3   SCOPE AND OBJECTIVES OF THE RESEARCH

The objectives of this research were:

- To investigate the application of CE for the separation of humic substances.
- To develop an interface to couple CE with ICP-MS (CE-ICP-MS).
- To characterise the interface and to optimise the operating conditions for both CE and ICP-MS.
- To investigate the application of CE-ICP-MS to metal species, particularly metal-humic complexes.
- To investigate the application of electrospray/ion spray ionisation-mass spectrometry to some common metal-ligand systems.

1.4   SUMMARY OF CHAPTERS

Chapter 2: The fundamentals of the CE technique covering the historical background, principles of separation, modes of operation, instrumentation, sample injection

3

techniques, column technology, buffer systems, detection techniques and selected applications.

Chapter 3: The principles, instrumentation, sample introduction systems, interferences and applications of ICP-MS and coupling of separation techniques with ICP-MS.

Chapter 4: A brief introduction to the principles of electrospray/ion spray-mass spectrometry.

Chapter 5: The origins and chemistry of humic substances, humic substances in natural waters, isolation, fractionation, characterisation of humic substances and complexation reactions with metals.

Chapter 6: Preliminary experimental work aimed at separating and characterising humic substances using CE with UV detection.

Chapter 7: Optimisation of the various operating parameters of the ICP-MS instrument using a standard concentric nebuliser and a high efficiency nebuliser and a comparison of these.

Chapter 8: Design and construction of an interface for CE-ICP-MS, evaluation and characterisation of the interface.

Chapter 9: Applications of the CE-ICP-MS system to the study of metal species.

Chapter 10: Applications of electrospray/ion spray-mass spectrometry to some common metal-ligand systems.

Chapter 11: General conclusions and recommendations for further work.

REFERENCES

1. Irgolic, K. J., *Trace Metal Analysis and Speciation*, Krull, I. S. (Ed), Elsevier, Amsterdam, 1991.

2. Ebdon, L., Hill, S. J., and Ward, R. W., *Analyst*, 1986, **111**, 1113.

3. Ebdon, L., Hill, S. J., and Ward, R. W., *Analyst*, 1987, **112**, 1.

4. Li, S. F. Y., *Capillary Electrophoresis: Principles, Practice and Applications*, J. Chromatogr. Library, Elsevier Scientific Publ., Amsterdam, 1992.

5. Camilleri, P., Brown, R., and Okafo, G., *Chem. Br.*, 1992, **28**, 800.

Chapter 2

CHAPTER TWO

CAPILLARY ELECTROPHORESIS

2.1   INTRODUCTION TO CHAPTER

This chapter discusses the technique of CE covering the historical background, theory, principles of the separation, modes of operation, instrumentation, sample injection techniques, column technology, buffer systems, detection techniques and selected applications.

2.2   HISTORICAL BACKGROUND

CE is the most recently introduced electrophoretic technique. Unlike conventional gel electrophoresis, the use of a supporting medium is not necessary and analysis can be carried out in free aqueous solution.

At the early stage of development, CE was originally described as free solution electrophoresis in capillaries. Hjerten [1] provided the first demonstration of free solution electrophoresis using a high electric field strength in 3 mm i.d. capillaries. Virtanen [2] described the use of smaller diameter glass capillaries, 0.2 - 0.5 mm i.d. and 50 - 100 mm length, as the separation columns. The sample was introduced by a microsyringe and detection by potentiometric methods (the potential drop detector).

Mikkers *et al.* [3] reported the separation of organic acids in a 0.2 mm i.d. polytetrafluoroethylene (PTFE) capillary. The sample was applied to one end of the capillary and the components migrated to the far end under the influence of an applied potential. The separated zones were detected by means of a UV and a conductivity detector. The separations obtained by Mikkers *et al.* were excellent, but the peak shape was poor. The detector also had insufficient sensitivity and thus

6

required relatively large sample loads. This led to a potential drop across the separated zones, giving the asymmetric peak shapes.

Jorgenson and Lukacs [4-6] demonstrated highly efficient separations based on the use of open glass capillaries with an i.d. of 75 μm. Voltages as high as 30 kV were applied across a 100 cm long capillary equipped with an on-column fluorescence detector. These workers exploited electroosmotic flow in their separations and with the inherent sensitivity of the detection system, symmetrical peaks were obtained.

For many years, investigators built their own CE instruments from a controllable high voltage power supply, two electrode assemblies, two buffer reservoirs, a fused-silica capillary with a viewing window and a UV detector. These early home-made CE systems, however, were inconvenient for routine analysis and too imprecise for quantitative analysis. At the end of the 1980s, commercial instruments became available [7]. With the rapid advances currently being made, CE is gaining popularity as an alternative analytical tool for some routine analyses. This is reflected in the numbers of papers published since the early 80s, as shown in Figure 2.1 [8].
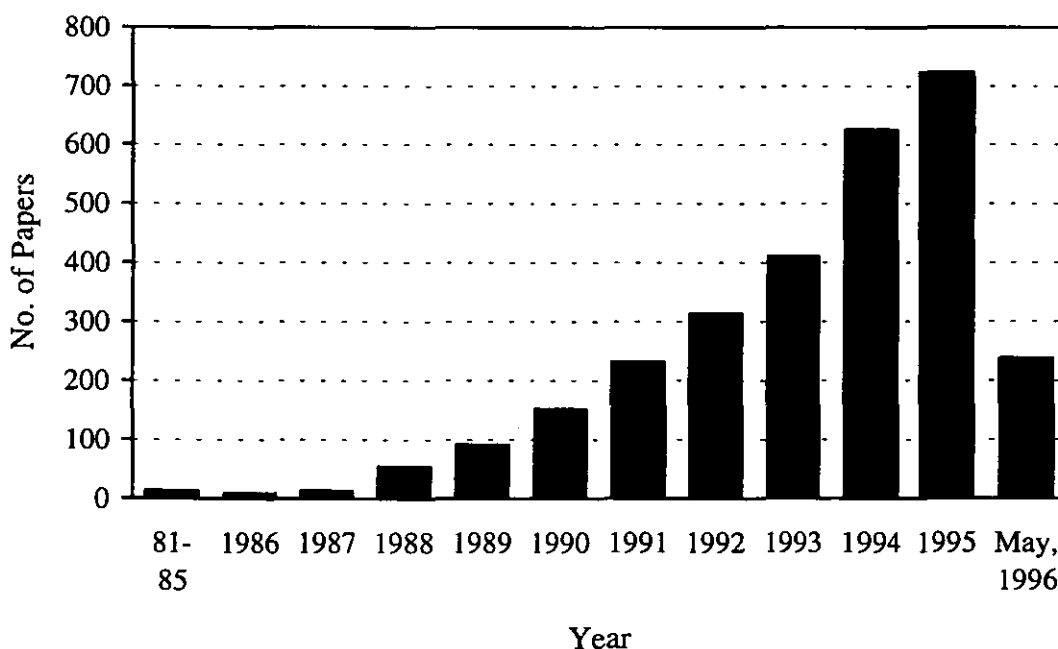
Figure 2.1: Frequency of published articles on CE based on a survey - May 1996.

7

2.3   THEORETICAL PRINCIPLES

CE is an analytical technique that can achieve rapid and high-resolution separation of water-soluble components present in small sample volumes.   Many excellent textbooks [9-16] and comprehensive reviews documenting the process of CE have been published [17-24].   Other reviews have covered modes of operation [25], methods and scope [26], terminology and nomenclature [27], instrumental aspects [28], sensitivity enhancement [29], column technology [30] and comparison of CE with liquid chromatography and conventional electrophoresis [31].

2.3.1   Theory of CE Separation

Separation by CE is based on the differences in electrophoretic mobility of ions in electrophoretic media in narrow bore capillaries, typically 25 to 75 μm i.d. and 10 to 100 cm in length.   The ionic electrophoretic mobility is always accompanied by an electroosmotic flow (EOF) of a certain magnitude.

2.3.1.1   Electrophoretic Mobility

The mobility (μ) of a charged molecule in an electric field is given by the sum of its electrophoretic mobility and electroosmotic mobility of the background electrolyte.

$$\mu = \mu_e + \mu_o \tag{2.1}$$

where μ_e is electrophoretic mobility and μ_o is electroosmotic mobility.

The electrophoretic mobility is the velocity of an ion in an electric field.   It is depends on the size of the ionic species and the nature, concentration and the temperature of the electrolyte.   This is reflected in the equation for electrophoretic mobility:

$$\mu_e = \frac{q}{6\pi\eta\, r} \tag{2.2}$$

8

where q is the ionic charge, η is the solution viscosity and r is the ionic radius of an analyte. Small species that are highly charged have high mobility, whereas large species with minimal charge have low mobility.

2.3.1.2   Electroosmotic Flow (EOF)

EOF is the bulk flow of liquid in the capillary and occurs as a consequence of the surface charge on the interior capillary wall. The EOF results from the effect of the applied electric field on the solution double-layer at the wall. The magnitude of the EOF can be expressed as,

$$\mu_o = \frac{\varepsilon\xi}{\eta}$$

(2.3)

where ε is the dielectric constant and ξ is the zeta potential.

Almost every surface carries charges. For fused silica the surface possess an excess of negative charges (SiO$^-$) resulting from ionisation of the silanol groups at pHs > 2. The surface charges are balanced by positive charges in the buffer. The capillary double layer is dominated by positive ions arranged in a static (Stern) and a diffuse layers at the surface. These create a potential difference very close to the wall, known as the zeta potential, as shown in Figure 2.2.

When voltage is applied across the capillary, the cations forming the diffuse double layer are attracted toward the cathode. An extreme, flat, piston-shaped flow profile results as shown in Figure 2.3. This leads to considerably less band broadening.

Several researchers have proposed methods for EOF rate determination [32-37] and for control of the flow [38-44]. The EOF can be altered by any of the following parameters:

9
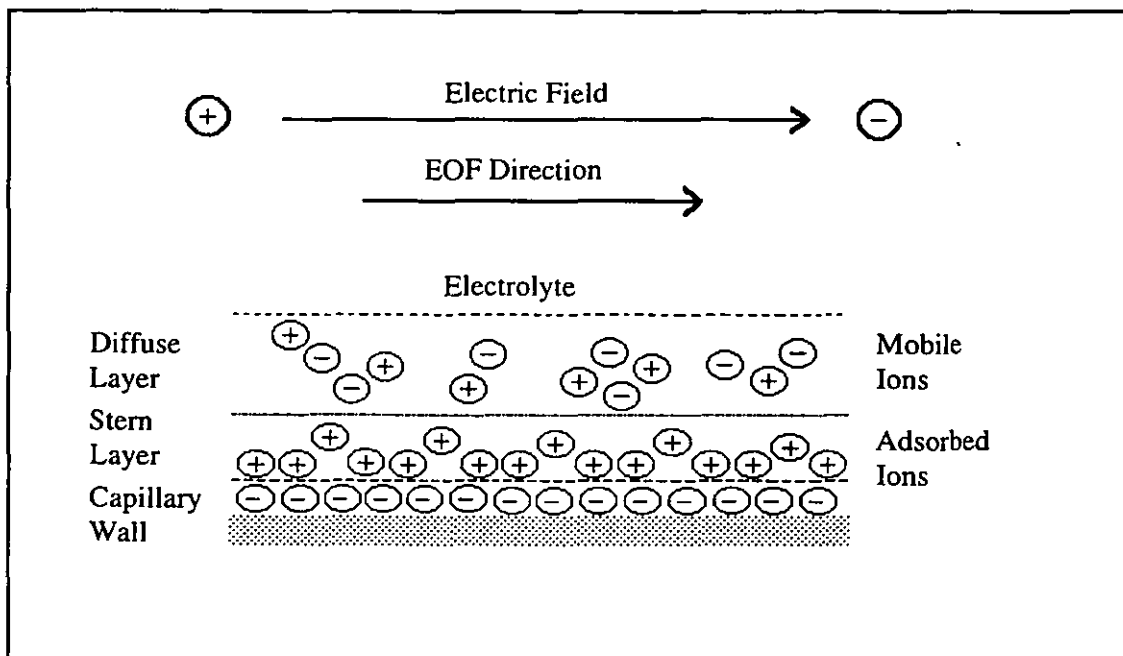
Figure 2.2:   Schematic diagram of the double layer at the capillary wall
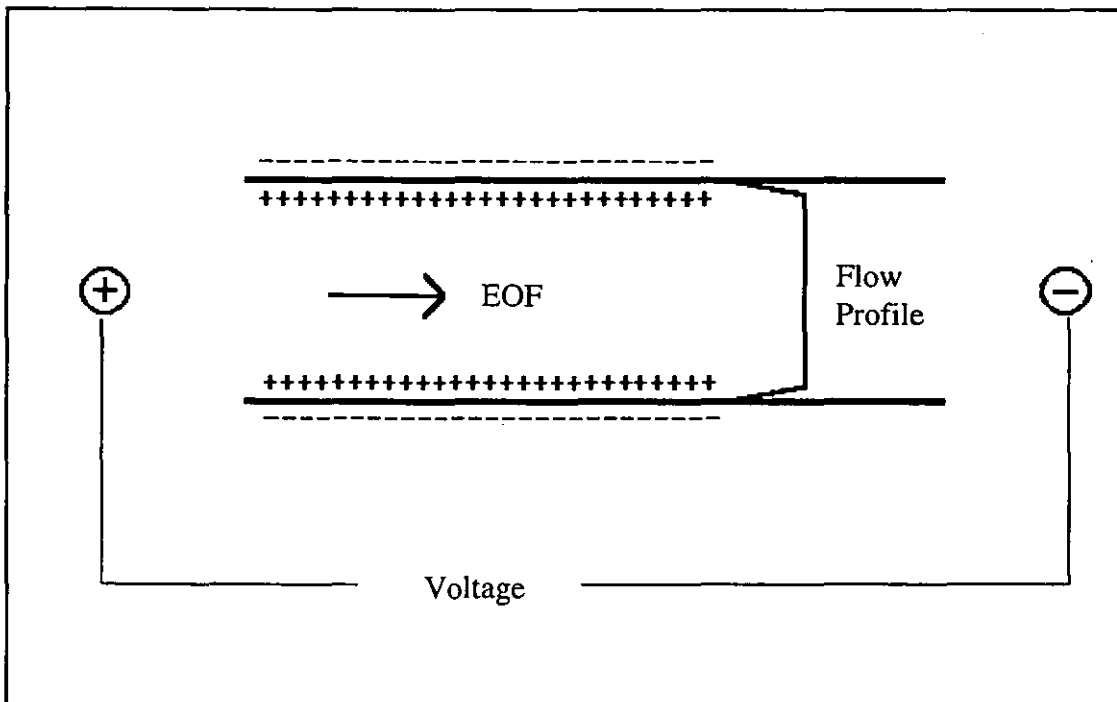
Figure 2.3:   Flow profile in CE capillary.

i. Changes in the electric field.

ii. Chemical modification of capillary wall.

iii. Adjustment of buffer pH.

iv. Addition of surfactant.

v. Changes in ionic strength or buffer concentration.

vi. Addition of an organic modifier.

vii. Changes in temperature.

2.3.1.3 Migration Time

Migration time is the time required for a solute to migrate to the point of detection. The migration time of an ion can be given by:

$$t = \frac{L^2}{(\mu_e + \mu_o)V} \qquad (2.4)$$

where, L is the capillary length, μ_e is the electrophoretic mobility, μ_o is the electroosmotic mobility and V is the applied voltage.

2.3.1.4 Efficiency and Resolution

The goal of both electrophoretic and chromatographic techniques is to keep separated zones as narrow as possible, that is the width at half height of the peak is a minimum. The efficiency of the CE separation is evaluated by calculation of the number of theoretical plates (although these do not have the same physical significance as in partition chromatography). The electrophoretic expression of theoretical plate number is given as:

$$N = \frac{(\mu_e + \mu_o)V}{2D} \qquad (2.5)$$

where D is diffusion coefficient of the solute. The separation efficiency will therefore increase if the applied voltage is increased.

The theoretical plate number also can be determined directly from an electropherogram using:

$$N = 5.54(\frac{t}{w_{1/2}})^2$$

(2.6)

where, t is the migration time and $w_{1/2}$ is the temporal peak width at half height.

The quality of the separation is called the resolution which is the ability of the system to separate two closely eluting species. The resolution in CE separation is given as [4]:

$$R = 0.177(\mu_1 - \mu_2)[\frac{V}{D(\mu_e + \mu_o)}]^{1/2}$$

(2.7)

where μ_1 and μ_2 are the electrophoretic mobilities of the two solutes, and μ_e is their average mobility. When the EOF is high, the resolution between two zones is poor. Good resolution can be obtained by balancing the EOF to the electrophoretic migration ($\mu_o = -\mu_e$). The cost of better resolution is longer analysis times. If the EOF coefficient has a greater absolute value than the electrophoretic mobilities of all the ions, then all the ions will move in the same direction, eluting in the following order: cations, neutral species and finally anions.

The factors that can lead to loss of efficiency and resolution in CE are Joule heating, the relative conductivity of the buffer and sample and adsorption of solutes onto the walls of the capillary. Joule heating occurs when a voltage induces a current to flow in the solution held in the capillary. In order to perform efficient separations it is essential that there is sufficient heat dissipation to avoid excessive temperature increase. Heating may change the mobilities of the solutes due to three effects. Firstly, changes in viscosity, secondly changes in partition ratios and finally changes in kinetic processes.

The conductivity of the sample and the electrolyte need to be well matched to avoid peak distortion. If the analytes have a higher mobility than the main co-ion of the electrolyte then peaks will exhibit fronting. Tailing peaks are due to analytes that have lower mobilities than the electrolyte co-ions. The optimum resolution and peak shape should be obtained when the mobility and charge of both the analyte and the electrolyte co-ion are similar.

A problem with silica capillaries is that solute molecules may adsorb onto the walls of the capillary. This can result in peak distortion and loss of sensitivity. When a voltage is applied across the capillary, the Stern layer forms and analyte ions may become trapped in this layer. The problem worsens: if the voltage applied is increased, the electrolyte cation charge is smaller than that of the analyte ion or if the concentration of the analyte is smaller. It is recommended that a highly charged electrolyte cation is best to minimise the adsorption of the analyte ions onto the Stern layer. The highly charged cation competes successfully with the analyte ions for the positively charged Stern layer. If the electrolyte cation has a smaller positive charge than the analyte ions then there will be significant loss of sensitivity due to adsorption.

2.4 MODES OF CE OPERATION

2.4.1 Classification of Modes

Different modes of CE separation can be performed using a standard CE instrument. The mode of separation depends on the composition of the electrolyte in different parts of the separation equipment. The distinct CE methods include capillary zone electrophoresis (CZE), capillary gel electrophoresis (CGE), micellar electrokinetic chromatography (MEKC), capillary isoelectric focusing (CIEF), and capillary isotachophoresis (CITP) [45]. Table 2.1 summarises the main separation modes encountered in the CE technique.

Table 2.1: Summary of CE separation modes.

Name	Abbreviation	Description	Basis of separation
Capillary electrophoresis	CE	General name for all electrophoretic separations in a capillary. Also known as High Performance Capillary Electrophoresis (HPCE)	-
Capillary zone electrophoresis	CZE	Originally synonymous with CE. Used mainly for counterelectroosmotic separations	Free solution mobility
Capillary gel electrophoresis	CGE	CE separations in gel filled capillaries	Size and charge
Micellar electrokinetic chromatography	MEKC	CE separations combined with interaction of analytes with micelles	Hydrophobic/ionic interactions with micelles
Capillary isoelectric focusing	CIEF	CE using a pH gradient inside the capillary	Isoelectric point or pI values
Capillary isotachophoresis	CITP	CE performed using a discontinuous buffer	Moving boundaries

2.4.2 Capillary Zone Electrophoresis (CZE)

CZE is the most widely used mode due to its simplicity of operation and its versatility [6]. The separation in CZE is based on the differences in the electrophoretic mobilities resulting in different velocities of migration of ionic species in the electrophoretic buffer contained in the capillary. Separation of anionic, cationic and neutral solutes is possible by CZE due to the EOF. EOF is toward the cathode, hence, a detector is placed at this end.

2.4.3 Capillary Gel Electrophoresis (CGE)

In CGE, the capillary is filled with a gel which acts as a molecular sieve to produce a size-based separation [46]. Various types of gel are used including acrylamide,

14

agarose, and cellulose. Gels are potentially useful for electrophoretic separations because of their anticonvective property. They can minimise solute diffusion, which contributes to zone broadening, prevent solute adsorption to the capillary walls and eliminate EOF which yields maximum resolution in short lengths of column.

2.4.4 Micellar Electrokinetic Chromatography (MEKC)

MEKC is a hybrid of CZE and micellar liquid chromatography [47]. The separation is based on the use of electroosmotically pumped micelles in a CE system to affect chromatographic separations of neutral compounds.

In this technique, anionic surfactants (especially sodium dodecyl sulphate, SDS) are added to the operating buffer and lead to the formation of micelles around the uncharged molecules. Since the micelles carry a negative charge, they migrate to the anode. However, most buffers exhibit an EOF larger than the rate of migration of the micelles, therefore, the micelles are transported to the detector at the cathode.

2.4.5 Capillary Isoelectric Focusing (CIEF)

CIEF is a high resolution electrophoretic technique used to separate sample constituents according to their isoelectric point. It is carried out in a pH gradient [48]. The pH gradient is generated by the electric current passing through a mixture of carrier ampholytes. Ampholytes are molecules that contain both an acidic and a basic moiety and can have isoelectric point values that span the desired pH range of the CIEF experiment.

The capillary is filled with the solution of the samples in the ampholytes mixture; dilute sodium hydroxide is introduced into the capillary at the anode side and phosphoric acid at the cathode side. When voltage is first applied, a high current flows and at the end of the focusing the current reduces to a constant low value. After the sample has been focused in the capillary, it is transported to the detector by changing the cathode electrolyte from NaOH to NaCl solution. This solution destroys

the pH gradient, mobilises the focused analytes and allows their transport to the detector.

2.4.6   Capillary Isotachophoresis (CITP)

CITP is performed in a discontinuous buffer system, with leading and terminating electrolytes. The leading electrolyte has the highest mobility and forms the front zone, the terminating electrolyte has the lowest mobility and forms the rear zone. Sample is introduced in between the zones. All ions with the same charge migrate at an equal rate. In a single CITP experiment either cations or anions can be analysed [49].

The steady state velocity in CITP occurs since the electric field varies in each zone. The field is self-adjusting to maintain constant velocity, with the lowest field across the zone with highest mobility. This phenomenon maintains very sharp boundaries between the zones. If an ion diffuses into a neighbouring zone its velocity changes and it immediately returns to its own zone.

2.5   INSTRUMENTATION

A CE instrument usually comprises a high voltage power supply, a detector and an electrophoresis compartment containing a capillary connecting two buffer reservoirs with high voltage electrodes as shown in Figure 2.4.

The basic instrumentation set-up can be enhanced with auto-samplers, multiple injection devices, sample/capillary temperature control, programmable power supplies, multiple detectors, fraction collection and computer interfacing.

2.5.1   High Voltage Power Supply

The power supply used in a CE instrument usually has an adjustable voltage within the range from - 30 to + 30 kV. Most instruments allow the polarity to be switched.
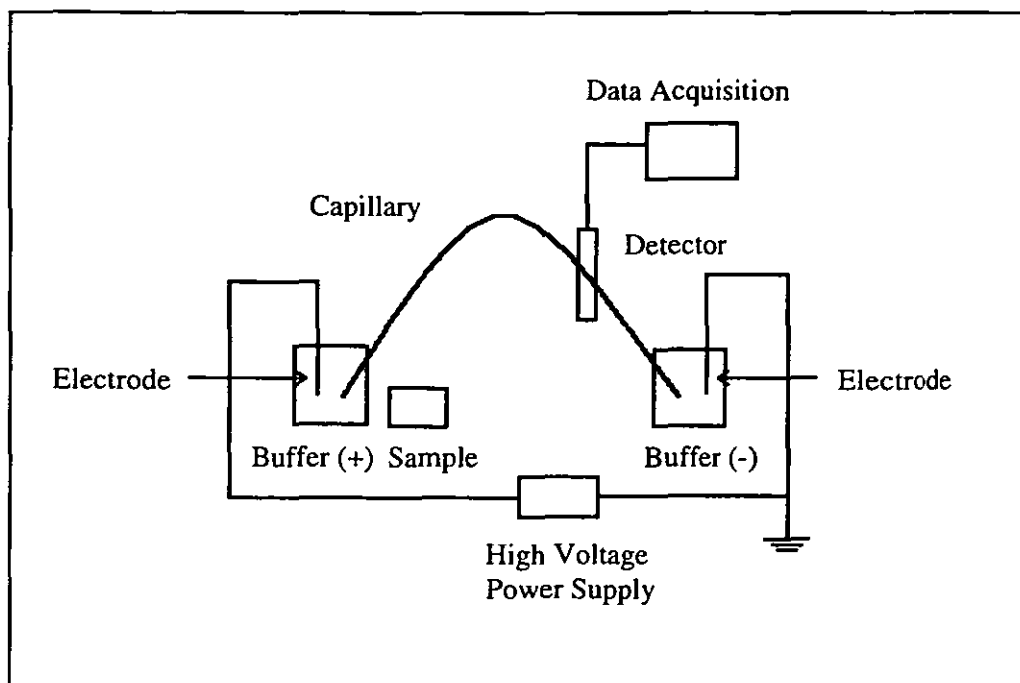
Figure 2.4:   Schematic diagram of a CE instrument.

The possibility to work with constant power or constant current, instead of constant voltage is an additional feature [28].

Recording of power, current and voltage is an important feature to control the stability of experimental conditions. This is necessary for proper validation and to explain failed experiments.

The driving force behind the migration of ions in CE is the field strength applied within the capillary, which is determined by the applied voltage dividing by the total capillary length. Since both the electrophoretic migration velocity and the EOF velocity are directly proportional to the electric field, highest field strengths will bring about the shortest analysis times.

2.5.2   Samples Injection Techniques

Injection of very small sample volumes, in the range of 1 to 50 nl, into the capillary is employed in CE in order to maintain high efficiency [50]. With respect to sample

overloading, the injection plug length is a more critical parameter than volume. The sample length should be less than 1 - 2% of the total length of the capillary. Various techniques for sample introduction have been studied including hydrodynamic [51], electrokinetic [4], rotary loop injector [52], split flow injector [53], electric sample splitter [54], and isotachophoretic methods [55]. The two most common quantitative methods are hydrodynamic and electrokinetic injection.

2.5.2.1   Hydrodynamic Injection

Hydrodynamic sample injection is based on pressure differential and there are three approaches; application of pressure at the injection end of the capillary; vacuum at the exit end of the capillary; or by siphoning action obtained by elevating the injection reservoir relative to the exit reservoir.

The volume of sample loaded can be calculated using the equation,

$$\text{Volume} = \frac{\Delta P r^4 \pi \ t}{8 \eta \ L} \tag{2.8}$$

where, ΔP is the pressure difference across the capillary, r is the capillary radius, t is injection time, η is the buffer viscosity and L is the total capillary length.

The amount of sample injected, Q (g or moles) is then;

$$Q = \frac{\Delta P r^4 \pi \ Ct}{8 \eta \ L} \tag{2.9}$$

where C is the sample concentration.

2.5.2.2   Electrokinetic Injection

Electrokinetic or electromigration injection is performed by replacing the injection end reservoir with the sample vial and applying the voltage. Analyte enters the

capillary by both migration and by the pumping action of the EOF. The quantity loaded is dependent on the electrophoretic mobility of the individual solutes.

The quantity injected, Q (g or moles), can be calculated by,

$$Q = \frac{(\mu_e + \mu_0)Vr^2\pi \ Ct}{L}$$

(2.10)

2.5.2.3 Reproducibility

The various factors that affect the reproducibility of sample introduction include: conductivity differences between the separation electrolyte and the sample solution [56], large differences in the concentrations of the various components of the sample and their electrophoretic mobility [57] and differences in the sample matrix [58].

2.5.3 Capillary Technology

Ideal properties for the capillary material include being chemically and electrically inert, UV/VIS transparent, flexible and robust, and inexpensive. Fused silica capillaries are mostly employed for CE separation. One disadvantage of using silica columns is that charged analytes can adsorb onto the surface of the wall leading to a decrease in the efficiency of separation and peak distortions. One solution involves deactivation of the silica surface by chemical modification. Coating of the interior surface of the capillary reduces or eliminates EOF and minimises the adsorption of solutes onto capillary walls [59]. Table 2.2 shows some common wall coatings and some comments on their stability and properties.

The fused silica capillaries used normally have i.d. ranging from 2 to 200 μm with o.d. of between 200 and 500 μm and a length typically between 10 and 100 cm. The use of shorter length capillaries is advantageous because these will give a very high field strength and thus short migration time and high separation efficiency, whilst the resolution remains almost the same [28]. The capillaries are often incorporated into a

Table 2.2:   Capillary coatings for CE [45].

Type	Comment
Silylation Coupling, (Si-O-Si-R). R= Polyacrylamide, Aryl penta fluoro, Protein or amino acid, Sulfonic acids, Maltose, PEG, Polyvinyl pyrrolidinone	Numerous usable functional groups, generally simple to prepare, Siloxane bond stable between pH 4 and 7, limited long term stability.
Direct Si-C Coupling: Polyacrylamide via Grignard	Si-C binding eliminates need for silylation, EOF practically eliminated, pH stable between 2 and 10, difficult to prepare.
Adsorbed Polymers: Cellulose, PEG, PVA	Poor long-term stability, low pH range (2-4), relatively hydrophobic.
Adsorbed, crosslinked polymers: Polyethyleneimine	Reverse EOF, useful for basic proteins, stable for physiological pH.
GC Phases: PEG, Phenylmethyl silicone	Hydrolytically unstable.
LC Phases: C_2, C_8, C_{18}	Can increase protein adsorption.

cartridge to eliminate the risk of capillary breakage. This also enables the capillary to be prealigned with a micro focusing lens system for sensitive and stable detection.

Both glass and Teflon capillaries have been used [3, 4], although not to the extent of fused silica because they are difficult to obtain with homogeneous inner bores and have poor heat transfer properties.

Capillary conditioning is one of the most important factors leading to good reproducibility. Base conditioning to remove adsorbates and refresh the surface by deprotonation of the silanol group is most commonly employed [26].

Capillary thermostating to control operating temperature is crucial if reproducible results are to be obtained. The approaches normally used are to bath the capillary in a high velocity air stream or in a liquid.

2.5.4 Buffer System

The selection of the electrophoresis buffer is extremely important because it fundamentally determines the migration behaviour of the analytes. A wide variety of buffer systems have been used to effect the required separation as shown in Table 2.3.

Table 2.3: Commonly used CE buffers [60].

Buffer	pK_a	pH Range
Phosphate (pK_1)	2.1	1.1 - 3.1
Phosphate (pK_2)	7.2	6.2 - 8.2
Phosphate (pK_3)	12.3	11.3 - 13.3
Citrate (pK_1)	3.1	2.1 - 4.1
Citrate (pK_2)	4.7	3.7 - 5.7
Citrate (pK_3)	5.4	4.4 - 6.4
Formate	3.8	2.8 - 4.8
Acetate	4.8	3.8 - 5.8
Tris	8.06	7.3 - 9.3
Borate	9.2	8.2 - 10.2

The suitability of a buffer system depends on many factors, the first of which is the pKa value of the buffer acid or base. For a buffer to be effective, its pH must be within ±1 of its pKa value (Table 2.3). Other factors include the solubility and stability of the analytes in the electrolyte, the effect of temperature and heat generation. Matching buffer ion mobility with solute mobility is important for minimising peak-shape distortion.

The pH of the buffer used affects the magnitude and direction of the EOF and the degree of ionisation of the analyte [61]. At pH above 2 in silica capillaries, the capillary wall is negatively charged. This causes the EOF to migrate towards the cathode. It should be noted that as the pH increases from 2, the magnitude of the EOF increases as the number of ionised silanol groups present on the capillary wall increases. To reverse the EOF, the pH can be taken to below 2. This causes the walls to become positively charged due to the presence of $SiOH_2^+$ groups. At ~ pH 2 the dissociation of the silanol groups is completely suppressed so the EOF should be minimal or zero.

Surfactants are amongst the most widely used additives in CE. Various types can be used, these include: anionic, cationic, zwitterionic and non-ionic. When added to the electrolyte in concentrations above the critical micelle concentration, droplets of the surfactant are formed. Analytes then interact with these to increase resolution in a CE separation. Many surfactants can also adsorb onto the capillary wall. This can modify the EOF and also decrease the potential for solute adsorption onto the walls. Depending on the surfactant charge, the EOF can be increased, reduced or reversed. Addition of an organic modifier, such as surfactant, to the electrophoretic buffer permits the analysis of some analytes which are not normally aqueous soluble.

2.5.5 Detection Techniques

Detection in CE is still the greatest technical problem owing to the small inside diameter of the separation capillary and the ultra-small analyte volume. Several detection techniques have been developed for use with CE including UV/VIS

absorption, fluorescence, electrochemical detectors, mass spectrometric detectors and indirect detection. Table 2.4 provides a summary.

2.5.5.1 Absorbance Detection

Most commercial CE instruments employ UV/VIS absorption as the detection technique. The popularity of UV/VIS detectors may be attributed to their easy implementation for on-column detection, their availability at relatively low cost, and their adequate sensitivity for chromophoric compounds. Detection is carried out in the capillary in order to avoid efficiency loss due to peak broadening outside the capillary. However, UV detection suffers from the disadvantages that sensitivity is limited by the short path length and limited time available to observe the sample as it passes the detector [69].

Capillaries with rectangular cross section [70] and a z-shaped flow cell [71] have been used to increased the optical path length. An alternative approach is to use a wide-bore capillary to perform the separations, this increases both the path length and the amount of sample introduced into the capillary [72]. The diode-array detector (DAD) has been used as an alternative to multiple wavelength absorption detectors [73]. These detectors provide additional spectral information during the run that can be used to assist in analyte identification, peak purity assessment and pre-run screening to determine the wavelength settings for optimum sensitivity.

2.5.5.2 Fluorescence Detection

Fluorescence detectors have been used in commercial instruments with deuterium, tungsten or xenon arc lamp sources [74]. Detection limits are excellent with fluorescence and the technique is highly selective. Relatively few compounds naturally fluoresce and thus there is a need for derivatisation. Compounds without native fluorescence are usually pre-column, on-column, or post-column labelled with a fluorescence tag.

Table 2.4:   CE detection techniques.

Method	Detection limit/(M)	Advantages	Disadvantages	References
UV/VIS absorption	$10^{-5} - 10^{-8}$	Universal, diode array offers spectral information	Sensitivity	62
Fluorescence	$10^{-7} - 10^{-9}$	Sensitive	Usually requires sample derivatisation	63
Laser induced fluorescence	$10^{-14} - 10^{-16}$	Extremely sensitive	Usually requires sample derivatisation, expensive	64
Amperometry	$10^{-10} - 10^{-11}$	Sensitive	Selective, but only for electroactive analytes, requires special electronics and capillary modification	65
Conductivity	$10^{-7} - 10^{-8}$	Universal	Requires special electronics and capillary modification	66
Mass spectrometry	$10^{-8} - 10^{-9}$	Sensitive and offers structural information	Interface between MS and CE complicated	67
Indirect UV, fluorescence, amperometery	10-100 times less than direct methods	Universal	Less sensitive than direct methods	68

Laser-induced fluorescence (LIF) detection is among the most sensitive detection techniques developed for CE. Much LIF work has been carried out using the helium-cadmium laser [75]. The lowest detection limits reported for the LIF system employed a sheath flow cuvette to reduce stray light levels [64].

2.5.5.3 Electrochemical Detection

Electrochemical techniques offer both sensitivity and selectivity for detection in CE. However, these techniques are not routinely used due to the difficulty of performing electrochemistry in the presence of the high-voltage electric field used for electrophoretic separation. Electrochemical detection schemes employed include methods based on potentiometric measurement [2], conductivity measurement [76-79] and amperometry [80-83].

Potentiometric detection is based on the measurement of the Nernst potential, either across an ion selective barrier or at an electrode surface, with respect to a reference electrode. The major advantage of this type of detector is its ability to response to extremely small amounts of ions through the use of a microelectrode.

Conductivity detection is based on the measurement of the conductivity, or a voltage drop between two indicator electrodes, when a small constant current is applied between them. It is advantageous to use a low ionic strength, poorly ionised buffer system to produce a low conductivity background.

Amperometric detection is based on the redox reaction of an analyte at the detection electrode during its passage through the detection cell. The sensitivity of amperometric detection for CE is relatively good, but it is not easily applied. The high current associated with the separation in the capillary interferes with the electrochemical measurement current.

2.5.5.4   CE-Mass Spectrometry

Coupling of CE to mass spectrometry (CE-MS) provides sensitive mass-selective detection, structural information as well as migration times [84-90]. The interfacing has been accomplished mainly by electrospray ionisation (ESI), ionspray (IS) or continuous-flow fast atom bombardment (CF-FAB).

The first successful coupling of CE with mass spectrometry was reported by Olivares *et al.* [91]. An electrospray ionisation interface was used for connection of the separation capillary to a quadrupole mass spectrometer. A thin sheath liquid flow outside the CE capillary was employed to make electrical contact with a steel capillary to complete the circuit.

Other CE-MS interface systems developed include: sheathless [92], coaxial sheath flow [93] and liquid junction interface [94, 95].

2.5.5.5   Indirect Detection

Indirect modes of detection provide a simple solution to the problem of universal detection, eliminating the need for pre- or post-column derivatisation to convert the analyte of interest into a species that gives a response at the detector. Because the analytes are not chemically altered, fraction collection and further studies are facilitated.

Several indirect detection modes for CE have been established including indirect UV absorbance [96], indirect fluorescence [97] and indirect amperometric detection [98]. This detection mode is based on signal perturbation of a continuously monitored background substance.

26

2.5.5.6   Other Detection Methods

Other detection methods such as Raman spectroscopy [99], on-line measurement of radioactivity [100], circular dichroism [101], refractive index [102] and capillary vibration [103] have been described in the literature. Interfacing sensitive and selective detectors with CE, such as microwave-induced helium plasma atomic emission [104] and inductively coupled plasma-mass spectrometry [105-107] have also been investigated.

2.6   APPLICATIONS OF CAPILLARY ELECTROPHORESIS

CE has been applied to a wide variety of analyte types including inorganic ion determination [108], peptides and protein separation [109], environmental analysis [110], DNA sequencing [111], organic acids separation [112], humic acid fractionation [113], amino acids separation [114], carbohydrates and oligonucleotides analysis [115], pharmaceuticals and clinical samples [116] and polymer analysis [117].

CE has also been extensively used for metal chelate studies. Timerbaev *et al.* [118, 119] studied the separation of metal ions (transition metal and aluminium) in the form of 8-hydroxyquinoline-5-sulphonic acid complexes (HQS). Metal chelates of Al(III), Co(III), Cr(III) and Fe(III) ions with 2,2'-dihydroxyazobenzene-5,5'-disulphonate have been investigated by Iki *et al.* [120]. Motomidzu *et al.* [121] examined metal chelates of the alkaline-earths (Ba, Sr, Ca, and Mg) with ethylenediaminetetraacetic acid (EDTA) using UV-absorptive detection. Other metal-chelate separations reported, included complexes with chelating agents such as diethylenetriaminepentaacetic acid (DTPA) [122], cyclohexanediaminetetraacetic acid (CyDTA) [123] and pyridylazoresorcinol (PAR) [124].

REFERENCES

1. Hjerten, S., *Chromatogr. Rev.,* 1969, **9**, 122.

2. Virtanen, R., *Acta Polytech. Scan.,* 1974, **123**, 1.

3. Mikkers, F. E. P., Everaerts, F. M., and Verheggen, T. P. E. M., *J. Chromatogr.,* 1979, **169**, 11.

4. Jorgenson, J. W., and Lukacs, K. D., *Anal. Chem.,* 1981, **53**, 1298.

5. Jorgenson, J. W., and Lukacs, K. D., *J. Chromatogr.,* 1981, **218**, 209.

6. Jorgenson, J. W., and Lukacs, K. D., *Science,* 1983, **222**, 266.

7. Warner, M., *Anal. Chem.,* 1994, **66**, 1137A.

8. Science Citation Index (SCI) Search on BIDS ISI Data Service Release 5.2.07, Bath Information and Data Services, UK.

9. Foret, F., Krivankova, L., and Bocek, P., *Capillary Zone Electrophoresis,* VCH Verlagsgesellschaft, Weinheim FRG, 1993.

10. Camilleri, P. (Ed.), *Capillary Electrophoresis: Theory and Practice,* CRC Press, Boca Raton, 1993.

11. Li, S. F. Y., *Capillary Electrophoresis: Principles, Practice and Applications,* J. Chromatogr. Library, Elsevier Scientific Publ., Amsterdam, 1992.

12. Jandik, P., and Bonn, G., *Capillary Electrophoresis of Small Molecules and Ions,* VCH Publishers, New York, 1993.

13. Guzman, N. A. (Ed.), *Capillary Electrophoresis Technology,* Chromatogr. Sci. Series, Vol. 64, Marcel Dekker, Inc., New York, 1993.

14. Weinberger, R., *Practical Capillary Electrophoresis,* Academic Press, Boston, 1993.

15. Kuhn, R., and Huffstetter-Kuhn, S., *Capillary Electrophoresis: Principles and Practice,* Springer-Verlag, New York, 1993.

16. Grossman, P. D., and Colburn, J. C. (Eds.), *Capillary Electrophoresis: Theory and Practice,* Academic Press, San Diego, 1992.

17. Gordon, M. J., Huang, X., Pentoney, S. L., and Zare, R. N., *Science,* 1988, **242**, 224.

18.   Ewing, A. G., Wallingford, R. A., and Olefirowics, T. M., *Anal. Chem.*, 1989, **61**, 292A.

19.   Kuhr, W. G., *Anal. Chem.*, 1990, **62**, 403R.

20.   Goodall, D. M., Lloyd, D. K., and Williams, S. J., *LC-GC Intl.*, 1990, **3**, 28.

21.   Campos, C. C., and Simpson, C. F., *J. Chromatogr. Sci.*, 1992, **30**, 53.

22.   Kuhr, W. G., and Monnig, C. A., *Anal. Chem.*, 1992, **64**, 389R.

23.   Marina, M. L., and Torre, M., *Talanta*, 1994, **41**, 1411.

24.   Monnig, C. A., and Kennedy, R. T., *Anal. Chem.*, 1994, **66**, 280R.

25.   Reijenga, J. C., *J. Radianal. Nucl. Chem.*, 1992, **163**, 155.

26.   Engelhardt, H., Beck, W., Kohr, J., and Schmitt, T., *Angew. Chem.*, 1993, **32**, 629.

27.   Knox, J. H., *J. Chromatogr.*, 1994, **680**, 3.

28.   Watzig, H., and Dette, C., *Fresenius J. Anal. Chem.*, 1993, **345**, 403.

29.   Albin, M., Grossman, P. D., and Moring, S. E., *Anal. Chem.*, 1993, **65**, 489A.

30.   Turner, K. A., *LC-GC Intl.*, 1991, **4**, 32.

31.   Lauer, H. H., and Ooms, J. B., *Anal. Chim. Acta*, 1991, **250**, 45.

32.   Altria, K.D., and Simpson, C. F., *Anal. Proc.*, 1986, **23**, 453.

33.   Huang, X., Gordon, M. J., and Zare, R. N., *Anal. Chem.*, 1988, **60**, 1837.

34.   Wanders, B. J., Van De Goor, A. A. A. M., and Everaerts, F. M., *J. Chromatogr.*, 1989, **470**, 89.

35.   Wanders, B. J., Van De Goor, A. A. A. M., and Everaerts, F. M., *J. Chromatogr.*, 1989, **470**, 95.

36.   Lee, T. T., Dadoo, R., and Zare, R. N., *Anal. Chem.*, 1994, **66**, 2694.

37.   Williams, B. A., and Vigh, G., *Anal. Chem.*, 1996, **68**, 1174.

38.   Hayes, M. A., Kheterpal, I., and Ewing, A. G., *Anal. Chem.*, 1993, **65**, 2010.

39.   Hoffstetter-Kuhn, S., Paulus, A., Gassmann, E., and Widmer, H. M., *Anal. Chem.*, 1991, **63**, 1541.

40.   Demana, T., Guhathakurta, U., and Morris, M. D., *Anal. Chem.*, 1992, **64**, 390.

41. Wu, D., and Regnier, F. E., *Anal. Chem.*, 1993, **65**, 2029.

42. Schwer, C., and Kenndler, E., *Anal. Chem.*, 1991, **63**, 1801.

43. Vindevogel, J., and Sandra, P. J., *J. Chromatogr.*, 1991, **541**, 483.

44. Kuhn, R., Stoecklin, F., and Erni, F., *Chromatographia*, 1992, **33**, 32.

45. Heiger, D. N., *High Performance Capillary Electrophoresis*, Hewlett-Packard Co., Waldbronn, 1992.

46. Cohen, A. S., and Karger, B. L., *J. Chromatogr.*, 1987, **398**, 409.

47. Vindevogel, J., and Sandra, P., *Introduction to MEC in Chromatographic Methods*, Huthig, Heidelberg, 1992.

48. Righetti, P. C., *Isoelectric Focusing: Theory, Methodology and Applications*, Elsevier, Amsterdam, 1983.

49. Bocek, P., Deml, M., Gebauer, P., and Dolnik, V., *Analytical Isotachophoresis*, VCH Verlagsgesellschaft, Weinheim FRG, 1988.

50. Sepaniak, M. J., and Cole, R. O., *Anal. Chem.*, 1988, **60**, 617.

51. Terabe, S., Otsuka, S., Ichikawa, K., Tsuchiya, A., and Ando, T., *Anal. Chem.*, 1984, **56**, 113.

52. Tsuda, T., Mizuno, T., and Akiyama, J., *Anal. Chem.*, 1987, **59**, 799.

53. Tehrani, J., Macomber, R., and Days, L., *J. High Res. Chromatogr.*, 1991, **14**, 10.

54. Deml, M., Foret, F., and Bocek, P., *J. Chromatogr.*, 1985, **320**, 159.

55. Foret, F., Sustachek, V., and Bocek, P., *J. Microcolumn Sep.*, 1990, **2**, 299.

56. Burton, D., Sepaniak, M. J., and Maskavinec, M., *Chromatographia*, 1986, **21**, 583.

57. Huang, X., Lucky, J. A., Gordon, M. J., and Zare, R. N., *Anal. Chem.*, 1989, **61**, 766.

58. Huang, X., Gordon, M. J., and Zare, R. N., *Anal. Chem.*, 1988, **60**, 375.

59. Wehr, T., *LC-GC Intl.*, 1992, **6**, 70.

60. Altria, K. D., Kelly, T., and Clark, B., *LC-GC Intl..*, 1996, 10, 408.

61. McCormick, R. M., *Anal. Chem.*, 1988, **60**, 2322.

62. Sepaniak, M. J., Swaile, D. F., and Powell, A. C., *J. Chromatogr.*, 1989, **480**, 185.

63. Roach, M. C., Gozel, P., and Zare, R. N., *J. Chromatogr.*, 1988, **426**, 129.

64. Wu, S., and Dovichi, N. J., *J. Chromatogr.*, 1989, **480**, 141.

65. Wallingford, K. A., and Ewing, A. G., *Anal. Chem.*, 1988, **60**, 1762.

66. Huang, X., Pang, T., Gordon, M. J., and Zare, R. N., *Anal. Chem.*, 1987, **59**, 1230.

67. Smith, R. D., Wahl, J. H., Goodlett, D. R., and Hofstadler, S. A., *Anal. Chem.*, 1993, **65**, 574A.

68. Kuhr, W. G., and Yeung, E. S., *Anal. Chem.*, 1991, **63**, 275A.

69. Milofsky, R. E., and Yeung, E. S., *Anal. Chem.*, 1993, **65**, 153.

70. Tsuda, T., Sweedler, J. V., and Zare, R. N., *Anal. Chem.*, 1990, **62**, 2149.

71. Chervet, J. P., van Soest, R. E. J., and Ursem, M., *J. Chromatogr.*, 1991, **543**, 439.

72. Altria, K. D., *LC-GC Int.*, 1992, **6**, 164.

73. Kobayaski, S., Ueda, T., and Kikumoto, M., *J. Chromatogr.*, 1989, **480**, 179.

74. Albin, M., Weinberger, R., Sapp, E., and Moring, S., *Anal. Chem.*, 1991, **63**, 417

75. Burton, D., Sepaniak, M. J., and Maskar, M. P., *J. Chromatogr. Sci.*, 1986, **24**, 347.

76. Beckers, J., Verheggen, T., and Everaerts, F., *J. Chromatogr.*, 1988, **452**, 591.

77. Huang, X., Gordon, M. J., and Zare, R. N., *J. Chromatogr.*, 1989, **480**, 285.

78. Huang, X., Zare, R. N., Sloss, S., and Ewing, A. G., *Anal. Chem* , 1991, **63**, 189.

79. Gebaur, P., Deml, M., Bocek, P., and Janak, K., *J. Chromatogr.*, 1983, **267**, 455.

80. Wallingford, R. A., and Ewing, A. G., *Anal. Chem.*, 1991, **59**, 678.

81. Yik, Y. F., Lee, H. K., Li, S. F. Y., and Khoo, S. B., *J. Chromatogr.*, 1991, **585**, 144.

82. Gaitonde, C. D., and Pathak, P. V., *J. Chromatogr.*, 1990, **514**, 389.

83. Olefirowicz, T. M., and Ewing, A. G., *J. Chromatogr.*, 1990, **499**, 713.

84. Niessen, W. M. A., Tjaden, U. R., and van der Greef, J., *J. Chromatogr.*, 1993, **636**, 3.

85. Cai, J., and Henion, J., *J. Chromatogr.*, 1995, **703**, 667.

86. Paulus, A., and Ohms, J. I., *J. Chromatogr.*, 1990, **507**, 113.

87. Smith, R. D., Barinaga, C. J., and Udseth, H. R., *Anal. Chem.*, 1988, **60**, 1948.

88. Wahl, J. H., Goodlett, D. R., Udseth, H. R., and Smith, R. D., *Anal. Chem.*, 1992, **64**, 3194.

89. Schomburg, G., *Chromatographia*, 1990, **30**, 500.

90. Mosely, M. A, Deterding, L. J., Tomer, K. B., and Jorgenson, J. W., *Anal. Chem.*, 1991, **63**, 109.

91. Olivares, J. A., Nguyen, N. T., Yonker, C. R., and Smith, R. D., *Anal. Chem.*, 1987, **59**, 1230.

92. Wahl, J. H., Gale, D. C., and Smith, R. D., *J. Chromatogr.*, 1994, **659**, 217.

93. Thibault, P., Pleasance, S., and Laycock, M. V., *J. Chromatogr.*, 1991, **542**, 483.

94. Lee, E. D., Muck, W., Henion, J. D., and Covey, T. R., *J. Chromatogr.*, 1988, **458**, 313.

95. Caprioli, R. M., Moore, W. T., Martin, M., DaGue, B. B., Wilson, K., and Moring, S., *J. Chromatogr.*, 1989, **480**, 247.

96. Foret, F., Fanali, S., Ossicini, L., and Bocek, P., *J. Chromatogr.*, 1989, **470**, 299.

97. Kuhr, W. G., and Yeung, E. S., *Anal. Chem.*, 1988, **60**, 2642.

98. Honda, S., Suzuki, K., Kataoka, M., Makino, A., and Kakehi, K., *J. Chromatogr.*, 1990, **515**, 653.

99. Chen, C., and Morris, M., *Appl. Spectrosc.*, 1988, **42**, 515.

100. Pentoney, S., and Zare, R. N., *Anal. Chem.*, 1989, **61**, 1643.

101. Christensen, P., and Yeung, E., *Anal. Chem.*, 1989, **61**, 1344.

102. Chen, C., Demana, T., Huang, S., and Morris, M., *Anal. Chem.*, 1989, **61**, 1593.

103. Wu, J., Odake, T., Katimori, T., Sawada, T., *Anal. Chem.*, 1991, **63**, 2216.

104. Liu, Y., and Lopez-Avila, V., *J. High Res. Chromatogr.*, 1993, **16**, 717.

105. Olesik, J. W., Kinzer, J. A., and Olesik, S. V., *Anal. Chem.*, 1995, **67**, 1.

106. Lopez-Avila, V., Liu, Y., Zhu, J. J., Wiederin, D., and Becket, W. F., *Anal. Chem*, 1995, **67**, 2020.

107. Barnes, R. M., Lu, Q., and Bird, S. M., *Anal. Chem*, 1995, **67**, 2949.

108. Chen, M., and Cassidy, R. M., *J. Chromatogr.*, 1993, **640**, 425.

109. Mattusch, J., and Dittrich, K., *J. Chromatogr.*, 1994, **680**, 279.

110. Kleiboehmer, W., Cammann, K., Robert, J., and Mussenbrock, E., *J. Chromatogr.*, 1993, **638**, 349.

111. Takahashi, S., Murakami, K., Anazawa, T., and Kambara, H., *Anal. Chem.*, 1994, **66**, 1021.

112. Kenney, B. F., *J. Chromatogr.*, 1991, **546**, 423.

113. Rigol, A., Lopez-Sanchez, J. F. and Rauret, G., *J. Chromatogr.*, 1994, **664**, 301.

114. Yu, M., and Dovichi, J., *Anal. Chem.*, 1989, **61**, 37.

115. Liu, J., Shirota, O., and Novotny, M., *Anal. Chem.*, 1991, **63**, 413.

116. Fujiwara, S., Iwase, S., and Honda, S., *J. Chromatogr.*, 1988, **447**, 133.

117. Jones, H. K., and Ballou, N. E., *Anal. Chem.*, 1990, **62**, 2484.

118. Timerbaev, A., Semenova, O., and Bonn, G., *Chromatographia*, 1993, **37**, 497.

119. Timerbaev, A., Semenova, O., and Bonn, G., *Chromatographia*, 1994, **38**, 255.

120. Iki, N., Hoshino, H., and Yotsuyanagi, T., *J. Chromatogr.*, 1993, **652**, 539.

121. Motomidzu, S., Oshima, M., Matsuda, S., Obata, Y., and Tanaka, H., *Anal. Sci.*, 1992, **8**, 619.

122. Buchberger, W., and Mulleder, S., *Mikrochimica Acta*, 1995, **119**, 103.

123. Motomidzu, S., Nishimura, Y., Obata, Y., and Tanaka, H., *Anal. Sci.*, 1991, **7** (supplement), 253.

124. Iki, N., Hoshino, H., and Yotsuyanagi, T., *Chem. Lett.*, 1993, **4**, 701.

Chapter 3

CHAPTER THREE

INDUCTIVELY COUPLED PLASMA - MASS SPECTROMETRY

3.1   INTRODUCTION TO CHAPTER

This chapter provides an introduction to ICP-MS, the theory, instrumentation, sample introduction methods and interferences.   The coupling of ICP-MS with chromatographic and CE techniques is also discussed. Finally, a review of selected applications will be presented.

3.2   ORIGINS AND DEVELOPMENT

The first known experiment with an inductively coupled plasma (ICP) was conducted by Babat [1] with a plasma discharge in air at low pressure. Reed [2] was the first to form a stable plasma operating at atmospheric pressure. The analytical potential of the technique was explored in the work of Greenfield *et al.* [3] and Wendt and Fassel [4].   The ICP was initially developed as a source for optical atomic emission spectroscopy (AES) [5-7].

ICP-MS was first introduced in 1980 by Houk and Gray and co-workers [8] and this was followed by the successful operation of an updated ICP-MS system by Date and Gray [9].   Publications before 1980, and several that have appeared since, have employed plasmas such as a capillary arc [10-12] or a microwave-induced plasma (MIP) [13] as the ion source.

Commercial ICP-MS instruments were first launched in 1983 by VG Isotopes, United Kingdom (PlasmaQuad) and by Sciex Incorporation, Canada (Elan) [14]. Reviews on the subject of ICP-MS have been written by Date [15], Gray [16, 17], Date and Gray [18], Houk [19], Douglas and Houk [20], Koppenaal [21, 22] and Horlick [23].

Other reviews on ICP-MS include developments and trends [24-26], instrumentation [27], comparison of ICP-MS, ICP-AES and AAS [28], interferences in ICP-MS [29] and Atomic Spectrometer Updates [30, 31]. Several books on ICP-MS [14, 32-34] and chapters on ICP-MS have been published in books [35, 36].

The technique of ICP-MS has received a great deal of attention as a method for sensitive elemental analysis as shown by the growth in numbers of publications since 1980 (Figure 3.1).
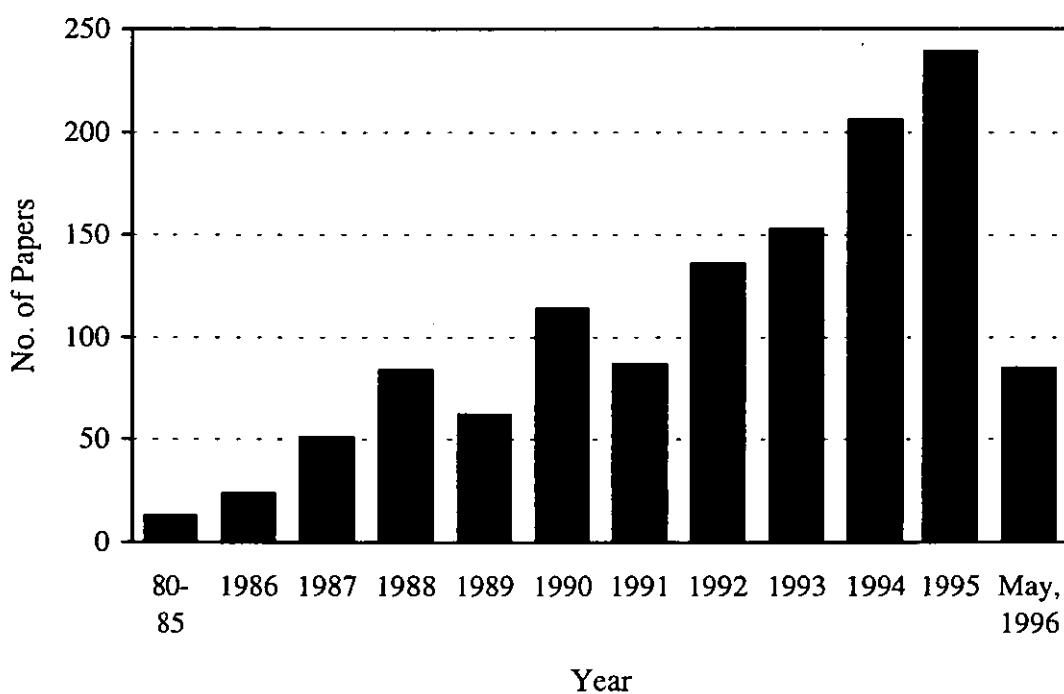
Figure 3.1: Frequency of published articles on ICP-MS based on a survey - May 1996 [37].

3.3   THEORY OF ICP-MS

ICP-MS employs an argon ICP as an ion source for mass spectrometry. Liquid samples are introduced into the center of the plasma as aerosols. The fine sample aerosol moves through the central channel of the plasma and undergoes several

processes in turn: desolvation, vaporisation, atomisation and finally ionisation. Ions are extracted from the atmospheric-pressure plasma into the low-pressure mass spectrometer, separated and analysed according to their mass-to-charge (m/z) ratios.

The advantages of the ICP-MS technique for elemental analysis include [38]:

- Low detection limits.
- Good precision.
- Broad linear dynamic range.
- Capability for multielement analysis.
- Speed of analysis.
- Rapid acquisition of mass spectra.
- Simple spectra.
- Capability for isotopic analysis.

The limitations of the ICP-MS include [38]:

- The total solute content of the sample should be less than 0.2%.
- Potential interferences from the background spectrum.
- Potential interferences from the matrix.
- Signal drift.
- Mass discrimination.

3.4   INSTRUMENTATION

A typical ICP-MS instrument consists of a radio frequency (rf) generator, torch box, sample introduction system, ion extraction interface, ion focusing system, quadrupole mass spectrometer, ion detector and a microcomputer for instrument control and data handling. Figure 3.2 shows a schematic diagram of an ICP-MS instrument.
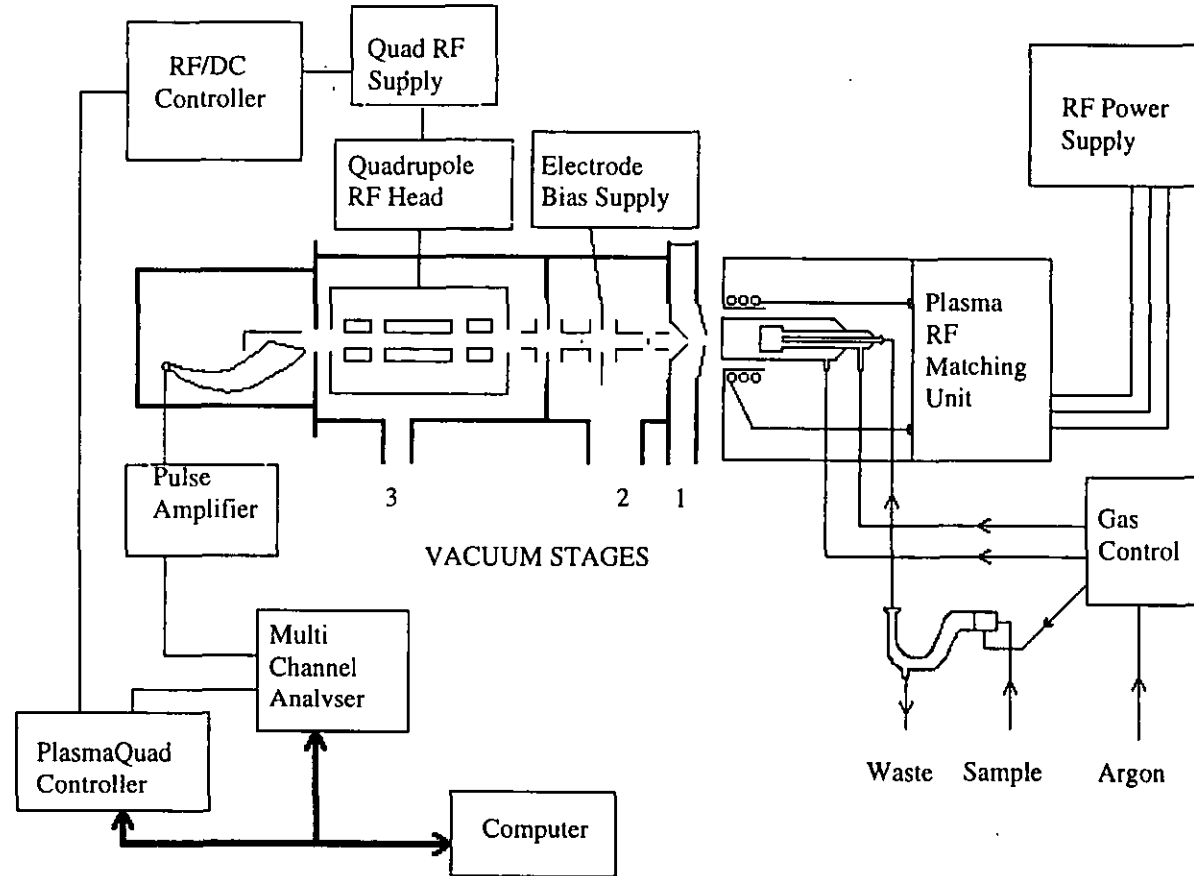
Figure 3.2: Schematic of ICP-MS instrument.

3.4.1 Plasma rf Generator

Radio frequency (rf) generators used to supply power to ICPs are oscillators that basically generate an alternating current at a desired frequency. The two types of oscillators mostly used in commercial instruments are crystal-controlled multistage rf oscillator/amplifiers and free-running rf generators [39].

The crystal-controlled type has a piezoelectric crystal to maintain a constant frequency of operation. The frequency of a free-running system is controlled by the oscillating circuit and load coil. Currently, generator frequencies of 27.12 and 40.68 MHz are available.

3.4.2 Torch

The ICP is an electrodeless discharge in a gas at atmospheric pressure, maintained by energy coupled to it from a rf generator. This is done by a suitable coupling coil, which functions as the primary of a rf transformer, the secondary of which is created by the discharged itself. The gas used is commonly argon although other gases are occasionally used, sometimes as additions to the main supply. The plasma is generated inside and at the open end of an assembly of quartz tubes known as the torch.

The torch commonly used for the ICP is based on the Scott Fassel design [40], has an outer tube inner diameter of 18 mm and is about 100 mm long. The torch typically consists of a series of annular tubes. The outer gas flow, the 'coolant flow', protects the tube walls and serves to sustain the plasma (usually 10-15 l min^{-1}). The second gas flow, the 'auxiliary flow' (0-1.5 l min^{-1}), is mainly used to ensure that the hot plasma is kept clear of the tip of the central injector tube to prevent it being melted. The central gas flow, known as the injector or carrier flow (usually about 1 l min^{-1}), carries the sample aerosol into the central channel of the plasma.

The coupling or load coil is located with its outer turn a few mm below the mouth of the torch. The rf current supplied from the generator produces a magnetic field which varies in time at the generator frequency. The discharge is usually initiated in a cold torch by a spark from a Tesla coil, which provides free electrons to couple with the magnetic field. Electrons in the plasma precess around the magnetic field lines in circular orbits and the electrical energy supplied to the coil is converted into kinetic energy of electrons. At atmospheric pressure the free electron path before collision with an argon atom, to which its energy is transferred, and thus the plasma is heated, forming a bright discharge or fireball. At the frequency used, the skin effect occurring in rf induction heating ensures that most of the energy is coupled into the outer or induction region of the plasma. The temperature in the induction region of the plasma may be as high as 10000 K, in the central channel the gas kinetic temperature is probably between 5000 K and 7000 K at the mouth of the torch.

3.4.3   Sample Introduction

Most commonly, sample solution is pumped using a peristaltic pump to a nebuliser where a high velocity of argon produces a fine aerosol. Larger droplets are removed by a spray chamber, thus ensuring that only small droplets (< 6 μm) pass to the plasma.

In the central channel of the plasma, the sample is converted to a mixture of ions and atoms, residual molecular fragments and unvolatilised particles and it is accompanied by a large quantity of argon. A fuller discussion on sample introduction systems is given in section 3.5.

3.4.4   Ion Extraction and Focusing

The physical interface between the plasma and the mass spectrometer comprises two cones. The first cone, designated the sampling cone, is used to sample the ions created in the plasma. The second cone, located behind the sampler cone, provides an ion skimming function and is called the skimmer cone.

Ions first flow through a sampling orifice (approximately 1 mm diameter in a cooled cone) into a mechanically pumped vacuum system, where a supersonic jet forms.

The central section of the jet flows through the skimmer orifice, which is also approximately 1 mm in diameter, into a second vacuum chamber. A series of cylindrical ion lenses focus charged species through a differential pumping aperture, and then into the quadrupole mass filter entrance. A photon stop, placed behind the skimmer, is used to prevent photons from the ICP reaching the detector when they would cause sparious 'ion' counts.

3.4.5 Mass Analyser and Ion Detection

A typical quadrupole mass filter for ICP-MS has rods of 12-18 mm diameter and about 200 mm long. The purpose of the quadrupole mass filter is to selectively transmit ions based on their mass-to-charge ratio. The mass analyser can be scanned very rapidly ($\leq$20 ms for one sweep from m/z 1-200) or the mass transmitted can be switched repetitively from peak to peak with only a few ms required between each jump. A mass resolution of about 0.6 amu is sufficient for elemental isotopic spectra.

Ions transmitted by the quadrupole mass filter are detected by an electron multiplier assembly. The most common ion detector used in ICP-MS instruments is the channeltron electron multiplier [41]. Pulse-counting ion detection is normally employed to discriminate against gain variation and unwanted pulses. Analogue ion current measurements can also be made.

3.4.6 Data Collection

Two types of data collection mode are employed, peak hopping or jumping and scanning. In peak jumping mode, the mass spectrometer is used to collect data at a number of fixed mass positions for each isotope of interest. The peak jumping mode is normally used when only a small number of isotopes are required (<20).

An alternative mode of operation is to collect data for a relatively large number of points so that the peak shape is defined for each isotope and the area under the curve is integrated. The advantage of the scanning mode of operation is that data are available not only for the isotopes of interest, but also over a wide range for archival purposes.

3.5   SAMPLE INTRODUCTION METHODS

A variety of sample introduction techniques can be used with ICP-MS. Solution nebulisation is the most common method for sample introduction, though the transport efficiency is poor [42]. Solid samples that cannot be digested or dissolved can be addressed with techniques such as laser ablation sampling. Samples may also be introduced as gases or vapours, for example, by hydride generation.

3.5.1   Nebulisation

Three different types of nebuliser are in common use; concentric [43], cross-flow [44], and Babington [45]. The nebuliser is coupled to a spray chamber to remove the large (> 6 μm) droplets and thus most of the sample solution is lost to the drain, with only 1-2% entering the plasma. Additionally, the nebuliser gas flow causes a dilution of the sample in the argon, which is further diluted in the plasma by the plasma gas. A comprehensive review on the operation and operating characteristics of pneumatic nebulisers has been published [46].

An alternative to the pneumatic nebuliser is the ultrasonic nebuliser which is more efficient and yields better sensitivities, primarily through increased analyte transport to the plasma [47, 48]. However, ultrasonic nebulisers suffer many disadvantages such as complexity, lack of reliability and greater memory effects. A comparison of the performances of pneumatic and ultrasonic nebulisers for ICP-MS has been made [49].

Another device for solution nebulisation is the thermospray [50]. This provides high efficiency and improvements in sensitivity by a factor of 20 have been reported compared to pneumatic nebulisation [51].

Other types of nebulisers that have been utilised include: the jet-impact nebuliser [52], the glass frit nebuliser [53], the high efficiency nebuliser (HEN) [54], the hydraulic high pressure nebuliser (HHPN) [55], direct injection nebulisation (DIN) [56], the microconcentric nebuliser (MCN) [57] and the monodisperse dried microparticulate injector (MDMI) [58].

3.5.2   Direct Sample Insertion

Direct sample introduction is performed by inserting the solution directly into or close to the base of the plasma. Atomisation is achieved as the sample is carried higher up the plasma. Methods of direct liquid sample introduction have made use of graphite rods [59], tungsten wire-loops [60] and graphite cups [61]. Improved detection limits were achieved compared with those obtained with pneumatic nebulisation [62].

Direct solid sample introduction for powders has been achieved utilising various techniques such as solid sample pneumatic nebulisation, vibrating sample chamber, swirl cups and fluidised bed chambers [63].

Gas samples have also been introduced directly into the ICP, either by continuous flow or by injection through a sampling loop [64].

3.5.3   Electrothermal Vaporisation

Coupling of electrothermal vaporisation (ETV) to ICP-MS can dramatically improve sensitivity and decrease interferences [65-67]. The sample is desolvated, the matrix ashed and the analyte vaporised in the ETV unit. Atomisation and ionisation occur in

the ICP. Solid samples can be handled using a graphite rod or crucible for sample vaporisation.

Electrothermal vaporisation for sample introduction to ICP-MS offers several advantages including [68]:

- High analyte transport efficiency resulting in higher sensitivity.
- Reduced polyatomic ion interferences.
- Reduced oxide formation of the analyte, plasma gas and matrix components.
- Small volume sampling.
- Improved performance using chemical modification techniques.

3.5.4 Flow Injection (FI)

Sample introduction into the ICP-MS using the FI technique is a preferred method for solutions of high salt content, high viscosity or high acid strength [69]. These types of samples can be handled without blockage or distortion of the sample interface because the analyte is dispersed in the carrier stream resulting in decreased total loading in the plasma.

Coupling of the FI technique to ICP-MS has several desirable features [38]:

- High sampling rate.
- Minimal sample consumption (~100 µl per injection).
- Ease of automation.
- Ability to perform rapid on-line pre-treatment chemistry.
- Minimal contamination.
- Continuous monitoring of the blank.

3.5.5 Chromatographic Techniques

Coupling of chromatographic techniques to ICP-MS provides a capability for elemental speciation. Various types of chromatographic techniques have been coupled with ICP-MS such as high performance liquid chromatography, gas

chromatography and supercritical fluid chromatography. This subject will be discussed in detail in section 3.7.

3.5.6 Laser Ablation

Laser ablation for sample introduction in ICP-MS was first described by Gray [70]. A laser is focused onto the sample and ablates 50 to 100 µg of material which is then swept into the plasma. This technique is normally used for the analysis of high-purity materials, such as pure metals and semiconductors where sample treatment must be kept to an absolute minimum.

The major problem associated with laser ablation ICP-MS is that of calibration. The use of closely matrix-matched standards and samples is crucial [71].

3.5.7 Arc Nebulisation

The arc nebulisation technique has been used to vaporise solid samples, mainly conducting solids, before atomisation in the ICP. The sample acts as a cathode in an intermittent arc, and must therefore be, or be made, conductive. The eroded sample condenses into particulates which are then transported into the ICP by a stream of argon [72, 73].

3.5.8 Slurry Nebulisation

Slurries of up to 1% w/v can be nebulised into an ICP using a high solids nebuliser; the Babington type has been commonly used [74]. This approach is particularly attractive for samples that are hard to dissolve. If used in conjunction with the flow injection technique, the risk of clogging of the ICP-MS interface by solid deposition is reduced.

3.5.9 Hydride Generation

The hydride generation technique is used to produce a gaseous sample for introduction into the ICP [75-78]. The elements that have been shown to form hydrides include antimony, arsenic, bismuth, cadmium, cobalt, copper, germanium, lead, mercury, and selenium [79].

The transport efficiency of the hydrides to the plasma is nearly 100%, giving an increase in signal. Two general approaches have been used to generate volatile hydrides for introduction into the ICP, continuous and batch generation.
In the continuous hydride generation scheme, the reagents and sample plug are pumped continuously into a reaction chamber. The mixture then passes through a gas-liquid separator. The liquid passes to waste and the gaseous mixture of volatile hydrides and hydrogen are directed into the ICP.

The batch hydride generation method involves reacting an aliquot of sample solution with an aliquot of $NaBH_4$ in a syringe. The syringe needle is then inserted into the uptake tube of the ICP and the gaseous products injected directly into the plasma.

3.6 INTERFERENCES IN ICP-MS

The interferences which occur in ICP-MS can be divided into two main groups, spectroscopic and non-spectroscopic. The first type may be further subdivided into four categories: those due to isobaric overlap, polyatomic ions, refractory oxide ions and doubly charged ions. Non-spectroscopic interference, or matrix effects, may be broadly divided into suppression and enhancement effects and physical effects caused by high total dissolved solid. Evans *et al.* [29] published a comprehensive review on interferences in ICP-MS including methods for their reduction.

3.6.1 Isobaric Overlap

This type of interference is caused by overlapping isotopes of different elements. Masses may actually differ by a small amount, but this cannot be resolved by the quadrupole mass analyser. As an example, an isobaric overlap occurs between ^{58}Fe and ^{58}Ni. This overlap can be corrected by monitoring more than one isotope of the interfering species and then using the known isotopic abundances to correct the interference.

3.6.2 Polyatomic Ions

Polyatomic or adduct ions result from the short lived combination of two or more atomic species. Species present in the plasma (Ar, H and O) and major elements present in the solvents or acids used during sample preparation (N, S and Cl) may combine with each other or with elements from the analyte matrix. Polyatomic formation depends on many factors including extraction geometry, operating parameters for the plasma and nebuliser system and the nature of the acids and sample matrix [80]. The most serious interferences from polyatomic ions arise from combination of the most abundant isotopes.

Tan and Horlick [81] have listed in some detail all the possible polyatomic interfering ions. Reed *et al.* [82] tabulated the major polyatomic interferences for elements m/z 6 to m/z 76 using data obtained from a high resolution ICP-MS instrument.

3.6.3 Refractory Oxides

These species occur either as a result of incomplete dissociation of the sample matrix or from recombination in the interface region. The interfering ions occur at 16, 17, 32 or 48 mass units above the elemental peak in the form of monoxide $-MO^+$, hydroxide $-MOH^-$, dioxide $-MO_2^+$ or trioxide $-MO_3^+$ ions. The levels of oxide

species are quoted with respect to the elemental peak, MO^+/M^+. Typical levels are 1-3 %.

The formation of oxides is influenced by the plasma operating conditions including rf forward power and nebuliser gas flow rate and by conditions in the extraction interface [83, 84].

3.6.4 Doubly Charged Ions

Most of the ions produced in the ICP are single charged ions, though some multiply charged species also occur. The formation of doubly charged ions, M^{2+} in the plasma is controlled by the second ionisation energy of the element and the conditions of the plasma equilibrium [85].

The effects of formation of the doubly charged ion are a small loss of sensitivity for the singly charged ions and a number of isotopic overlaps at one half of the mass of the parent element. Nebuliser gas flow rates particularly affect the level of doubly charged ions produced. At very low flow rates, plasma temperature is increased and the equilibrium is shifted toward a higher yield of doubly charged species.

3.6.5 Matrix Effects

Some matrix elements cause an enhancement in the analyte signal, while others cause suppression by exerting an influence on sample transport, ionisation in the plasma, ion extraction or ion transmission. A high concentration of matrix elements leads to blocking of the sampling and skimmer cone orifices and therefore erratic loss of signal.

A number of methods have been used to overcome non-spectroscopic interferences including dilution of the sample [86], use of internal standards [87] and instrumental optimisation [88].

3.7 CHROMATOGRAPHY COUPLED WITH ICP-MS

ICP-MS is an excellent elemental detector and coupled with the separation power of chromatography provides speciation capability. Hill *et al.* [89] and Uden [90] have published comprehensive reviews on coupling chromatography with ICP-MS covering various applications. The benefits of coupling chromatographic separation with ICP-MS detection include element specificity, real time chromatograms, the ability to separate peaks of interest from interferences, multielement capability and low levels of detection.

Liquid chromatography (LC) is the most common separation method coupled to ICP-MS, primarily because of the physical simplicity of the interface. Gas chromatography (GC) has not found extensive use with ICP-MS because of the limited number of metal compounds with sufficient volatility and thermal stability for GC separation. Supercritical fluid chromatography (SFC) offers a complementary alternative to the traditional LC and GC methods.

3.7.1 Liquid Chromatography-ICP-MS

LC is commonly used for separating ionic, polar and non-polar compounds as well as complex ions and neutral species. Various modes of liquid chromatography, coupled to ICP-MS have been investigated including: reversed-phase [91-95], reversed-phase ion pair [96-98], ion-exchange chromatography [99-101], size-exclusion chromatography [102-105], and ion chromatography [106-108].

Interfacing LC with ICP-MS employs a transfer line that connects the outlet of the liquid chromatography column with the liquid flow inlet of the nebuliser. The transfer line is usually composed of an inert material, such as Teflon or PEEK tubing, and connections are made with conventional liquid chromatography fittings. Typically LC flow rates, on the order of 0.5 to 2 ml min^{-1}, are within the range usually required for liquid sample introduction to the plasma with traditional pneumatic nebulisation.

3.7.2 Gas Chromatography-ICP-MS

GC is used for the analysis of volatile and thermally stable compounds or for derivatives of the compounds with these same characteristics. GC is advantageous as a sample introduction method because it by-passes the nebulisation step and provides 100% transport efficiency. This leads to better detection capabilities.

Coupling GC to ICP-MS can be accomplished using a heated transfer line for connecting the column to the inner tube of the torch. The temperature of the transfer line is maintained to ensure that all compounds will remain in the gas phase.

One of the first papers to report the coupling of GC to ICP-MS was by Chong and Houk [109]. Olson *et al.* [110] have reviewed the technique in general and indicated both the advantages and the problems.

3.7.3 Supercritical Fluid Chromatography-ICP-MS

SFC is used to separate wide range of materials such as thermally labile, non-volatile and high molecular weight compounds with shorter analysis times and higher efficiency. Separation by SFC is performed with the mobile phase in the supercritical state and detection occurs whilst still in supercritical state, frequently with on line detection.

Coupling SFC to ICP-MS requires a heated transfer line. A restrictor is connected to the end of the column to maintain the supercritical condition in the column. The transfer line after the restrictor is positioned flush with the end of the torch inner tube. Interfacing of the two techniques was first reported by Shen *et. al.* [111]. In general, the operating conditions of both the SFC and ICP-MS require no modification [112].

3.8   CAPILLARY ELECTROPHORESIS COUPLED WITH ICP-MS

CE is a separation technique with the ability to separate a range of species, from small molecules and ions to large biomolecules. CE technology has advanced rapidly and in its various modes of operation the technique is fast, reliable and selective [113]. The major drawback with CE is its poor concentration sensitivity owing to the fact that sample introduction volumes in CE are very low [114].

Coupling CE with ICP-MS has the potential to provide rapid and quantitative elemental speciation information that is complementary to that provided by other separation techniques. However, the challenges for coupling CE to ICP-MS are the small sample volume and the low flow rate which limits the choice of nebuliser. The other problem is how to apply the high voltage across the capillary since the detector end is no longer in a buffer reservoir.

An efficient interface to connect the end of the CE separation capillary with the ICP is critical to the success of the coupling of these two techniques. Olesik *et al.* [115] were the first to publish their research in this area. A fused silica capillary was inserted into the centre tube of a standard Meinhard nebuliser. The end of the capillary was 0.5 mm away from the tip of the nebuliser. The capillary was coated with silver paint providing a connection between the solution at the end of the capillary to ground. The paint also ensured that the capillary fitted tightly into the centre tube of the concentric nebuliser. The problem with the silver paint was that under circumstances where a ligand was present in high concentrations in the sample, this could complex with the silver and cause contamination.

The spray chamber was specially constructed, similar to the ARL conical type, but without the impact bead. This was done to improve the sample transport efficiency. Results showed though that only about 2% of the sample aerosol reached the plasma.

Using this interface they separated iron and chromium species in 100 seconds using ICP-AES detection. The neutral iron and chromium species co-eluted, but they were

50

still detected simultaneously by the ICP-AES at two different wavelengths. Using CE-ICP-MS, Sr, Cr, As and Sn were detected, again the analysis was completed in approximately 100 seconds. The detection limits for CE-ICP-MS were 6-200 times worse than for conventional sample introduction techniques.

Barnes *et al.* [116] described an interface with the CE capillary inserted into a commercial glass concentric nebuliser. The capillary was placed inside the central glass tube of the nebuliser with the end approximately 2 cm away from the tip of the nebuliser. Another fused silica capillary was then placed around the one inside the nebuliser, this only reached as far as the glass joint of the nebuliser gas tube. Due to the arrangement of the capillaries, the distance between the two tips was adjustable from 0 mm to 18 mm. This outer tube had a make up flow of 10 mM NaCl. The liquid sheath of the make up flow provided the connection to ground.

A conical spray chamber containing an impact bead was employed. A Teflon adapter was used to connect the torch and the spray chamber outlet. Samples were introduced by air pressure produced by a piston displacement. The injection system could also generate negative pressure created by withdrawing the piston.

The samples analysed were isoforms of the metallothioeins and ferritins. The position of the capillary in the nebuliser affected the results; as the capillary was inserted further into the nebuliser, the signal intensity of the Cd was found to increase. This was because less make up flow was able to enter the nebuliser and hence the sample was less diluted. However, resolution was lost and migration time reduced as the capillary was placed further into the capillary due to increased suction inside the capillary. The reverse was found when the capillary was withdrawn from the nebuliser.

One way of overcoming the loss of resolution resulting from the ICP-MS interface was to apply a negative pressure in the inlet vial while separation was in progress. Once this was done, the resolution was found to be almost as good as with UV

detection. Detection limits for CE-ICP-MS were poorer than those for conventional ICP-MS and this was attributed to the small sample sizes used.

Lopez-Avila *et al.* [117] built an interface where the CE capillary was placed concentrically inside the central fused-silica tube of a direct injection nebuliser (DIN). A make-up liquid was pumped into the fused-silica sample transfer capillary via a connector and this served as a continuous and stable electrical contact to the grounding terminus. The make up flow could be adjusted independently of the CE system ensuring efficient sample introduction. The system was used for the speciation of selenium, arsenic, various alkali, alkali earth and heavy metals. Detection limits were found to be up to 600 times poorer than those obtained with the DIN-ICP-MS system alone, although the majority were found to be up to 15 times as poorer.

Tomlinson *et al.* [118] used a modified Meinhard nebuliser to interface CE to ICP-MS. Initial attempts were made by applying pressure to the capillary after the electrophoretic separation had taken place. This proved unsuccessful because the flow then became laminar and the resolution between peaks was lost.

Later a glass frit nebuliser was used. The capillary and grounding electrode were inserted through a stainless steel tube through which the make up flow was passed. The electrical connection to ground was made at the point of aerosol formation. Two lead compounds ($PbCl_2$ and $C_4H_9Pb(O_2CH_3)$) were resolved and detected by ICP-MS. It was found that the flow rate of the buffer solution affected the behaviour of the glass frit nebuliser. Slow flow rates caused pulsing and high background and high flow rates diluted the analyte too much.

3.9   APPLICATIONS OF ICP-MS

ICP-MS has been applied to a very wide range of sample types. Selected applications of the technique for elemental speciation are given in Table 3.1.

Table 3.1:   Selected applications of coupled chromatography-ICP-MS to elemental speciation.

Element	Species	Sample	Separation Method	Reference
As	Arsenobetaine Arsenocholine Trimethylarsine oxide Trimethylarsonium ion Dimethylarsinate Arsenite Arsenate	Tuna Fish	HPLC- Cation Exchange	119
As	DMA, MMA As(III), As(V)	SRM Urine	Micellar HPLC	120
Cr	Cr(III), Cr(IV)	SRM 1641c	LC-Ion Exchange	121
Cr	Cr(III), Cr(IV)	Aquatic Sample	IC	122
V	V(V), V(IV)	Coal Fly Ash	HPLC	123
Sn	Inorganic tin Trimethyl tin Triethyl tin Triprophyl tin Tributyl tin Triphenyl tin	Sediment, Water	LC	95
Sn	Tributyl tin Triphenyl tin	Fish Tissue	SFC	124
Se	Se(IV), Se(VI)	Test Sample	CE	117
Se	Se(IV), Se(VI)	Human Serum	SEC	101
I	Iodide, Iodate	Mineral Water	IC	125
Pb	Inorganic lead Triethyl lead Triphenyl lead Tetraethyl lead	Reference Fuel	HPLC - Ion Pair Reversed Phase	126
Hg	Hg^{2+} $MeHg^{+}$ $EtHg^{+}$ $PhHg^{+}$	SRM 2670 Urine Reference Material	HPLC - Ion Pair Reversed Phase	127
Pb	Pb^{2+} $(Me)_3Pb^{+}$ $(Et)_3Pb^{+}$			
Hg	$HgCl_2$ C_2H_2HgCl CH_3HgCl	Dogfish Muscle Reference Material	LC - Reversed Phase	128

REFERENCES

1. Babat, G. I., *J. Inst. Elect. Eng.*, 1947, **94**, 27.

2. Reed, T. B., *J. Appl. Phys.*, 1961, **32**, 821.

3. Greenfield, S., Jones, I. Ll., and Berry, C. T., *Analyst*, 1964, **89**, 713.

4. Wendt, R. H., and Fassel, V. A., *Anal. Chem.*, 1965, **37**, 920.

5. Fassel, V. A., and Kniseley, R. N., *Anal. Chem.*, 1974, **46**, 1110A.

6. Fassel, V. A., *Science*, 1978, **202**, 183.

7. Barnes, R. M., *Crit. Rev. Anal. Chem.*, 1978, **7**, 203.

8. Houk, R. S., Fassel, V. A., Flesch, G. D., Svec, H. J., Gray, A. L., and Taylor, C. E., *Anal. Chem.*, 1980, **52**, 2283.

9. Date, A. R., and Gray, A. L., *Analyst*, 1981, **106**, 1255.

10. Gray, A. L., *Anal. Proc.*, 1974, **11**, 182.

11. Gray, A. L., *Anal. Chem.*, 1975, **47**, 600.

12. Gray, A. L., *Analyst*, 1975, **100**, 289.

13. Douglas, D. J., and French, J. B., *Anal. Chem.*, 1981, **53**, 37.

14. Gray, A. L., in *Applications of Inductively Coupled Plasma-Mass Spectrometry*, Date, A. R. and Gray, A. L. (Eds.), Blackie, Glasgow, 1989, pp. 1-42.

15. Date, A. R., *Spectrochim. Acta Rev.*, 1991, **14**, 3.

16. Gray, A. L., *Spectrochim. Acta*, 1985, **40B**, 1525.

17. Gray, A. L., *Anal. Proc.*, 1994, **31**, 371.

18. Date, A. R., and Gray, A. L., *Analyst*, 1983, **108**, 159.

19. Houk, R. S., *Anal. Chem.*, 1986, **58**, A97.

20. Douglas, D. J., and Houk, R. S., *Prog. Anal. At. Spectrosc.*, 1985, **8**, 1.

21. Koppenaal, D. W., *Anal. Chem.*, 1990, **62**, 303R.

22. Koppenaal, D. W., *Anal. Chem.*, 1992, **64**, 320R.

23. Horlick, G., *J. Anal. At. Spectrom.*, 1994, **9**, 593.

24. Hieftje, G. M., and Vickers, G. H., *Anal. Chim. Acta*, 1989, **216**, 1.

25. Hieftje, G. M., Galley, P. J., Glick, M., and Hanseiman, D. S., *J. Anal. At. Spectrom.*, 1992, **7**, 69.

26. Boumans, P., *J. Anal. At. Spectrom.*, 1993, **8**, 767.

27.   Newman, A., *Anal. Chem.*, 1996, **68**, 46A.

28.   Tyler, G., *Spectroscopy Europe*, 1995, **7**, 14.

29.   Evans, E. H., and Giglio, J. J., *J. Anal. At. Spectrom.*, 1993, **8**, 1.

30.   Bacon, J. R., Ellis, A. T., McMahon, A. W., Potts, P. J., and Williams, J. G., *J. Anal. At. Spectrom.*, 1994, **9**, 267R.

31.   Bacon, J. R., Chenery, S. R. N., Ellis, A. T., Fisher, A., McMahon, A. W., Potts, P. J., and Williams, J. G., *J. Anal. At. Spectrom.*, 1995, **10**, 2537R.

32.   Jarvis, K. E., Gray, A. L., Jarvis, I., and Williams, J. G. (Eds.), *Plasma Source Mass Spectrometry*, Royal Society of Chemistry, Cambridge, 1990.

33.   Jarvis, K. E., Gray, A. L., and Houk, R. S., *Handbook of Inductively Coupled Plasma-Mass Spectrometry*, Blackie Academic and Professional, Glasgow, 1992.

34.   Holland, G., and Eaton, A. N., *Applications of Plasma Source Mass Spectrometry II*, Royal Society of Chemistry, Cambridge, 1993.

35.   Thompson, M., and Walsh, J. N., *Handbook of Inductively Coupled Plasma Spectrometry*, 2nd edn., Blackie, Glasgow, 1989, Chapter 11.

36.   Montaser, A., and Golightly, D. W. (Eds.), *Inductively Coupled Plasmas in Analytical Atomic Spectrometry*, VCH, New York, 1987, Chapter 10.

37.   Science Citation Index (SCI) Search on BIDS ISI Data Service Release 5.2.07, Bath Information and Data Services, UK.

38.   Beauchemin, D., *Trends Anal. Chem.*, 1991, **10**, 71.

39.   Greenfield, S., in *Inductively Coupled Plasmas in Analytical Atomic Spectrometry*, Montaser, A., and Golightly, D. W. (Eds.), VCH, New York, 1987, pp. 123-161.

40.   Scott, R. H., and Fassel, V. A., *Anal. Chem.*, 1974, **6**, 76.

41.   Kurz, E. A., *Am. Lab.*, 1979, **11**, 67.

42.   Browner, R. F., and Boorn, A. W., *Anal. Chem.*, 1984, **56**, 786A.

43.   Meinhard, J. E., *ICP Inf. Newsl.*, 1976, **2**, 163.

44.   Kniseley, R. H., Amenson, H., Butler, C. C., and Fassel, V. A., *Appl. Spectrosc.*, 1974, **28**, 285.

45.   Suddendorf, R. F., and Boyer, K. W., *Anal. Chem.*, 1978, **50**, 1769.

46.   Sharp, B. L., *J. Anal. At. Spectrom.*, 1988, **3**, 613.

47.   Thompson, J. J., and Houk, R. S., *Anal. Chem.*, 1986, **58**, 2541.

48.   Olson, K. W., Haas, W. J., and Fassel, V. A., *Anal. Chem.*, 1977, **49**, 632.

49.   Thompson, J. J., and Houk, R. S., *Appl. Spectrosc.*, 1987, **41**, 801.

50.   Meyer. G. A., Roeck, J. S., and Vestal, M. L., *ICP Inf. Newsl.*, 1985, **10**, 955.

51.   Thomas, C., Jakubowski, N., and Stuewer, D., *J. Anal. At. Spectrom.*, 1995, **10**, 583.

52.   Doherty, M. P., and Hieftje, G. M., *Appl. Spectrosc.*, 1984, **38**, 405.

53.   Layman, L. R., and Lichte, F. E., *Anal. Chem.*, 1982, **54**, 638.

54.   Tan, H., Meinhard, B. A., and Meinhard, J. E., *Presented at FACSS XXIX*, Philadelphia, USA, 1992.

55.   Jakubowski, N., Feldmann, I., Stuewer, D., and Berndt, H., *Spectrochim. Acta*, 1992, **47B**, 119.

56.   Wielderin, D. R., Smith, F. G., and Houk, R. S., *Anal. Chem.*, 1991, **63**, 219.

57.   Debrah, E., Beres, S. A., Gluodenis, T. J., Thomas, R. J., and Denoyer, E. R., *At. Spectrosc.*, 1995, **16**, 197.

58.   Dziewatkoski, M. P., Daniels, L. B., and Olesik, J. W., *Anal. Chem.*, 1996, **68**, 1101.

59.   Kirkbright, G. F., and Li-Xing, Z., *Analyst*, 1982, **107**, 617.

60.   Boomer, D. W., Powell, M., Sing, R. L. A., and Salin, E. D., *Anal. Chem.*, 1986, **58**, 975.

61.   Umemoto, M., and Kubota, M., *Spectrochim. Acta*, 1987, **42B**, 491.

62.   Umemoto, M., and Kubota, M., *Spectrochim. Acta*, 1989, **44B**, 713.

63.   Darke, S. A., *Ph. D. Thesis*, Loughborough University of Technology, UK, 1989.

64.   LaFreniere, B. R., Houk, R. S., Wiederin, D. R., and Fassel, V. A., *Anal. Chem.*, 1988, **60**, 23.

65.   Gregoire, D. C., *Anal. Chem.*, 1990, **62**, 141.

66.   Whittaker, P. G., Lind, T., Williams, J. G., and Gray, A. L., *Analyst*, 1989, **114**, 675.

67.   Carey, J. M., and Caruso, J. A., *Crit. Rev. Anal. Chem.*, 1992, **23**, 397.

68.   Gregoire, D. C., Lamoureux, M., Chakrabati, C. L., Al-Maawali, S., and Byrne, J. P., *J. Anal. At. Spectrom.*, 1992, **7**, 579.

69.   Dean, J. R., Ebdon, L., Crews, H. M., and Masey, R. C., *J. Anal. At. Spectrom.*, 1988, **3**, 349.

70.   Gray, A. L., *Analyst*, 1985, **110**, 551.

71.   Darke, S. A., Long, S. E., Pickford, C. J., and Tyson, J. F., *Anal. Proc.*, 1989, **26**, 159.

72.   Jiang, S. J., and Houk, R. S., *Anal. Chem.*, 1986, **58**, 1739.

73.   Jiang, S. J., and Houk, R. S., *Spectrochim. Acta*, 1987, **42B**, 93.

74.   Ebdon, L., Foulkes, M. E., Parry, H. G. M., and Tye, C. T., *J. Anal. At. Spectrom.*, 1988, **3**, 753.

75.   Heitkemper, D. A., and Caruso, J. A., *Appl. Spectrosc.*, 1990, **44**, 228.

76.   Olson, L. K., Vela, N. P., and Caruso, J. A., *Spectrochim. Acta*, 1995, **50**, 355.

77.   Wang, X., and Barnes, R. M., *J. Anal. At. Spectrom.*, 1988, **3**, 1091.

78.   Pickford, C. J., *Analyst*, 1981, **106**, 464.

79.   Carey, J. M., Byrdy, F. A., and Caruso, J. A., *J. Chromatogr. Sci.*, 1993, **31**, 330.

80.   Gray, A. L., and Williams, J. G., *J. Anal. At. Spectrom.*, 1987, **2**, 599.

81.   Tan, S. H., and Horlick, G., *Appl. Spectrosc.*, 1986, **40**, 445.

82.   Reed, N. M., Cairn, R. O., Hutton, R. C., and Takaku, Y., *J. Anal. At. Spectrom.*, 1994, **9**, 881.

83.   Horlick, G., Tan, S. H., Vaughan, M. A., Rose, C.A., *Spectrochim. Acta*, 1985, **40B**, 1555.

84.   Gray, A. L., and Williams, J. G., *J. Anal. At. Spectrom.*, 1987, **2**, 81.

85.   Jarvis, K. E., Gray, A. L., and McCurdy, E., *J. Anal. At. Spectrom.*, 1989, **4**, 743.

86.   Ridout, P. S., Jones, H. R., and Williams, J. G., *Analyst*, 1988, **113**, 1383.

87.   Thompson, J. J., and Houk, R. S., *Appl. Spectrosc.*, 1987, **41**, 801.

88.   Wang, J., Shen, W. L., Sheppard, B. S., Evans, E. H., Caruso, J. A., *J. Anal. At. Spectrom.*, 1990, **5**, 445.

89.   Hill, S. J., Bloxham, M. J., and Worsfold, P. J., *J. Anal. At. Spectrom.*, 1993, **8**, 499.

90.   · Uden, P. C., *J. Chromatogr.*, 1995, **703**, 393.

91. Bushee, D. S., *Analyst*, 1988, **113**, 1167.

92. Al-Rashdan, A., Heitkemper, D., and Caruso, J. A., *J. Chromatogr.*, 1991, **29**, 98.

93. Huang, C., and Jiang, S., *J. Anal. At. Spectrom.*, 1993, **8**, 681.

94. Beauchemin, D., Bednas, M. E., Berman, S. S., McLaren, J. W., Siu, K. W. M., and Sturgeon, R. E., *Anal. Chem.*, 1988, **60**, 2209.

95. Yang, H. J., Jiang, S. J., Yang, Y. J., and Hwang, C. J., *Anal. Chim. Acta*, 1995, **312**, 141.

96. Thomas, P., and Sniatecki, K., *Fresenius J. Anal. Chem.*, 1995, **351**, 410.

97. Yang, K. L., and Jiang, S. J., *Anal. Chim. Acta*, 1995, **307**, 109.

98. Suyani, H., Creed, J., Davidson, T., and Caruso, J. A., *J. Chromatogr. Sci.*, 1989, **27**, 139.

99. Byrdy, F. A., Olson, L. K., Vela, N. P., and Caruso, J. A., *J. Chromatogr.*, 1995, **712**, 311.

100. Garsiaalonso, J. I., Sanzmedel, A., and Ebdon, L., *Anal. Chim. Acta*, 1993, **238**, 261.

101. Shum, S. C. K., and Houk, R. S., *Anal. Chem.*, 1993, **65**, 2972.

102. Owen, L. M. W., Crews, H. M., Massey, R. C., and Bishop, N. J., *Analyst*, 1995, **120**, 705.

103. Rottmann, L., and Heumann, K. G., *Anal. Chem.*, 1994, **66**, 3709.

104. Mason, A. Z., Storms, S. D., and Jenkins, K. D., *Anal. Biochem.*, 1990, **186**, 187.

105. Crews, H. M., Dean, J. R., Ebdon, L., and Massey, R. C., *Analyst*, 1989, **114**, 895.

106. Feldmann, J., *Anal. Comm.*, 1996, **33**, 11.

107. Pantsarkallio, M., and Manninen, P. K. G., *Anal. Chim. Acta*, 1996, **318**, 335.

108. Thompson, J. J., and Houk, R. S., *Anal. Chem.*, 1986, **58**, 2541.

109. Chong, N. S., and Houk, R. S., *Appl. Spectrosc.*, 1987, **41**, 66.

110. Olson, L. K., Heitkemper, D. T., and Caruso, J. A., *ACS Symp. Ser.*, 1992, **479**, 288.

111.   Shen, W., Vela, N. P., Sheppard, B. S., and Caruso, J. A., *Anal. Chem.*, 1991, **63**, 1491.

112.   Carey, J. M., and Caruso, J. A., *Trends Anal. Chem.*, 1992, **11**, 287.

113.   Engelhardt, H., Beck, W., Kohr, J., and Schmitt, T., *Angew. Chem.*, 1993, **32**, 629.

114.   Camilleri, P., Brown, R., and Okafo, G., *Chem. Br.*, 1992, **28**, 800.

115.   Olesik, J. W., Kinzer, J. A. and Olesik, S. V., *Anal. Chem.*, 1995, **67**, 1.

116.   Barnes, R. M., Lu, Q. and Bird, S. M., *Anal. Chem*, 1995, **67**, 2949.

117.   Lopez-Avila, V., Liu, Y., Zhu, J. J., Wiederin, D., and Becket, W. F., *Anal. Chem*, 1995, **67**, 2020.

118.   Tomlinson, M. J., Lin, L., and Caruso, J. A., *Analyst*, 1995, **120**, 583.

119.   Larsen, E. H., Pritzi, G., and Hansen, S. H., *J. Anal. At. Spectrom.*, 1993, **8**, 1075.

120.   Ding, H., Wang, J. S., Dorsey, J. G., and Caruso, J. A., *J. Chromatogr.*, 1995, **694**, 425.

121.   Tomlinson, M. J., and Caruso, J. A., *Anal. Chim. Acta*, 1996, **322**, 1.

122.   Pantsarkallio, M., and Manninen, P. K. G., *Anal. Chim. Acta*, 1996, **318**, 335.

123.   Wang, J. S., Tomlinson, M. J., and Caruso, J. A., *J. Anal. At. Spectrom.*, 1995, **10**, 601.

124.   Kumar, U. T., Vela, N. P., Dorsey, J. G., and Caruso, J. A., *J. Chromatogr.*, 1993, **655**, 340.

125.   Heumann, K. G., Rottmann, L., and Vogl, J., *J. Anal. At. Spectrom.*, 1994, **9**, 1351.

126.   Al-Rashdan, A., Vela, N. P., Caruso, J. A., and Heitkemper, D. T., *J. Anal. At. Spectrom.*, 1992, **7**, 551.

127.   Shum, S. C. K., Pang, H. M., and Houk, R. S., *Anal. Chem.*, 1992, **64**, 2444.

128.   Huang, C. W., and Jiang, S. J., *J. Anal. At. Spectrom.*, 1993, **8**, 681.

Chapter 4

CHAPTER FOUR

ELECTROSPRAY/ION SPRAY IONISATION-MASS SPECTROMETRY

4.1   INTRODUCTION TO CHAPTER

This chapter deals with the historical perspective of electrospray/ion spray ionisation-mass spectrometry, the ionisation processes, instrumentation and selected applications of the technique.

4.2   HISTORICAL PERSPECTIVE

The electrospray phenomenon is a process of disintegration of a liquid surface in the presence of a strong electric field to produce a spray of fine and highly charged droplets.   Since it was first reported by Zeleny [1, 2] more than 70 years ago, electrospray has found wide applications in electrostatic painting, fuel atomisation in combustion systems, rocket propulsion, crop spraying and electrospray ionisation.   In the late 1960's, Dole *et al.* [3, 4] used electrospray ionisation to produce gas-phase macro-ions.   However, because a mass spectrometer was not available, only ion retardation or ion mobility measurements were feasible.

Yamashita and Fenn [5] first described combined electrospray ionisation-mass spectrometry. They replaced the retarding grid Faraday cage assembly used in Dole's work with a quadrupole mass spectrometer.   Negative ion mode electrospray ionisation-mass spectrometry was also demonstrated [6].   Nearly simultaneously, Aleksandrov *et al.* [7] reported the successful interfacing of an electrospray ion source to a magnetic sector mass spectrometer. They also demonstrated on-line combination of liquid chromatography with electrospray ionisation-mass spectrometry and its application to various oligosaccharides and polypeptides [8, 9].

Subsequently several workers have initiated new developments in electrospray ionisation-mass spectrometry with the introduction of more efficient ionisation sources suitable for quadrupole mass spectrometry [10, 11]. Henion *et al.* [12-14] used a coaxial flow of nitrogen to facilitate spraying, thus effecting a lower optimum polarising voltage or a higher maximum operable flow rate than electrospray. This technique has been given the name *ion spray*.

4.3   THE IONISATION PROCESS

The electrospray/ion spray technique allows ions to be transferred from a solution to the gas phase at atmospheric pressure in the presence of a strong electric field. There are three major processes in electrospray ion production [15]: the production of charged droplets from electrolyte, solvent evaporation and repeated droplet disintegrations and gas-phase ion production.

Electrospray is generally produced by application of a high electric field to a small flow of liquid, 0.01-10 μl min^{-1}, from a capillary tube. A voltage of 2-5 kV is applied to the capillary, which is typically 0.1 mm i.d. and 0.2 mm o.d. and located 1-3 cm from a larger planar counter electrode.

Because the capillary tip is very narrow, the electric field in the air at the capillary tip is high, ~ 10^6 V m^{-1}. The high electric field results in disruption of the liquid surface and formation of highly charged liquid droplets. Positively or negatively charged droplets can be produced depending upon the capillary bias. The negative ion mode requires the presence of an electron scavenger, such as oxygen, to inhibit electrical discharge.

In the electrospray technique, the used of an electric field for nebulisation leads to some practical restrictions on the range of liquid conductivity [16], dielectric constant [17] and surface tension [18]. A fluid with higher surface tension requires a higher threshold voltage for stable electrospray production. Conductivity and dielectric

constant are also important in that they influence charge transport to the aerosol. Although high surface tension, low conductivity solvents, such as pure water, can be sprayed by appropriate capillary tip geometry [19] or raising the capillary voltage [20], the onset of corona discharge sets an upper limit. Henion and co-workers [12-14] employed a concentric double-walled capillary in which the inner tube carries the solution while the outer tube is used for the nitrogen nebulising gas. This ion spray technique is very much more tolerant of solvent properties and liquid flow rates and allows the stable production of ions at lower capillary voltages than would otherwise possible.

The formation of ions requires conditions that produce evaporation of the initial droplet population. This can be accomplished at higher pressures by a flow of dry gas at moderate temperatures (~60 °C), by heating during transport through the interface, and by energetic collisions at relatively low pressure. Two mechanisms have been proposed for ion formation from the charged droplets; droplet fission at the Rayleigh limit [21] and direct field evaporation of ions [22].

For large droplets (r > 1 μm), the droplets shrink by evaporation of solvent molecules until they come close to the Rayleigh limit. The droplets become unstable and undergo fission into smaller droplets until the electric field at the droplet surface is sufficient for ion evaporation. Later Kebarle and co-workers [16] supported the idea of ion evaporation which they also referred to as electrophoretic ionisation.

4.4   ELECTROSPRAY/ION SPRAY IONISATION-MASS SPECTROMETRY

The coupling of electrospray/ion spray ionisation to mass spectrometry is one of the most widely utilised and fastest growing mass spectrometric techniques. A recent review by Hofstadler *et al.* [23] described in detail the instrumentation and spectral interpretation of the technique.

Electrospray/ion spray devices are also used to couple separation techniques, including CE [24-27] and HPLC [28-30] to mass spectrometry. Direct coupling of the separation technique and the ionisation technique is accomplished in a number of ways including the addition of a conductive sheath liquid or the application of an electrically conductive coating to the terminus of the separation capillary.

An electrospray interface with a sample uptake rate of 10 µl min^{-1}, for coupling micro-bore HPLC to ICP- AES, has been reported [31].

4.5 APPLICATIONS OF ELECTROSPRAY/ION SPRAY IONISATION-MASS SPECTROMETRY

Electrospray/ion spray ionisation-mass spectrometry has been routinely used for the characterisation of macromolecules, particularly important classes of biomolecules [32-34] such as peptides, proteins and nucleic acids. Additionally, electrospray/ion spray ionisation-mass spectrometry provides an inherently 'soft' ionisation that has been shown to produced intact ions from thermally labile biological molecules and even biologically relevant noncovalent complexes [35, 36].

Speciation studies utilising electrospray/ion spray ionisation-mass spectrometry for the determination of inorganic species [37], inorganic complexes [38], metalloporphyrins [39], anticancer drugs [40], phosphopeptides [41] and pesticides [42] have been reported.

Agnes *et al.* [43-46] showed the applicability of electrospray/ion spray ionisation-mass spectrometry for the elemental speciation of chlorine, iodine, sulphur, iron and organometallic compounds. Agnes and Horlick [47] have shown that electrospray/ion spray ionisation-mass spectrometry can also provide information about valence state, molecular form and composition of the solvation sphere (i.e. ligands and counter-ions) for both cations and anions.

63

Comparative studies on the use of electrospray/ion spray ionisation and ICP sources for MS were reported by Caruso *et al.* [48]. Both qualitative and quantitative aspects of electrospray/ion spray ionisation and ICP sources were investigated for the determination of Rb, Cs, V, Cr, Ni, Co, Cu, Zn, Ba and Cu. The results showed that electrospray/ion spray ionisation-mass spectrometry detection limits were 2-3 orders of magnitude poorer than those found using the ICP source.

REFERENCES

1. Zeleny, J., *Phys. Rev.*, 1917, **10**, 1.

2. Zeleny, J., *Phys. Rev.*, 1920, **16**, 102.

3. Dole, M., Mack, L. L., Hines, R. L., Mobley, R. C., Ferguson, L. D., and Alice, M. B., *J. Chem. Phys.*, 1968, **49**, 2240.

4. Mack, L. L., Kralik, P., Rheude, A., and Dole, M., *J. Chem. Phys.*, 1970, **52**, 4977.

5. Yamashita, M., and Fenn, J. B., *J. Chem. Phys.*, 1984, **88**, 4451.

6. Yamashita, M., and Fenn, J. B., *J. Chem. Phys.*, 1984, **88**, 4671.

7. Aleksandrov, M. L., Gall, L. N., Krasnov, V. N., Nikolaev, V. I., Pavenko, V. A., Shkurov, V. A., Baram, G. I., Gracher, M. A., Knorre, V. D., and Kusner, Y. S., *Bioorg. Khim.*, 1984, **10**, 710.

8. Aleksandrov, M. L., Baram, G. I., Gall, L. N., Krasnov, V. N., Kusner, Y. S., Mirgorodskaya, O. A., Nikolaev, V. I., and Shkurov, V. A., *Bioorg. Khim.*, 1985, **11**, 700.

9. Aleksandrov, M. L., Besuklandnikov, P. V., Grachev, M. A., Elyakova, L. A., Zyyaginsteva, T. N., Kondratsev, V. M., and Kusner, Y. S., *Bioorg. Khim.*, 1986, **12**, 1689.

10. Fenn, J. B., Mann, M., Meng, C. K., Wong, S. F., and Whitehouse, C. M., *Science*, 1989, **246**, 46.

11. Smith, R. D., Loo, J. A., Orgozalek-Loo, R. R., Busman, M., and Udseth, H. R., *Mass Spectrom. Rev.*, 1991, **10**, 359.

12. Bruins, A. P., Covey, T. R., and Henion, J. D., *Anal. Chem.*, 1987, **59**, 2642.

13. Covey, T. R., Bonner, R. F., Shushan, B. I., and Henion, J. D., *Rapid Commun. Mass Spectrom.*, 1988, **2**, 249.

14. Huang, E. C., and Henion, J. D., *J. Am. Soc. Mass Spectrom.*, 1990, **1**, 158.

15. Kebarle, P., and Tang, L., *Anal. Chem.*, 1993, **65**, 972A.

16. Tang, L., and Kebarle, P., *Anal. Chem.*, 1991, **63**, 2709.

17. Drozin, V. G., *J. Colloid Sci.*, 1955, **10**, 158.

18. Smith, D. P. H., *IEEE Trans. Ind. Appl.*, 1986, **IA-22**, 527.

19. Chowdhury, S. K., and Chait, B. T., *Anal. Chem.*, 1991, **63**, 1660.

20. Ikonomou, M. G., Blades, A. T., and Kebarle, P., *Anal. Chem.*, 1990, **62**, 957.

21. Rayleigh, J. W. S., *Philos. Mag.*, 1882, **14**, 184.

22. Muller, E. W., *Phys. Rev.*, 1956, **102**, 618.

23. Hofstadler, S. A., Bakhtiar, R., and Smith, R. D., *J. Chem. Edu.*, 1996, **73**, A82.

24. Smith, R. D., Loo, J. A., Barinaga, C. J., Edmonds, C. G., and Udseth, H. R., *J. Chromatogr.*, 1989, **480**, 211.

25. Smith, R. D., Barinaga, C. J., and Udseth, H. R., *Anal. Chem.*, 1988, **60**, 1948.

26. Smith, R. D., Loo, J. A., Edmonds, C. G., Barinaga, C. J., and Udseth, H. R., *J. Chromatogr.*, 1990, **516**, 157.

27. Thompson, T. J., Foret, F., Vourus, P., and Karger, B. L., *Anal. Chem.*, 1993, **65**, 900.

28. Whitehouse, C. M., Dreyer, R. N., Yamashita, M., and Fenn, J. B., *Anal. Chem.*, 1985, **57**, 675.

29. Siu, K. W. M., Geuvremont, R., Le Blanc, J. C. Y., Gardner, G. J., and Berman, S. S., *J. Chromatogr.*, 1991, **554**, 27.

30. Bruins, A. P., *J. Chromatogr.*, 1991, **554**, 39.

31. Gotz, R., Elgersma, J. W., Kraak, J. C., and Poppe, H., *Spectrochim. Acta*, 1994, **49B**, 761.

32. Smith, R. D., Loo, J. A., Edmonds, C. G., Barinaga, C. J., and Udseth, H. R., *Anal. Chem.*, 1990, **62**, 882.

33. Burlingame, A. L., Baillie, T. A., and Russel, D. H., *Anal. Chem.*, 1992, **64**, 467.

34. Przybylski, M., and Glocker, M. O., *Angew. Chem.*, 1996, **35**, 806.

35. Ganem, B., Li, Y. T., and Henion, J. D., *J. Am. Chem. Soc.*, 1991, **113**, 6294.

36. Schwartz, B. L., Light-Wahl, K. J., and Smith, R. D., *J. Amer. Soc. Mass Spectrom.*, 1994, **5**, 201.

37. Siu, K. W. M., Gardner, G. J., and Berman, S. S., *Anal. Chem.*, 1989, **61**, 2320.

38. Blades, A. T., Jayaweera, P., Ikonomou, M. G., and Kebarle, P., *J. Phys. Chem.*, 1990, **10**, 5900.

39. Van Berkel, G. J., McLuckey, S. A., and Glish, G. L., *Anal. Chem.*, 1992, **64**, 1586.

40. Poon, G. K., Bisset, G. M. F., and Mistry, P., *J. Amer. Soc. Mass Spectrom.*, 1993, **4**, 588.

41. Huddlestone, M. J., Annan, R. S., Bean, M. F., and Carr, S. A., *J. Amer. Soc. Mass Spectrom.*, 1993, **4**, 710.

42. Lin, H. Y., and Voyksner, R. D., *Anal. Chem.*, 1993, **65**, 451.

43. Agnes, G. R., and Horlick, G., *Appl. Spectrosc.*, 1992, **46**, 401.

44. Agnes, G. R., and Horlick, G., *Appl. Spectrosc.*, 1994, **48**, 649.

45. Agnes, G. R., and Horlick, G., *Appl. Spectrosc.*, 1994, **48**, 655.

46. Agnes, G. R., Steward, I. I., and Horlick, G., *Appl. Spectrosc.*, 1994, **48**, 1347.

47. Agnes, G. R., and Horlick, G., *Appl. Spectrosc.*, 1995, **49**, 324.

48. Brown, F. B., Olson, L. K., and Caruso, J. A. *J. Anal. At. Spectrom.*, 1996, **11**, 633.

Chapter 5

CHAPTER FIVE

HUMIC SUBSTANCES

5.1   INTRODUCTION TO CHAPTER

This chapter discusses the origin and chemistry of humic substances, humic substances in natural waters, their analysis and characterisation and their complexation with metals.

5.2   THE ORIGINS AND CHEMISTRY OF HUMIC SUBSTANCES

Humic substances are the dark coloured acidic material widely present in soils and natural waters. Humic substances form when living matter, especially plants, die and decay. Many are formed in soil and eventually find their way into lakes, rivers and streams. Others are formed directly within aquatic systems, for example in ocean waters.

Humic substances contain three major fractions and other minor components. Humic acid is the component which is soluble in bases, but precipitates from solution below pH 2. Fulvic acid is the component which is soluble in both acids and bases. Humin is the fraction that is not soluble at any pH value [1]. Generally, fulvic acids are more water soluble because they contain more carboxylic and hydroxyl functional groups and are lower in molecular weight [2].

Humic substances contain a wide variety of aromatic and aliphatic structures bearing many oxygen-containing functional groups, with atomic masses ranging from a few hundred to thousands of Daltons. The major functional groups include carboxylic acids, phenolic and alcoholic hydroxyl groups, and ketonic functional groups [3]. A full structure elucidation of humic substances has not been achieved although various

68

model structures have been proposed by researchers such as Fuchs, Schnitzer, Dragunov, Kleinhempel and Lignin [4]. Since there is a wide variety of possible precursors, molecules of humic substances from different sources need not be chemically and structurally identical. A suggested classification is in term of molecular weight [5].

5.3 HUMIC SUBSTANCES IN NATURAL WATER

The forms found in natural water are called aquatic humic substances. They constitute 40 to 60 percent of dissolved organic carbon and are the largest fraction of natural organic matter in water. The concentrations of aquatic humic substances are low, ranging from 10 mg l^{-1} in certain inland waters to less than 0.5 mg l^{-1} in oceanic waters [6].

Some water-borne humic substances are simply leachate from the land, so they have their origins in soil humification processes and have similar properties. However, other aquatic humics are derived from decomposition of aquatic plants. Marine humics are generated from material released by phytoplankton, small free floating micro organisms [7].

Humic substances in natural water are composed of both fulvic and humic acids. Typically, 90% of the dissolved humic substances in natural waters consist of fulvic acids and the remaining 10% of humic acids [8].

Humic substances possess ion-exchange and complexing properties and are associated with most constituents of water, including toxic elements and organic micropollutants. They act as a vehicle for the transportation of these materials [9].

5.4 ANALYSIS AND CHARACTERISATION OF HUMIC SUBSTANCES

5.4.1 Isolation of Humic Substances

Before humic substances can be thoroughly characterised, they must be isolated from other organic compounds and background inorganic species and then be concentrated. The final product should be free from chemical impurities and should be in a form that can resist biological and chemical degradation.

The isolation and concentration of humic substances begins by separating the sample into the dissolved and particulate fractions. Filtration through a 0.45 μm filter using silver, glass fibre or cellulose acetate membranes is the accepted method [10].

Samples of naturally occurring organic matter are subject to both biological and chemical degradation. It is imperative to filter the samples immediately to remove organisms such as bacteria. Biological activity can be further suppressed by the addition of a biocide to the filtered sample. Adjustment of sample pH is another effective measure to minimise biological degradation. Biological degradation can also be greatly retarded by chilling the sample with ice or by refrigeration. Humic substances can also degrade chemically. Preservation techniques such as UV irradiation or storage at high temperature should be avoided because of chemical alteration.

Numerous concentration and isolation methods are available such as coprecipitation, electrodialysis, liquid extraction, freeze concentration, reverse osmosis, ultrafiltration and sorption methods employing alumina or charcoal, ion exchange or non-ionic macro porous sorbents [1].

Coprecipitation can remove up to 95% of dissolved organic matter, but the technique is a slow and tedious for large volumes of water. Sorption using charcoal is much simpler, however, humic substances cannot be eluted efficiently from charcoal. Isolation on non-ionic macro porous resins such as Amberlite XAD is generally

considered to be the best method of isolation [11]. The XAD resins adsorb and desorb humic substances efficiently.

5.4.2 Fractionation and Characterisation of Humic Substances

Fractionation is the subdividing of humic substances according to some property related to their composition. One reason for carrying out a fractionation is to determine the range of variation found for properties such as molecular weight, functional group content or elemental composition. This information can also be used as a fingerprint for humic material from a particular source. A second reason is that the measurement of many chemical or physical parameters is made difficult if the molecules being studied exhibit a wide range for the particular property being measured. Fractionation procedures have been used as a preliminary step to spectral measurements, elemental analyses and functional group analyses.

5.4.3 Elemental Analysis

Humic substances comprise mainly carbon, hydrogen, oxygen, nitrogen, sulphur, phosphorus and halogens. Elemental composition falls within certain ranges, depending on the source of the sample, and the isolation and fractionation procedure as shown in Table 5.1.

Table 5.1:   Elemental composition of aquatic humic substances [4].

Elements	Humic/%	Fulvic/%
C	53.8 - 58.7	40.7 - 50.6
H	3.2 - 6.2	3.8 - 7.0
O	32.8 - 38.3	39.7 - 49.8
N	0.8 - 4.3	0.9 - 3.3
S	0.1 - 1.5	0.1 - 3.6

For humic substances it is not the absolute percentage of element present that is important. Elemental ratios of H/C, O/C and N/C are more useful in identifying types of humic substances and for devising structural formulae.

5.4.4   Functional Group Determination

Numerous methods for the analysis of functional groups in humic substances have been published [12]. These include direct, indirect and continuous titrations, indirect titration coupled with distillation or ultrafiltration steps and thermometric titration methods. The two most frequently used tests are the barium hydroxide total acidity determination and the calcium acetate exchange method for the determination of carboxyl groups.

5.4.5   Determination of Molecular Weight

Various methods for determining the molecular weights of humic substances based on colligative properties such as lowering of vapour pressure, depression of freezing point, elevation of boiling point and osmometry have been used. However, there are problems associated with determining the molecular weights of mixtures in that the usual methods yield an average molecular weight.

Methods which attempt to fractionate, whilst determining molecular weight have been widely applied. These include ultracentrifugation, ultrafiltration, gel permeation chromatography, high performance size exclusion chromatography (HPSEC) and small angle X-ray scattering.

There are no definitive values for the molecular weights of humic substances. The ranges, from compilations of data by various methods, are; fulvic acid: 500 to 2000 Daltons, and humic acid: 2000 to 5000 Daltons, and sometimes much higher up to 100000 Daltons [2].

5.4.5.1   Ultracentrifugation

Two types of ultracentrifugation method are used to determine molecular weight, equilibrium ultracentrifugation and sedimentation velocity ultracentrifugation. Wilkinson *et al.* [13] used sedimentation velocity ultracentrifugation for the determination of the molecular weight of humic substances from natural waters.

5.4.5.2   Ultrafiltration

Macromolecules are separated by filtration under an applied hydrostatic pressure through a polymeric membrane. The membranes used have a variety of pore sizes with nominal molecular cut-off values ranging from 50 to 100000 Daltons with numerous filters within the range.

Under hydrostatic pressure, solute molecules within the cut-off range of the membrane pass, along with the solvent, through the micropores of the membrane. Large solutes are retained and concentrated. Various problems arise, the membrane does not provide a perfect cut-off and the separation is non-uniform. It has also been observed that humic substances interact with the membrane leading to a sorption effect which can interfere with the filtration process. In addition, the filtration process depends on both the pressure and concentration gradient [14].

5.4.5.3   Gel Permeation Chromatography

Gel permeation chromatography (GPC) utilises a synthetic gel matrix of cross-linked polymers which have pores of uniform size. The method is based on the fact that different sized molecules travel through the matrix at different rates which are proportional to the size of the molecule.

Most studies on humic substances have employed Sephadex gels and an aqueous solvent. However, Swift and Posner reported interaction of humics with Sephadex, due to both electrostatic and adsorption effects [15]. Another problem with GPC is

that humic substances form aggregates in solution as a function of pH and ionic strength, therefore, making the humic substances behave in a non-ideal fashion [16].

However, although many problems concerning adsorption phenomena and inter- and intramolecular solute interactions remain to be solved , the technique is well accepted and used because of it simplicity [17-20].

5.4.5.4   High Performance Size Exclusion Chromatography

The use of high performance size exclusion chromatography (HPSEC) techniques in the study of humic substances has been widely reported [21-25].

Recently, Chin *et al.* [25] found that HPSEC could be used to measure reliably the molecular weights of humic and fulvic acids. The molecular weights for a large number of aquatic humic substances measured by HPSEC were compared with published values determined by vapour pressure osmometry, ultracentrifugation and field flow fractionation. The results obtained were in relatively good agreement with previously reported values.

Other chromatographic methods used for the study of humic substances include thin layer chromatography [26], ion-exchange chromatography [27] and gas chromatography [28].

5.4.6   Spectroscopic Methods

5.4.6.1   IR Spectroscopy

The striking feature of IR spectra obtained from humic substances is their overall simplicity consisting of relatively few bands that are very broad [1]. This simplicity is more apparent than real. Humic substances comprise a complex mixture, each type of functional group therefore exists in a wide diversity of chemical environments. As a result, there is severe overlapping of absorption bands from the individual

constituents. Stevenson [29] reported differences in the IR spectra of humic substances derived from different sources.

5.4.6.2 NMR Spectroscopy

NMR spectroscopy has been used for the characterisation of humic substances and provides functional group analysis, elemental composition and structural information as a whole [30-33]. The analysis can be carried out using either solid-state or solubilised samples. The advantages of solid-state NMR spectroscopy are that the whole untreated sample can be analysed directly and needs only a few hours to record the spectrum.

5.4.6.3 UV/VIS Spectroscopy

The UV/VIS spectra of humic substances are generally featureless with the absorption increasing towards lower wavelengths [34].

The ratio of absorbance at two different wavelengths is of value in comparing humic substances from various sources. Chen *et al.* [35] discussed the relationship between the E_4/E_6 ratio, the ratio of absorbance at 465 nm and 665 nm, and molecular weight. The higher the ratio, the lower the molecular weight. Others have proposed the E_2/E_3 ratio (ratio of absorbance at 250 nm to that at 365 nm) because of the low absorbance at 665 nm [36].

5.4.6.4 Fluorescence Spectroscopy

Humic substances are known to fluoresce and in order to fluoresce, they must first absorb some UV/VIS radiation [37]. However, only a small fraction of the molecules that absorb radiation undergo fluorescence. Since humic substances are comprised of a multicomponent mixture, it is likely that the fluorescence spectra represent a small fraction of the molecular moieties.

Although the fluorescent structures appear to constitute a minor component of the humic macro-molecule, the variety and the dependence of the spectra on several molecular and environmental parameters make them particularly useful for obtaining information about the general nature and chemistry of humics [38]. Attempts have also been made to differentiate between humics from different environments based on fluorescence spectra [39].

5.4.6.5   Mass Spectrometry

Mass spectrometry, especially when coupled with separation techniques, gives assurance of correct compound identification [40]. Structural characterisation of humic substances by GC-MS indicated that aquatic humic substances contain both aromatic and aliphatic components. The aromatic rings contain mainly 3-6 alkyl substituents, polynuclear aromatic and fused ring structures are also present. Aliphatic components are relatively short chains (2-4 methylene units) and branched structures [3].

5.4.7   Separation of Humic Substances by CE

Application of CE to characterisation of humic substances is possible because of their ionic nature. The high separation efficiency and resolution of CE allows the production of electropherograms that are characteristic of humic substances with shorter migration times compared to liquid chromatography. Several studies have been reported on the use of CE for humic substances utilising UV detection.

Rigol *et al.* [41] used CE for the separation of commercial humic acids from Fluka, Aldrich and Janssen. The electropherograms obtained showed two fractions and were similar for different humic acids. A linear relationship between the signals and the concentration of humic acids was observed.

Characterisation of humic substances using CE for samples from difference sources and locations with various types of buffer solutions and ranges of pH has been

demonstrated [42]. Ciavatta *et al.* [43] characterised humic acid fractions of different molecular weight using the CE technique. In all cases, the main peak in the CE profile appeared in progressively shorter times as the molecular size of the humic fractions decreased.

Finger-print characterisation of humic and fulvic acids of different origin was investigated using CE [44]. The electropherograms of the humic and fulvic acids exhibited characteristic, individual patterns depending on their origin.

Other electrophoretic techniques used for characterising humic substances include: polyacrylamide gel electrophoresis [45], gradient gel electrophoresis [46], isotachophoresis [47] and isoelectric focusing [48].

5.5   COMPLEXATION OF METALS BY HUMIC SUBSTANCES

An important property of humic substances is their ability to form complexes with metal ions, minerals and organics, including toxic pollutants, to form water-soluble and water-insoluble associations of widely differing chemical and biological stabilities [49]. Ionisable groups, particularly carboxylic -COOH and phenolic -OH, found in humic and fulvic acids are responsible for the ion binding. Environmentally significant interactions occur with protons and cationic forms of alkaline earth, transition and heavy metals, and radionuclides [50].

Study of the binding of metal ions by humic substances normally involves the understanding of the strength of binding constants, stability constants and the type of binding sites. Several review papers on the interaction of metal ions with humic substances have been published [51-56].

For the complex-formation reaction between metal ion (M) and organic ligand (A);

$$aM + bA \rightleftharpoons M_aA_b \qquad (5.1)$$
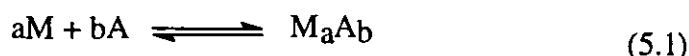
The stability constant, K is given by;

$$K = \frac{[M_aA_b]}{[M]^a[A]^b}$$

(5.2)

where [M], [A] and [MA] are the concentrations, a and b are the coefficients of the reaction and the charges of the species have been omitted. The stability constant is determined by measuring the concentration of the metal ion, ligand and the ligand-metal ion complex [57].

Due to the many structural variations, the acidic functional groups in humic substances constitute a vast collection of proton- or metal-binding sites that have relatively broad distributions of complex stability constants.

Other factors that affect the stability constant of metal-humic complex include the source, the isolation procedure, concentration, temperature and pH of the solution.

Gamble and Schnitzer [58] postulated that there are two types of reactions involved in metal-humic interaction. The first reaction involves metal displacing a hydrogen from a phenolic group that is adjacent to a carboxylic group in a salicylate ligand. The other type of reaction involves only carboxylic groups in a phthalate ligand. Figure 5.1 shows the two possible reactions of metal with humic substances.

Various models have been used to explain the interactions of metal ions with humic substances including a discrete ligand model and a continuous distribution model. The discrete ligand model [59-61] applies for single metal ion complexes with one site type on the humic molecule. Theoretically, the metal complexation site type may be a free site, a site already occupied by a proton or a site already occupied by a metal.
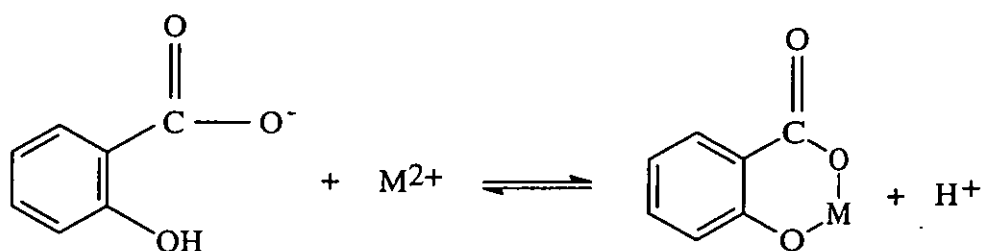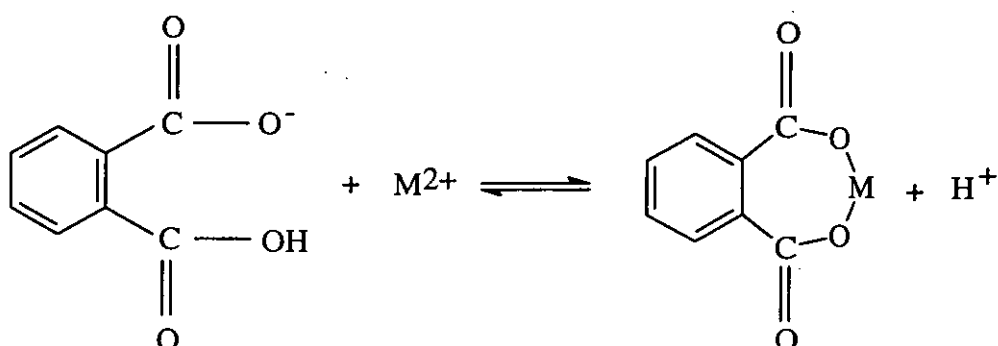
Figure 5.1:   Chelation reactions of metal-humic substances (a) Salicylate ligand and
(b) Phthalate ligand.

In the continuous distribution model [4], humic substances act as heterogeneous mixtures and contain a variety of sites in a large number of environments, each with a particular affinity for metal ions. It is assumed that a large number of different sites are involved and that these can be described by a continuous distribution of stability constants.

A variety of methods are employed to measure the extent of complexation of humic substances with metals and they can be classified as non-separation and separation techniques. Non-separation techniques include: potentiometric titration [62], UV/VIS spectrometry [63], ion-selective electrodes [64], anodic stripping voltammetry [65], ion-exchange [66] and fluorescence spectrometry [67].

Separation techniques used include: ion chromatography, reversed-phase chromatography, size-exclusion chromatography in combination with atomic absorption spectrometry [68-70] or radioanalytical techniques [71].

CE, with on-column UV detection, has also been used to study metal-humic interaction [72]. Humic and fulvic acids were titrated with Fe(III) and Cu(II) cations, as an increasing amount of these cations was added, flocculation of the metal-humic complexes occurred. The complexes were characterised as to total carbon content (TOC) and molecular weight by gel permeation chromatography and average electrophoretic mobility by CE. The extent of flocculation correlated with both TOC and quantitative CE measurements.

Gardner *et al.* [73] investigated the interaction of Mg and Ca with organic matter in natural water using high performance liquid chromatography (HPLC) with a gel filtration column coupled to ICP-AES detection.

Rottmann and Heumann [74] determined the interaction between heavy metals and different fractions of dissolved organic matter in natural aquatic systems. HPLC with a size exclusion column, coupled to ICP-MS was used. Direct coupling was applied and on-line isotope dilution mass spectrometry was performed to quantify the heavy metal accurately. Different distribution patterns for heavy metals were observed depending on the type of aquatic system.

Metal-humic complex formation can affect the behaviour of metals in the environment by altering their mobility within soils and sediments, or in aquatic systems, or by changing their availability for uptake by plant roots. Humic and fulvic acids may complex with metal pollutants and thereby affect their transport mechanism, toxicity, bioavailability and the effectiveness of recovery and clean-up procedures [75].

REFERENCES

1. Aiken, G. R., McKnight, D. M., Wershaw, R. L., and MacCarthy, P., *Humic Substances in Soil, Sediment and Water*, John Wiley, New York, 1985.

2. Thurman, E. M., *Organic Geochemistry of Natural Waters*, Martinus Nijhoff, Dordrecht, 1985.

3. Liao, W., Christman, R. F., Johnson, J. D., Millington, D. S., and Hass, J. R., *Environ. Sci. Technol.*, 1982, **16**, 403.

4. Buffle, J., *Complexation Reactions in Aquatic Syatems: An Analytical Approach*, John Wiley, New York, 1988.

5. Josephson, J., *Environ. Sci. Technol.*, 1982, **16**, 20A.

6. Gillam, A. H., and Riley, J. P., *Anal. Chim. Acta*, 1982, **141**, 287.

7. Harvey, G. R., Boran, D. A., Chesal, L. A., and Tokar, J. M., *Mar. Chem.*, 1983, **12**, 119.

8. Suffet, I. H., and MacCarthy, P., *Aquatic Humic Substances*, American Chemical Society, Washington, 1989.

9. Schnitzer, M., and Khan, S. V., *Humic Substances in the Environmental*, Marcel Dekker, New York, 1972.

10. Danielson, L. G., *Water Res.*, 1982, **16**, 179.

11. Thurman, E. M., and Malcolm, R. L., *Environ. Sci. Technol.*, 1981, **15**, 463.

12. Stevenson, F. J., and Butler, J. H. A., *Organic Geochemistry*, Eglington, G., and Murphy, M. T. J. (Eds.), Springer-Verlag, New York, 1969.

13. Wilkinson, A. E., Hesketh, N., Higgo, J. J. W., Tipping, E., and Jones, M. N., *J. Coll. Surf.*, 1993, **73**, 19.

14. Cross, R. A., and Strathmann, H., *Introduction to Separation Science*, John Wiley, New York, 1973.

15. Swift, R. S., and Posner, A. M., *J. Soil Sci.*, 1971, **22**, 237.

16. Wershaw, R. L., and Pinckney, D. J., *J. US Geol. Surv.*, 1973, **1**, 361.

17. Plechanov, N., *Org. Geochem.*, 1983, **5**, 143.

18. Kolesnikov, M. P., *Sov. Soil Sci.*, 1978, **10**, 174.

19. Goh, K. M., and Williams, M. R., *J. Soil Sci.*, 1979, **30**, 747.

20. Dawson, H. J., Hrutfiord, B. F., Zasoski, R. J., and Ugolini, F. C., *Soil Sci.*, 1981, **132**, 191.

21. Mori, S., Hiraide, M., and Mizuike, A., *Anal. Chim. Acta*, 1987, **193**, 231.

22. Morrison, A. R., Park, J. S., and Sharp, B. L., *Analyst*, 1990, **115**, 1429.

23. Warwick, P., Hall, A., and Patterson, M., *Radiochim. Acta*, 1992, **58/59**, 137.

24. Mile, C. J., and Brezonik, P. L., *J. Chromatogr.*, 1983, **259**, 499.

25. Chin, Y. P., Alken, G., and O'Loughlin, E., *Environ. Sci. Technol.*, 1994, **28**, 1853.

26. Kastelan-Macan, M., Cerjan-Stefanovic, S., and Jalsovec, D., *Wat. Sci. Tech.*, 1992, **26**, 2567.

27. Zhou, J. L., and Banks, C. J., *Environ. Technol.*, 1990, **11**, 1147.

28. Garcia, C., Hernandez, T., Costa, F., Ceccanti, B., and Calcinai, M., *Sci. Tot. Environ.*, 1992, **119**, 157.

29. Stevenson, F. J., *Humus Chemistry: Genesis, Composition, Reactions*, Wiley-Interscience, New York, 1982.

30. Wilson, M. A., Jones, A. J., and Williamson, B., *Nature*, 1978, **276**, 487.

31. Hatcher, P. G., Rowan, R., and Mattingly, M. A., *Org. Geochem.*, 1980, **2**, 77.

32. Hatcher, P. G., Breger, I. A., Dennis, L. W., and Maciel, G. E., in *Aquatic and Terrestrial Humic Materials*, Christman, R. F., and Gjessing, E. T. (Eds.), Ann Arbor Sci. Publ., Michigan, 1983, pp. 37-81.

33. Thorn, K., Rice, J., Wershaw, R., and MacCarthy, P., *Sci. Tot. Environ.*, 1987, **62**, 185.

34. Robert, P. V., *Sci. Tot. Environ.*, 1987, **62**, 27.

35. Chen, Y., Senesi, N., and Schnitzer, M., *Soil Sci. Soc. Am. J.*, 1977, **40**, 682.

36. De Haan, H., in *Aquatic and Terrestrial Humic Materials*, Christman, R. F., and Gjessing, E. T. (Eds.), Ann Arbor Sci. Publ., Michigan, 1983, pp. 165-182.

37. Schnitzer, M., in *Soil Biochemistry*, McLaren, A. D., and Skujins, J. (Eds.), Marcel Dekker, New York, 1971.

38. Senesi, N., Teodoro, M. M., Maria, R. P., and Brunetti, G., *J. Soil Sci.*, 1991, **152**, 259.

39. Visser, S. A., in *Aquatic and Terrestrial Humic Materials*, Christman, R. F., and Gjessing, E. T. (Eds.), Ann Arbor Sci. Publ., Michigan, 1983, pp. 183-202.

40. Swift, R. S., Leonard, R. L., Newman, R. H., and Theng, B. K. G., *Sci. Tot. Environ.*, 1992, **117/118**, 53.

41. Rigol, A., Lopez-Sanchez, J. F., and Rauret, G., *J. Chromatogr.*, 1994, **664**, 301.

42. Garrison, A. W., Schmitt, P. and Kettrup, A., *Wat. Res.*, 1995, **29**, 2149.

43. Ciavatta, C., Govi, M., Sitti, L., and Gessa, C., *Commun. Soil Sci. Plant Anal.*, 1995, **26**, 3305.

44. Pompe, S., Heise, K., and Nitsche, H., *J. Chromatogr.*, 1996, **723**, 215.

45. Trubetskoj, O. A., Trubetskaya, O. E., and Khomutora, T. E., *Soil Biol. Biochem.*, 1992, **24**, 893.

46. Baxter, R. M., and Malysz, J., *Chemospere*, 1992, **24**, 1745.

47. Kopacek, K., Kaniansky, D., and Hejzlar, J., *J. Chromatogr.*, 1991, **545**, 461.

48. de Nobili, M., *J. Soil Sci.*, 1988, **39**, 437.

49. Rainville, D. P., and Weber, J. H., *Can. J. Chem.*, 1982, **60**, 1.

50. Gamble, D. S., Underdown, A. W., and Langford, C. H., *Anal. Chem.*, 1980, **52**, 1901.

51. Fish, W., Dzombak, D. A., and Morel, F. M. M., *Environ. Sci. Technol.*, 1986, **20**, 676.

52. Perdue, E. M., MacCarthy, P., Gamble, D. S., and Smith, G. C., in *Humic Substances: Volume 3 - Interactions with Metals, Minerals, and Organic Chemicals*, Swift, R., Hayes, M., MacCarthy, P., and Malcolm, R. (Eds.), Wiley, Chichester, 1988.

53. Sposito, G., *CRC Crit. Rev. Environ. Control*, 1986, **16**, 193.

54. Cabaniss, S. E., Shuman, M. S., and Collins, B. J., in *Complexation of Trace Metals in Natural Waters*, Kramer, C. J. M., and Juinker, J. C. (Eds.), Junk, The Hague, 1984.

55. Livens, F. R., *Environ. Pollut.*, 1991, **70**, 183.

56. Langford, C. H., *ACS Symposium Series*, 1994, **565**, 404.

57. Lerman, A., and Childs, C. W., in *Trace Metals and Metal-Organic Interactions in Natural Waters*, Singer, P. C. (Ed.), Ann Arbor Sci. Publ., Michigan, 1973, pp. 201-235.

58. Gamble, D. S., and Schnitzer, M., in *Trace Metals and Metal-Organic Interactions in Natural Waters*, Singer, P. C. (Ed.), Ann Arbor Sci. Publ., Michigan, 1973, pp. 265-302.

59. Buffle, J., Greter, F. L., and Haerdi, W., *Anal. Chem.*, 1977, **49**, 216.

60. Perdue, E. M., and Lytle, C. R., in *Aquatic and Terrestrial Humic Materials*, Christman, R. F., and Gjessing, E. T. (Eds.), Ann Arbor Sci. Publ., Michigan, 1983, pp. 295-313.

61. Sposito, G., Bingham, F. T., Yadav, S. S., and Inouye, C. A., *Soil Sci. Soc. Am. J.*, 1982, **46**, 51.

62. Stevenson, F. J., and Chen, Y., *Soil Sci. Soc. Am. J.*, 1991, **55**, 1586.

63. Tuschall, J. R., and Brezonik, P. L., *Anal. Chim. Acta*, 1983, **149**, 47.

64. Town, R. M., and Powell, H. K. J., *Anal. Chim. Acta*, 1993, **279**, 221.

65. Powel, H. K. J., and Town, R. M., *Anal. Chim. Acta*, 1991, **248**, 95.

66. Tao, Z. Y., and Gao, H. X., *Radiochimica Acta*, 1994, **65**, 121.

67. Susetyo, W., Carreira, L. A., Azarraga, L. V., and Grimm, M. D., *Fresenius J. Anal. Chem.*, 1991, **339**, 624.

68. Burba, P., and Willmer, P. G., *Fresenius J. Anal. Chem.*, 1992, **342**, 167.

69. Truitt, R. E., and Weber, J. H., *Anal. Chem.*, 1981, **53**, 337.

70. Hiraide, M., Arima, Y., and Mizuike, A., *Anal. Chim. Acta*, 1987, **200**, 171.

71. Warwick, P., and Hall, T., *Analyst*, 1992, **117**, 151.

72. Schmitt, P., Kettrup, A., Freitag, D., and Garrison, A. W., *Fresenius J. Anal. Chem.*, 1996, **354**, 915.

73. Gardner, W. S., Landrum, P. F., and Yates, D. A., *Anal. Chem.*, 1982, **54**, 1196.

74. Rottmann, L., and Heumann, K. G., *Anal. Chem.*, 1994, **66**, 3709.

75. Patterson, J. W. and Passino, R., *Metals Speciation, Separation and Recovery*, Lewis, Chelsea, 1987.

Chapter 6

CHAPTER SIX

SEPARATION OF HUMIC ACID BY CAPILLARY ELECTROPHORESIS

6.1   INTRODUCTION TO CHAPTER

This chapter discusses preliminary experiments aimed at optimising the conditions for the separation and characterisation of humic acid using CE with UV detection. The humic acid samples used were from commercial humic acid and from surface water samples. The reaction of humic acid with metals, particularly nickel, was also investigated.

6.2   EXPERIMENTAL

6.2.1   Instrumentation

The experiments were performed using a HPE 100 High-Performance Capillary Electrophoresis System (Bio-Rad Labs, Herts, UK). The power supply was capable of supplying up to 12 kV at current levels of 100 μA. It also had the capability to switch the polarity from positive to negative. The fused silica capillaries used were enclosed in cartridges and coated on their internal surfaces with a covalently bonded linear polymer, significantly reducing both adsorption and EOF. The capillaries used had 50 μm i.d. and 35 cm total length.

In the HPE 100 unit, a grating monochromator is used to select wavelengths from a deuterium lamp and light is directed through a window in the cartridge that houses the capillary. The built-in variable-wavelength UV detector has a micro focusing lens system that eliminates the problem of light loss and baseline drift. Microprocessor control of load times, run times, detector parameters and power supply variations are controlled from a touch panel. Chemically resistant reservoirs are provided for

buffers and electrode contacts. A needle valve directs flow through the capillary for flushing and filling. For these experiments, electropherograms were recorded using a Bio-Rad Econo-Recorder (Model 1325, Bio-Rad Labs, Herts, UK).

The operating conditions used throughout the CE experimentation, unless otherwise stated, are summarised in Table 6.1.

Table 6.1:   Standard CE experimental conditions.

Parameter		Condition
Capillary	:	Coated fused silica (50 μm x 35 cm)
Separation voltage	:	10 kV
Polarity	:	Negative (at the injection end)
Sample introduction	:	Electrokinetic, 20 s at 10 kV
Detection wavelength	:	254 nm
Buffer solution	:	0.30 M borate with polymer modifier, pH 8.5

6.2.2 Chemicals

A solution of 15 mg l^{-1} humic acid was prepared from stock solution of 200 mg l^{-1} humic acid. Stock solution was prepared by dissolving 0.20 g humic acid (Fluka, Gillingham, Dorset, UK) in 1 ml 0.20 M sodium hydroxide (A.R., Fisons, Loughborough, UK) and diluting to 1 litre with deionised water (Liquipure, Bichester, UK).

A natural water sample was collected from a small isolated clough in the Derbyshire Peak District and filtered through a 0.45 μm filter membrane (Gelman Sciences, Northampton, UK). The filtered water was then rotary evaporated at 33 °C to increase the concentration up to 4 times [1].

Spiked samples of humic acid and the water sample were prepared by adding maleic acid (A.R., Fisons, Loughborough, UK) to a final concentration of 1×10^{-3} M.

For preconditioning of the capillary surface, rinsing with 0.10 M sodium hydroxide solution (HPCE grade, Fluka, Gillingham, Dorset, UK) and then with buffer solution was employed. The buffer solutions used are describe in Section 6.3.1. The buffer was chosen because its means of preconditioning would be mechanical; that is, it has no chemical effect on the capillary wall, but would rinse away any particulate matter and fill the capillary with fresh buffer. Sodium hydroxide was chosen for its ability to remove the older silica and expose a fresh surface. Rinsing with 0.10 M sodium hydroxide and buffer solution was employed for every new experiment and rinsing with buffer solution only was employed for every measurement.

6.3 OPTIMISATION OF THE CAPILLARY ELECTROPHORESIS SEPARATION

6.3.1 Buffer Solutions and pH

A solution of 15 mg l^{-1} humic acid was used for the CE separation using various buffer solutions and pHs. Other CE parameters were as given in Table 6.1. The buffer solutions used in this experiment were readily available in our laboratory. All buffer solutions were used as received without any modification or dilution. Seven different buffer solutions with different pHs were investigated:

(a)   0.10 M phosphate with polymer modifier, pH 2.5 (Bio-Rad Labs, Herts, UK)

(b)   0.20 M borate, 0.10 M phosphate, pH 4.1 (Bio-Rad Labs, Herts, UK)

(c)   0.20 M borate, pH 6.0 (Bio-Rad Labs, Herts, UK)

(d)   0.02 M phosphate, pH 7.0 (Fluka, Gillingham, Dorset, UK)

(e)   0.30 M borate with polymer modifier, pH 8.5 (Bio-Rad Labs, Herts. UK)

(f)   0.02 M borate, 20 mM phosphate, 150 mM SDS, pH 9.0 (Bio-Rad, Herts, UK)

(g)   0.10 M borate, pH 10.0 (Fisons, Loughborough, UK)

During CE separation, the electrophoretic mobility of the humic acid was toward the detector and the EOF of the buffer was toward the inlet reservoir. Changes in pH of the buffer solution will change the EOF which directly affected the migration times of separated components. Separations with phosphate buffer solutions of pH 2.5, 4.1 and 7.0 show shorter migration times because lower pH may essentially reduced the EOF. At lower pH, hydrogen ions could neutralise anions at the capillary surface and hence lower the zeta potential. A buffer solution of pH 9.0 increased the EOF and thus gave longer migration times. Separation of humic acid with borate buffer at pH 10.0 was only suitable for lower separation voltage since a high voltage induced a high current.

Borate buffer with a concentration of 0.30 M at pH 8.5 produced a better separation for 15 mg l^{-1} humic acid compared to other buffer solutions investigated. Figure 6.1 shows the electropherogram of 15 mg l^{-1} humic acid separated using this buffer with a polymer modifier. Electrophoretic separation of humic acid produced two peaks; a sharp peak with migration time at 4.30 min followed by a broad peak at 7.18 min.

The chemical composition of the buffer, as well as its pH, probably had some influence on these electropherograms because there could be chemical interactions between the buffer chemicals and the humic acid. The addition of modifier into the buffer system could also decrease the EOF by binding to the capillary wall, hence shielding the surface charge. It also increases the viscosity of the solution.

6.3.2 Separation Voltage

Separation voltages ranging from 4 to 12 kV were investigated for the separation of humic acid by CE. Other experimental conditions were set as in Table 6.1.

Electropherograms of humic acid for separation voltages of 4, 6, 8, 10 and 12 kV using 0.30 M borate buffer with polymer modifier, pH 8.5, are shown in Figure 6.2. Generally, the separation patterns were identical, but the migration times for different voltages were changed. The highest voltage resulted in the shortest separation time
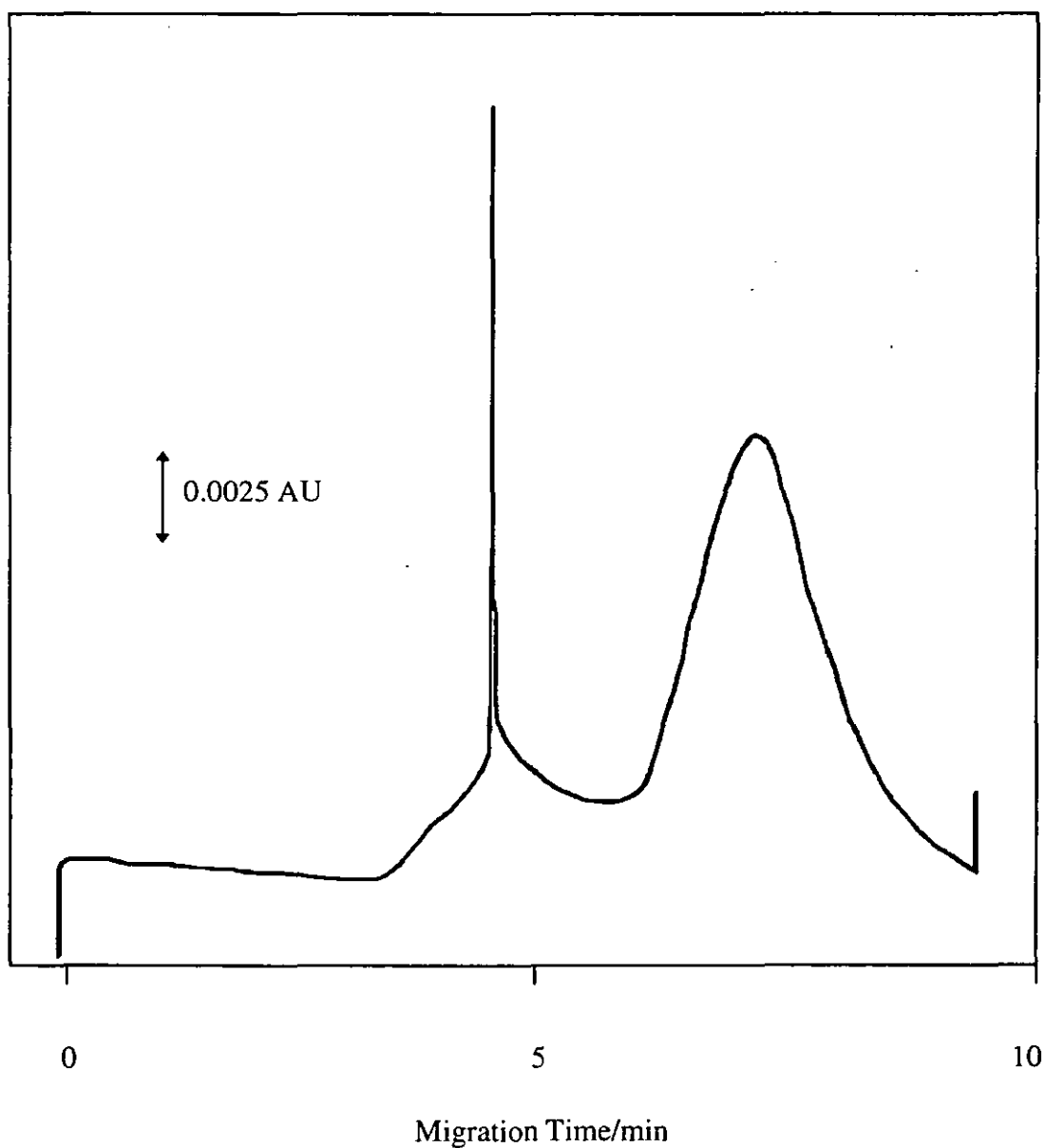
Figure 6.1:   Typical electropherogram of 15 mg l^{-1} humic acid.   Separation
conditions: 0.30 M borate buffer with polymer modifier, pH 8.5, 10 kV
separation voltage, 20 s electrokinetic sample injection, 254 nm
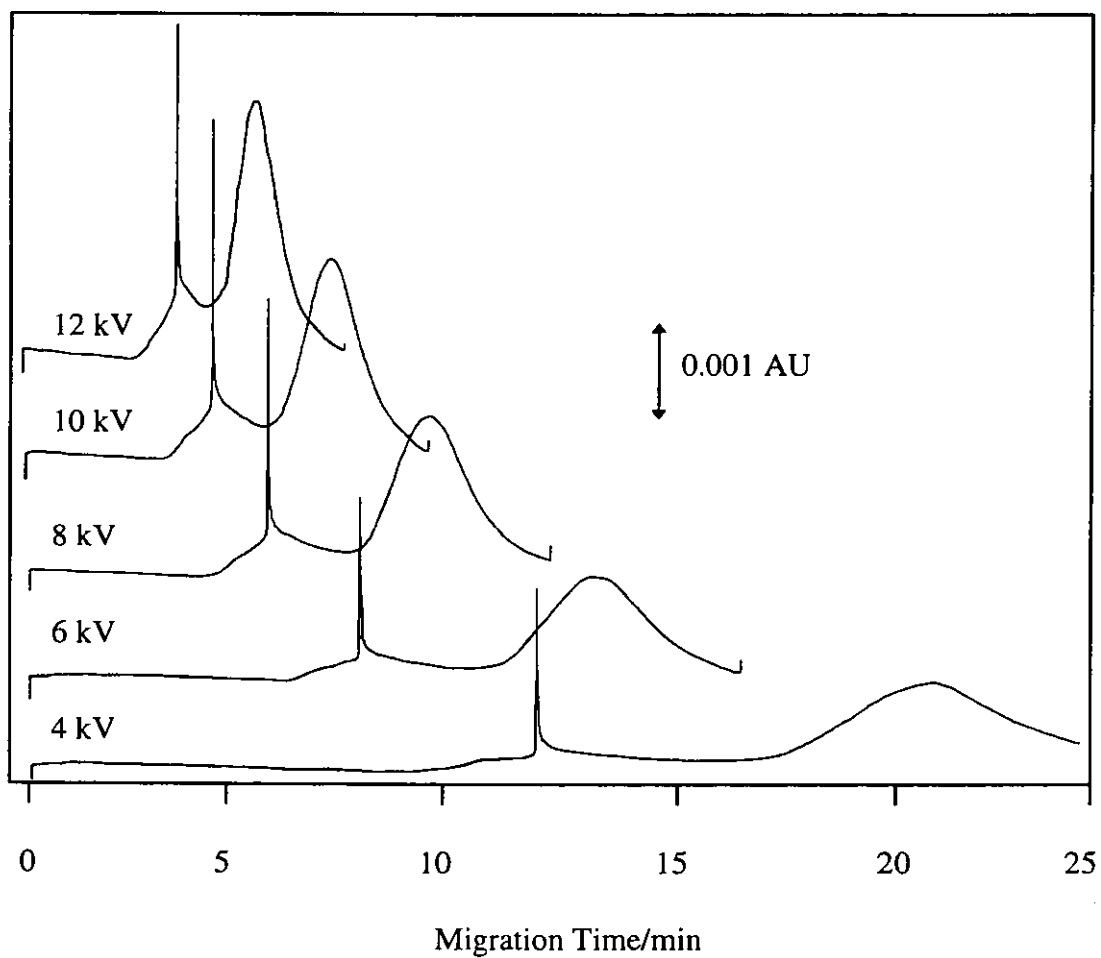detection wavelength and 50 μm x 35 cm capillary.

Figure 6.2: Electropherograms of humic acid for various separation voltages; (a) 4 kV, (b) 6 kV, (c) 8 kV, (d) 10 kV and (e) 12 kV. Separation conditions: 0.30 M borate buffer with polymer modifier, pH 8.5, 20 s electrokinetic sample injection, 254 nm detection wavelength and 50 µm x 35 cm capillary.

which in turn produced the highest separation efficiency as shown in Table 6.2. The number of theoretical plate, N calculated is based on the second eluting peak. The small N values, obtained because the peak corresponded to the humic acid polymeric mixture of different molecular weights. It was also observed that a linear relationship was obtained for peak heights versus separation voltages with a correlation coefficient better than 0.98.

Table 6.2:   Field strengths, migration times, peak heights and N values for various separation voltages.

Voltage/ kV	Field Strength/ $V\,cm^{-1}$	Migration Time/ min	Peak Height/ mm	N
4.0	114	21.28	19.00	113
6.0	171	13.41	24.00	118
8.0	228	9.39	37.00	122
10.0	285	7.18	47.00	126
12.0	342	5.40	60.00	133

6.3.3   Sample Injection Time

15 mg l^{-1} humic acid solutions were loaded electrokinetically for 8, 12, 16, 20, 24, 28, and 32 s at 10 kV injection voltage. Other experimental conditions were set as Table 6.1.

Injection times have little effect on the electrophoretic separation of humic acid as shown in Figure 6.3. The zone migration times were almost constant for the various injection times applied as shown in Table 6.3. An increase in peak height was observed as injection times increased. Longer injection times mean that more sample entered the capillary and thus larger signals and lower limits of detection.
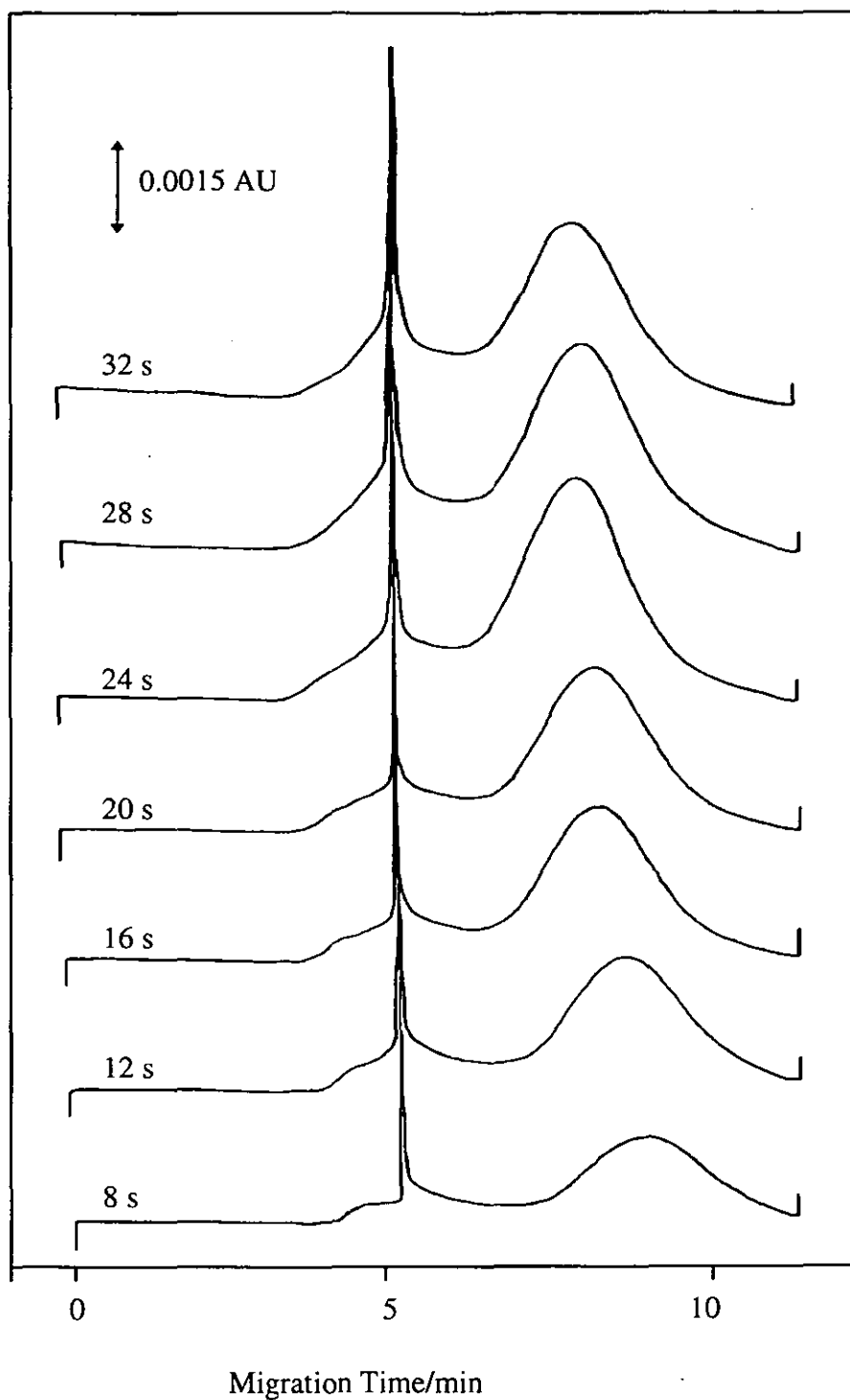
Figure 6.3:   Electropherograms of humic acid for various injection times; (a) 8 s, (b) 12 s, (c) 16 s, (d) 20 s, (e) 24 s, (f) 28 s and (g) 32 s.   Separation conditions: 0.30 M borate buffer with polymer modifier pH 8.5, 10 kV separation voltage, 254 nm detection wavelength and 50 μm x 35 cm capillary.

Table 6.3: Migration times and peak heights for various injection times.

Injection Time/s	Migration Time/min	Peak Height/mm
8.0	8.42	15.00
12.0	8.27	25.00
16.0	8.07	30.00
20.0	8.00	33.00
24.0	7.55	43.00
28.0	7.56	40.00
32.0	7.55	34.00

6.3.4 Detection Wavelength

The UV absorption spectrum of 15 mg l^{-1} humic acid was measured using a UV/VIS spectrometer (Unicam 8700 Series, ATI Unicam, Cambridge, UK). The UV spectrum at wavelengths from 200 to 380 nm is shown in Figure 6.4. Humic acid possess no maximum absorption at any wavelength in the UV spectrum.

Separation of the humic acid by CE with measurement at wavelengths of 200, 230, 254 and 280 nm was investigated. Other experimental conditions were set as in Table 6.1. The separation at the wavelengths of 200, 230, 254 and 280 nm exhibited, as expected, similar electropherograms as shown in Figure 6.5. The different in migration time observed with 200 nm detection is reproducible and not expected. More work needed to explain this phenomenon. Detection at the wavelength of 200 nm also showed absorption by low molecular weight inorganic compounds, but this was not observed for detection at the higher wavelengths.
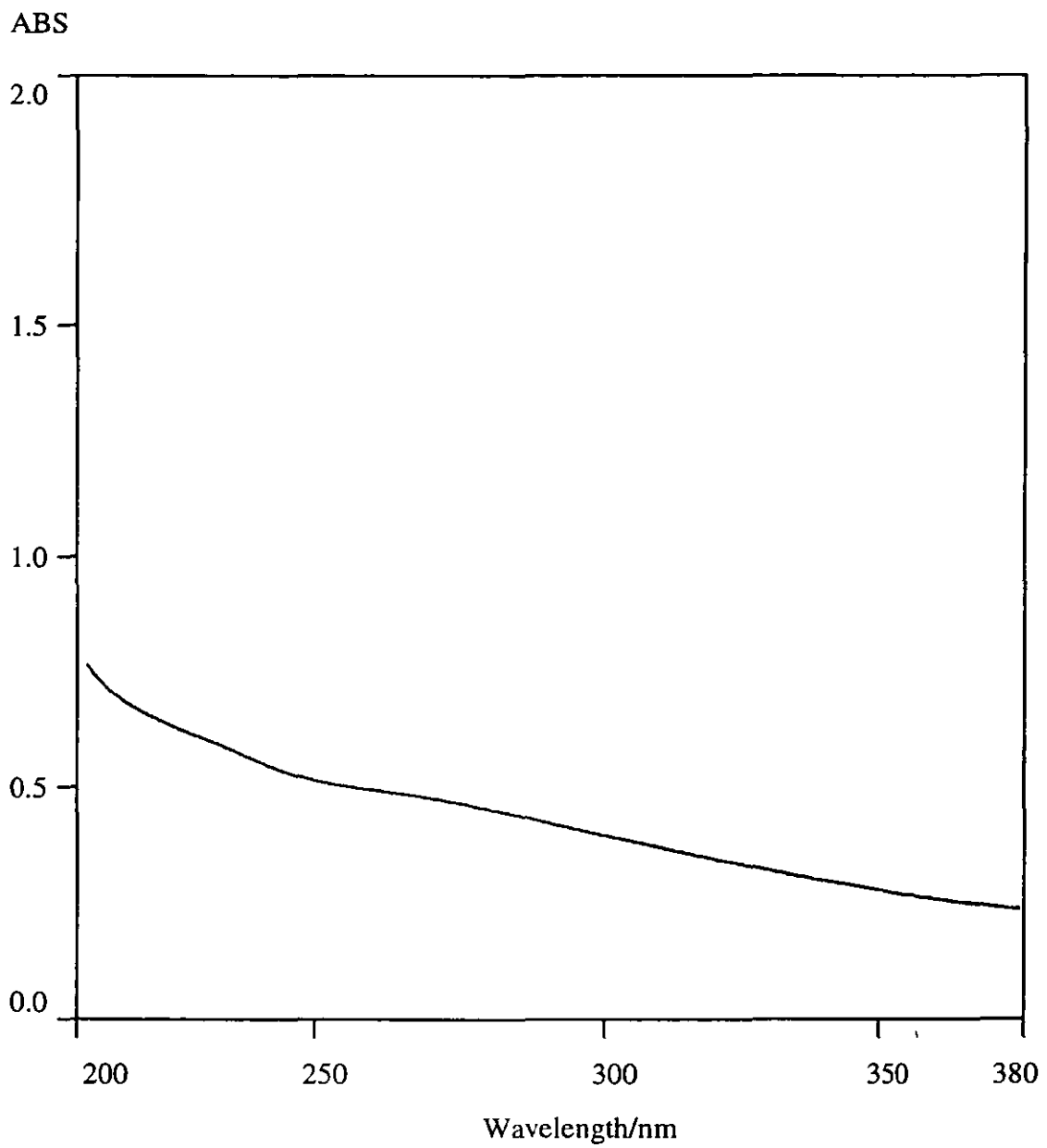
Figure 6.4: UV spectrum of 15 mg l^{-1} humic acid (supplied by Fluka).
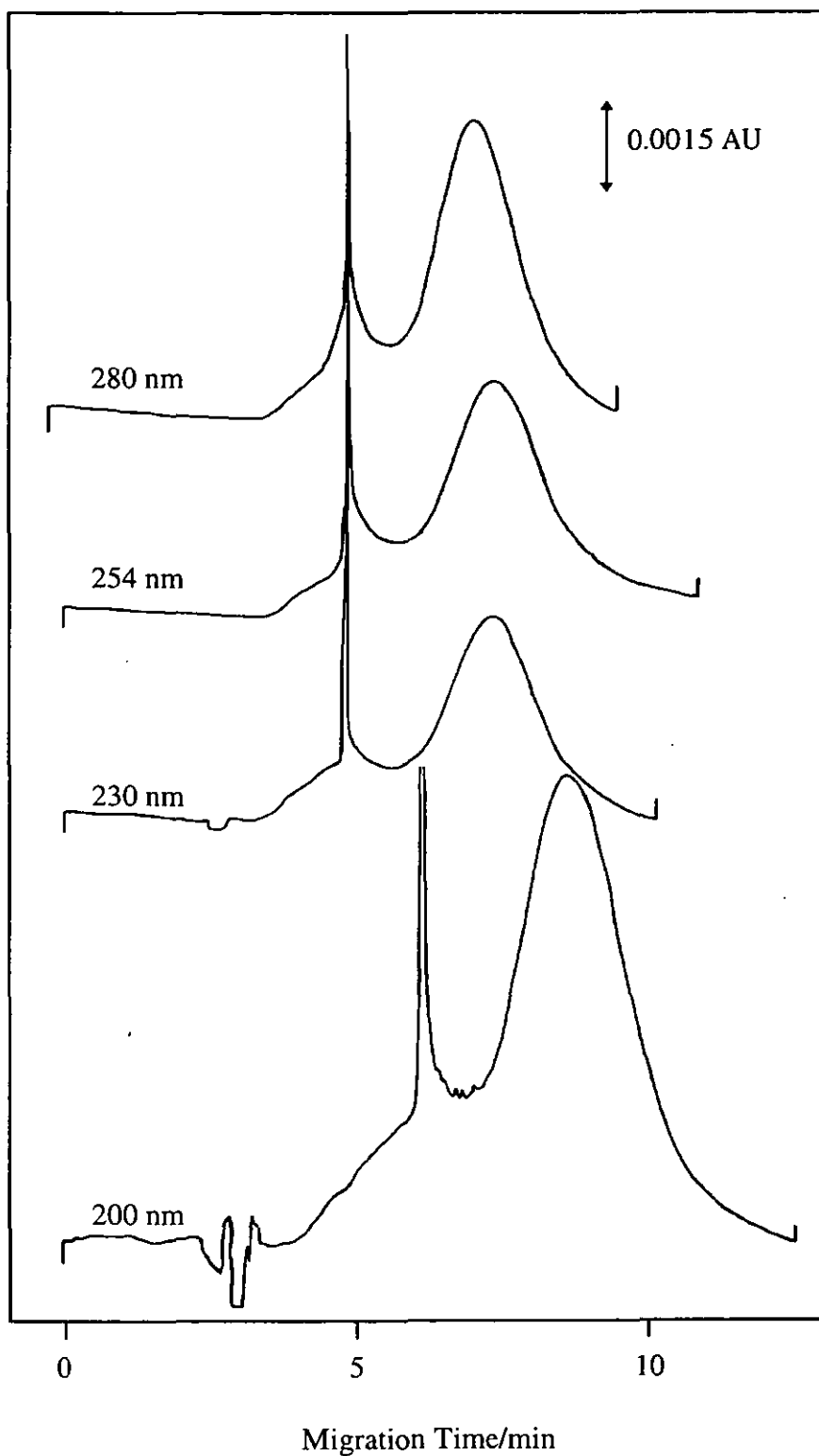
Figure 6.5: Electropherograms of humic acid at different detection wavelengths; (a) 200 nm, (b) 230 nm, (c) 254 nm and (d) 280 nm. Separation conditions: 0.30 M borate buffer with polymer modifier, pH 8.5, 10 kV separation voltage, 20 s electrophoretic injection time and 50 μm x 35 cm capillary.

6.4   ELECTROPHORETIC SEPARATION OF HUMIC ACID

The CE separation of 15 mg l^{-1} humic acid, natural water sample, humic acid and water sample spiked with maleic acid employed the previously established optimum conditions.

The electropherogram of the commercial humic acid showed two fractions with migration times of 4.50 and 6.49 min respectively as shown in Figure 6.6(a). The first peak was principally due to the low relative molecular mass fulvic acid, although it may also contain some humic material. The second peak was due to the high relative molecular mass humic acid.

The electropherogram for the natural water sample is shown in Figure 6.6(b) and consists of 3 peaks at migration times 4.17, 4.37 and 6.29 min respectively. A probable interpretation is that the peak at 4.37 min is due to the low relative molecular mass fulvic acid and the peak at 6.29 min is due to high relative molecular mass humic acid. The peak at 4.17 min is thought to be due to low molecular mass organic acid. The fulvic acid content in natural water is normally around 90% and this illustrated by the broad second peak.

Separations of the humic acid and water sample spiked with 1×10^{-3} M maleic acid are shown in Figure 6.6(c) and 6.6(d) respectively. These show that the first peak, with lower migration time, has characteristics similar to a typical low relative molecular mass organic acid.   The picture is not simple because of possible interactions between the components and the possibility that the maleic acid might form dimers and higher polymers. The splitting of the first peak observed is due to the detector running over range.
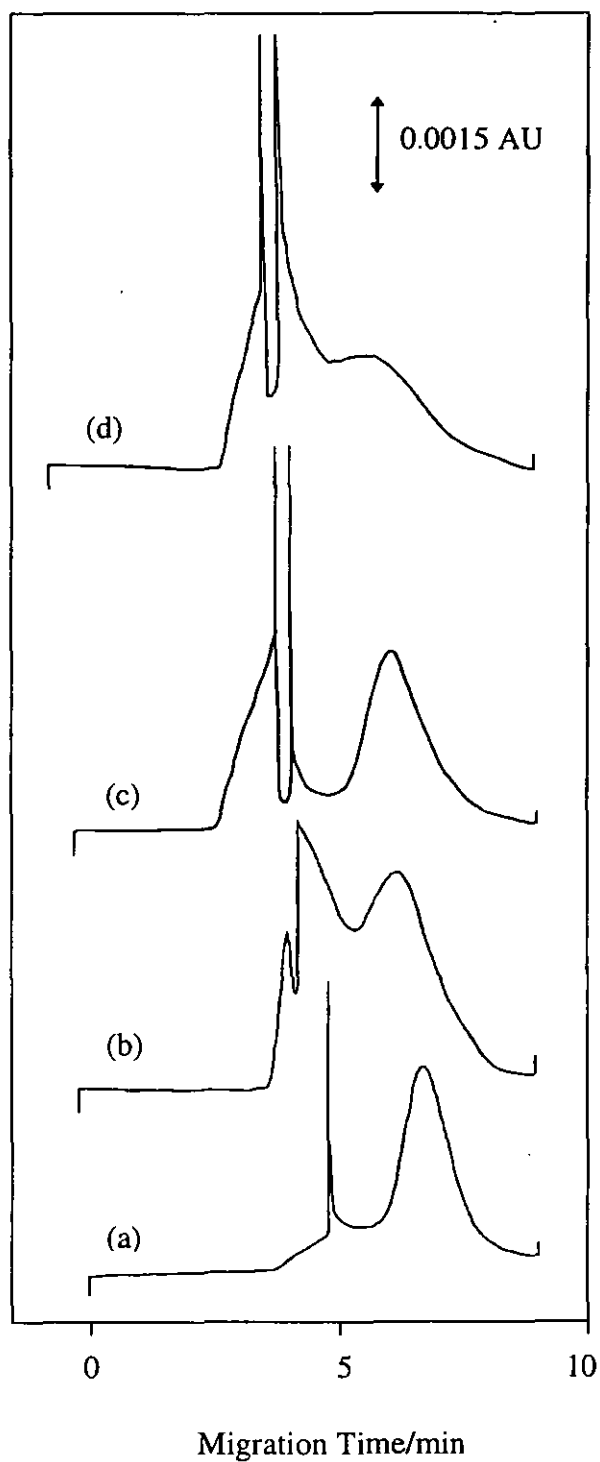
Figure 6.6: Electropherograms of (a) Commercial humic acid, (b) Water sample, (c) Spiked humic acid with maleic acid and (d) Spiked water sample with maleic acid. Separation conditions: 0.30 M borate buffer with polymer modifier, pH 8.5, 10 kV separation voltage, 20 s electrokinetic injection time, 254 nm detection wavelength and 50 μm x 35 cm capillary.

6.5 FRACTIONATION AND SEPARATION OF HUMIC ACID

6.5.1 Fractionation of Humic and Fulvic Acids

The procedure used is that outlined in Figure 6.7. A solution of humic acid (50 mg l^{-1}) was acidified with concentrated hydrochloric acid (A.R., Fisons, Loughborough, UK) to bring the pH below 1 and allowed to stand overnight. The precipitated humic acid was filtered off and thoroughly washed with deionised water. The solid humic acid was weighted and redissolved in deionised water (final volume = 10 ml) with a small amount of 0.10 M sodium hydroxide (A.R., Fisons, Loughborough, UK) to aid dissolution. Finally, the pH of the purified humic acid was adjusted to 6.3 with hydrochloric acid. The supernatant known as purified fulvic acid solution, was adjust to pH 6.3 with sodium hydroxide.

Humic Substances

Extract with alkali

(Insoluble) Humin

(Soluble)

Treat with acid

(Precipitate) Humic Acid

(Not Precipitate) Fulvic Acid

Redissolve in base

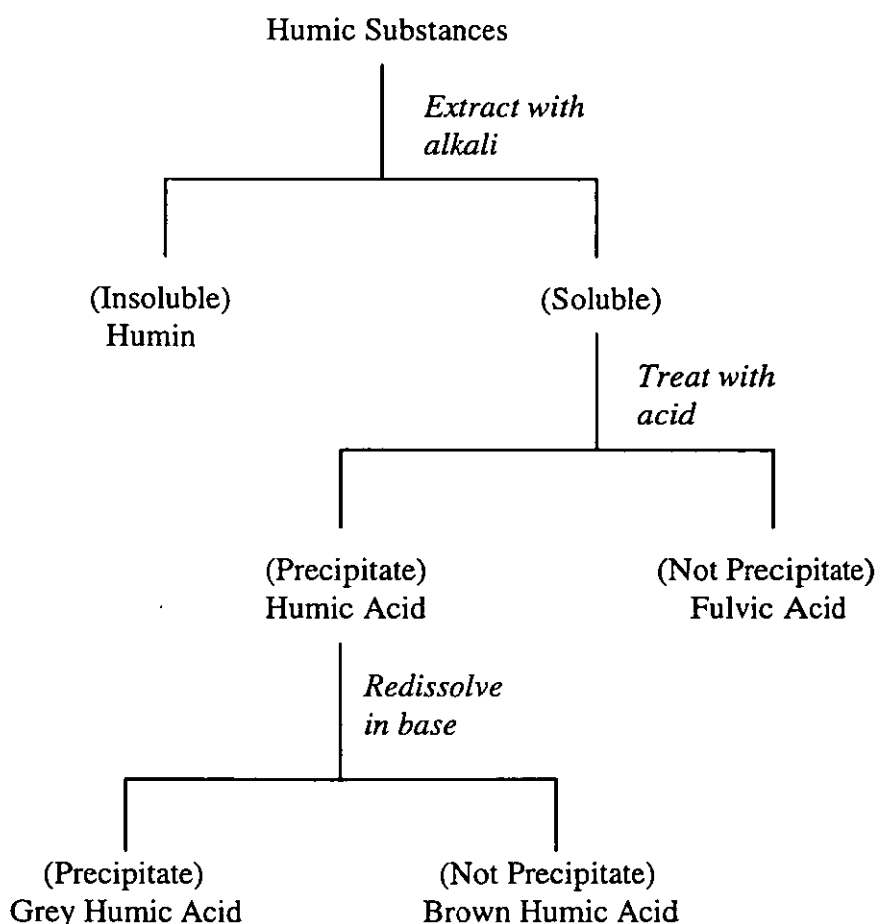(Precipitate) Grey Humic Acid

(Not Precipitate) Brown Humic Acid

Figure 6.7: The classical extraction scheme of humic material [2].

UV spectra for the humic acid, purified humic acid and purified fulvic acid at wavelengths from 200 to 380 nm are shown in Figure 6.8. The spectra are featureless with no maximum absorption peak.

6.5.2 Separation of Purified Humic and Fulvic Acids

Electrophoretic separations of purified humic and fulvic acids by CE were carried out utilising the optimum separation parameters (see section 6.3).

The electropherograms for the separations of humic acid, purified humic acid and purified fulvic acid are shown in Figure 6.9. The electropherogram of purified humic acid, as shown in Figure 6.9(b), consists of two peaks; the first peak which is small and sharp is probably due to the low relative molecular mass humic acid, but could also be residual fulvic material. This peak is smaller than the peak obtained from the original humic acid, Figure 6.9(a), indicating that the fulvic acid had been largely eliminated from the solution. The second peak is due to the high relative molecular mass humic acid and is similar to the peak obtained from the original humic acid solution.

The electropherogram of purified fulvic acid is shown in Figure 6.9(c) and has only one small peak at the lower migration time. It would have been expected that the peak in solution (c) should be of approximately the same magnitude as the first peak in (a). That it is not indicates that the fractionation procedure has modified the material that was responsible for the first peak. It is known that acidification causes the soluble material to increase its molecular weight by increased hydrogen bonding. This would account for an apparent loss of the fulvic material.

6.6 COMPLEXATION OF METAL BY HUMIC ACID

Solutions of nickel were prepared from nickel nitrate (A.R. grade, Fluka, Dorset, UK) having concentrations ranging from 1×10^{-3} to 1×10^{-9} M and then 1 ml aliquots of
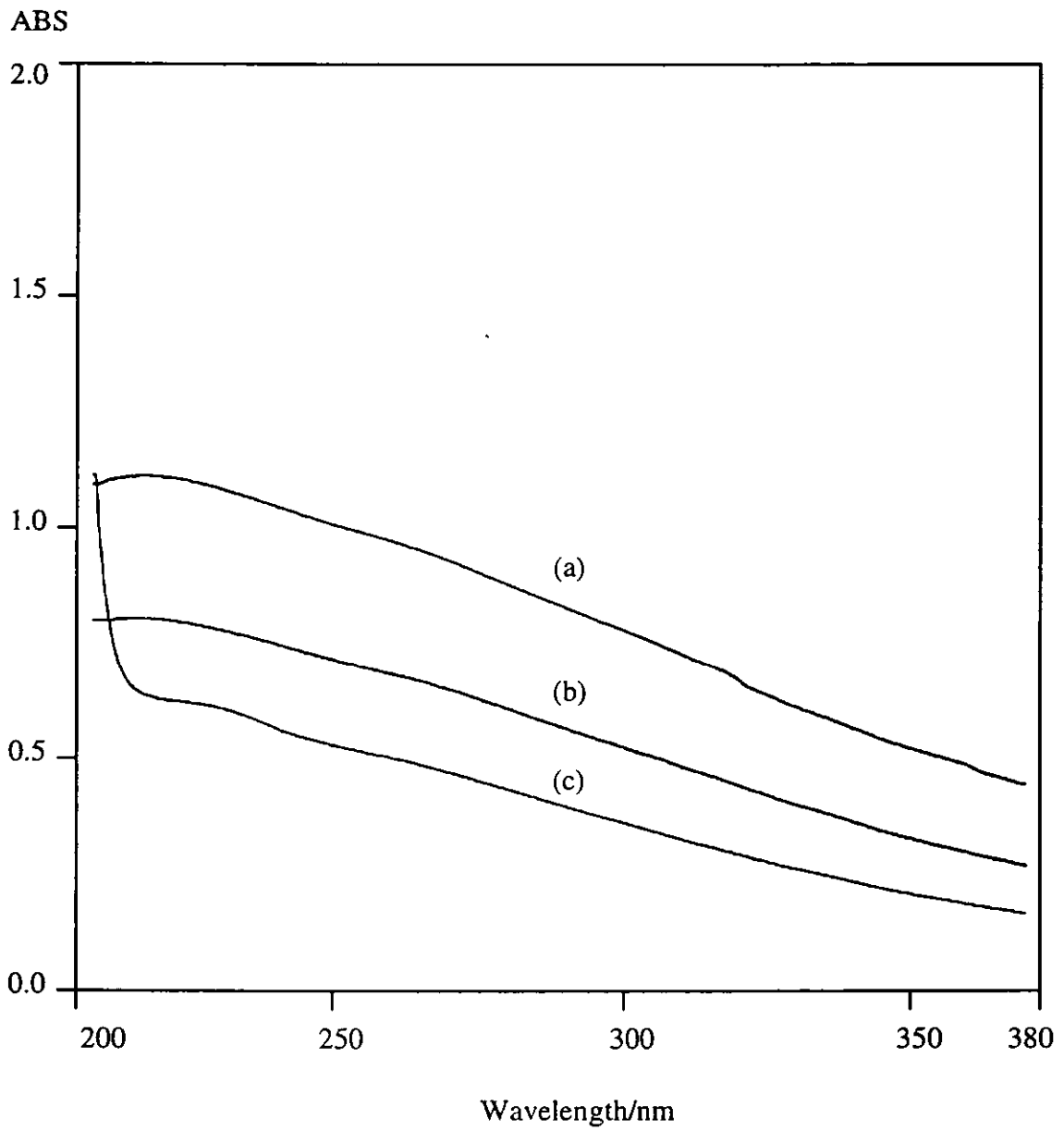
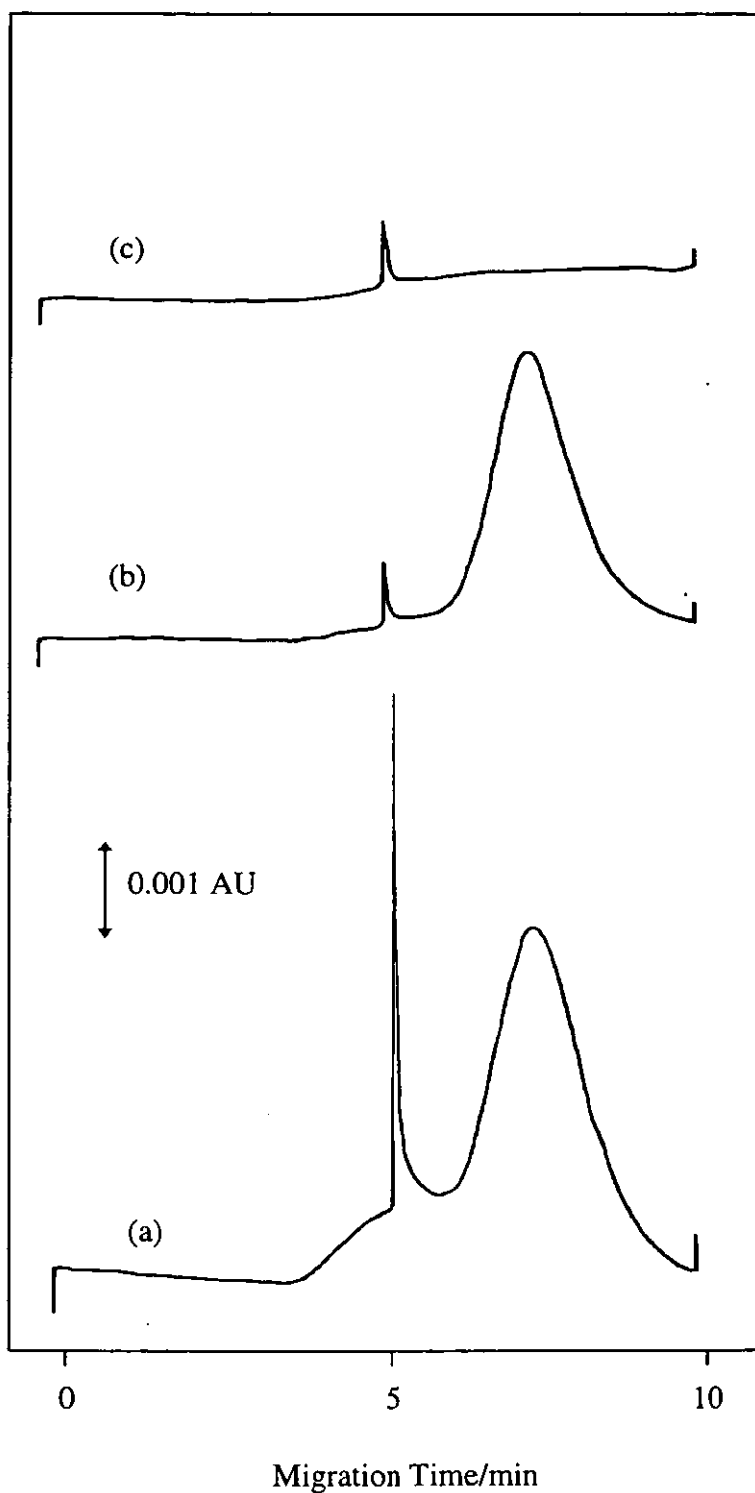Figure 6.8:   UV spectra of (a) Humic acid, (b) Purified humic acid and (c) Purified fulvic acid.

Figure 6.9:   Electropherograms of (a) Humic acid, (b) Purified humic acid and (c) Purified fulvic acid.   Separation conditions: 0.30 M borate with polymer modifier pH 8.5, 10 kV separation voltage, 20 s electrokinetic injection time, 254 nm detection wavelength and 50 μm x 35 cm capillary.

these solutions were added to 9 ml of humic acid solution (16.67 mg l^{-1}). The final solutions had nickel concentration ranging from 1 x 10^{-4} to 1 x 10^{-10} M and a humic acid concentration of 15 mg l^{-1}.

After allowing 24 hours for the mixture to reach equilibrium at 20 °C, each solution was analysed by CE utilising the optimum separation parameters.

The effect of adding nickel to the humic acid is illustrated in Figure 6.10. Zone migration times of the nickel-humic complexes were found to be proportional to the logarithm of the nickel concentration added as shown in Figure 6.11. On the other hand, increased nickel concentration for nickel-humic complexes resulted in lower peak heights. Above 1 x 10^{-4} M of nickel added to the humic acid, the broad peak disappeared from the electropherogram.

These observation suggest that as nickel was added, the negative charge centres on the complex was gradually neutralised, firstly resulting in slower migration, but ultimately leading to neutral species which could no longer be detected. The increase in the size of the first peak is due to the detection of NO_3^- which is a strong absorber at 254 nm. Note that NO_3^- appears slightly earlier.

6.7   CONCLUSIONS

Investigation of the optimum instrument operating parameters showed that the best electrophoretic separation for aqueous humic acid samples could be achieved in a borate buffer, pH 8.5 at 10 kV separation voltage, 20 s electrokinetic sample injection time and UV detection at 254 nm. Electrophoretic separation of humic acid showed that humic acids consist of 2 major components: a fraction at lower migration time contained the low relative molecular mass fulvic acid and humic acid and a fraction at higher migration time which contains the high relative molecular mass humic acid.
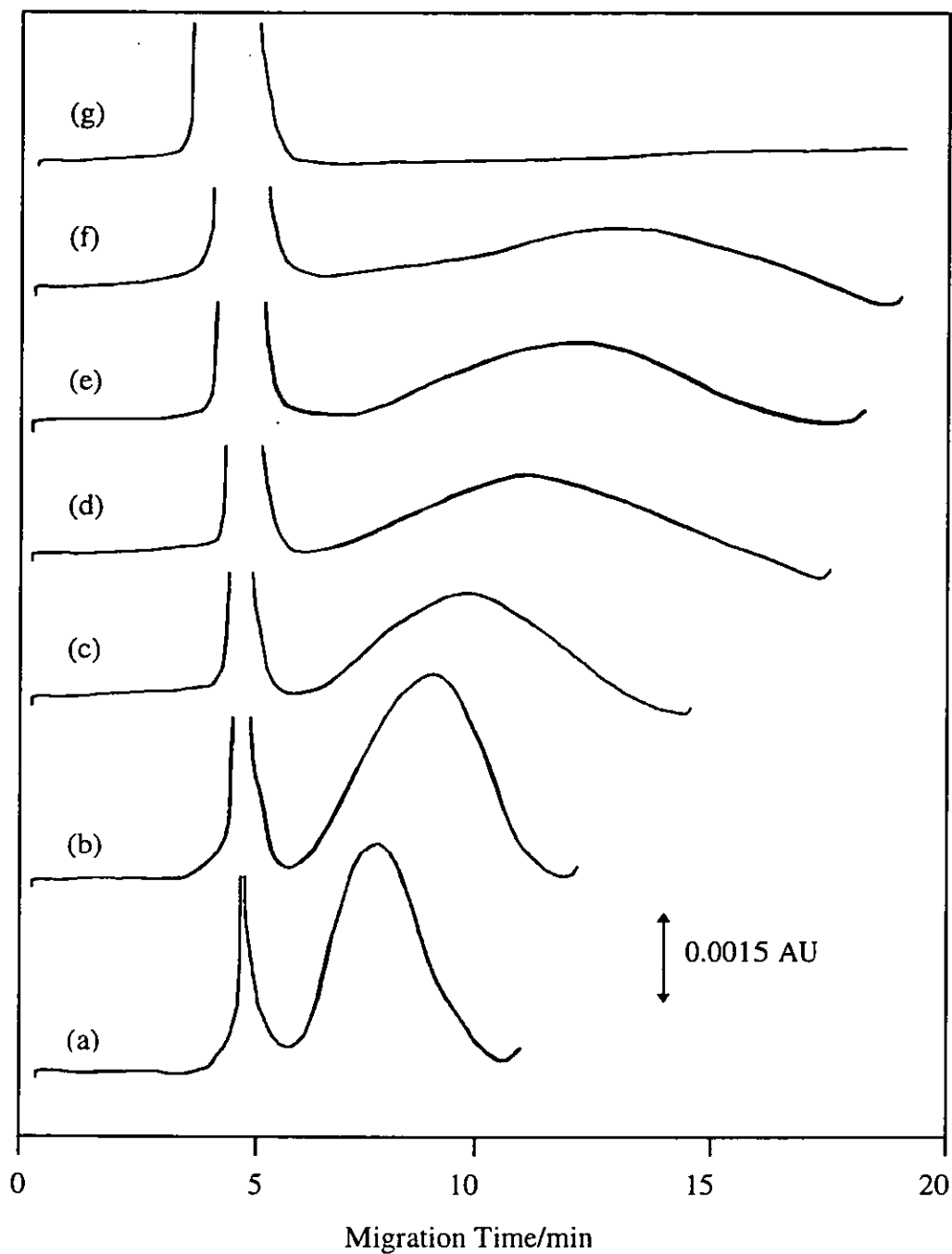
Figure 6.10: Electropherograms of Ni^{2+}:humic acid complexes; (a) 1 x 10^{-10} M:15 mg l^{-1}, (b) 1 x 10^{-9} M:15 mg l^{-1}, (c) 1 x 10^{-8} M:15 mg l^{-1}, (d) 1 x 10^{-7} M:15 mg l^{-1}, (e) 1 x 10^{-6} M:15 mg l^{-1}, (f) 1 x 10^{-5} M:15 mg l^{-1} and (g) 1 x 10^{-4} M:15 mg l^{-1}. Separation conditions: 0.30 M borate with polymer modifier, pH 8.5, 10 kV separation voltage, 20 s electrokinetic injection time, 254 nm detection wavelength and 50 μm x 35 cm capillary.
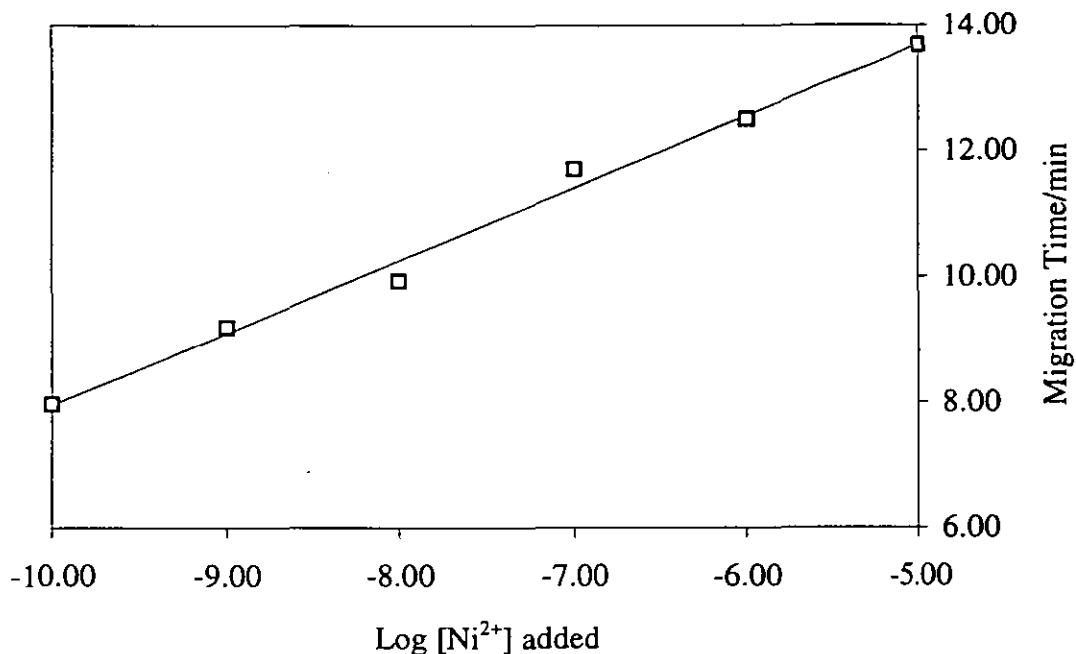
Figure 6.11:   Effects of nickel concentrations on zone migration time for
electrophoretic separation of nickel-humic complexes.

Electrophoretic separation of a neutral water sample indicated that water sample consisted of 3 major components; low molecular mass organic acid, low relative molecular mass fulvic acid and humic acid, and high relative molecular mass humic acid.

The tentative allocation of peaks to different mass fraction was confirmed by electrophoresis on fractionated solution. Here only the high mass peak was present for humic acid solution and similarly only the low mass peak was present for fulvic acid solution.

The separation of nickel-humic acid complexes showed that the presence of nickel had affected the zone migration times and peaks heights. This was attributed to nickel complexing on the negative charge sites (-COOH, -OH) of the humic acid.

REFERENCES

1. Patterson, M., *Ph.D. Thesis*, Loughborough University of Technology, UK, 1995.

2. Stevenson, F. J., *Humus Chemistry: Genesis, Composition, Reaction*, Wiley, New York, 1982.

Chapter 7

CHAPTER SEVEN

COMPARISON OF A HIGH EFFICIENCY NEBULISER WITH A STANDARD CONCENTRIC NEBULISER FOR INDUCTIVELY COUPLED PLASMA- MASS SPECTROMETRY

7.1   INTRODUCTION TO CHAPTER

This chapter describes optimisation of the ICP-MS instrument with a high efficiency nebuliser and a standard concentric nebuliser. A comparison study of the analytical and fundamental characteristics of these nebulisers in terms of sensitivities, detection limits, short and long term stabilities, oxide ratios, doubly charged ratios and relative isotopic ratios under optimal conditions is also discussed.

7.2   EXPERIMENTAL

7.2.1   ICP-MS Instrument

The ICP was powered by a 27.12 MHz crystal controlled oscillator (Model HFP 2500F, Plasma Therm Inc., Kresson, NJ, USA) with an APCS-1 automatic power supply and AMN-PS-1 automatic impedance matching network.

The ICP torch was a Fassel fused silica torch of 18 mm i.d. Power was coupled from a 3 turn load coil of 6 mm copper tube grounded at the torch mouth and cooled by a water flow. The plasma was centred about the sampling orifice which was in the region of 12 mm above the load coil. The torch box was mounted on an optical bench that provided motion for alignment in three directions.

The glass concentric nebuliser (Type TR-30-C2, J. E. Meinhard Associates Inc., Santa Ana, CA, USA) was coupled to a water cooled single pass spray chamber (VG

Elemental, Winsford, Cheshire, UK). The high efficiency nebuliser (Type HEN-170-AA, J. E. Meinhard Associates Inc., Santa Ana, CA, USA) employed a home-made U-shape spray chamber. For the HEN-170-AA nebuliser, the aerosol had to be directed from the spray chamber to the torch via a 50 cm long flexible tubing (4 mm i.d.) due to space restriction around the instrument.

The mass spectrometer (MS) unit was a VG Micromass quadrupole assembly (Model 12-12S, VG Analytical Ltd., Altrincham, Cheshire, UK) having a mass range of 0 - 800 u. The ion detector was a continuous dynode channel electron multiplier (Model 4870V, Galileo Electro-Optics Corporation, Sturbridge, MA, USA).

For evacuating the interface and MS chamber, various types of vacuum pumps were used:

- Stage 1 (Expansion Chamber) used a mechanical pump (Trivac B Model S25B, Leybold AG, Koln, Germany) operated at a pump speed of 7.13 l s^{-1} to remove more than 95% of gas load entering the system at the interface.

- Stage 2 (Intermediate Chamber), comprising part of the ion focusing system employed a diffusion pump (Diffstak MK2 Model 250, Edwards High Vacuum, Crawley, Sussex, UK) with pump speed of 1700 l s^{-1} backed by a rotary pump (Model EDM 12, Edwards High Vacuum, Crawley, Sussex, UK).

- Stage 3 (Analyser Chamber) which houses the remainder of the lens, the quadrupole and the detector, used a diffusion pump (Diffstak MK2 Model 100, Edwards High Vacuum, Crawley, Sussex, UK) with pump speed of 280 l s^{-1} and a backing rotary pump (Model EDM 6, Edwards High Vacuum, Crawley, Sussex, UK).

The plasma sampling interface was of the type found in VG PlasmaQuad instruments. The sample cone had a 1.0 mm aperture and the skimmer cone a 0.7 mm aperture, both cones were machined from pure nickel (VG Elemental, Winsford, Cheshire, UK). A modified lens stack (VG Elemental, Winsford, Cheshire, UK) was used for ion focusing in which lenses L3 and L4 were of reduced length to enable the

assembly to fit into the vacuum chamber. No noticeable deterioration in performance occurred from making this modification.

Data acquisition was controlled by a microcomputer, using PQVision software version 4.1.2 (Fisons plc, Uxbridge, Middlesex, UK), connected to the instrument via an IEEE 488 interface.

A peristaltic pump (Model Minipuls 2, Gilson Medical Electronic, Villiers-Le-Bel, France) was used for solution delivery to the nebuliser.

The ICP-MS operating conditions utilised for this work, unless otherwise stated, were those shown in Table 7.1.

Routine optimisation and calibration procedures were performed following a warm up period of approximately 30 min. A 50 ng ml^{-1} tune solution containing Be, Mg, Co, In, Ce, Pb and U in 1% HNO_3 was used to optimised the instrument. The sampling depth, the nebuliser gas flow rate and the lens stack potentials were sequentially and iteratively tuned to provide maximum signal response at 115 m/z for ^{115}In. A full scan spectrum of the tune solution was obtained and analysed for the signal response of ^{115}In, the oxide ratio value of $^{140}CeO^+:^{140}Ce^+$ and the doubly charged species ratio of $^{238}U^{2+}:^{238}U^+$.

Calibration of the instrument, which involved mass calibration and detector calibration, was performed on a weekly basis. Response calibration was performed on a daily basis prior to analysis.

7.2.2 Chemicals

All standards used in this work were 10,000 µg ml^{-1} ICP standard solution (Specpure, Johnson Matthey, Royston, Herts, UK) or 1,000 µg ml^{-1} standard solution (SpectrosoL, BDH Ltd., Poole, Dorset, UK). All working solutions were stored in polypropylene bottles (Analytical Supplies Ltd., Little Easton, Derbyshire, UK).

Table 7.1:   Optimised ICP-MS operating condition.

Parameter	TR-30-C2	HEN-170-AA
Incident power	1.30 kW	1.30 kW
Reflected power	< 5 W	< 5 W
Plasma gas flow rate	12.0 l min^{-1}	12.0 l min^{-1}
Auxiliary gas flow rate	1.2 l min^{-1}	1.4 l min^{-1}
Nebuliser gas flow rate	0.75 l min^{-1}	1.0 l min^{-1}
Solution uptake rate	0.55 ml min^{-1}	40 µl min^{-1}
Sampling distance	12 mm a.l.c.	12 mm a.l.c.
1st vacuum stage pressure	1.8 mbar	1.8 mbar
2nd vacuum stage pressure	1 x 10^{-4} mbar	1 x 10^{-4} mbar
3rd vacuum stage pressure	3 x 10^{-6} mbar	3 x 10^{-6} mbar
Extraction potential	-325 V	-325 V
Collector potential	-2.5 V	-2.5 V
L1 potential	-2.5 V	-2.5 V
L2 potential	-35 V	-35 V
L3 potential	0 V	0 V
L4 potential	-74 V	-74 V
Pole Bias	0 V	0 V
Quadrupole Resolution	0.6 u (at 5% peak height)	
Quadrupole rest mass	150 u	
Detector supply voltage	-2750 V	
Detector dead time	40 x 10^{-9} s	
Discriminator level	64 x 10^{-3} V	

The nitric acid used was Aristar grade nitric acid (BDH Ltd., Poole, Dorset, UK). The high purity water used to prepare the solutions was obtained from a Liquipure pure water system (Liquipure, Bichester, Oxfordshire, UK) or Maxima (ELGA, High Wycombe, Bucks, UK) operated at 18 MΩ.

7.3   ICP-MS OPTIMISATION

Optimisation of the operating conditions was typically performed using a single element, often indium, but this single element optimisation has been considered to be disadvantageous for applications in the multielement mode of operation.   Other method of optimisation are usually performed as a series of cyclical univariate searches or simplex optimisation. These two methods rely on a skilled operator and are time consuming, but once the optimisation is achieved, the settings are kept constant.   Only minor trimming is needed, especially to the ion optics settings, without repeated optimisation throughout the working day even though a variety of different sample types and chemistries may be run.

Several reports on optimisation studies for ICP-MS based on univariate optimisation have been published.   Horlick *et al.* [1-3] reported studies of the effect of plasma operating parameters on several analyte ion signals, oxide, hydroxide and doubly charged analyte species signals. Long and Brown [4] optimised a commercial ICP-MS system as a function of a number of parameters associated with sample introduction and plasma operation.   The effects of solution uptake rate, nebuliser pressure and rf power on M^+, $MO^+:M^+$ and $M^{2+}:M^+$ were investigated.   Gray and Williams [5] discussed the effect of operating parameters on ICP-MS performance for routine analysis. Browner and Zhu [6] studied the effects of nebuliser flow-rate, rf plasma power, sampling depth and ion lens voltages on ion populations, ratios of singly charged to doubly charged ions, ratios of singly charged to oxide and hydroxide ions. A more rigorous optimisation procedure for ICP-MS systems is simplex optimisation [7-9].

In this work, the alternating variable search was preferred to simplex optimisation because more information was required on response of the system to parametric variation.

7.3.1 Effects of Nebuliser Pressure

Studies of the effect of nebuliser pressure on ion signals, oxide and doubly charged ion ratios were performed by varying nebuliser pressures from 24 to 32 psi for the standard concentric nebuliser (TR-30-C2) and from 125 to 165 psi for the high efficiency nebuliser (HEN-170-AA). Other operating parameters were set as in Table 7.1. 50 ng ml^{-1} multielement solution was used as a test solution.

Indium was used as the major analyte since its first ionisation energy (5.79 eV) is low and its second ionisation energy (18.86 eV) is well above the first of argon (15.76 eV). It can be assumed to be ionised to singly charged ions. ^{115}In has an abundance of 95.72%. Ion signals for ^{140}Ce and ^{238}U were included for comparison. For the oxide ion ratio, ^{140}CeO$^+$ and ^{140}Ce$^+$ were used since cerium has a high neutral metal-oxygen bond strength (795 kJ mol^{-1}), but a low oxide percentage. Its first ionisation energy is 5.21 eV and it has an abundance of 88.48%. For the doubly charged ion ratio, ^{238}U^{2+} and ^{238}U$^+$ were measured since uranium has a low second ionisation energy of about 12 eV (first ionisation energy = 6.08 eV) and can produce doubly charged ions at high plasma temperature. ^{238}U has an abundance of 99.27%.

Plots of the effects of varying the nebuliser pressure on ^{115}In, ^{140}Ce and ^{238}U signals with the TR-30-C2 and HEN-170-AA nebulisers are presented in Figures 7.1 and 7.2 respectively. The points plotted were the means of 4 measurements. The relative standard deviations are better than 10% in all instances. The signals were not corrected for background as it was determined that background was negligible for all the conditions studied.

The maximum signal for the TR-30-C2 nebuliser was achieved at a pressure of 28 psi which yield a gas flow rate of 0.75 l min^{-1}. For the HEN-170-AA nebuliser, a
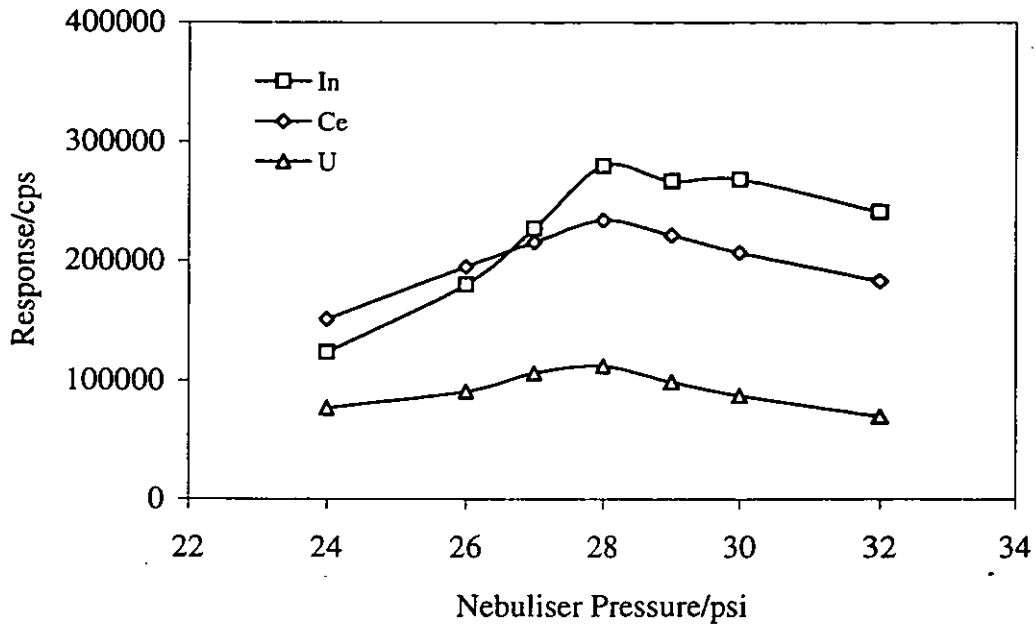
Figure 7.1:   Dependence of ion signals on nebuliser pressure with the TR-30-C2
               nebuliser.
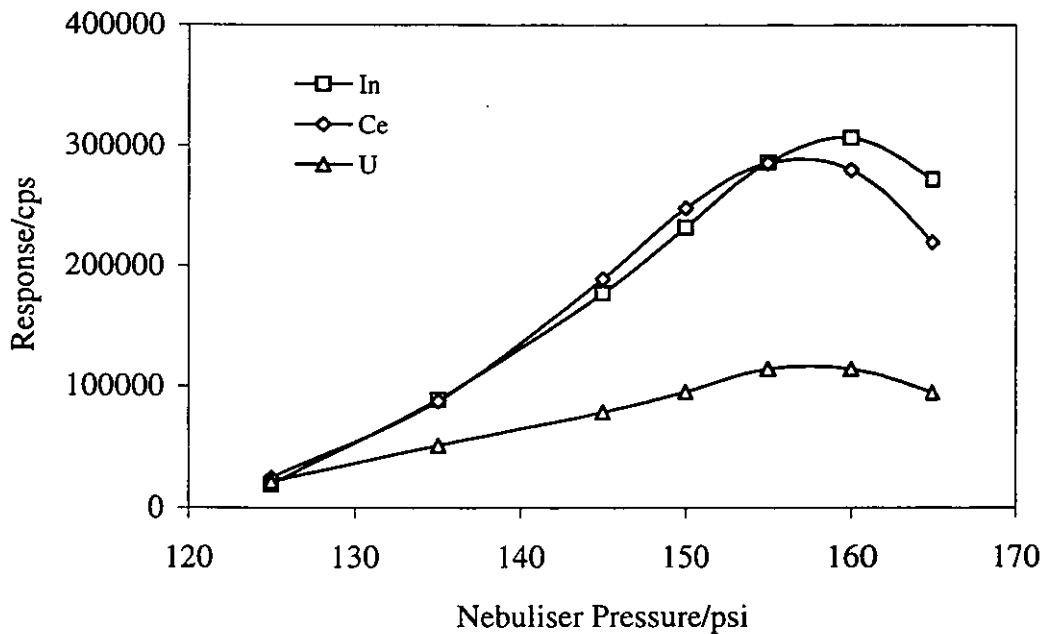

Figure 7.2:   Dependence of ion signals on nebuliser pressure with the
               HEN-170-AA nebuliser.

pressure of 155 psi gave the maximum signal which is equivalent to 1.0 l min^{-1}. There were changes in signals upon varying the nebuliser pressure since it affects both the aerosol density and gas flow rate into the central channel of the ICP. This in turn affects the structure of the central channel. It was interesting to note that a more defined maximum was obtained with the HEN, particularly for the high ionisation potential elements. This phenomenon is due to the quality of the aerosol produced by the HEN which is finer and more homogenous in size than the aerosol produced by the standard nebuliser.

The ratios of the oxides ($CeO^+:Ce^+$) and doubly charged ($U^{2+}:U^+$) ions to singly charged ions for the TR-30-C2 and HEN-170-AA nebulisers are tabulated in Table 7.2. The oxide and doubly charged ratios, showed low ratios, at the sensitivity maxima for the TR-30-C2 and HEN-170-AA nebulisers. At the highest flow rate, the oxide and doubly charged ratios were higher. Dissociation, which requires a finite residence time in the hottest part of the plasma, occurs further along the axis at higher flows. Similarly, low ratios were obtained in the range 150-160 psi for HEN which is the pressure range which yield good sensitivity.

Table 7.2: Dependence of oxide and doubly charged ion ratios on nebuliser pressures.

Pressure/ psi	TR-30-C2		Pressure/ psi	HEN-170-AA	
	%CeO^+/Ce^+	%U^{2+}/U^+		%CeO^+/Ce^+	%U^{2+}/U^+
24	2.08	2.27	125	3.58	4.01
26	1.79	2.26	135	0.78	1.59
27	1.73	2.26	145	0.46	2.36
28	2.04	2.51	150	0.39	2.26
29	2.34	2.90	155	0.43	2.58
30	2.81	3.50	160	0.52	3.35
32	5.01	4.40	165	4.01	5.54

7.3.2 Effects of rf Generator Forward Power

The rf generator forward powers were varied from 0.85 to 1.30 kW for measurements of ion signals, oxide and doubly charged ratios for both the TR-30-C2 and HEN-170-AA nebulisers. Other ICP-MS operating parameters were set as in Table 7.1 and 50 ng ml^{-1} multielement solution was used.

Figures 7.3 and 7.4 illustrate the effects of rf generator forward power applied to the plasma for the TR-30-C2 and HEN-170-AA nebulisers respectively. Ion signals continually increase with power for the standard Meinhard, but plateau for the HEN. This may reflect the plasma being more able to process the finer aerosol produced from the HEN. Increase in rf power also affects the ionisation temperature of the plasma and zone structure relative to the sampling orifice. The maximum rf generator power tested was 1.30 kW. Gray and Date [10] pointed out that very high powers (>1.4 kW) could cause excessive temperature build-up in the expansion stage which might lead to component failure.

The effects of rf generator forward power on the ratios of oxides and doubly charged ions to singly charged ions with the TR-30-C2 and the HEN-170-AA nebulisers are shown in Table 7.3. Ratios are decreased as the rf power increased. The effect of higher powers on oxide ratios is predictable, but it might be expected that doubly to singly charged ratios would increase with power. However, this observation cannot be taken in isolation from the changes in zone structure and effective sampling depth.

7.3.3 Effects of Sampling Depth

The sampling depth is the distance from the tip of the sampling cone to the top of the load coil of the ICP torch. It is an important parameter because ion densities vary with position in the plasma.
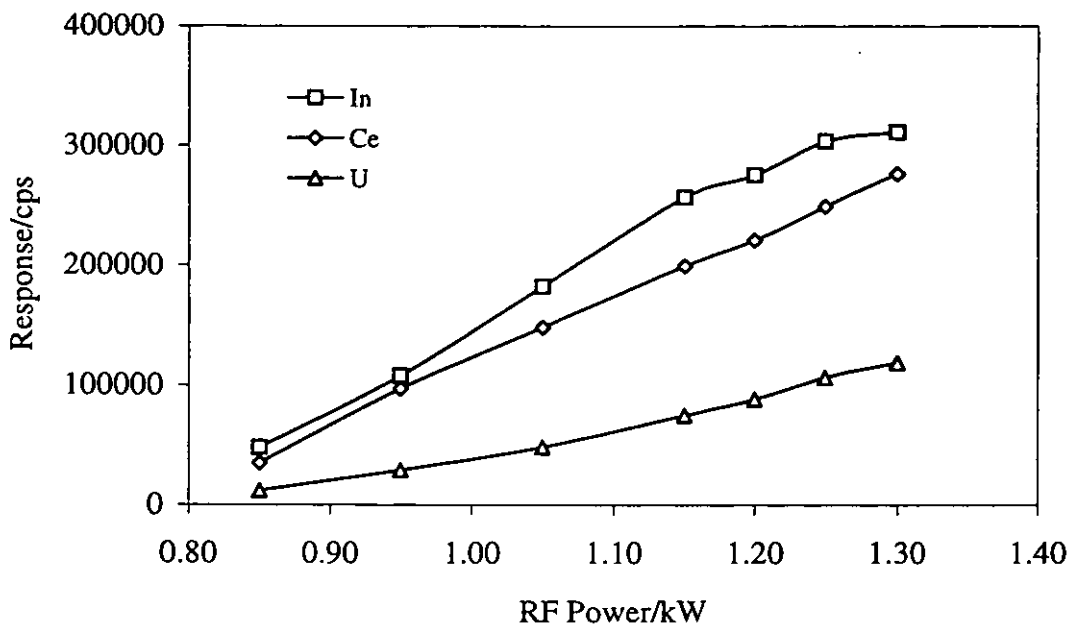
Figure 7.3:   Dependence of ion signals on rf generator forward power with
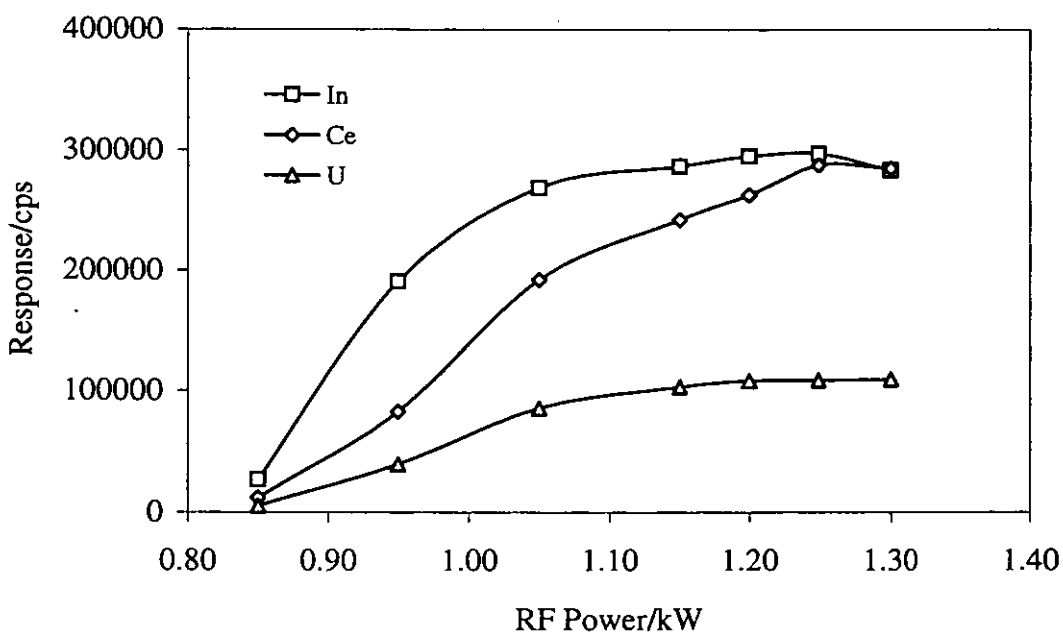   TR-30-C2 nebuliser.

Figure 7.4:   Dependence of ion signals on rf generator forward power with
              HEN-170-AA nebuliser.

Table 7.3: Dependence of oxide and doubly charged ion ratios on rf generator forward power (TR-30-C2 operating at 0.75 l min^{-1} and HEN-170-AA operating at 1.0 l min^{-1}).

rf Power/ kW	TR-30-C2		HEN-170-AA	
	%CeO$^+$/Ce$^+$	%U^{2+}/U$^+$	%CeO$^+$/Ce$^+$	%U^{2+}/U$^+$
0.85	9.89	26.83	74.41	19.80
0.95	4.44	7.88	45.99	10.50
1.05	3.68	5.34	6.53	7.15
1.15	2.21	3.71	0.93	4.34
1.20	2.02	3.14	0.49	3.56
1.25	2.17	3.02	0.43	3.43
1.30	1.83	2.77	0.38	3.01

For studying the effects of sampling depth on ion signals, oxide and doubly charged ion ratios, the sampling depth was varied from 8.5 mm to 12.5 mm, while the other operating parameters were set as in Table 7.1.

The effects of sampling depth on ion signals with the TR-30-C2 and HEN-170-AA nebulisers are shown in Figures 7.5 and 7.6 respectively. The maximum ion signal was obtained at 12.00 mm sampling depth for both the TR-30-C2 and HEN-170-AA nebulisers. This was expected because the optimum plasma temperature for ionisation is about 7500 K which occurs 12 - 14 mm above load coil.

The ratios of the oxides and doubly charged ions to singly charged ions with the TR-30-C2 and HEN-170-AA nebulisers are shown in Table 7.4. Low levels of oxide and doubly charged ratios were observed at the various sampling depths. Over the range studied, the distance between the sampling cone and the load coil did not have much effect on the formation of oxide and doubly charged ions.
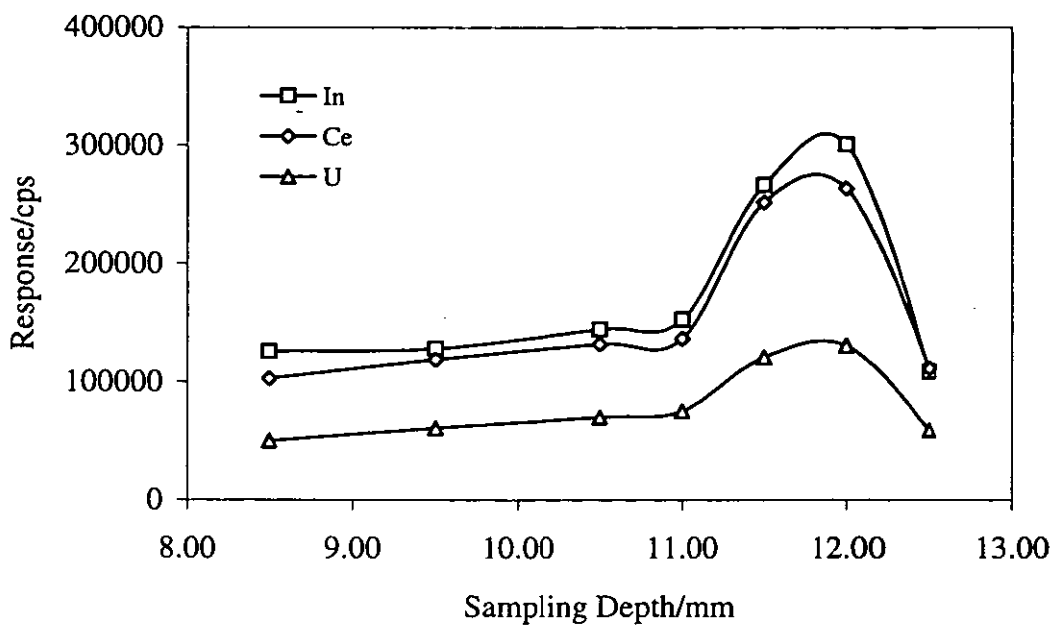
Figure 7.5:   Dependence of ion signals on sampling depth with TR-30-C2
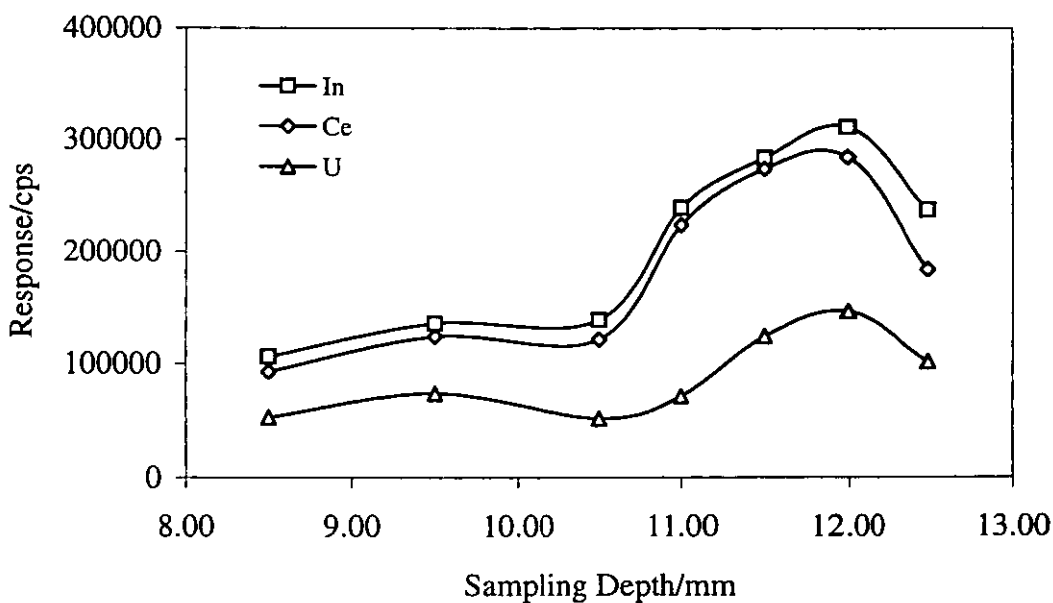nebuliser.

Figure 7.6:   Dependence of ion signals on sampling depth with HEN-170-AA
nebuliser.

Table 7.4:   Dependence of oxide and doubly charged ion ratios on sampling depth.

Sampling Depth/mm	TR-30-C2		HEN-170-AA	
	%CeO$^+$/Ce$^+$	%U^{2+}/U$^+$	%CeO$^+$/Ce$^+$	%U^{2+}/U$^+$
8.50	1.68	2.78	0.78	2.62
9.50	1.71	2.37	0.83	2.94
10.50	1.79	2.07	2.19	2.78
11.00	1.83	1.73	1.79	2.39
11.50	2.05	2.68	1.23	2.23
12.00	2.35	2.47	0.93	2.08
12.50	2.24	2.01	0.89	2.36

7.3.4   Ion Lens Optimisation

The extraction, collector, L1 and L3 lenses were included in the optimisation, the other lenses have little effect and were excluded.   The ion lens optimisation was conducted at the optimum plasma conditions as shown in Table 7.1.

For the ion optics experiments, the voltage on one lens was varied while the remaining lenses were kept at the voltages listed in Table 7.5.

Table 7.5:   Ion lens standard operating condition.

Lenses	Dial Setting	Voltages/V
Extraction	2.5	-325.0
Collector	7.5	- 2.5
L1	7.5	- 2.5
L2	5.0	- 35.0
L3	5.0	0.0
L4	2.0	- 74.0
Pole Bias	5.0	0.0

Values set for the experiments were referred to the lens digitpot setting which were directly related to the voltage ranges of each lens elements as shown in Table 7.6.

Table 7.6: Lens supply voltage.

Control	Voltage Range	
	Dial Set at 0.00	Dial Set at 10.00
Extraction	-100	-1000
Collector	-100	+ 30
L1	-100	+ 30
L2	-100	+ 30
L3	- 30	+ 30
L4	-100	+ 30
Pole bias	+ 30	- 30

7.3.4.1   Extraction Electrode

In normal operation, the negative voltage on the extraction electrode extracts positive ions and directs them through the slide valve aperture toward the collector. Negatively charged species are repelled and neutral atoms and molecules diffuse away from the system axis toward the intermediate stage diffusion pump. Low values of extraction potential generally give the clearest spectra; if high settings are necessary there is probably a leak in the ICP glassware connections or a torch or nebuliser blockage.

The effects of extraction electrode voltage on ion signal with the TR-30-C2 and HEN-170-AA nebulisers are shown in Figures 7.7 and 7.8 respectively. Maximum ion signals were obtained at an extraction electrode setting of 2.50 for both nebulisers which is equal to -325 V.
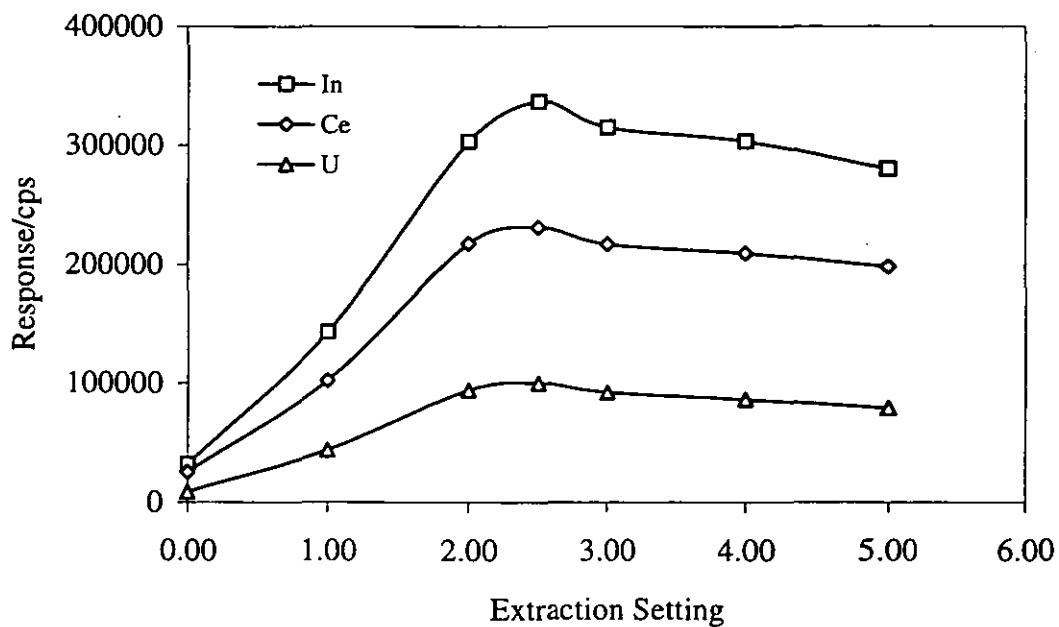
Figure 7.7:   Dependence of ion signals on extraction electrode voltage with
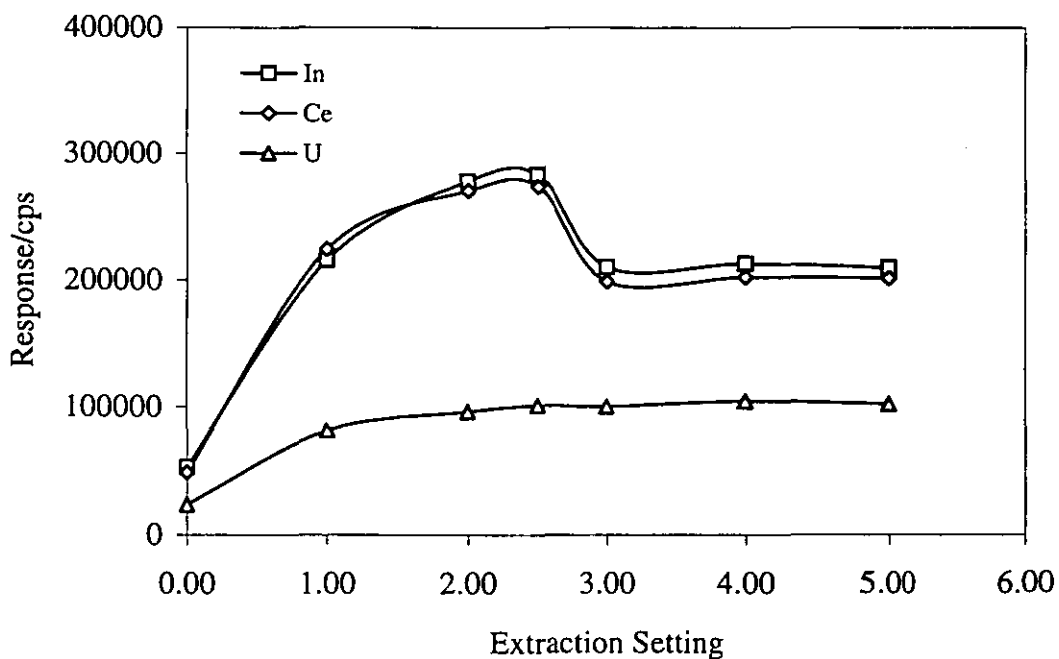TR-30-C2 nebuliser.

Figure 7.8:   Dependence of ion signals on extraction electrode voltage with
HEN-170-AA nebuliser.

The effects of extraction electrode voltage on the ratios of oxide and doubly charged ions to singly charged ions with the TR-30-C2 and HEN-170-AA nebulisers are shown in Table 7.7.

Table 7.7: Dependence of oxide and doubly charged ion ratios on extraction electrode voltage.

Dial Setting	TR-30-C2		HEN-170-AA	
	$\%CeO^+/Ce^+$	$\%U^{2+}/U^+$	$\%CeO^+/Ce^+$	$\%U^{2+}/U^+$
0.00	4.54	10.72	0.64	2.42
1.00	3.12	4.62	0.50	3.18
2.00	2.36	3.86	0.44	3.11
2.50	2.46	3.40	0.46	2.99
3.00	2.34	3.58	0.50	1.99
4.00	2.21	3.91	0.41	2.14
5.00	2.24	3.75	0.48	1.70

7.3.4.2 Collector Electrode

Having passed through the slide valve aperture, the ions are entrained by the collector electrode and defocused around the photon stop. An on-axis photon stop mounted close to the collector, prevents light and neutral species from passing down the otherwise unobstructed system axis and being detected by the electron multiplier.

The effects of collector electrode voltage on ion signal with the TR-30-C2 and HEN-170-AA nebulisers are shown in Figures 7.9 and 7.10 respectively. Maximum ion signals were obtained at a collector electrode setting of 7.50 for both nebulisers which was equal to -2.5 V.

The effects of collector electrode voltage on the ratios of oxide and doubly charged ions to singly charged ions for the TR-30-C2 and HEN-170-AA nebulisers are shown in Table 7.8.
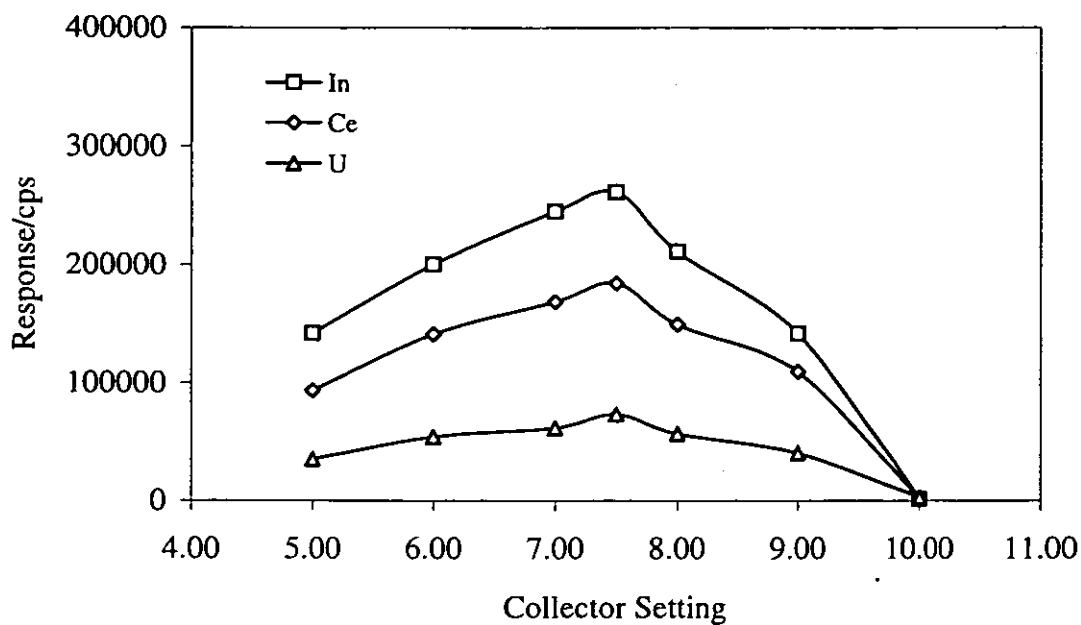
Figure 7.9: Dependence of ion signals on collector electrode voltage with TR-30-C2 nebuliser.
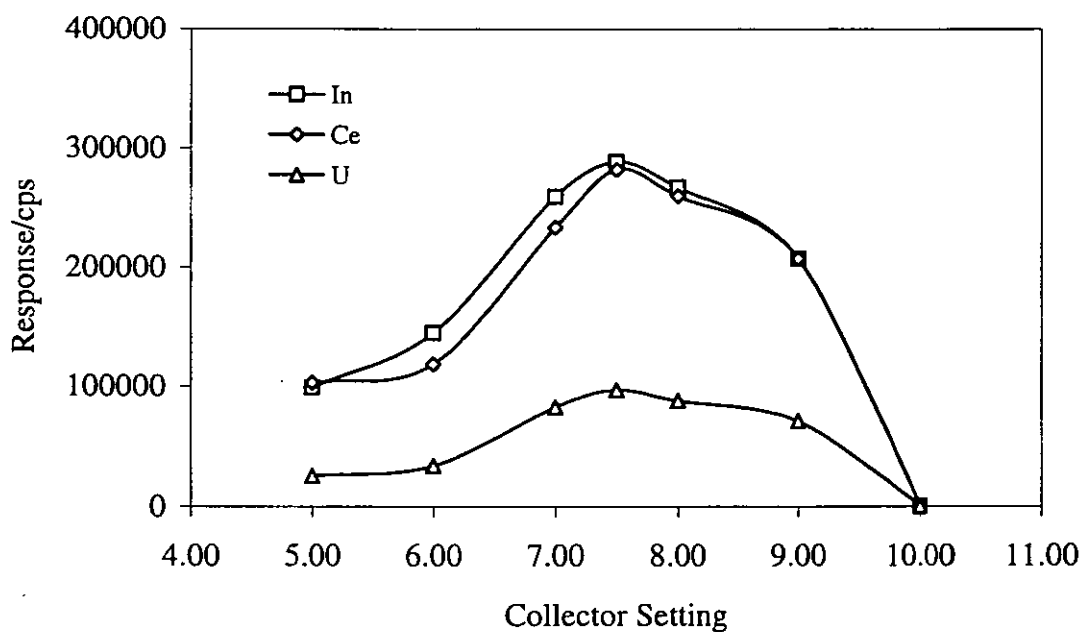

Figure 7.10: Dependence of ion signals on collector electrode voltage with HEN-170-AA nebuliser.

Table 7.8: Dependence of oxide and doubly charged ion ratios on collector electrode voltage.

Dial Setting	TR-30-C2		HEN-170-AA	
	$\%CeO^+/Ce^+$	$\%U^{2+}/U^+$	$\%CeO^+/Ce^+$	$\%U^{2+}/U^+$
5.00	2.57	5.46	0.53	5.42
6.00	2.60	4.68	0.49	5.85
7.00	2.57	4.86	0.51	3.76
7.50	2.62	4.05	0.43	3.42
8.00	2.38	4.57	0.42	3.59
9.00	2.14	3.85	0.50	2.89
10.00	13.95	6.33	14.42	16.16

7.3.4.3 L1 Lens

Ions passing around the photon stop are focused through the differential pumping aperture by lens elements L1 and L2. Effects of L1 lens voltage on ion signal with the TR-30-C2 and HEN-170-AA nebulisers are shown in Figures 7.11 and 7.12 respectively. The maximum ion signal was obtained at the L1 lens setting of 7.50 for both nebulisers which was equal to -2.5 V.

The effects of L1 lens voltage on the ratios of oxide and doubly charged ions to singly charged ions for the TR-30-C2 and HEN-170-AA nebulisers are shown in Table 7.9.
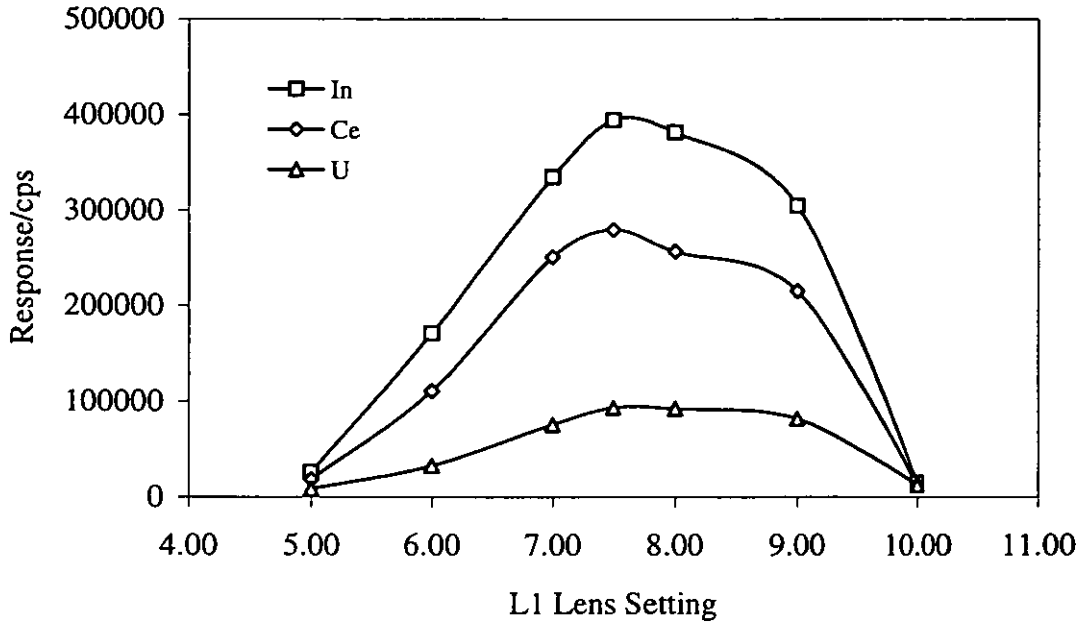
Figure 7.11:   Dependence of ion signals on L1 lens voltage with TR-30-C2
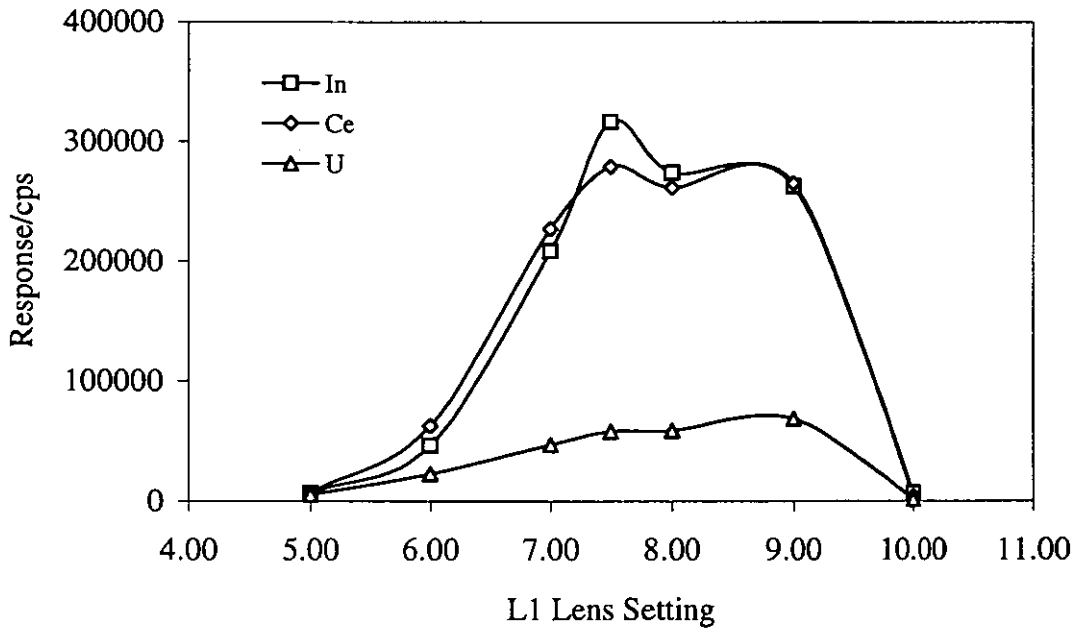nebuliser.

Figure 7.12:   Dependence of ion signals on L1 lens voltage with HEN-170-AA
nebuliser.

Table 7.9:   Dependence of oxide and doubly charged ion ratios on L1 lens voltage.

Dial Setting	TR-30-C2		HEN-170-AA	
	%CeO$^+$/Ce$^+$	%U^{2+}/U$^+$	%CeO$^+$/Ce$^+$	%U^{2+}/U$^+$
5.00	1.75	3.90	1.37	2.03
6.00	2.07	5.49	0.60	1.78
7.00	2.69	5.44	0.45	4.17
7.50	2.47	4.88	0.41	5.67
8.00	2.62	4.89	0.46	5.12
9.00	2.36	4.39	0.46	4.60
10.00	7.53	6.02	4.87	13.71

7.3.4.4   L3 Lens

The final lens elements L3 and L4 serve to refocus the ions emerging from the differential aperture into the entrance aperture of the quadrupole. The focusing fields are produced by the difference in voltage between the two elements of lens pairs (L1, L2) and (L3, L4).

The effects of L3 lens voltage on ion signal with the TR-30-C2 and HEN-170-AA nebulisers are shown in Figures 7.13 and 7.14 respectively. The maximum ion signal was obtained at the L3 lens setting of 5.00 for both nebulisers which was equal to 0 V.

The effects of L3 lens voltage on the ratios of oxide and doubly charged ions to singly charged ions for the TR-30-C2 and HEN-170-AA nebulisers are shown in Table 7.10.
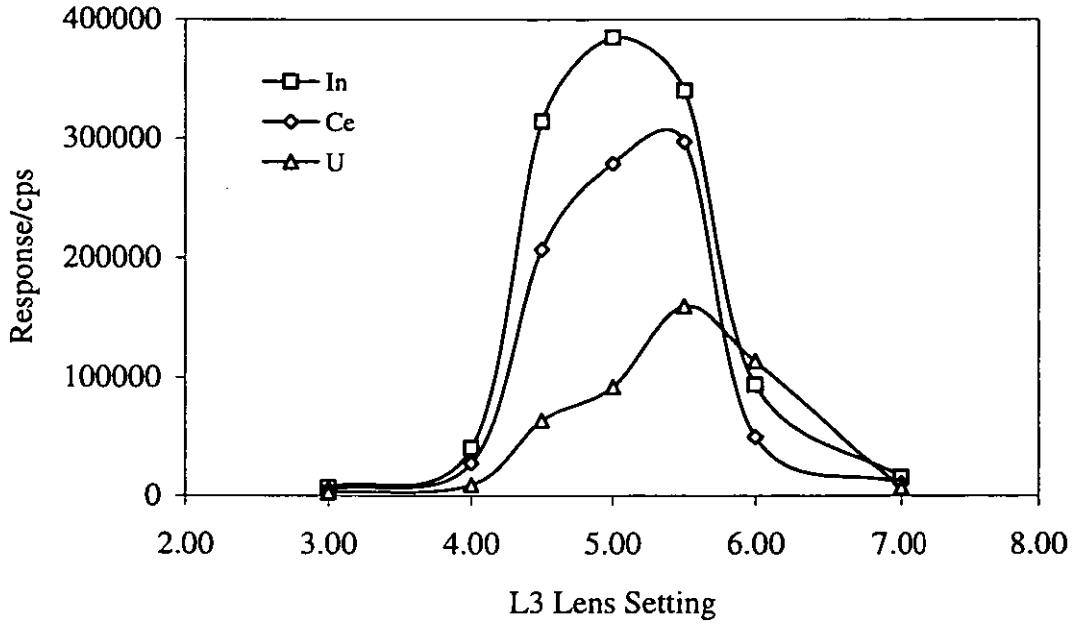
Figure 7.13: Dependence of ion signals on L3 lens voltage with TR-30-C2 nebuliser.
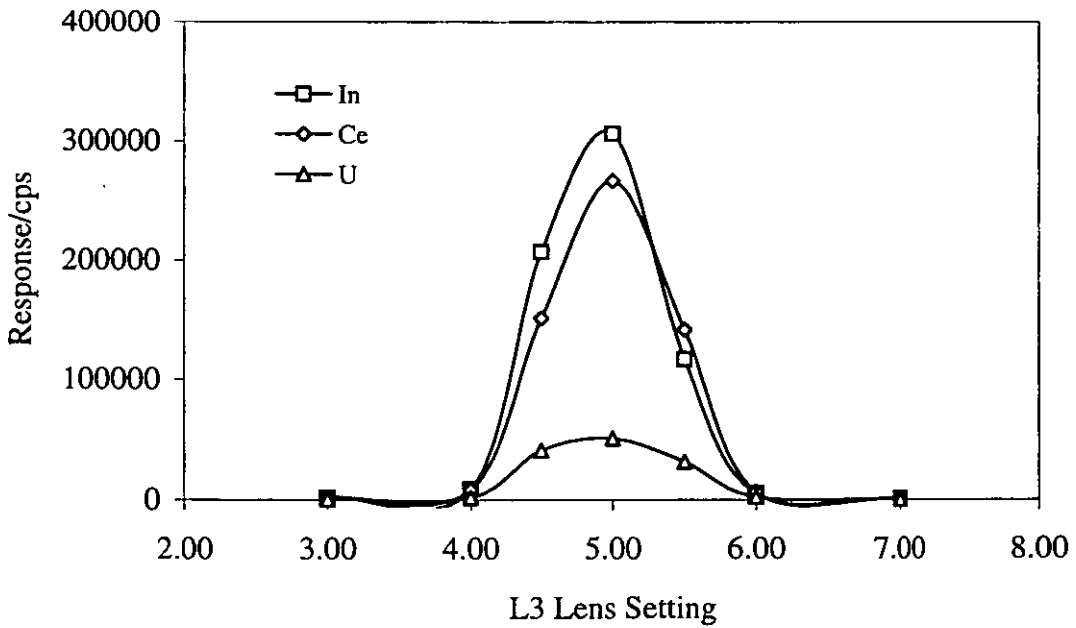

Figure 7.14: Dependence of ion signals on L3 lens voltage with HEN-170-AA nebuliser.

Table 7.10: Dependence of oxide and doubly charged ion ratios on L3 lens voltage.

Dial Setting	TR-30-C2		HEN-170-AA	
	$\%CeO^+/Ce^+$	$\%U^{2+}/U^+$	$\%CeO^+/Ce^+$	$\%U^{2+}/U^+$
3.00	16.33	38.47	3.84	22.26
4.00	5.90	17.76	1.91	11.64
4.50	2.44	6.66	0.39	4.61
5.00	2.67	4.91	0.44	6.08
5.50	2.46	2.31	0.49	4.81
6.00	3.95	1.41	1.82	4.11
7.00	9.67	17.53	5.90	13.37

The ion lens voltages did not have a very significant effect on the production of oxide and doubly charged ions. The oxide ratios at the settings for maximum ion signal were in the range 0.40 - 2.60 %. Slightly higher ratios were observed for doubly charged, but within accepted values.

7.3.5 Effects of Solution Uptake Rate

For solution delivery, standard PVC manifold tubes (Omnifit, Cambridge, UK) were used with a peristaltic pump (Model Minipuls 2, Gilson Medical Electronic, Villiers-Le-Bel, France). The internal diameters of the tubes used were 0.76 mm (black tagged) for the TR-30-C2 nebuliser and 0.25 mm (orange/blue tagged) for the HEN-170-AA nebuliser.

Calibrations of the solution uptake rate at different pump settings were achieved by weighing the solutions at 1 min intervals. For the TR-30-C2 nebuliser, pump settings of 100 to 900 were used and pump settings of 25 to 300 were used for the HEN-170-AA nebuliser.

The experiments on varying solution uptake rate were carried using the multielement solution containing 50 ng ml^{-1} Ni, In, Ce, Pb and U. Optimum ICP-MS operating parameters were set as in Table 7.1.

Calibration graphs of solution uptake versus pump settings for the TR-30-C2 and HEN-170-AA nebulisers are shown in Figures 7.15 and 7.16 respectively.

For the TR-30-2C nebuliser, the ion signal reached a peak at a pump setting 500 which corresponded to a solution uptake rate of 0.55 ml min^{-1}, as shown in Figure 7.17. For the HEN-170-AA nebuliser, the highest signal was obtained at a pump setting 125 which correspond to a solution uptake rate of 40 µl min^{-1}, as shown in Figure 7.18.

There was little variation in the count rates for solution uptake rates above 0.55 ml min^{-1} for TR-30-C2 nebuliser and above 40.0 µl min^{-1} for HEN-170-AA nebuliser. Further increase in solution uptake rate gave constant signals for both nebulisers. The increase in nebuliser mass transport, as the uptake rate was increased, was balanced by a lower nebuliser transport efficiency so that the net mass transport rate to the plasma remained roughly constant.

7.4   INSTRUMENT SENSITIVITY AND DETECTION LIMITS

7.4.1   Sensitivity

Sensitivity in ICP-MS is determined by the production of ions in the plasma and the efficiency of extraction and transmission of these ions through the interface region, the ion optics, the mass analyser and finally to the detector.

Sensitivity determinations with TR-30-C2 and HEN-170-AA nebulisers at the optimum instrument conditions were performed using scanning mode, with data
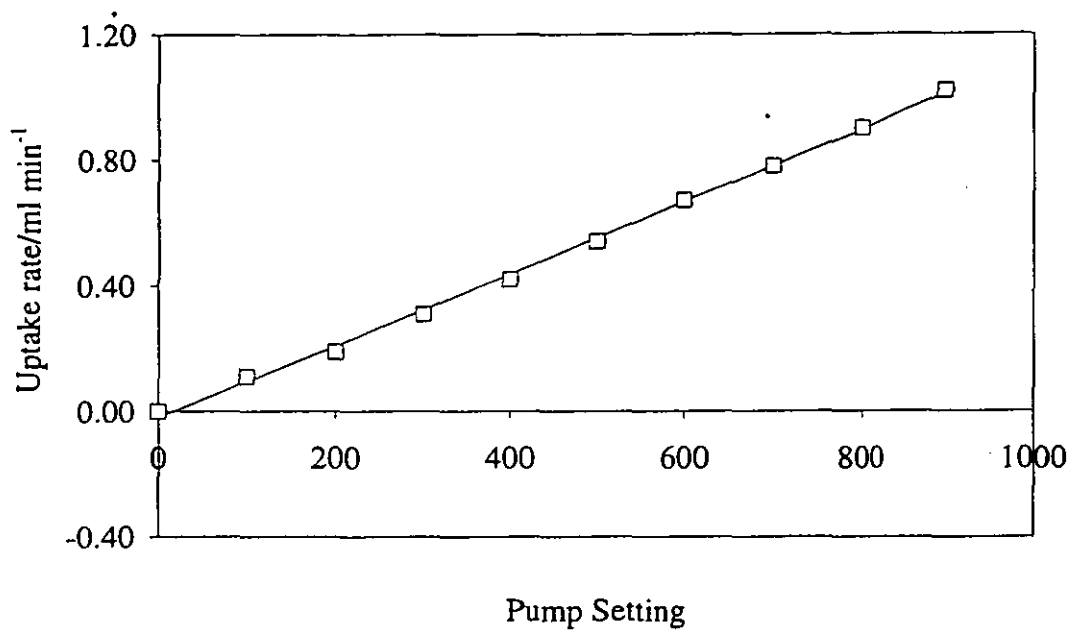
Figure 7.15: Calibration of solution uptake rate with 0.76 mm i.d. tube with TR-30-C2 nebuliser.
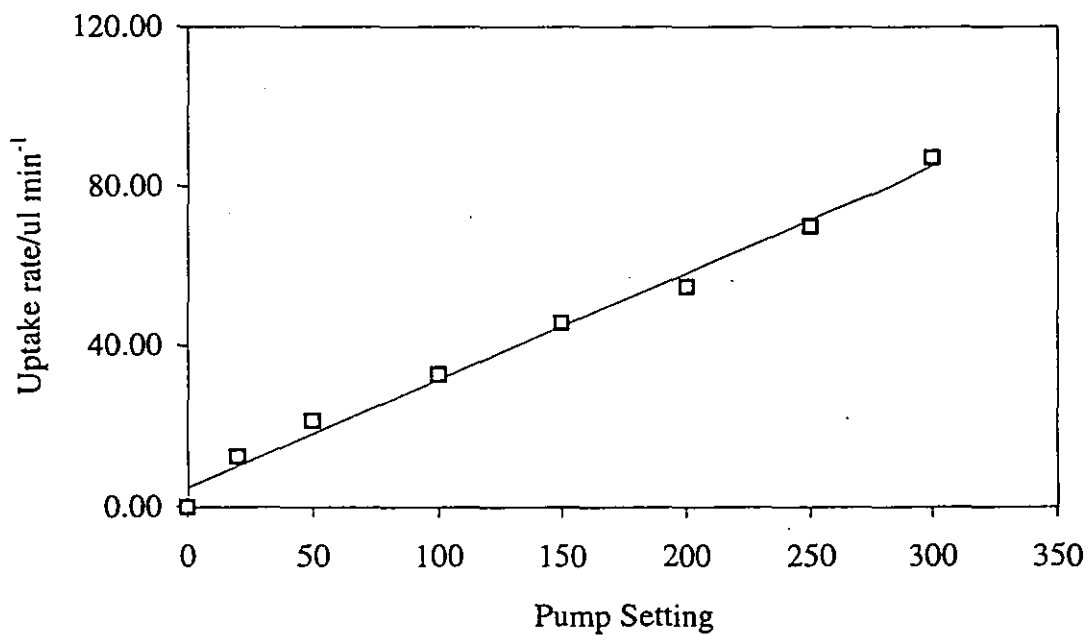

Figure 7.16: Calibration of solution uptake rate with 0.25 mm i.d. tube with HEN-170-AA nebuliser.
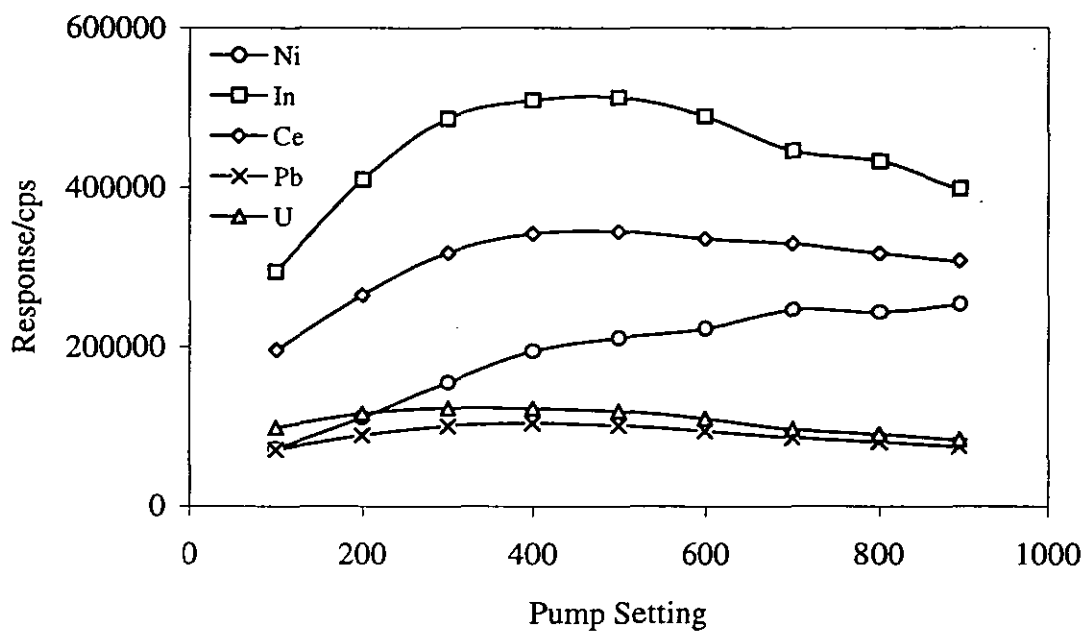
Figure 7.17:   Dependence of ion signals on solution uptake rate with TR-30-C2
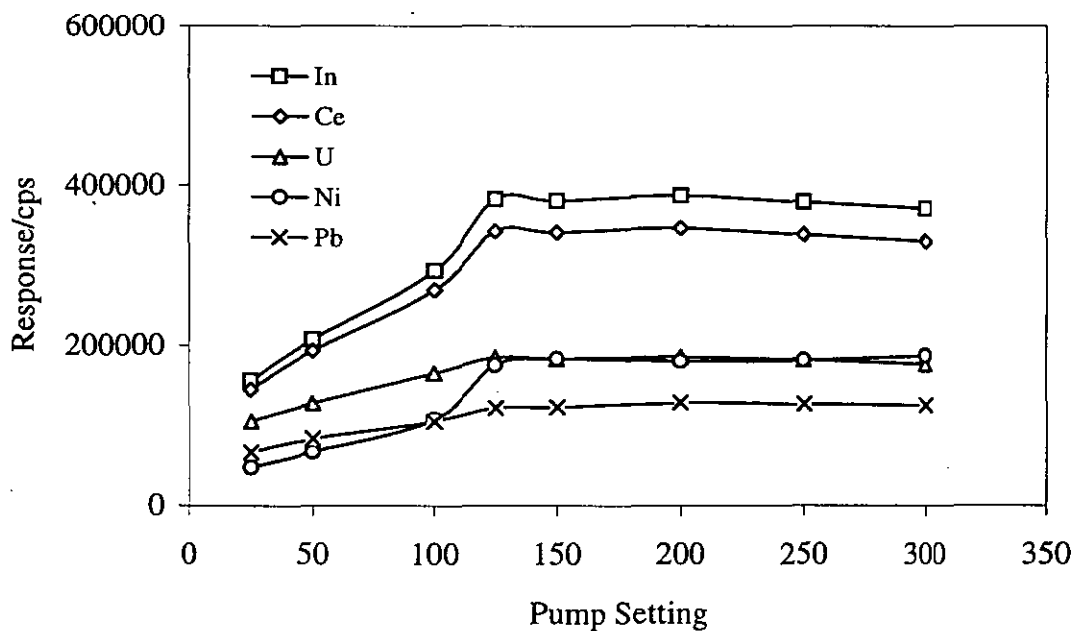   nebuliser.

Figure 7.18:   Dependence of ion signals on solution uptake rate with HEN-170-AA
                nebuliser.

acquisition parameters: dwell time 320.0 μs, 25 channels per amu and 0.5 s per sweep for 7 elements. Each data point was the mean of 4 measurements.

Sensitivity is reported in counts s^{-1} per μg ml^{-1} as shown in Table 7.11.

Table 7.11: Sensitivities for nebulisation with TR-30-C2 and HEN-170-AA.

Elements	Abundance/%	Sensitivities/cps per μg ml^{-1}	
		TR-30-C2	HEN-170-AA
^{9}Be	100.00	2.65x10^6	3.27x10^6
^{59}Co	100.00	7.58x10^6	5.99x10^6
^{60}Ni	58.27	6.19x10^6	6.86x10^6
^{115}In	95.70	1.06x10^7	1.00x10^7
^{140}Ce	88.48	7.79x10^6	8.54x10^6
^{208}Pb	52.40	3.87x10^6	5.61x10^6
^{238}U	99.27	2.41x10^6	2.17x10^6

The sensitivity obtained for the HEN-170-AA nebuliser was as good and in most cases better than that obtained with the TR-30-C2 nebuliser although the uptake rate was μl compared with ml min^{-1}. The transport efficiency for the HEN has been shown to be the order of 20 % compared with only 1-2 % for the standard nebuliser [11].

7.4.2 Detection Limits

Detection limits is defined as the concentration giving a signal equivalent to 3 times the noise. Noise was calculated from the standard deviation of 11 repetitive measurements of the background intensity using a 3 s integration time. Detection limit can be calculated as:

$$\text{Detection limit} = \frac{3\sigma \text{ of counts blank}}{(\text{counts analyte} - \text{counts blank})} \times \text{concentration of analyte} \quad (3.1)$$

Detection limits with the TR-30-C2 and HEN-170-AA nebulisers were measured at the optimum instrument conditions as given in Table 7.1. 11 determinations of a blank solution (1% HNO_3) at 3 s integration time each were acquired using single ion monitoring. 3 times the standard deviation of the data was calculated. This was followed by an integration for a 10 ng ml^{-1} solution of the elements. The detection limits were calculated using equation 3.1 above.

The detection limits measured with TR-30-C2 and HEN-170-AA nebulisers are shown in Table 7.12.

Table 7.12: Detection limits for nebulisation with TR-30-C2 and HEN-170-AA nebulisers

Elements	Detection Limit/ng l^{-1}	
	TR-30-C2	HEN-170-AA
^{9}Be	44.6	35.7
^{59}Co	8.1	10.3
^{60}Ni	31.8	28.5
^{115}In	28.2	29.9
^{140}Ce	9.4	8.6
^{208}Pb	26.4	18.1
^{238}U	40.4	44.9

Detection limits obtained using the HEN and standard nebuliser were very similar despite the fact that the liquid sample uptake rate for the HEN is more than 10 times smaller. The production of finer droplets and the higher transport efficiency in the HEN were the contributed factors.

7.5 SHORT TERM AND LONG TERM STABILITY TEST

For the short term stability test, the RSD of the signal intensity was calculated for 60 successive sweeps, recorded in 6 min using the peak jumping method for 5 elements with 3 points per peak and 20.48 ms dwell time yielding an integration time of 1 s mass^{-1}.

For the determination of long term stability, data was acquired every 5 min over a 4 hour period using the same conditions as for the short term stability test.

The stability tests are performed on the instrument and not just the nebulisers, but nevertheless, any significant differences between the nebulisers should be apparent. Also the TR-30-C2 nebuliser is working in conjunction with the standard spray chamber and the HEN-170-AA nebuliser with the U-shaped spray chamber connected with 50 cm long tubing to the torch.

The summarised data for the short and long term stability tests with the TR-30-C2 and HEN-170-AA nebulisers are shown in Table 7.13.

Table 7.13:   Short and long term stability test.

Elements	Short Term Stability (RSD/%)		Long Term Stability (RSD/%)	
	TR-30-C2	HEN-170-AA	TR-30-C2	HEN-170-AA
^{60}Ni	3.25	2.79	3.14	4.26
^{115}In	2.10	2.40	1.76	3.25
^{140}Ce	2.51	2.36	2.58	3.41
^{208}Pb	1.67	2.34	3.67	4.54
^{238}U	2.09	2.86	2.97	3.81

The RSD for short term stability obtained for the HEN was similar to that for the standard nebuliser. For the long term stability test, the RSD measured for the HEN was slightly poorer than the standard nebuliser.

7.6   RELATIVE ISOTOPIC RATIO

The ICP-MS technique is capable of both elemental detection and isotope ratio measurements. Although a few elements have only one isotope, the majority have two or more. There are potentially, therefore, many elements for which isotope ratio determinations can be made. Measurements of isotopic ratios can provide important information in many areas including geological dating, biological studies and nutrition [12-14].

A 50 ng ml^{-1} multielement solution containing Be, Mg, Co,, Ni, In, Ce, Pb and U in 1% HNO_3 was used for isotopic ratios measurement with the TR-30-C2 and HEN-170-AA nebulisers. ICP-MS operating conditions were set at the optimum. Peak jumping data acquisition mode with 3 points per peak and 20.48 ms dwell time was employed for the determination of isotopic ratios [15]. 10 measurements were made for the calculation of the isotopic ratios of ^{58}Ni:^{60}Ni and ^{208}Pb:^{206}Pb.

Table 7.14 shows the isotopic ratios for ^{58}Ni:^{60}Ni and ^{208}Pb:^{206}Pb with the TR-30-C2 and HEN-170-AA nebulisers.

Table 7.14:   Isotopic ratios for ^{58}Ni:^{60}Ni and ^{208}Pb:^{206}Pb.

Ratio	Percentage of the Ratio		
	TR-30-C2	HEN-170-AA	Accepted Value
$^{58}Ni/^{60}Ni$	2.61	2.48	2.24
$^{208}Pb/^{206}Pb$	2.10	2.02	2.17

Surprisingly the values are different for the nebulisers perhaps indicating that mass bias effects differ depend on the type of nebuliser used.

7.7 CONCLUSIONS

In this investigation, the various ICP-MS operating parameters have been studied in order to optimise ion signals and minimise possible spectroscopic interferences from oxide and doubly charged ions for the TR-30-C2 and HEN-170-AA nebulisers. The solution uptake rate for the TR nebuliser was 0.55 ml min^{-1} and for the HEN nebuliser 40 μl min^{-1}. The optimised plasma conditions for both nebulisers were nebuliser flow rate 0.75 l min^{-1} for the TR and 1.0 l min^{-1} for the HEN, rf forward power of 1.30 kW and sampling depth of 12.00 mm. For the ion lenses, extraction voltage was -325 V, collector -2.5 V, L1 lens -2.5 V and L3 lens 0 V.

The sensitivities and detection limits obtained were similar for the seven elements measured, even though the uptake rate for both nebulisers were very different. Similar findings have been reported by other workers [16].

The short term stability test yielded RSD's of 1.67 - 3.25 % for the TR-30-C2 and 1.76 - 4.54 % for the HEN-170-AA nebuliser. This short term precision was similar for both nebulisers, but long term stability was slightly better for the TR than for the HEN nebuliser. Occasional blockage was also a problem with the HEN.

The isotopic ratio data obtained with the TR-30-C2 and HEN-170-AA nebulisers were comparable to the accepted values from the literature [17]. The ^{58}Ni/^{60}Ni ratio had errors of 16.5% and 10.7%, compared to the accepted value, when measured with TR and HEN nebulisers respectively. The ratios for ^{208}Pb/^{206}Pb were much better, error values of 3.2% and 6.9% were obtained for the TR and HEN nebulisers respectively.

The use of the HEN-170-AA nebuliser, with a very low solution uptake rate, as an alternative to the TR-30-C2 nebuliser is very useful when a small volume of sample is available or when coupled to a device with a low solution output. It has been shown that the HEN nebuliser can give comparable analytical performance to the TR nebuliser.

REFERENCES

1.   Horlick, G., Tan, S. H., Vaughan, M. A., and Rose, C. A., *Spectrochim. Acta*, 1985, **40B**, 1555.

2.   Vaughan, M. A., and Horlick, G., *Appl. Spectrosc.*, 1986, **40**, 434.

3.   Vaughan, M. A., Horlick, G., and Tan, H., *J. Anal. At. Spectrom.*, 1987, **2**, 765.

4.   Long, S. E., and Brown, R. M., *Analyst*, 1986, **111**, 901.

5.   Gray, A. L., and Williams, J. G., *J. Anal. At. Spectrom.*, 1987, **2**, 599.

6.   Zhu, G., and Browner, F., *Appl. Spectrosc.*, 1987, **41**, 349.

7.   Schmit, J. P., and Chauvette, A., *J. Anal. At. Spectrom.*, 1989, **4**, 755.

8.   Evans, E. H., and Ebdon, L., *J. Anal. At. Spectrom*, 1991, **6**, 421.

9.   Evans, E. H., and Caruso, J. A., *Spectrochim. Acta*, 1992, **47B**, 1001.

10.   Gray, A. L., and Date, A. R., *Analyst*, 1983, **108**, 1033.

11.   Olesik, J. W., Kinzer, J. A., and Harkleroad, B., *Anal. Chem.*, 1994, **66**, 2022.

12.   Russ Ill, J. P., Bazan, J. M., and Date, A. R., *Anal. Chem.*, 1987, **59**, 984.

13.   Whitaker, P. G., Barrett, J. F. R., and Williams, J. G., *J. Anal. At. Spectrom.*, 1992, **7**, 109.

14.   Campbell, M. J., and Delves, H. T., *J. Anal. At. Spectrom.*, 1989, **4**, 235.

15.   Begley, I. S., and Sharp, B. L., *J. Anal. At. Spectrom*, 1994, **9**, 171.

16.   Nam, S. H., Lim, J. S., and Montaser, A., *J. Anal. At. Spectrom*, 1994, **9**, 1357.

17.   Date, A. R., and Gray, A. L., *Spectrochim. Acta*, 1983, **38B**, 29.

Chapter 8

CHAPTER EIGHT

COUPLING OF CAPILLARY ELECTROPHORESIS TO INDUCTIVELY COUPLED PLASMA-MASS SPECTROMETRY

8.1   INTRODUCTION TO CHAPTER

This chapter describes a laboratory designed and constructed CE system and an interface to couple it with ICP-MS. Evaluation and optimisation of the CE system and the interface also will be discussed.

8.2   DESIGN AND CONSTRUCTION OF THE CE SYSTEM

A CE system designed and constructed in our laboratory consisted of a high voltage power supply, buffer and sample reservoirs, high voltage electrodes, separation capillary, sample injection system and safety compartment as shown in Figure 8.1. A regulated high voltage power supply (Brandenburg Model 805, Croydon, Surrey, UK) delivering 0-30 kV and current range of 0-20 mA was used to drive the electrophoresis process. Electrophoretic currents were measured using a digital multimeter (Model ISO-Tech 90 Series, RS Components, Corby, Northants, UK) in the ammeter mode placed between the electrical connection to outlet end of the capillary and the ground of the high voltage power supply. The power supply could be switched to positive or negative output depending on the application requirements. The operator was protected from accidental contact with the high voltage through an interlock system.

The buffer and sample reservoirs assembly consisted of two 1 ml polyethylene vials mounted on a base with a stand which held the electrode and capillary into the solutions. The base, stand and holder were specially designed and made of PTFE to avoid electrical isolation problems. The terminal electrodes used were a platinum

wire at the inlet end and a platinum-iridium (Pt-Ir) tube at the outlet end. Fused silica capillaries (SGE Limited, Milton Keynes, UK) with 100 μm i.d., 330 μm o.d. and total length of 100 cm were used. The capillaries were coated with ES2 coating (SGE Limited, Milton Keynes, UK) which has the characteristics of hydrophilic and hydrolytic stability and provides surface deactivation.

Two types of injection technique could be applied for sample introduction. The electrokinetic method had the capillary and electrode dipped into the sample vial, whilst a voltage was applied for a short interval causing the components of the sample to migrate into the separation capillary. The hydrodynamic method took advantage of a difference in level between the buffer reservoir and the sample vial for the introduction of small sample volumes.

The whole CE set-up (except the high-voltage power supply) was placed in a perspex box. For safety, an automatic shut-off switch was mounted on the door and a safety light was installed as an additional precaution. Opening the box automatically cut off the high voltage in the event that the operator has neglected to turn off the voltage manually. The detection system for the CE was an ICP-MS (as described in Chapter 7) with a specially designed interface.

8.3   DEVICE FOR FILLING AND FLUSHING CAPILLARIES

The capillaries used in the CE technique normally display a high hydrodynamic resistance and require a high pressure for their filling and flushing. A simple device was constructed as a means of conveniently introducing and changing buffer or conditioning solution in the capillary. The device consisted of easily available components as shown in Figure 8.2.

A luer adapter was connected with a PTFE union to a PTFE tube. The PTFE tube was connected to a silicone rubber tube (0.4 mm i.d.) for a tight insertion of the capillary column. Buffer or conditioning solutions were introduced using a 1 ml
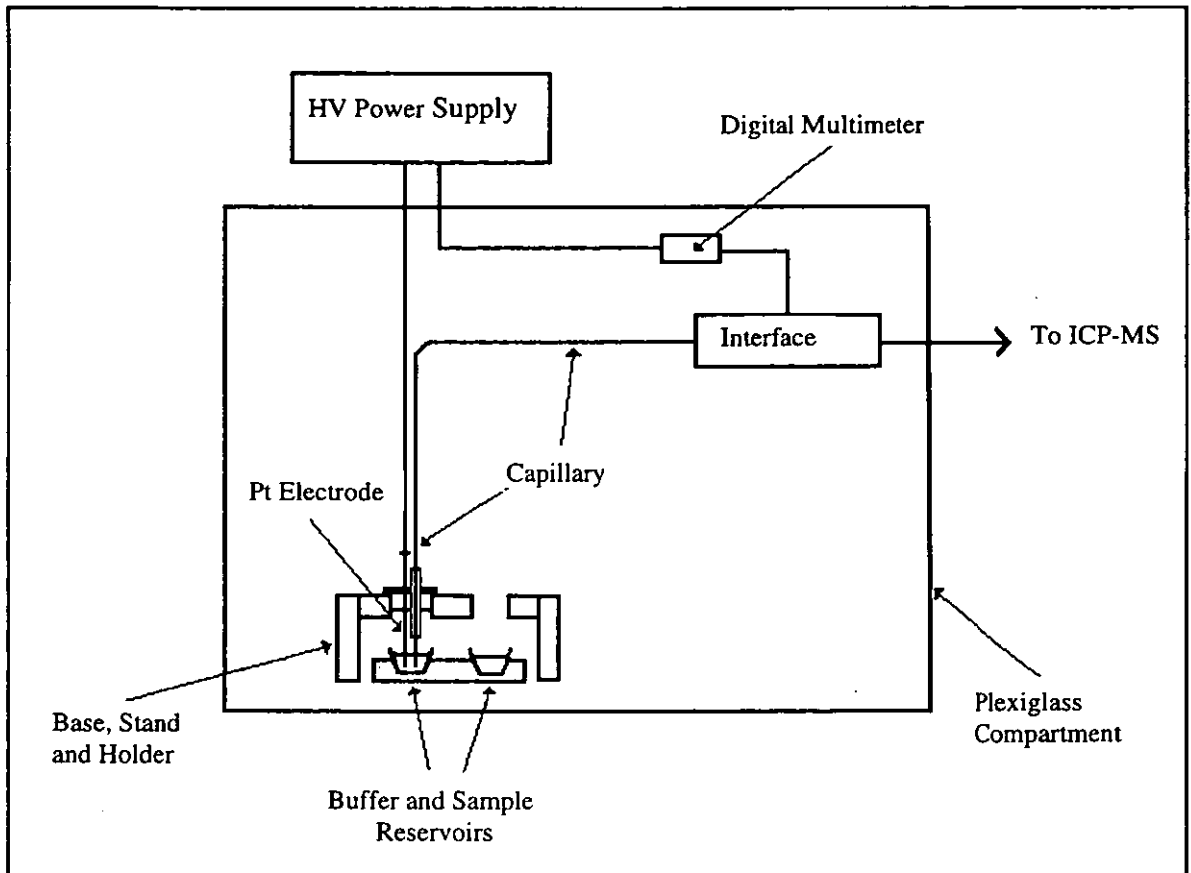
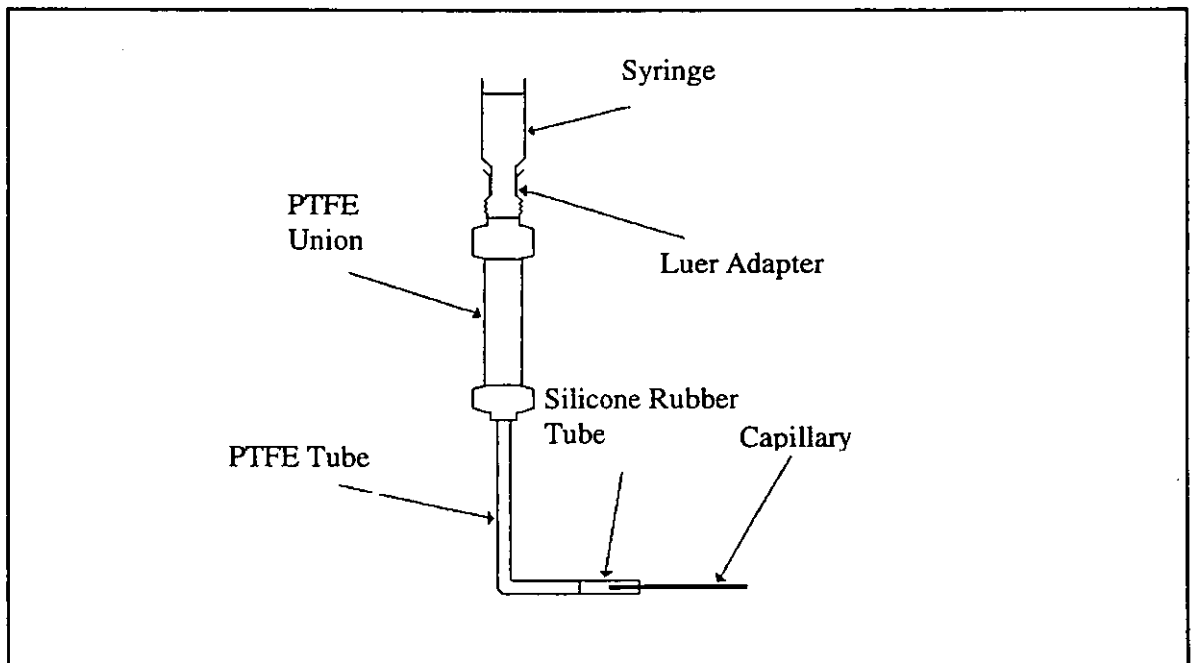Figure 8.1:   Schematic of the laboratory built CE.

Figure 8.2:   Simple device for filling and flushing capillaries.

syringe, either manually, or by syringe pump. Connection and disconnection of the capillary must be easy to avoid the risk of breaking or damaging the delicate tube.

8.4   INTERFACE FOR CE-ICP-MS

A specially designed and fabricated interface was used to couple the CE system to the ICP-MS instrument as shown in Figure 8.3. The outlet end of the CE capillary was inserted through a 0.5 mm i.d. Pt-Ir tube. Both the capillary and the Pt-Ir tube were placed into the inlet of the centre tube of a nebuliser. A silicone rubber tube was used to effect air tight fitting between the Pt-Ir tube and the nebuliser.

A PTFE block adapter was fabricated to hold the interface in place. To obtain a leak proof connection between the capillary, the Pt-Ir tube and the PTFE block, they were sealed with polyimide resin (Fluka, Gillingham, Dorset, UK). The Pt-Ir tube acted as an electrode and was connected to the power supply ground by a liquid sheath flow of electrolyte.

Two nebulisers, a high efficiency nebuliser (Type HEN-170-AA, J. E. Meinhard Associates Inc., Santa Ana, CA, USA) and a standard concentric nebuliser (Type TR-30-C2, J. E. Meinhard Associates Inc., Santa Ana, CA, USA) were used. They were coupled to a home-made U-shaped spray chamber (28.5 ml internal volume), which was connected by a 50 cm, 4 mm i.d. flexible tube to the ICP-MS torch. Makeup liquid flowing in the sheath outside the CE capillary also allowed the nebuliser to be optimised independently of the CE system for efficient sample introduction to the ICP-MS instrument. The make-up solution was delivered using a peristaltic pump (Model Minipuls2, Gilson Medical Electronic, Villiers-Le-Bel, France). A syringe pump (Model 341A, Sage Instruments, Orion Research Inc., Cambridge, MA, USA) was used with the special device for filling and flushing the CE capillaries.
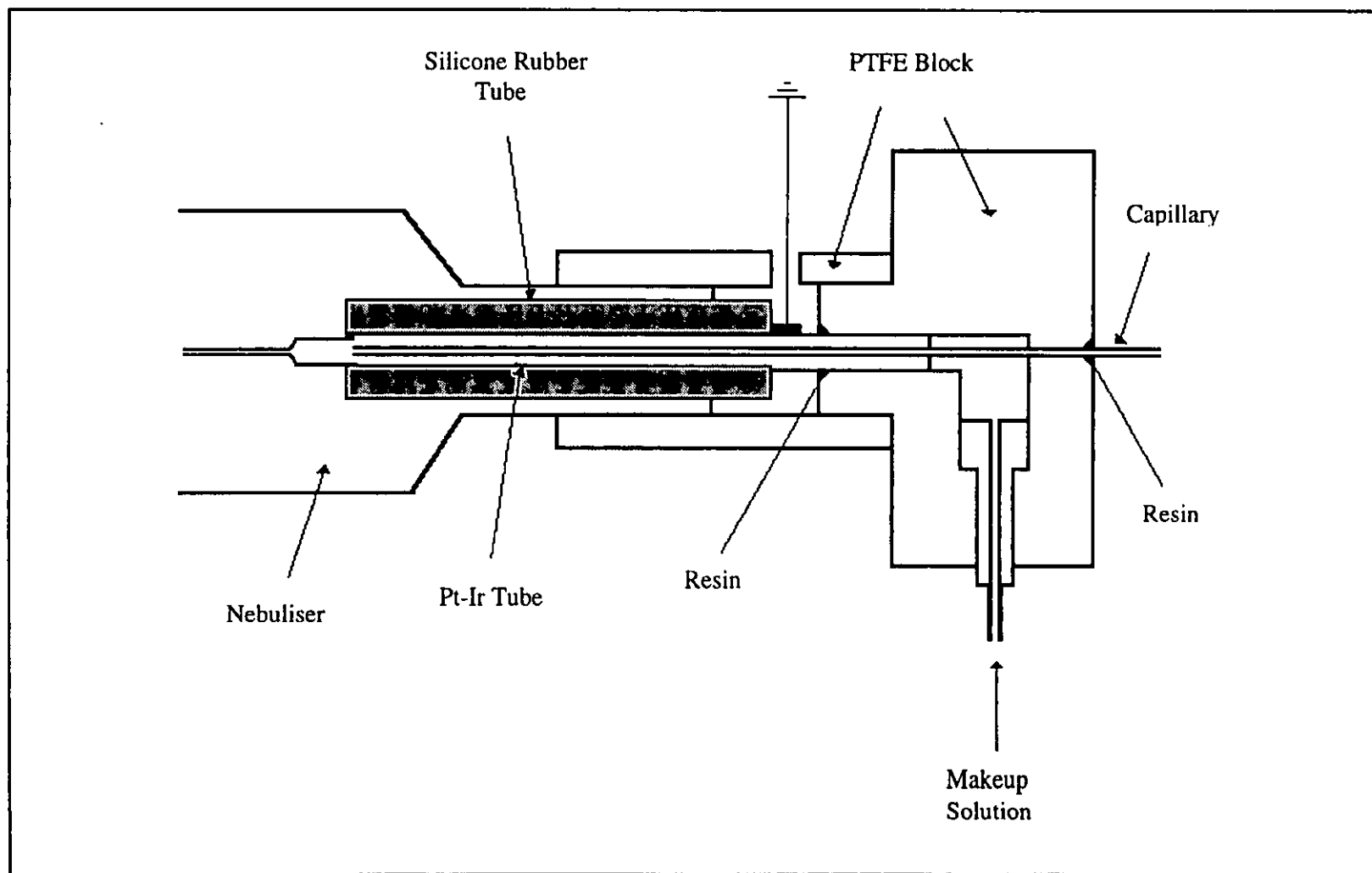
Figure 8.3:   Layout of CE-ICP-MS Interface.

8.5 OPERATION PROTOCOL FOR THE CE-ICP-MS

The following routine was adopted to operate the CE-ICP-MS system.

8.5.1 ICP-MS Operation Protocol

The ICP-MS system was switched on and allowed to stabilised for approximately 30 min. The ICP-MS operation protocol is described in Appendix A.

8.5.2 CE Capillaries Flushing and Filling

While waiting for the ICP-MS instrument to stabilise, the CE capillary was pre-treated with 0.10 M sodium hydroxide solution for 2 min, deionised water for 2 min and buffer solution for 5 min in turn prior to each day of analysis. Flushing with buffer solution was employed before each measurement.

8.5.3 ICP-MS Optimisation

For ICP-MS optimisation, 50 ng ml^{-1} multielement solution was delivered through the makeup flow of the CE system to the ICP-MS. A solution flow rate about 40 μl min^{-1} was employed. ICP-MS operating conditions when coupled with the CE system were the same to the optimised operating conditions as stated in Table 7.1, Chapter 7.

8.5.4 CE Sample Injection

Samples were introduced into the CE system by hydrodynamic injection at 15 cm height different for 10 s. Peristaltic pumping of the makeup solution was switched off during sample injection to avoid back pressure in the capillary. The nebuliser gas flow was turned to minimum to stop the nebuliser natural aspiration which cause suction on the capillary.

142

8.5.5 CE Operation Protocol

For successful CE separation, it was important to follow the operation procedure as shown below:

- Switch on the multimeter in ammeter mode.

- Dip the CE capillary and electrode into the buffer reservoir.

- Close the box lid.

- Switch on the peristaltic pump.

- Switch on the high voltage power supply; MAIN and followed by HT.

- Increase the voltage up to 15 kV.

- Start the timer.

- Increase the nebuliser gas pressure up to 155 psi (for HEN-170-AA) and 28 psi (for TR-30-C2).

- Start the TRAnalysis software.

8.5.6 Data Acquisition and Processing

ICP-MS data acquisition during CE-ICP-MS analyses was performed in time resolved analysis mode using TRAnalysis software, version 4.1.2 (Fisons plc, Uxbridge, Middlesex, UK). The TRAnalysis software was installed on a personal computer (Dell 486/L, Dell Computer Corporation, Austin, Texas, USA) running O/S2 Presentation Manager Graphical User Interface (IBM United Kingdom Limited, Portsmouth, UK).

The TRAnalysis software permitted data to be acquired at specified intervals over a period of time. The signals were monitored in peak jumping mode for an appropriate time of analysis. Data were converted into comma separated variable (CSV) files and exported into Microsoft Excel version 4.0 (Microsoft Corporation, Redmond, WA, USA) for further analysis.

8.6   CHEMICALS

The borate buffer used was prepared from disodium tetraborate (Fisons, Loughborough, UK). 0.10 M, 0.01 M, 0.05 M and 0.005 M borate solutions containing 10 ng ml^{-1} indium (SpectroSol, BDH, Poole, Dorset, UK) were prepared by dissolving appropriate amounts of the chemicals in deionised water and adjusting the pH of the solution to 8.50 with 0.10 M ammonium hydroxide (Biochemika, Fluka, Gillingham, Dorset, UK) or 0.10 M nitric acid (Aristar, BDH, Poole, Dorset, UK).

A solution of 0.01 M ammonium chloride (A.R., Fisons, Loughborough, UK) containing 10 ng ml^{-1} cerium (SpectroSol, BDH, Poole, Dorset, UK) was used as the makeup solution. A olution of 0.1 M sodium hydroxide (HPCE Grade, Biochemika, Fluka, Gillingham, Dorset, UK) was used to precondition the CE capillary.

For optimisation of the ICP-MS system, a 50 ng ml^{-1} multielement solution containing Be, Mg, Co, Ni, In, Ce, Pb and U in 1% HNO_3 (SpectroSol, BDH, Poole, Dorset, UK or Specpure, Johnson Matthey, Royston, Herts, UK) was used.

High purity water (18 MΩ) was used for sample preparation, obtained from a Maxima pure water system (ELGA, High Wycombe, Bucks, UK).

8.7   INJECTION VOLUME AND PLUG LENGTH

The hydrodynamic injection method was used throughout the experiments to introduce sample into the separation capillary. The sample vial was elevated 15 cm above the nebuliser end of the capillary for a duration of 10 s. The volume injected and plug length can be calculated as follows:

$$\text{Volume injected, } V = \frac{\Delta P r^4 \pi \, t}{8 \eta \, L} \tag{8.1}$$

Pressure difference, $\Delta P = \rho \, g\Delta h$ $\qquad\qquad$ (8.2)

Plug length, $I = \dfrac{\Delta P r^2 t}{8\eta \, L}$ $\qquad\qquad$ (8.3)

Capillary volume $= \pi \, r^2 L$ $\qquad\qquad$ (8.4)

where, ΔP is the pressure difference across the capillary, r is the capillary radius, t is the injection time, η is the buffer viscosity, L is the total capillary length, ρ is the buffer density, g is the gravitational constant and Δh is the height differential of the reservoir.

Thus,

$$\Delta P = 9.9821 \times 10^2 \text{ kg m}^{-3} \times 9.8067 \text{ m s}^{-2} \times 15 \times 10^{-2} \text{ m}$$
$$= 1.4683 \times 10^3 \text{ kg m}^{-1}\text{s}^{-2} \text{ or Pa}$$

$$V = \frac{1.4683 \times 10^3 \text{ Pa} \times (50 \times 10^{-6})^4 \text{ m}^4 \times 3.1415 \times 10 \text{ s}}{8 \times 0.001002 \text{ Pa s} \times 1 \text{ m}}$$
$$= 3.5965 \times 10^{-11} \text{ m}^3$$
$$= 35.96 \text{ nl}$$

$$I = \frac{1.4683 \times 10^3 \text{ Pa} \times (50 \times 10^{-6})^2 \text{ m}^2 \times 10 \text{ s}}{8 \times 0.001002 \text{ Pa s} \times 1 \text{ m}}$$
$$= 4.5790 \times 10^{-3} \text{ m}$$
$$= 0.45 \text{ cm}$$

Capillary volume $= 3.1415 \times (50 \times 10^{-6})^2 \text{ m}^2 \times 1 \text{ m}$
$$= 7.8539 \times 10^{-9} \text{ m}^3$$
$$= 7.85 \, \mu\text{l}$$

Calculation of the percentage of the volume injected and the percentage of the plug length of the CE capillary occupied by the sample are as follow:

$$\text{Percentage of volume injected, } \%V = \frac{35.96 \times 10^{-3} \, \mu l}{7.85 \, \mu l} \times 100 \%$$

$$= 0.45 \%$$

$$\text{Percentage of plug length, } \%I = \frac{0.45 \, cm}{100 \, cm} \times 100 \%$$

$$= 0.45 \%$$

The sample plug length must be less than 1 to 2 % of the total length of the capillary to minimise the dispersion [1].

8.8   EVALUATION AND OPTIMISATION OF THE CE-ICP-MS INTERFACE

8.8.1   Capillary Flow Rate

Solution flows in the capillary were measured by weighing the mass of buffer transferred from the inlet reservoir to outlet reservoir or vice versa over a time period using an Oertling digital balance (Model NA114, GEC Avery, Warley, West Midland, UK). A 0.005 M borate solution was used as buffer solution flow through the capillary and 0.01 M ammonium chloride solution flow through the makeup liquid sheath flow.

8.8.1.1   Effects of Makeup Flow Rate

This experiment was carried out to measure the effects of makeup solution flow rate on the capillary flow rate. The nebuliser gas flow rate was fixed at 1 l min^{-1}, the CE

high voltage was switched off and the makeup flow rate was varied up to 40 μl min^{-1}. The results shown in Table 8.1 are the average values of at least two measured flows.

The capillary flow rate decreased as the makeup flow rate was increased. The capillary flow was due to the natural aspiration of the nebuliser which caused a slight vacuum in the capillary. As the makeup flow rate increased, the vacuum in the capillary was reduced as the nebuliser demand was satisfied.

Table 8.1: Dependence of the capillary flow rate on makeup flow rate. (Positive values indicate flow from the buffer reservoir to the detector).

Makeup Flow/Setting	Capillary Flow Rate/μl min^{-1}
Off	3.97
0	3.81
5	3.75
10	3.73
25	3.68
50	3.63
75	3.61
100	3.59
125	3.43

8.8.1.2   Effects of Voltage without Nebuliser Gas Flow

This experiment was carried out to determine the effects of CE voltage on the capillary flow rate when the nebuliser gas flow was turned off. The makeup flow rate was fixed at the maximum setting of 125 and the voltage was varied up to 20 kV. The high voltage output was set to negative polarity (negative at the inlet end). The results are shown in Table 8.2 and are the average of at least two values.

8.8.1.3   Effects of Voltage with Nebuliser Gas Flow

This experiment was carried out to measure the effects of CE voltage on the capillary flow rate when the nebuliser gas flow rate was set at 1 1 min^{-1}. The makeup flow rate was fixed at the setting of 125 and the voltage was varied up to 20 kV. The high voltage output was set to negative polarity. The results again are shown in Table 8.2.

Table 8.2:   Dependence of capillary flow rate on applied voltage.
(Positive values indicate flow from the buffer reservoir to the detector and negative values for vice versa).

Voltage/kV	Capillary Flow Rate/μl min^{-1}	
	Nebuliser = Off	Nebuliser = On
2.5	-0.05	3.38
5.0	-0.09	3.32
7.5	-0.12	3.31
10.0	-0.13	3.27
12.5	-0.19	3.24
15.0	-0.23	3.19
20.0	-0.30	3.15

The capillary flow, when the high voltage was applied across the capillary without the nebuliser gas flow, was due to EOF. Since the inlet end of the capillary was set to negative polarity, the EOF was going towards the inlet reservoir. This is shown as a negative reading in Table 8.2. As the high voltage was increased, the EOF rate was increased because the magnitude of the EOF is dependent on the applied electric field.

When the nebuliser gas flow was applied, capillary flow resulted from the natural aspiration of the nebuliser overcoming the flow rate induced by EOF. This resulted in positive capillary flow, as shown in column 3 of Table 8.2.

8.8.2 Natural Aspiration of the Nebuliser

As shown above, the nebuliser produced a slight vacuum which drew solution from the reservoir into the capillary. These experiments were to measure the time taken for the solution from the reservoir to reach detector because of the natural aspiration.

Two conditions were set for the measurements. The first measurement was with the high voltage off and the other was with the high voltage on. Other experimental conditions were: nebuliser flow rate at 1 l min^{-1}, 0.005 M borate buffer solution, 0.01 M ammonium chloride makeup solution at a flow rate of 40 μl min^{-1}. A solution of 20 ppm nickel:20 ppm humic acid was used as a test sample. Signals for ^{60}Ni were measured.

Figure 8.4 shows that the time taken for the sample to reach the detector was 2.06 min when high voltage was not applied. When high voltage was applied across the capillary, the time taken for the sample to reach the detector increased to 2.19 min. This was due to the effect of EOF which was contra to the nebuliser natural aspiration.

8.8.3 Response Time

A 50 ng ml^{-1} multielement solution was introduced through the makeup flow at a flow rate of 40 μl min^{-1}, whilst the high voltage was switched off. A 0.005 M borate solution was used as buffer solution in the capillary. Signals for ^{115}In and ^{60}Ni were detected to measure the time needed for the signals to equilibrate. The results are shown in Figure 8.5.

The ^{115}In signal needed approximately 18 s to reached equilibrium and the ^{60}Ni signal needed slightly longer times. This is much longer than is desirable and will add to peak broadening, although dispersion is much less than expected in aerosol flow [2]. It is a problem associated with using very low flow rate nebulisers. Higher flow rates
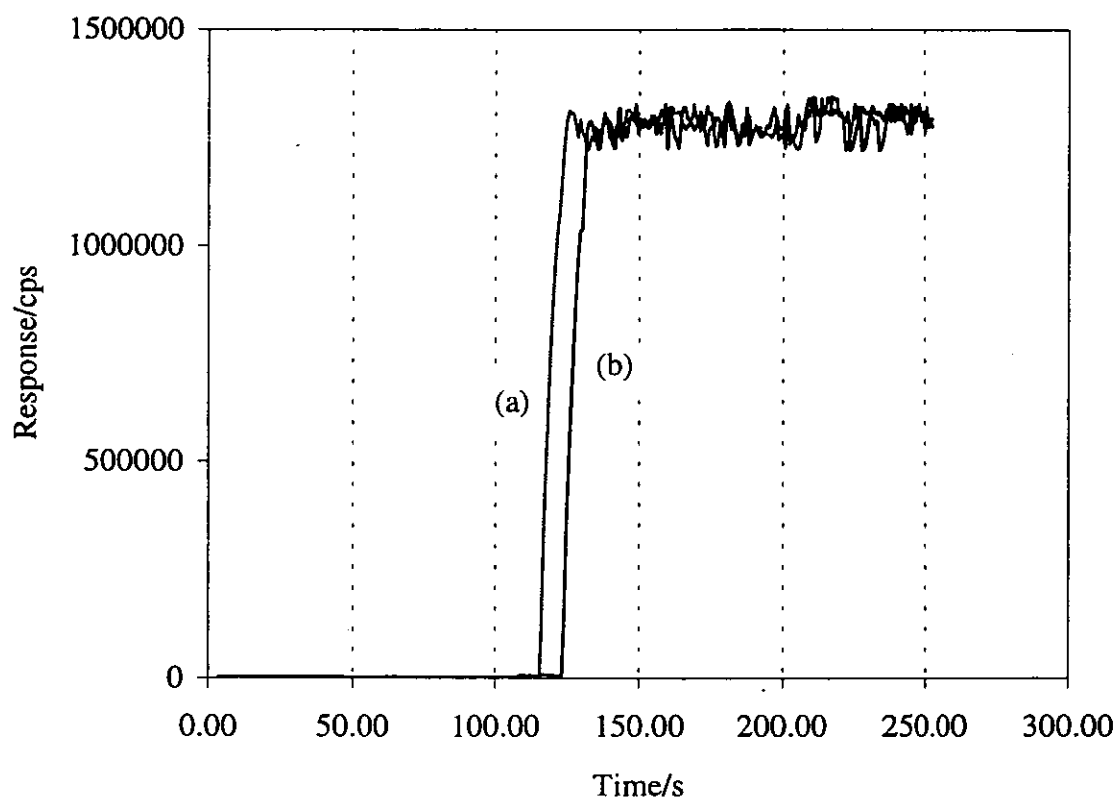
Figure 8.4:   Nebuliser natural aspiration; (a) Voltage off and (b) Voltage on.

can lead to more rapid equilibration, but at the expense of sensitivity. A solution to this problem would be to use a direct injection nebuliser [3].

8.8.4 Washout Time and Memory Effect

A 50 ng ml^{-1} multielement solution was replaced by a blank solution (1% nitric acid) in the normal sequence of throughput. Signal decay was observed for ^{115}In. A sharp drop from the full signal was observed after less than 30 s but after that the rate of decay became much lower as shown in Figure 8.6. This indicates that more than one process was responsible for the decay. The initial fall is due to aerosol wash-out, but the longer delay is probably due to memory effects in the solution phase in the interface.

8.8.5 Effects of Buffer Concentration

A series of borate solutions with concentrations of 0.10 M, 0.01 M, 0.05 M and 0.005 M, containing 10 ng ml^{-1} indium, were introduced through the makeup sheath flow at a rate of 40 μl min^{-1}. The same solution was used for both the makeup flow and as the buffer inside the CE capillary. The CE high voltage was set at 15 kV and the nebuliser gas flow rate was fixed at 1 l min^{-1}.

^{115}In signals were observed for each buffer concentration as shown in Figure 8.7. Stable signals indicated that the CE-ICP-MS system was operating satisfactorily. The electrophoretic current and RSD of the signals recorded for these buffer solutions are shown in Table 8.3.
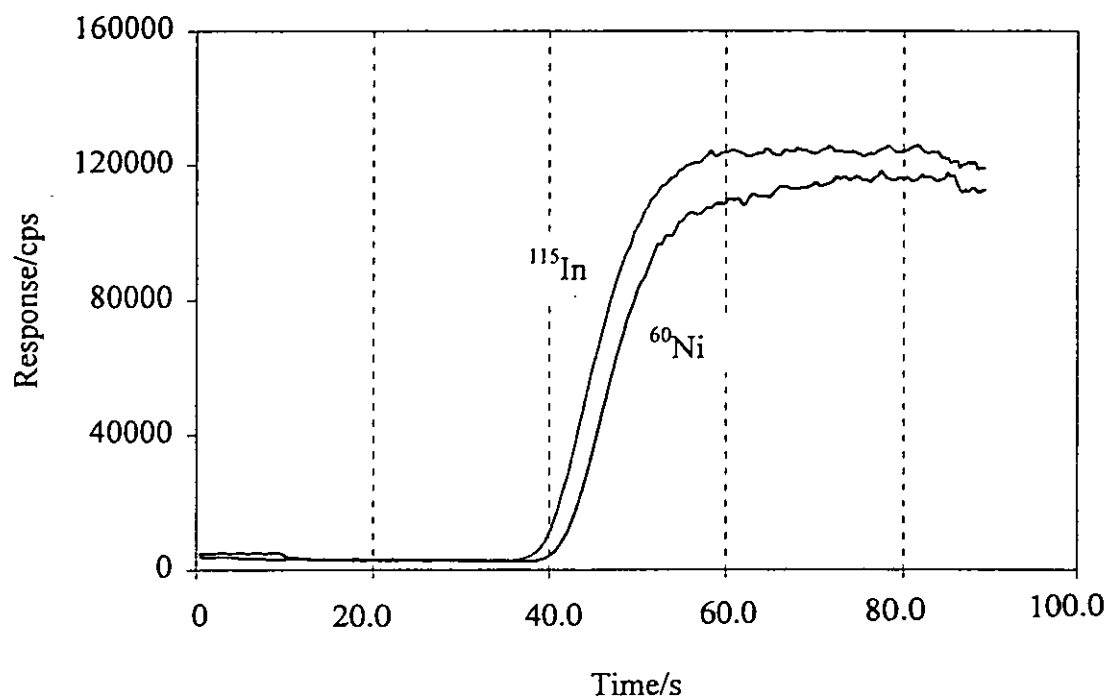
Figure 8.5:   Plot of signal equilibration times for ^{115}In and ^{60}Ni.
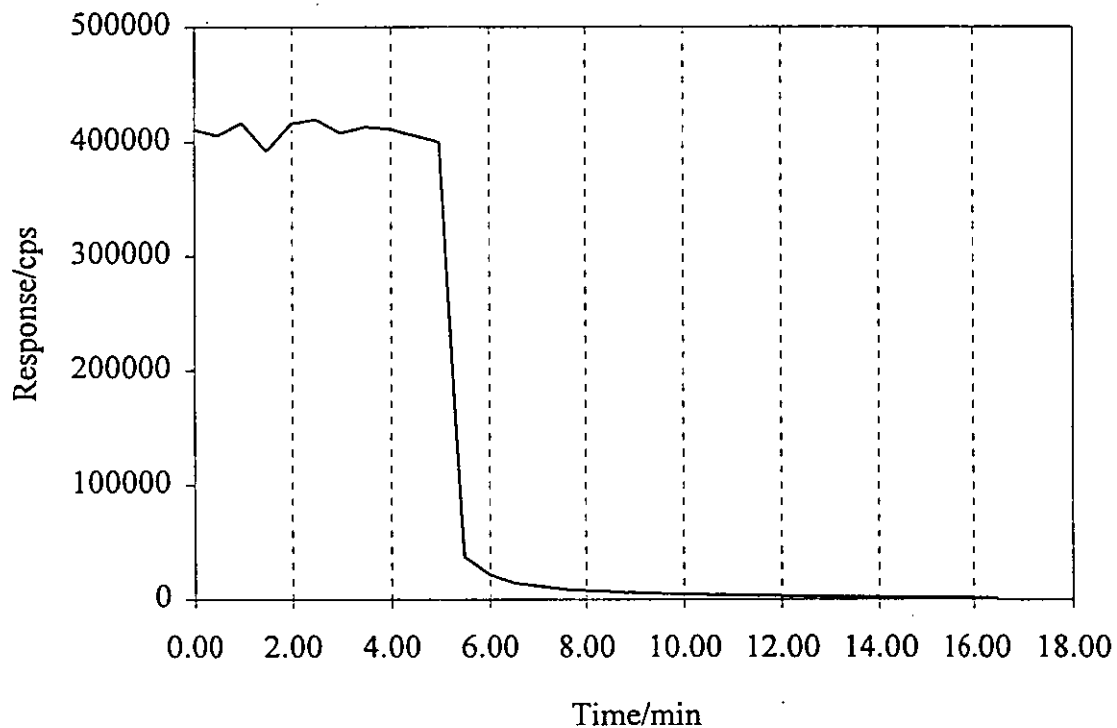

Figure 8.6:   Decay of response with time on substitution of the analyte solution by a blank.

Table 8.3: Electrophoretic currents and RSD of ^{115}In signals for various buffer concentrations introduced as makeup flow.

Buffer concentration/M	Current/μA	RSD Counts/%
0.10	88.7	4.18
0.01	51.3	7.97
0.05	43.3	6.96
0.005	31.0	2.80

As shown all these buffers worked satisfactorily and provided an electrical connection to the ground. Earlier experiments displayed a repeated pattern of signal fluctuation as shown in Figure 8.8. This type of fluctuation was thought to be due to leakage in the CE interface. After the leak was repaired, a steady signal was observed.

8.8.6 Effects of Separation Voltage

A 0.005 M borate solution, containing 10 ng ml^{-1} In, was introduced through the makeup flow at a rate of 40 μl min^{-1}. The same solution was used for both the makeup flow and as the buffer inside the CE capillary. The CE voltage was varied from 2.5 kV to 15.0 kV and the nebuliser gas flow rate was fixed at 1 l min^{-1}.

Signals of ^{115}In were recorded for the different CE voltages applied as shown in Figure 8.9. Different separation voltages did not affect the count rates and stable signals were observed. Electrophoretic currents and RSD of the signals are shown in Table 8.4.

The relation between the voltage applied and the electrophoretic current induced is shown in Figure 8.10. The plot shows that the electrophoretic current is, as expected, proportional to the separation voltage.
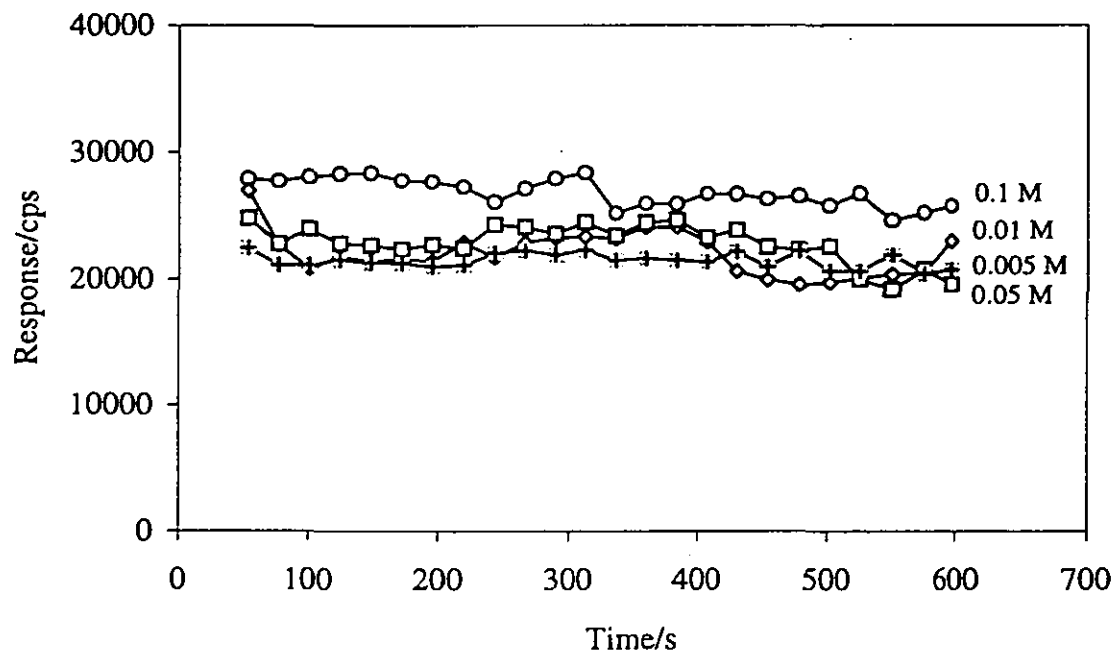
Figure 8.7:   Effects of buffer concentration on signals.
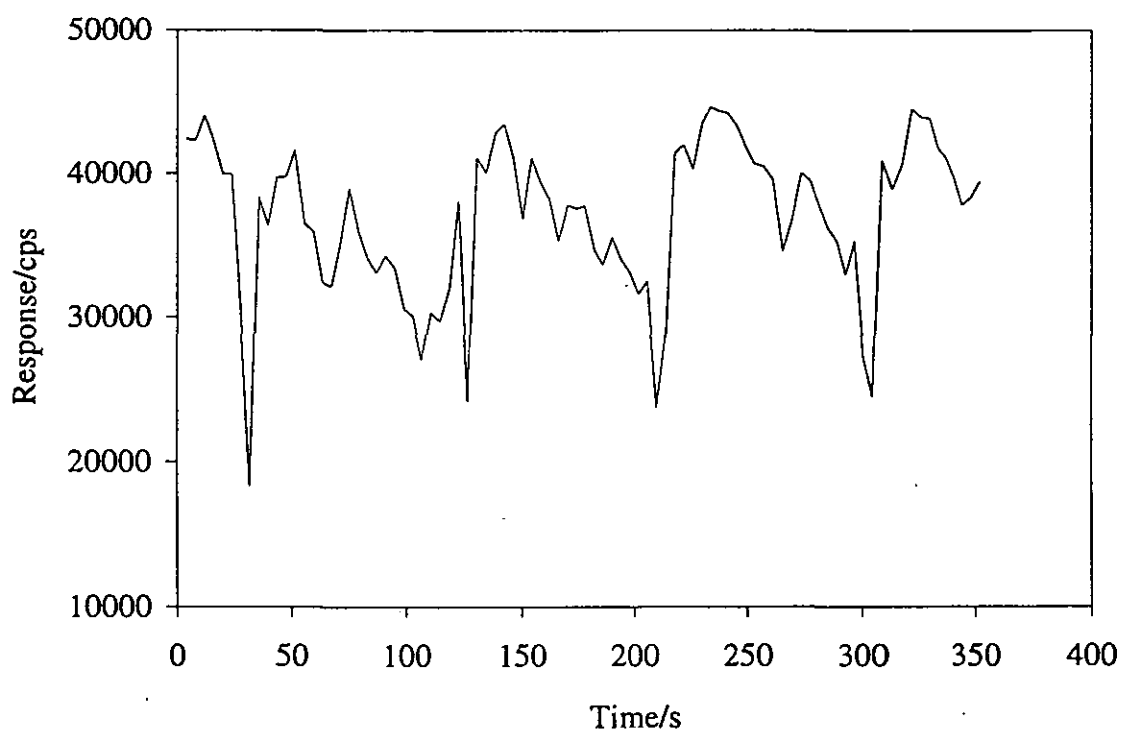

Figure 8.8:   Signal fluctuation due to leakage in the CE-ICP-MS interface.
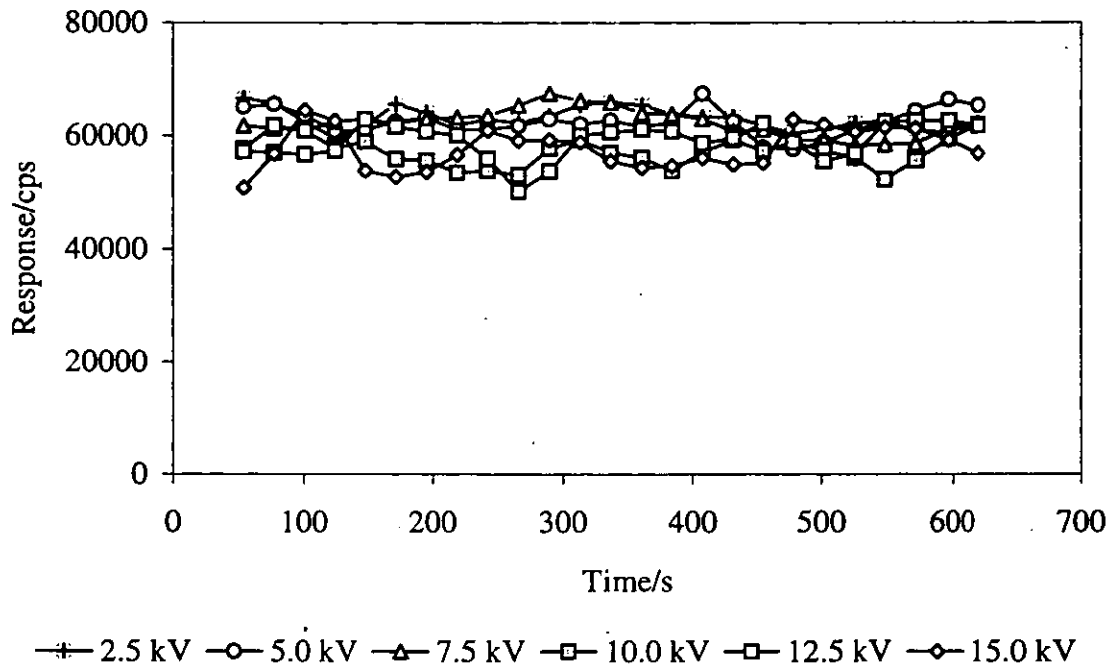
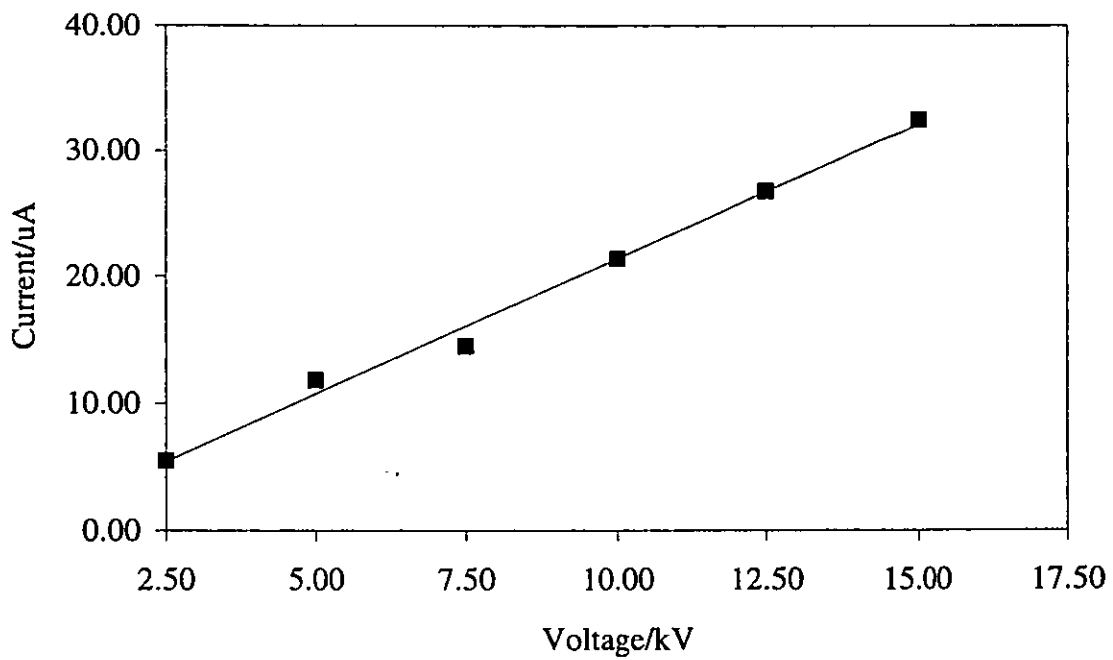Figure 8.9:   Effects of separation voltage on signals.

Figure 8.10:   Electrophoretic current versus applied CE voltage.

Table 8.4: Electrophoretic currents and RSD of the ^{115}In signals for different separation voltages.

Voltage/kV	Current/μA	RSD Counts/%
2.5	5.50	3.04
5.0	11.80	3.82
7.5	14.50	3.93
10.0	21.40	4.58
12.5	26.80	5.35
15.0	32.50	6.26

8.8.7 Effects of Makeup Liquid Flow Rate

A solution of 0.005 M borate buffer, containing 10 ng ml^{-1} was introduced through the makeup flow at various pump speeds up to the maximum setting of 125. The same solution was used for both the makeup flow and as the buffer inside the CE capillary. The nebuliser gas flow rate was fixed at 1 l min^{-1} and the CE high voltage was switched off. Signals of ^{115}In were observed.

Signals increased as the makeup flow rate was increased as shown in Figure 8.11 because more analyte entered the plasma. The makeup liquid flow rate, mean and RSD of the signals are shown in Table 8.5.

A solution flow rates below 18 μl min^{-1} showed poor stability because the nebuliser operated in a less stable manner and also ion counts were lower i.e. the noise was increased.

Table 8.5:   Makeup flow rate, mean and RSD of the ^{115}In signals for various pump settings.

Pump Setting	Makeup Flow Rate/ μl min^{-1}	Mean Counts/ cps	RSD Counts/ %
Off	0.00	4373	14.74
0	4.85	38943	8.06
5	6.20	35429	15.71
10	7.50	34676	11.94
25	11.50	47280	12.00
50	18.20	79427	1.38
75	24.90	92042	1.56
100	31.55	102215	5.91
125	38.25	123173	2.51

8.8.8   Effects of Nebuliser Gas Flow Rate

A 0.005 M borate solution, containing 10 ng ml^{-1} In, was introduced through the makeup flow at a rate of 40 μl min^{-1} to measure the effect of nebuliser gas pressures on signals. The same solution was used for both the makeup flow and as the buffer inside the CE capillary. The nebuliser gas pressures were varied from 120 psi to 160 psi and the CE high voltage was switched off. Signals of ^{115}In were observed.

The signals increased as the nebuliser pressures were increased, as shown in Figure 8.12, because the increased gas flow transported more analyte to plasma. The nebuliser flow rate, mean and RSD of the signals are shown in Table 8.6.
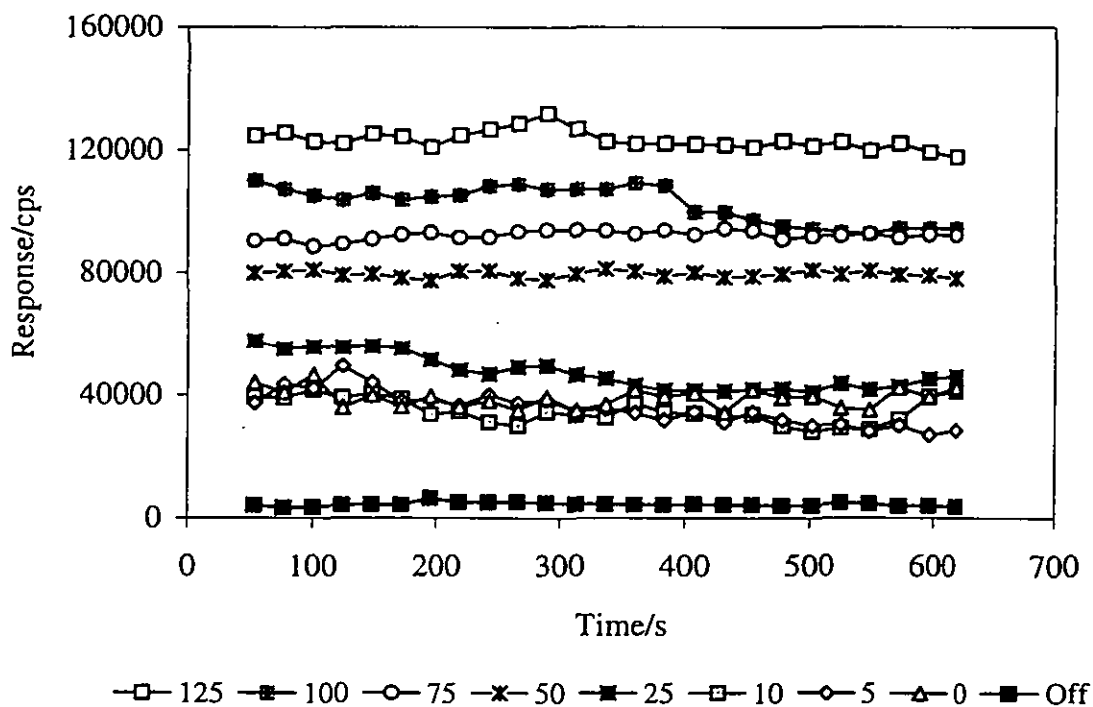
Figure 8.11:   Effects of makeup flow rate on ^{115}In signals.

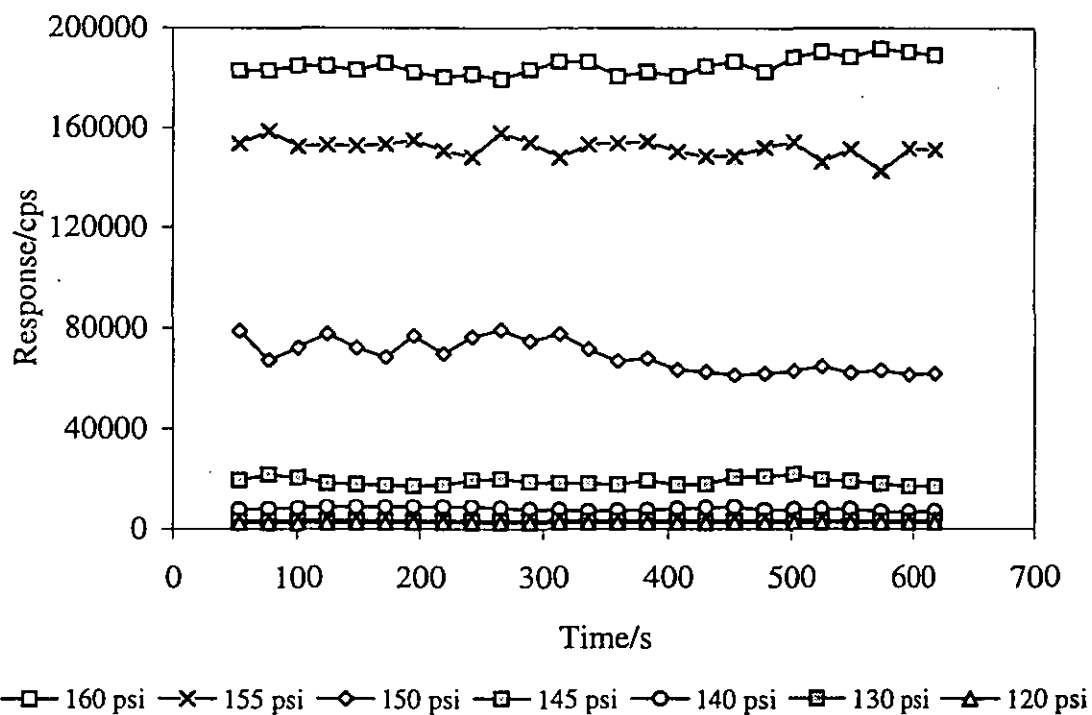(Shown as makeup flow pump setting, see Table 8.5 for flow rate)

Figure 8.12:   Effects of nebuliser pressures on ^{115}In signals.

Table 8.6:   Nebuliser flow rate, mean and RSD of the ^{115}In signals for various
            nebuliser pressures.

Pressure/psi	Nebuliser Flow Rate/ $l\ min^{-1}$	Means Counts/ cps	RSD Counts/ %
120	0.78	2474	2.34
130	0.84	3214	2.34
140	0.91	7885	8.72
145	0.94	19008	7.79
150	0.98	69046	9.17
155	1.00	151947	2.30
160	1.04	184746	1.88

These data are in contradiction to those observed when the HEN was used independently of the CE interface (see Section 7.3.1 in Chapter 7). The reason for this requires further investigation, but it could be that the pressure of the interface is modifying the nebuliser performance.

8.8.9   Responses of EOF and Makeup Liquid

A 0.005 M borate solution containing 10 ng ml^{-1} In was used as buffer solution inside the CE capillary and 0.01 M ammonium chloride solution containing 10 ng ml^{-1} Ce, flow through the makeup flow at a rate of 40 µl min^{-1}. The nebuliser gas flow rate was set at 1 l min^{-1} and the CE high voltage was switched off. After 90 s, the CE high voltage was switched on for another 90s and then switched off again for the remaining times. Signals of ^{115}In and ^{140}Ce were observed.

A typical example of the time plots of ^{115}In and ^{140}Ce responses obtained is shown in Figure 8.13. Ce^{2+} ions were added into the makeup liquid to monitor the operation of the interface and the ICP-MS. A stable signal indicated that the interface was working satisfactorily and the ICP-MS was in stable condition. In^{2+} ions were also added to the buffer solution to monitor the stability of the EOF. When the electrophoresis voltage was turned on, the ^{115}In response diminished and the ^{140}Ce
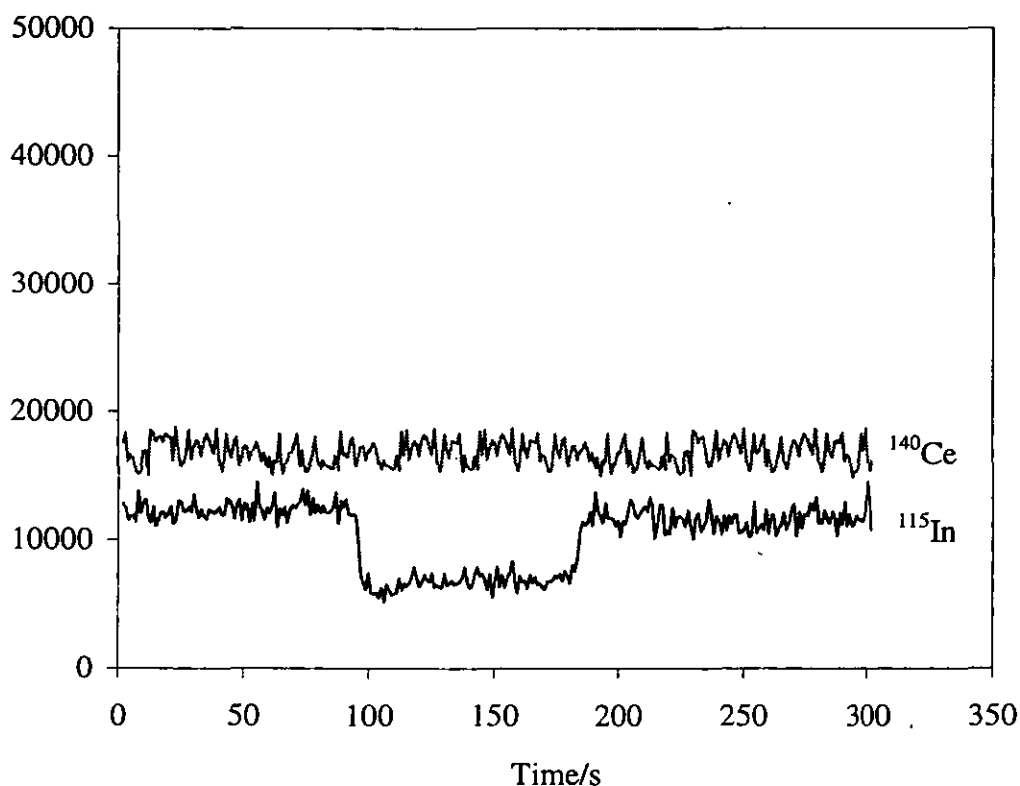
Figure 8.13:   Time plots of ^{115}In and ^{140}Ce response indicative
of EOF and makeup liquid flow, respectively.

response remain relatively stable. The results indicated that the EOF was directed to the inlet reservoir when there was current flow through the capillary.

8.9   CONCLUSIONS

A CE system was successfully constructed. This CE was coupled to ICP-MS with a specially designed interface. The interface was based on the use of a high efficiency nebuliser, although later it was found that a standard Meinhard nebuliser could also be used. The CE-ICP-MS interface was optimised and evaluated.

Capillary flows were between 3.40 and 4.00 μl min^{-1} when the makeup flow rates were varied with the nebuliser gas flow rate at 1 l min^{-1} and the high voltage switched off. When the CE voltage was varied, the makeup flow rate at 40 μl min^{-1} and the nebuliser gas flow was off, the capillary flow moved towards the reservoir with a rate between 0.05 and 0.30 μl min^{-1}. The capillary flow moved towards the detector with a flow rate between 3.13 and 3.38 μl min^{-1} when the CE voltage was varied, the makeup flow rate at 40 μl min^{-1} and the nebuliser gas flow rate at 1 l min^{-1}.

Under the optimised CE interface conditions, sample normally reached the detector after 2.06 min when the high voltage was not applied and 2.19 min with the high voltage on. The longer time was required because the EOF was directed toward the reservoir.

Studies of response time showed that the signals of ^{115}In and ^{60}Ni stabilised in about 18 s. It required less than 30 s for the signal to reduce to 1 % of its initial value once a blank solution was introduced into the interface.

Further evaluation of the CE-ICP-MS interface showed that the concentration of buffer solutions used and CE voltage applied did not affect the signal counts. Steady and stable signals were observed. CE current was, as expected, proportional to applied voltage. The makeup liquid flow rate and nebuliser gas flow rate had significant effects on signal counts. Increase in flow rates resulted in higher signal counts for a test analyte introduced in the makeup flow. However, higher makeup flow will have a different effect on analytes coming from the CE column.

It has been shown that addition of test elements to the makeup liquid flow and the buffer solution is a valuable means of monitoring the performance of the CE, interface and ICP-MS.

REFERENCES

1. Heiger, D. N., *High Performance Capillary Electrophoresis,* Hewlett-Packard Co., Waldbronn, 1992.

2. Koropchak, J. A., Allen, L., and Davis, J. M., *Appl. Spectrosc.*, 1992, **46**, 682.

3. Houk, R. S., Shum, S. C. K., and Wiederin, D. R., *Anal. Chim. Acta*, 1991, **250**, 61.

Chapter 9

CHAPTER NINE

APPLICATIONS OF CE-ICP-MS FOR METAL SPECIES STUDIES

9.1 INTRODUCTION TO CHAPTER

This chapter deals with the application of CE-ICP-MS to the separation of elements in a multielement solution, metal-ligand complexes, particularly metal-EDTA, and metal-humic acid and elemental speciation studies.

9.2 INSTRUMENTATION

The CE-ICP-MS system described in Chapter 8 was used throughout these experiments. The CE operating conditions used are summarised in Table 9.1. The operating parameters for ICP-MS were unchanged from the standard parameters given in Table 7.1, Chapter 7. The operating procedures for the CE-ICP-MS were as described in Section 8.5, Chapter 8.

Table 9.1:   Standard CE operating conditions.

Capillary	:	Coated fused silica ($100\ \mu m$ x 100 cm)
Separation voltage	:	15 kV
Injection method	:	Hydrodynamic injection,
		elevated at 15 cm for 10 s.
Buffer system	:	0.005 M borate containing $10\ ng\ ml^{-1}$ In,
		pH 8.5
Makeup solution	:	0.01 M ammonium chloride
Makeup flow rate	:	$40\ \mu l\ min^{-1}$
Polarity	:	Negative (at the inlet end)

Data acquisition was performed using TRAnalysis software (Fisons plc, Uxbridge, Middlesex, UK) run in the PQVision software, version 4.1.2 (Fisons plc, Uxbridge, Middlesex, UK). The parameters used were as shown in Table 9.2.

Table 9.2:   Time-resolved analysis parameters.

Acquisition mode	:	Peak jumping
Time per slice (s)	:	1.00
Total acquire time (min)	:	4-5
Points per peak	:	3
Detector mode	:	PC (Pulse Counting)
No. of selected isotopes	:	Varied depending on the experiment

9.3   CHEMICALS

A 10 μg ml^{-1} multielement solution containing Mn^{2+}, Ni^{2+}, Cu^{2+}, Ba^{2+} and Pb^{2+} was prepared from standard solutions (SpectroSol, BDH, Poole, Dorset, UK). A solution of Mn(VII), as MnO_4^-, was prepared from potassium permanganate, $KMnO_4$ (Analar, BDH, Poole, Dorset, UK). Nickel-EDTA and copper-EDTA complexes were prepared from standard solutions of nickel and copper (SpectroSol, BDH, Poole, Dorset, UK) and the diammonium salt of ethylendiamine tetraacetic acid (Chemika, Fluka, Gillingham, Dorset, UK).

Humic acid and dimethyl glyoxime (DMG) complexes with nickel were prepared from commercial humic acid (Fluka, Gillingham, Dorset, UK), nickel standard solution (SpectroSol, BDH, Poole, Dorset, UK) and DMG (Puriss, Fluka, Gillingham, Dorset, UK).

A mixture of 10 μg ml^{-1} of Cr(III) and Cr(VI) solution at pH~6 was prepared from Cr(III) chloride (BDH, Poole, Dorset, UK) and potassium dichromate (Riedel-de Haen, Phillip Harris Scientific, Lichfield, Staffordshire, UK).

0.005 M borate buffer containing 10 ng ml^{-1} indium was prepared from disodium tetraborate (Fisons, Loughborough, UK) and indium standard solution (SpectroSol, BDH, Poole, Dorset, UK). The pH solution was adjusted to 8.50 with 0.1 M ammonium hydroxide (Biochemika, Fluka, Gillingham, Dorset, UK) or 0.1 M nitric acid (Aristar, BDH, Poole, Dorset, UK).

Solution of 0.01 M ammonium chloride (A.R., Fisons, Loughborough, UK) containing 10 ng ml^{-1} cerium (SpectroSol, BDH, Poole, Dorset, UK) was used for makeup solution. Solution of 0.10 M sodium hydroxide (HPCE Grade, Biochemika, Fluka, Gillingham, Dorset, UK) was used for preconditioning the CE capillary.

High purity grade water (18 MΩ) for sample preparation was obtained from a Maxima pure water system (ELGA, High Wycombe, Bucks, UK).

9.4   ANALYSIS OF A MULTIELEMENT SOLUTION

A 10 μg ml^{-1} multielement solution containing Mn^{2+}, Ni^{2+}, Cu^{2+}, Ba^{2+} and Pb^{2+} was separated and detected using the CE-ICP-MS system. The CE and ICP-MS operating conditions given in Section 9.2 were used. The HEN-170-AA nebuliser was used at the interface. Isotopes of ^{55}Mn, ^{60}Ni, ^{65}Cu, ^{138}Ba and ^{208}Pb were detected using time-resolved analysis parameters as shown in Table 9.2.

The multielement electropherogram showed a single broad peak and the isotopes could not be separated and assigned. This would be similar to the signal obtained from a general purpose detector such as a single wavelength absorption detector. However, because the ICP-MS is an element-selective detector, there is no need to electrophoretically separate the isotopes. The multielement electropherogram can be

resolved into single element electropherograms as shown in Figure 9.1(a)-(e). All the elements were detected within 150 to 200 s.

The electrophoretic mobilities of the elements and the EOF of the buffer solution were toward the inlet reservoir since the polarity of the high voltage is negative at the inlet end. Natural aspiration of the nebuliser overcame the mobilities and pulled the solution toward the detector. An increase in the migration times was observed as the m/z increased. The order of the migration times were: $Mn^{2+} < Ni^{2+} < Cu^{2+} < Ba^{2+} < Pb^{2+}$ as expected. Band broadening is expected to occur because of the different movement directions of the electrophoretic mobility, EOF and the nebuliser natural aspiration.

9.5   SEPARATION OF A NEGATIVELY CHARGED SPECIES

A negatively charged species was analysed by the CE-ICP-MS system employed the same conditions described in Section 9.4.

An electropherogram of 100 μg ml^{-1} MnO_4^- showed a sharp peak at a migration time of 143 s, as shown in Figure 9.2. The electrophoretic mobility of this negatively charged species was toward the detector. Although the EOF of the buffer was toward the reservoir, combination of the electrophoretic mobility and the natural aspiration of the nebuliser resulted in a shorter migration time compared with those obtained for cationic species in Section 9.4.

9.6   SEPARATION OF METAL/METAL-EDTA COMPLEXES

Solutions of $Ni^{2+}/[Ni-EDTA]^{2-}$ and $Cu^{2+}/[Cu-EDTA]^{2-}$ were separated and detected using the CE-ICP-MS system. The conditions given in Section 9.2 were employed with the HEN-170-AA nebuliser.
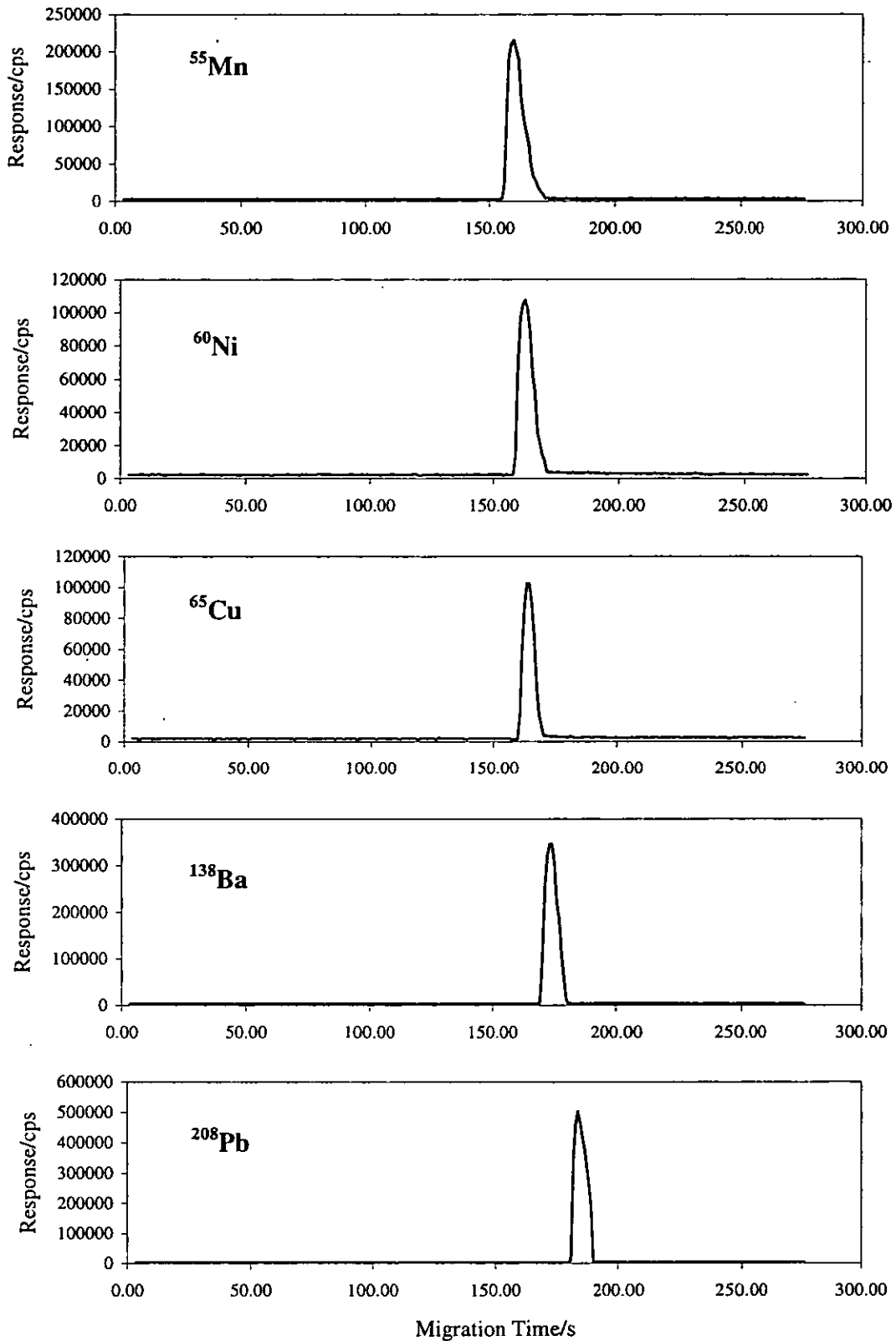
Figure 9.1: CE-ICP-MS electropherograms of 10 μg ml^{-1} multielement solution containing Mn^{2+}, Ni^{2+}, Cu^{2+}, Ba^{2+} and Pb^{2+}. All electropherograms were obtained with a single injection of the multielement sample.
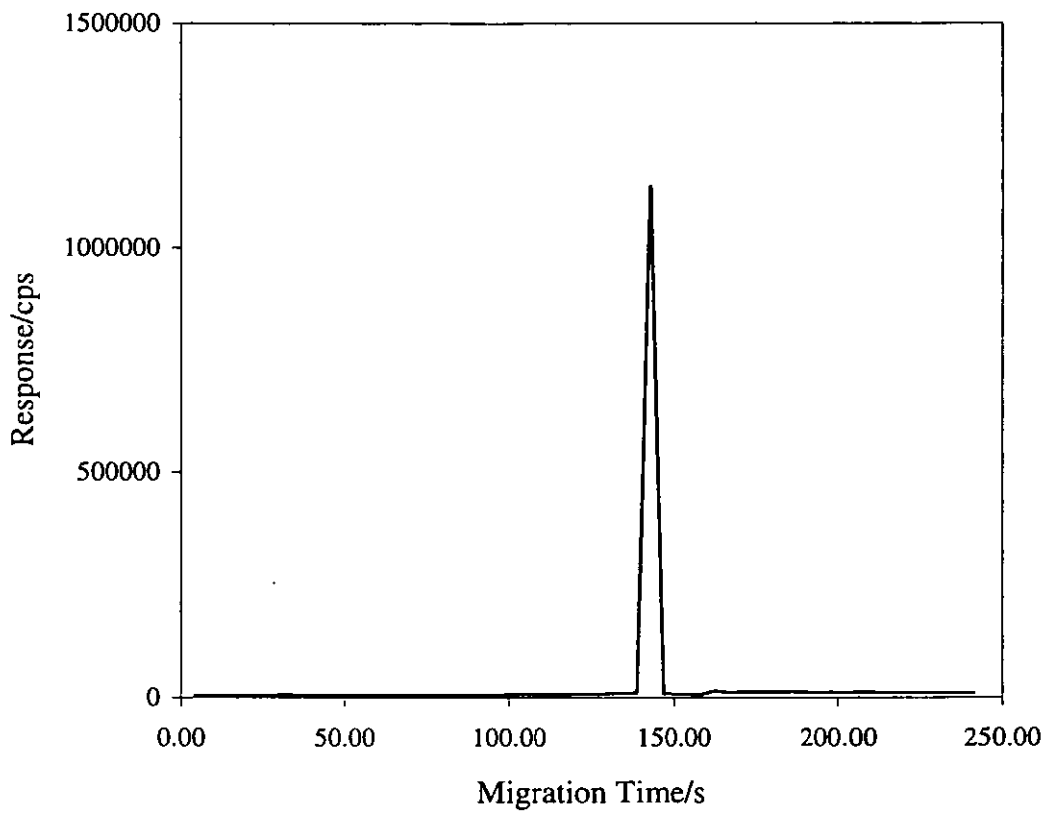
Figure 9.2: CE-ICP-MS electropherogram of 100 μg ml^{-1} MnO$_4^-$, detected as ^{55}Mn.

The separation of Ni^{2+}/[Ni-EDTA]$^{2-}$ and Cu^{2+}/[Cu-EDTA]$^{2-}$ mixtures by the CE-ICP-MS are shown in Figures 9.3 and 9.4 respectively. The Ni^{2+}:EDTA (20 μg ml^{-1}:10 μg ml^{-1}) solution showed 2 peaks which are attributable to the [Ni-EDTA]$^{2-}$ at a migration time 146.5 s and the free nickel at 178 s. The negatively charged species moved towards the detector and was detected first. The excess nickel in the solution moved toward the reservoir and was detected later.

Similar electropherograms were observed for Cu^{2+}:EDTA (20 μg ml^{-1}:10 μg ml^{-1}) solutions. The first peak at a migration time of 150 s was due to the [Cu-EDTA]$^{2-}$ complex and the second peak at 185 s was due to the free copper.

9.7   SEPARATION OF HUMIC ACID SPECIES

A 2000 μg ml^{-1} purified humic acid was separated and detected by the CE-ICP-MS and SEC-ICP-MS systems. The isotopes of ^{24}Mg, ^{27}Al, ^{39}K, ^{44}Ca, ^{56}Fe, ^{60}Ni and ^{65}Cu were included in the element menu for the ICP-MS detection.

The separation of purified humic acid using CE-ICP-MS showed lower sensitivities compared to the separation by SEC-ICP-MS. Figure 9.5 is the CE-ICP-MS electropherogram for the commercial humic acid and shows that only 2 elements i.e. ^{56}Fe and ^{60}Ni could be detected. For comparison, the SEC-ICP-MS chromatogram, shown in Figure 9.6, shows that at least 4 elements were detected. Higher background counts were observed for ^{39}K and ^{56}Fe as expected, due to the molecular ions, ^{38}Ar^{1}H and ^{40}Ar^{16}O respectively.

The separation of humic acid by the CE-ICP-MS had shown the advantages of using CE as the separation method. The elements could be detected at a shorter migration times compared to when SEC is used and that all the elements should appear at nearly the same migration times. This is because there should be less problem with weak complexes dissociating as they pass through the column.
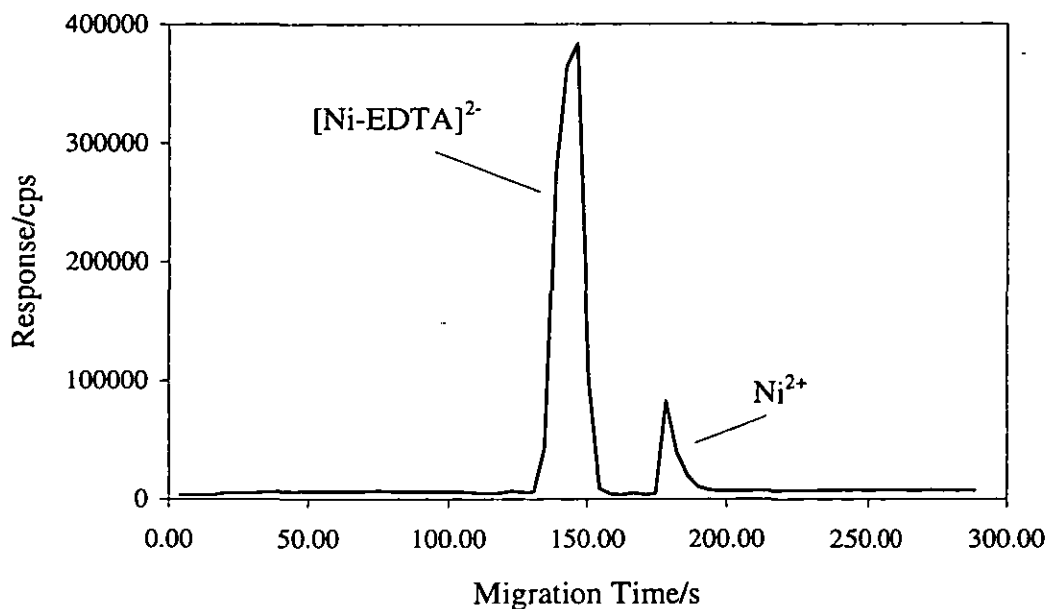
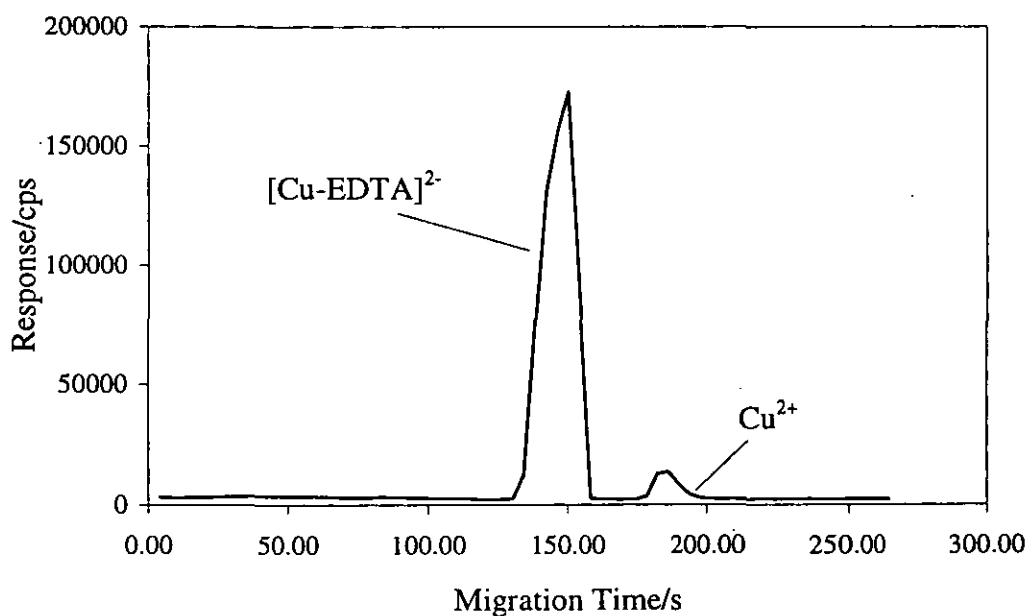Figure 9.3: Electropherogram of 20 $\mu g\ ml^{-1}$ nickel-10 $\mu g\ ml^{-1}$ EDTA mixture, detected as ^{60}Ni.

Figure 9.4: Electropherogram of 20 $\mu g\ ml^{-1}$ copper-10 $\mu g\ ml^{-1}$ EDTA mixture, detected as ^{65}Cu.
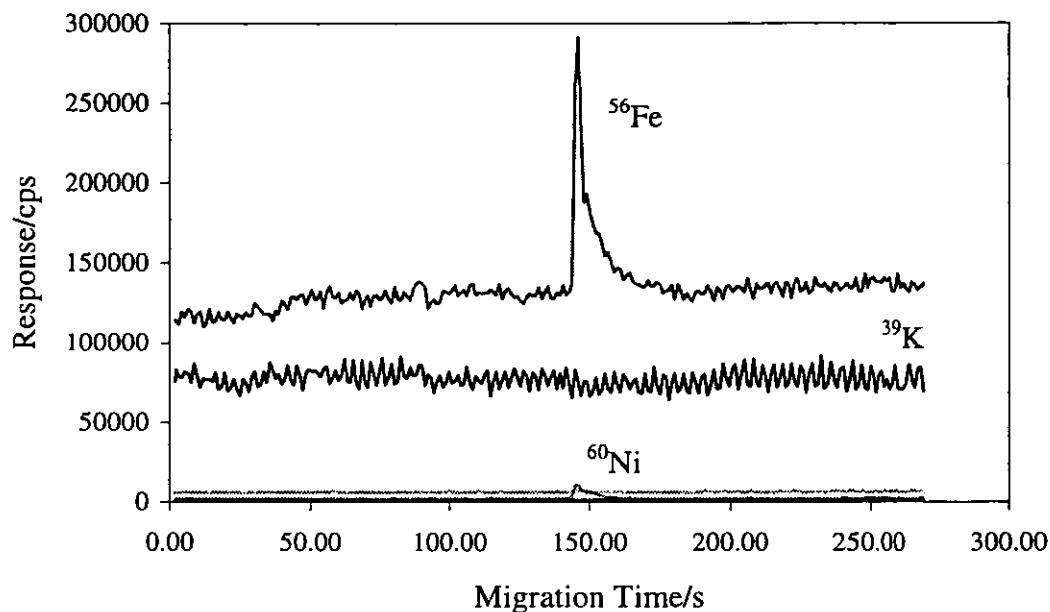
Figure 9.5: CE-ICP-MS electropherogram of 2000 μg ml⁻¹ purified humic acid. Separation conditions as described in Section 9.2. 36 nl sample was injected and TR-30-C2 nebuliser was used at the interface.
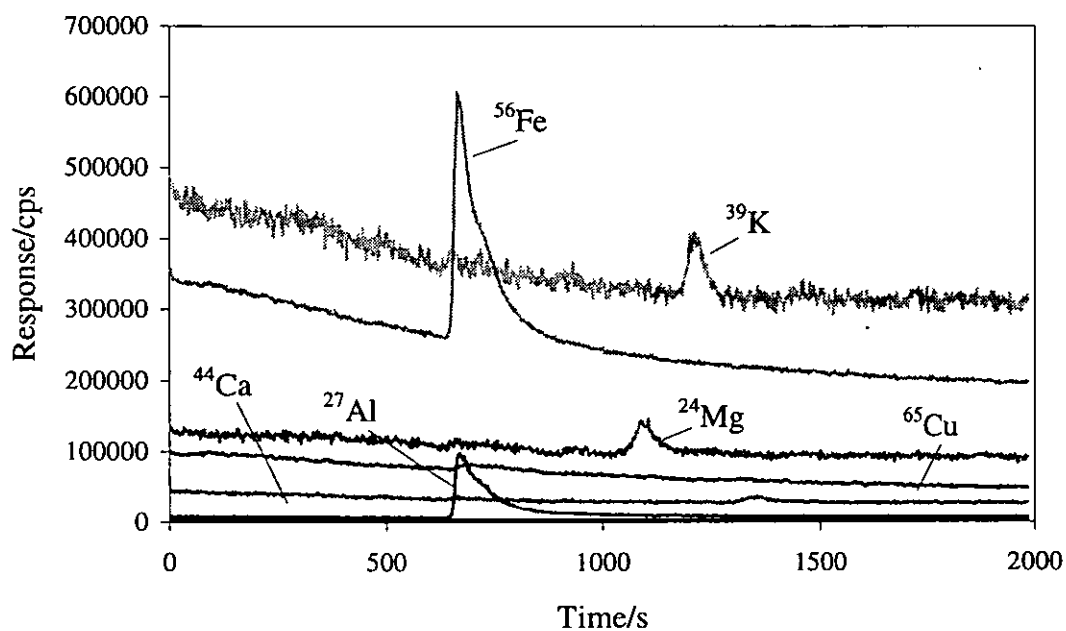

Figure 9.6: SEC-ICP-MS chromatogram of 2000 μg ml⁻¹ purified humic acid. 7.8 x 300 mm Ultrahydrogel column, 0.05 M phosphate, pH 6.5 mobile phase, 0.5 ml min⁻¹ flow rate and 20 μl sample injected.

171

9.8   SEPARATION OF NICKEL-HUMIC COMPLEX

A solution of nickel:humic acid (20 µg ml^{-1}: 20 µg ml^{-1}) was analysed with the CE-ICP-MS system and the conditions given in Section 9.2 was employed. The TR-30-C2 nebuliser was used at the interface. Two peaks were observed at migration times of 146 and 173 s respectively as shown in Figure 9.7(c). The first peak is a broad peak (typical of those obtained with UV detection) which is due to the nickel-humic acid complex. Humic acid is a very large molecule with many binding sites to which the nickel could attach. This complex is either neutral or negatively charged depending on the amount of nickel added. Negatively charged species have electrophoretic mobility toward the detector and are detected first. The second peak, which is sharp, was due to the free nickel in the solution. Because nickel is positively charged, its migration is toward the reservoir, however, the aspiration of the nebuliser pulled the nickel toward the detector where it appeared after the complex.

A mixture of nickel, DMG and humic acid solution (20 µg ml^{-1}:5 µg ml^{-1}:20 µg ml^{-1}) produced 3 peaks as shown in Figure 9.7(d). The complex of nickel with DMG is neutral and therefore it acts as a marker for the EOF. The first broad peak at a migration time 137 s is very similar to the first peak in the Figure 9.7(c) probably due to the nickel-humic acid complex. The second peak at 167 s is due to the nickel-DMG complex and the third peak at 177 s is due to the free nickel in the solution.

Solutions of nickel:DMG (10 µg ml^{-1}:5 µg ml^{-1}) and nickel (5 µg ml^{-1}) were analysed to confirm that the sharp peaks observed previously were due to the nickel-DMG complex and the free nickel. Figure 9.7(b) shows the separation of the nickel:DMG solution which consists of 2 sharp peaks. Nickel solution alone produced only one sharp peak as shown in Figure 9.7(a). Since the nickel-DMG complex is a neutral species, its mobility is dependent on the electroosmotic mobility. The mobility of the free nickel is attributable to both the electrophoretic and electroosmotic mobilities which are directed toward the reservoir. However, the movement of the species was toward the detector because of the dominant affect of nebuliser aspiration. Thus the
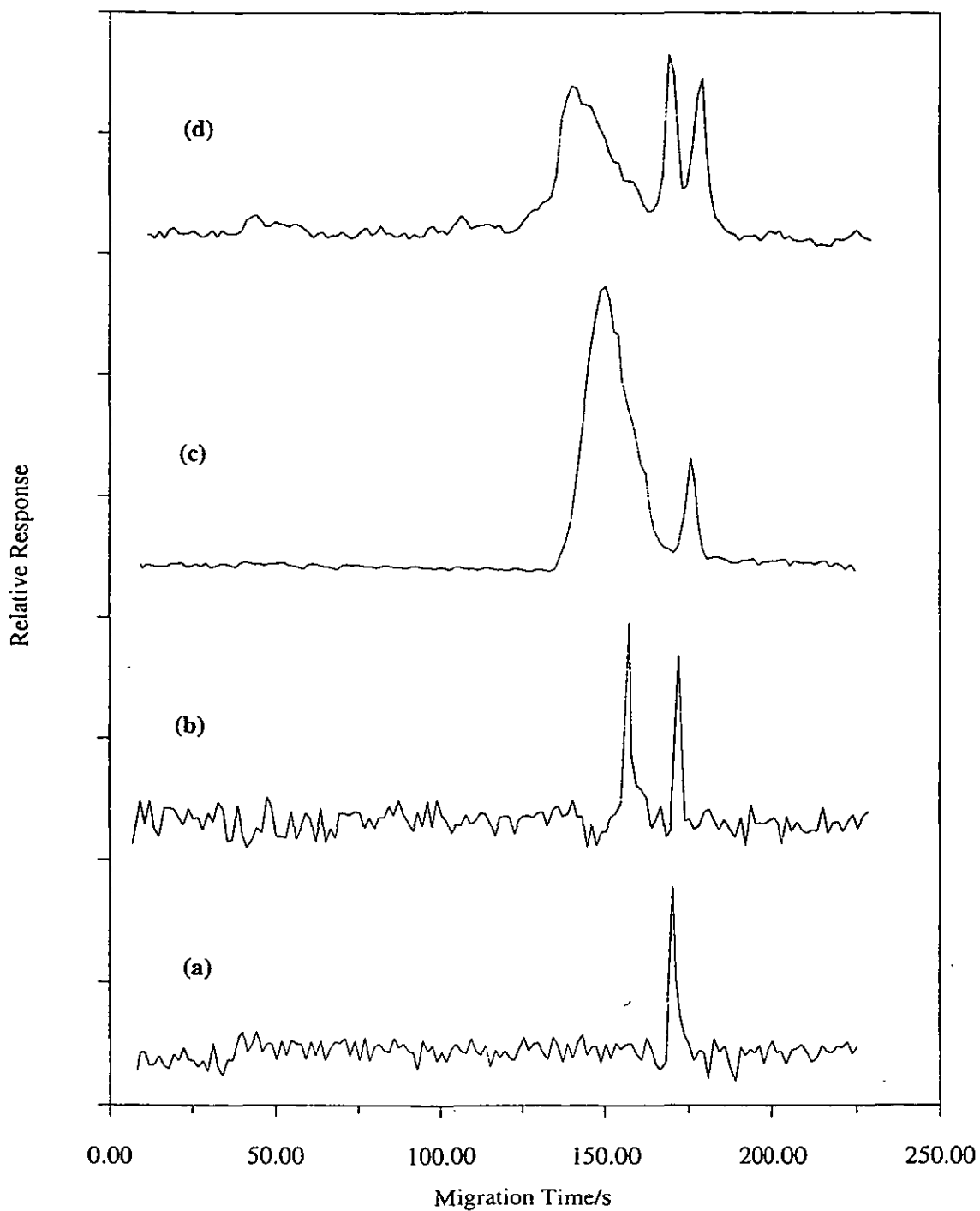
Figure 9.7: Electropherograms of: (a) 20 $\mu g\ ml^{-1}$ Ni^{2+}, (b) 20 $\mu g\ ml^{-1}$ Ni^{2+}:5 $\mu g\ ml^{-1}$ DMG, (c) 20 $\mu g\ ml^{-1}$ Ni^{2+}:20 $\mu g\ ml^{-1}$ HA and (d) 20 $\mu g\ ml^{-1}$ Ni^{2+}: 5 μg ml^{-1} DMG:20 $\mu g\ ml^{-1}$ HA; detected as ^{60}Ni.

first peak detected was due to the nickel-DMG complex and the second peak was due to the free nickel.

9.9 SPECIATION OF CHROMIUM

Chromium in aqueous solution can exist as Cr(III) and Cr(VI). Cr(III) exists as several species including $Cr(H_2O)_6^{3+}$, $Cr(H_2O)_5OH^{2+}$, $Cr(H_2O)_4(OH)_2^{+}$, $Cr(OH)_3^{0}$, and $Cr(OH)_4^{-}$, but exists primarily as $Cr(H_2O)_6^{3+}$ under acidic conditions. Cr(VI) exists as $HCrO_4^{-}$ and $Cr_2O_7^{2-}$ at similar pHs [1].

A mixture of 10 μg ml^{-1} of Cr(III) and Cr(VI) in solution was analysed by CE-ICP-MS and the conditions given in Section 9.2 was employed. The TR-30-C2 nebuliser was used at the interface. The electropherogram is shown in Figure 9.8. The negatively charged species moved toward the detector and thus $Cr_2O_7^{2-}$ was detected first. $Cr(H_2O)_6^{3+}$ moved toward the reservoir and separated from the negatively charged chromium and was detected later. The calculated resolution for these two peaks is 2:67.

9.10 CONCLUSIONS

The application of CE-ICP-MS to the analysis of metals in a multielement solution, metal-ligand complexes and speciation studies showed that it has the advantages of faster separations, small amount of samples used and requires a small volume of electrolyte. The negatively charged species were detected first, then the neutrals and later the positively charged species because of the different directions of the electrophoretic and electroosmotic mobilities. Element specific detection by ICP-MS has the advantage that different elements that are eluted at the same time can still be detected and assigned. It also has been shown that elemental speciation e.g. for Cr(III)/Cr(VI), is possible using the CE-ICP-MS system.
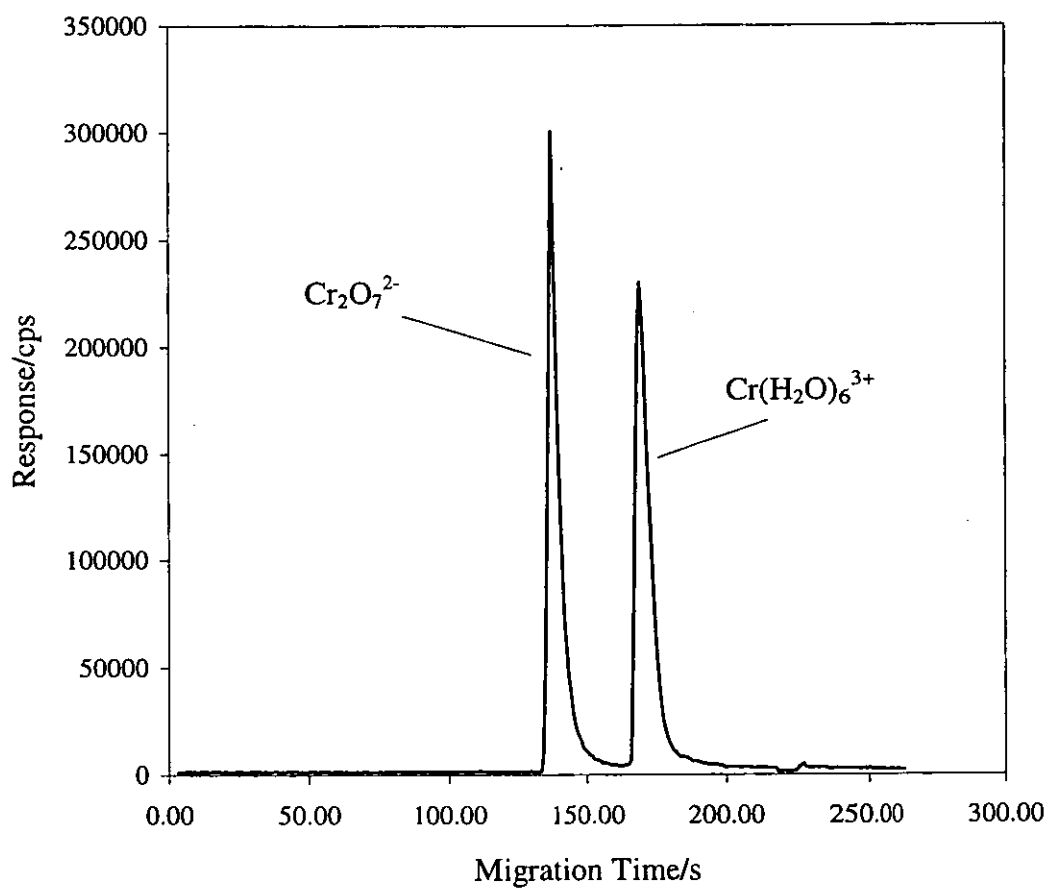
Figure 9.8:   CE-ICP-MS electropherogram of 10 μg ml⁻¹ Cr(III) and Cr(VI) mixture, detected as ^{52}Cr.

The use of HEN-170-AA and TR-30-C2 nebulisers at the CE-ICP-MS interface had no significant effect on the migration times for the samples tested. All samples were separated and detected within 4 min.

Sensitivity is a problem for CE-ICP-MS because of the minute volume of sample introduced, although this problem is less with modern instruments. Because of limited sensitivity the CE-ICP-MS technique will only be a competitor for conventional HPLC in specific applications such as for the separation of high molecular weight complexes and sensitive complexes. The very low volume samples required in the CE-ICP-MS technique is useful in the radio-active materials work where the waste is to be kept minimum.

REFERENCE

1.   Sperling, M., Xu, S., and Welz, B., *Anal. Chem.*, 1992, **64**, 3101.

Chapter 10

CHAPTER TEN

ELECTROSPRAY/ION SPRAY IONISATION-
MASS SPECTROMETRY FOR METAL-LIGAND SYSTEMS

10.1   INTRODUCTION TO CHAPTER

This chapter describes preliminary results obtained using the electrospray/ion spray-mass spectrometry technique for the study of some common metal-ligand systems.

10.2   INSTRUMENTATION

A triple quadrupole mass spectrometer (Quattro II, Micromass, Altrincham, Cheshire, UK) with an atmospheric pressure ionisation (API) source (Micromass, Altrincham, Cheshire, UK) was used, as shown in Figure 10.1. The API system employed was an electrospray/ion spray, consisted of two capillaries made from stainless-steel. A piece of smaller bore tubing (0.127 mm i.d., 0.229 mm o.d.) known as sample capillary is placed inside a piece of a larger bore tubing (0.330 mm i.d., 0.635 mm o.d.). Nebulising gas (N_2) flows in the annulus between the inner and outer tubes. For MS/MS experiments, argon was used as the collision gas in the collision cell (hexapole) located after the first detector. Instrument control and data acquisition were performed using Mass Lynx software (Micromass, Altrincham, Cheshire, UK).

A syringe pump (Model 341 B, Sage Instrument, Orion Research Inc., Cambridge, MA, USA) was used for sample solution delivery to the ionisation system.

The experimental conditions, shown in Table 10.1, were employed throughout the experiments unless otherwise stated.
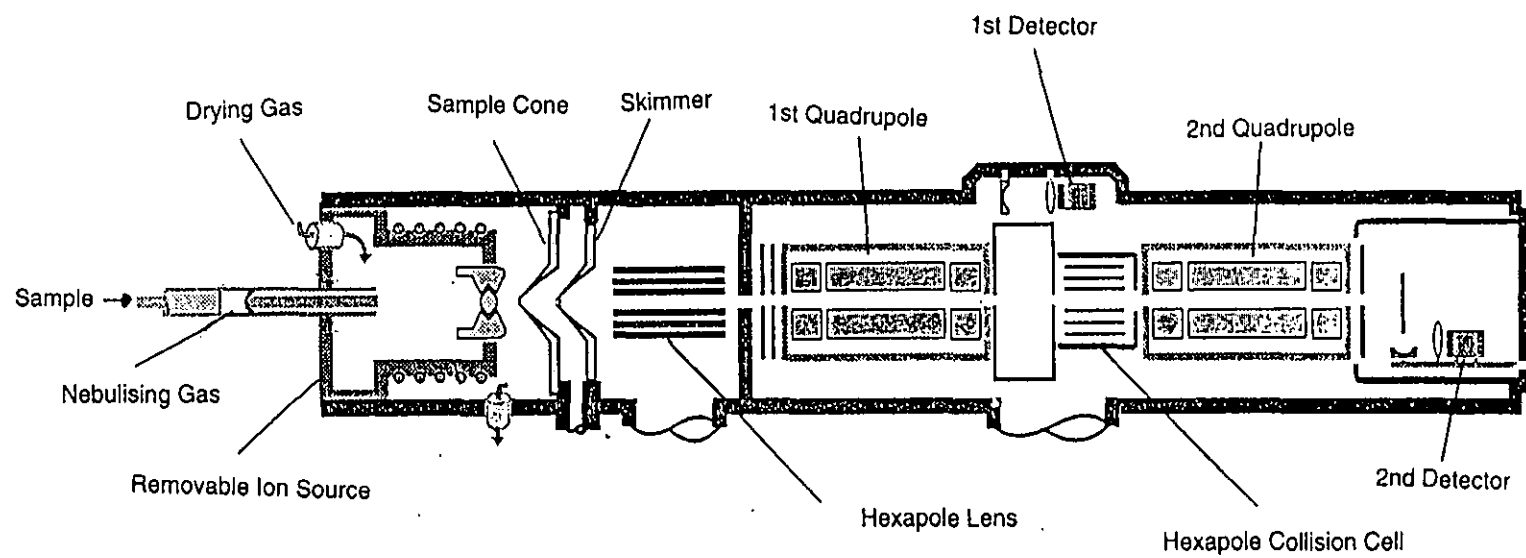
Figure 10.1:   Schematic of an API-mass spectrometer.

Table 10.1: Experimental conditions.

Source and Interface		
Capillary voltage	:	2.5 - 3.0 kV
Sample flow rate	:	5 µl min^{-1}
Nebulising gas flow rate (N$_2$)	:	0.25 l min^{-1}
Curtain gas flow rate (N$_2$)	:	1.67 l min^{-1}
Gas temperature	:	65 °C
Sampler-skimmer		
Cone pressure	:	1.2 mbar
Collision cell		
d.c. Potential on rods	:	70 V
Gas pressure	:	1.5 - 5.0 mbar
Collision gas	:	Ar

10.3 CHEMICALS

Citric acid solution was prepared from anhydrous citric acid (Microselect., Fluka, Gillingham, Dorset, UK). EDTA solution was prepared from EDTA diammonium salt (Puriss, Fluka, Gillingham, Dorset, UK). Humic acid from commercial humic acid (Fluka, Gillingham, Dorset, UK) and ferritin was a Type I from horse spleen (Sigma, Poole, Dorset, UK). Nickel and aluminium solutions were prepared from standard solutions (Spectrosol, BDH Ltd., Poole, Dorset, UK).

All working solutions were prepared by dilution of appropriate amounts of the chemicals with ultra-pure water obtained from a Maxima system (ELGA, High Wycombe, Bucks, UK).

10.4   CITRIC ACID ANALYSIS

A solution of 1×10^{-4} M citric acid was introduced into the ion spray-mass spectrometer under "soft" experimental conditions for both positive and negative ion detection modes.   The capillary voltage was 2.5 kV and the cone voltages i.e. the sampling orifice to skimmer voltage [1], were set at 10 or 20 V.

An equimolar (1×10^{-4} M) solution of aluminium and citric acid mixture was also measured under the same condition.   The citric acid/Al system is relatively weak complex with the stability constant of 7.0 in acidic conditions [2], e.g. can be found in the stomach and gut.

Figure 10.2(a) shows the citric acid spectrum for positive ion detection mode.   The main peak appeared at m/z 215.0 and corresponds to $[L + Na]^+$ where L is the citric acid molecule (RMM = 192.027).   Sodium is ubiquitous and has a strong tendency to form adducts.   Unlike in solution, however, metal addition does not occur by lost of a proton. Na^+ binds preferentially to the carbonyl oxygens, as found in protein and peptide molecules [3], as depicted in Figure 10.3.
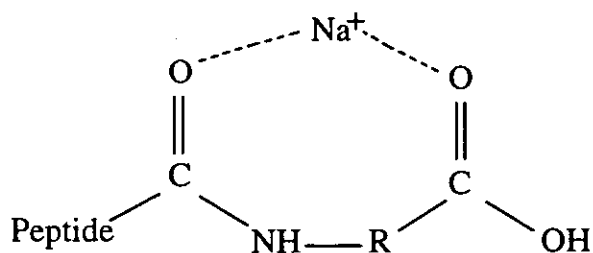

Figure 10.3:   Possible Na^+ attachment to carbonyl oxygen.

The negative ion detection mode spectrum for citric acid is much simpler and is shown in Figure 10.2(b).   The dominant peaks at m/z 191.1 and 95.1 are due to $[L - H]^-$ and $[L - 2H]^{2-}$ respectively.

(a)

$[L + Na]^+$

215.0

Scan ES+
2.39e7

Citric Acid ($C_6H_8O_7$)

CH_2 COOH
|
CH(OH) COOH
|
CH_2 COOH

RMM = 192.027

100

%

0

74.1
64.1 | 75.1
57.1   93.1
41.2   113.0   115.0   143.1   212.0
       135.1 154.5   193.0   231.0   251.0   308.0

100

%

0

(b)

191.1

$[L - H]^-$

$[L - 2H]^{2-}$

62.2   95.1
         104.1   192.1

m/z
20 40 60 80 100 120 140 160 180 200 220 240 260 280 300 320 340 360 380 400
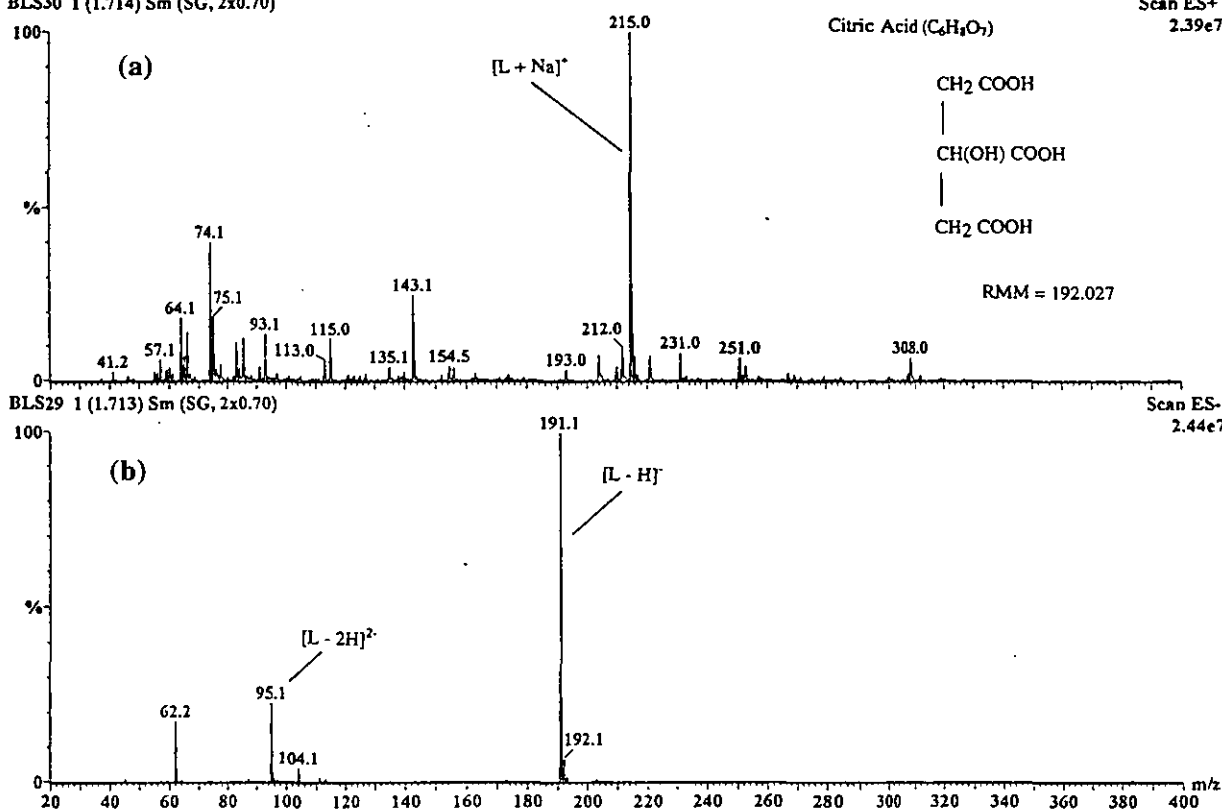
Figure 10.2:   Mass spectra of 1 x 10^{-4} M citric acid acquired at cone voltage 20 V; (a) Positive ion detection mode and (b) Negative ion detection mode.

The addition of equimolar Al^{3+} to the citric acid solution suppressed the $[L + Na]^+$ peak (m/z 215.0) previously observed and replaced it by a peak at m/z 193.0 as shown in Figure 10.4(b). This particular peak can be assigned to the major ligand species, $[L + H]^+$. However, peaks at m/z 298.0 and 253.0 were also observed which are due to $[LAl(NO_3)(OH)]^+$ and $[LAl(OH)_2]^+$ respectively. Note that once again the ligand has retained its protons. Other peaks from the same series present were; m/z 115, $[Al(H_2O)_3(OH)_2]^+$; m/z 133, $[Al(H_2O)_4(OH)_2]^+$; m/z 142, $[Al(H_2O)_2(NO_3)(OH)]^+$; m/z 160, $[Al(H_2O)_3(NO_3)(OH)]^+$ and m/z 178, $[Al(H_2O)_4(NO_3)(OH)]^+$.

Similar peaks were observed at a cone voltage of 10 V as shown in Figure 10.4(c). $^{93}M^+$ appears in several of the spectra, but could not be attributed to either Na or Al. Under gentle conditions (cone voltage = 10 V), it acquired another water molecule to become $^{111}M^+$.

10.5 ANALYSIS OF NICKEL

The mass spectra of nickel, as 1×10^{-3} M nickel nitrate solution at various cone voltages up to 200 V, are illustrated in Figure 10.5(a)-(h). Ion extraction for nickel species is inefficient below cone voltages of 30 V as shown in Figures 10.5(a)-(c), but again $^{93}M^+$ is ubiquitous.

Figures 10.5(d)-(h) show that nickel species started to appear above a cone voltage of 40 V, for example, the peak at m/z 174 is due to $[Ni(NO_3)(H_2O)_3]^+$. The peaks at m/z 197 and 202 always appeared and have the correct isotope ratio for nickel, but no assignment has been made.

Bare $^{58}Ni^+$ and $^{60}Ni^+$ began to appear above a cone voltage of 100 V, as shown in Figures 10.5(g)-(h). Higher cone voltage induced higher collisional energy of the ions in the jet expansion and hence rapid solvent declustering from the ion occurred.
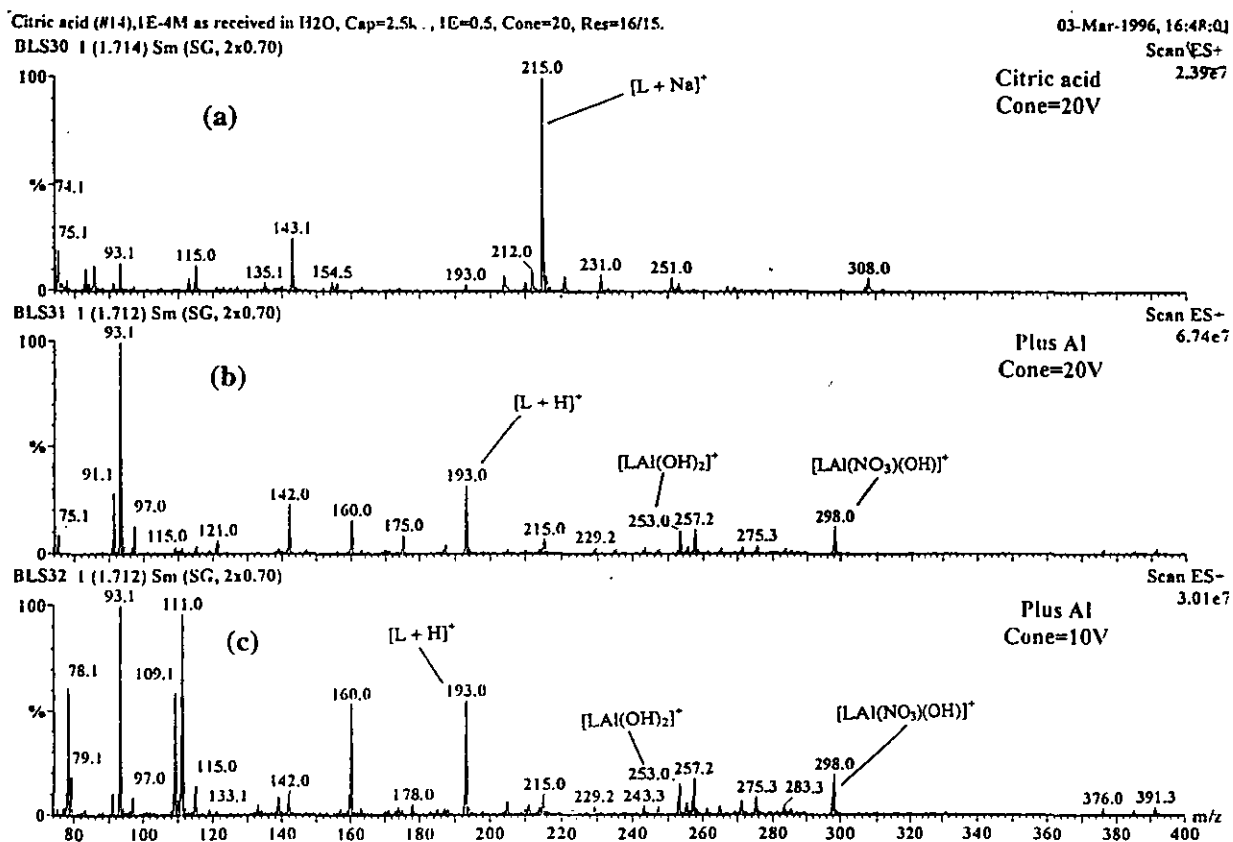
BLS30 1 (1.714) Sm (SG, 2x0.70)   Scan ES+
100   215.0   Citric acid   2.39e7
                                                        [L + Na]⁺   Cone=20V

                    (a)

% 74.1
   75.1   143.1
   93.1   115.0   212.0
             135.1   154.5   193.0   231.0   251.0   308.0
0

BLS31 1 (1.712) Sm (SG, 2x0.70)   Scan ES+
100   93.1   Plus Al   6.74e7
                                                                       Cone=20V
                    (b)
                                           [L + H]⁺

%
   91.1   142.0   [LAl(OH)₂]⁺   [LAl(NO₃)(OH)]⁺
   75.1   97.0   160.0   193.0
          115.0   121.0   175.0   215.0 229.2 253.0 257.2 275.3 298.0
0

BLS32 1 (1.712) Sm (SG, 2x0.70)   Scan ES+
100   93.1 111.0   Plus Al   3.01e7
                                                                       Cone=10V
                    (c)   [L + H]⁺
   78.1   109.1
                    160.0   193.0
% 79.1   [LAl(OH)₂]⁺   [LAl(NO₃)(OH)]⁺
   97.0   115.0   142.0   253.0 257.2   298.0
          133.1   178.0   215.0 229.2 243.3   275.3 283.3   376.0 391.3
0
   80   100   120   140   160   180   200   220   240   260   280   300   320   340   360   380   400   m/z

Figure 10.4:   Mass spectra of: (a) Citric acid, cone voltage 20 V,

(b) Equimolar mixture of Al:citric acid, cone voltage 20 V and

(c) Equimolar mixture of Al:citric acid, cone voltage 10 V,

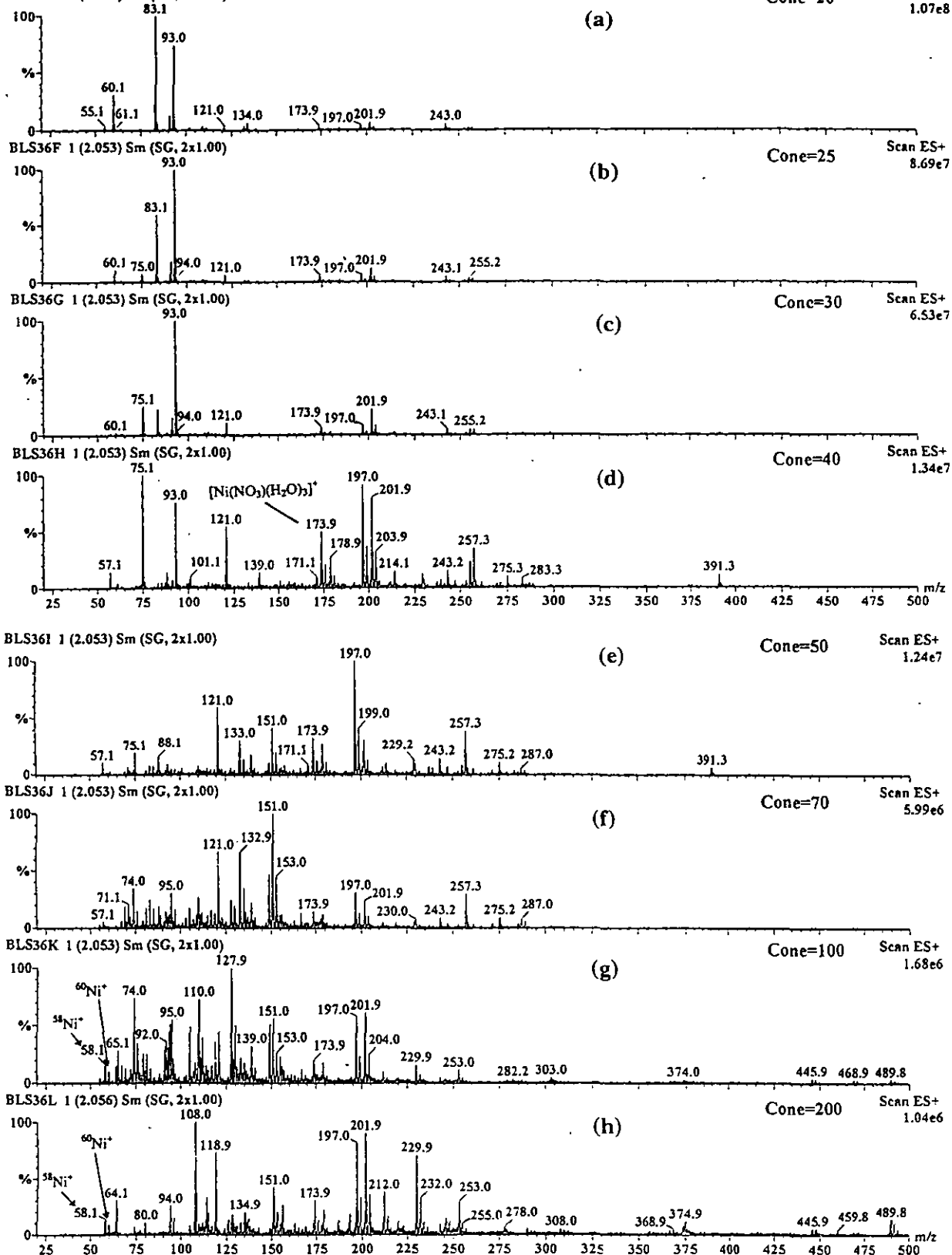acquired with positive ion detection mode. All concentrations

were 1 x 10⁻⁴ M.

Figure 10.5:   Mass spectra of 1 x 10^{-3} M nickel nitrate solution at various cone

voltages; (a) 20 V, (b) 25 V, (c) 30 V, (d) 40 V, (e) 50 V, (f) 70 V,

(g) 100 V and (h) 200 V acquired with positive ion detection mode.

10.6   EDTA/METAL-EDTA ANALYSIS

A solution of 1×10^{-4} M EDTA (RMM 292.1) was analysed in both positive and negative ion detection modes at a cone voltage of 25 V. EDTA is a stronger complexing agent than citric acid and can form very stable complexes with divalent metals such as nickel. The stability constant for Ni-EDTA complex is 18.62 [4].

The mass spectrum for positive ion detection mode shows that the principal ligand species appeared at m/z 315.1 and 293.2. These peaks are attributed to $[L + Na]^+$ and $[L + H]^+$ respectively, as shown in Figure 10.6(a). The negative ion detection mode spectrum, shown in Figure 10.7(a), consists of peaks at m/z 145.0 and 291.2 which are due to $[L - 2H]^{2-}$ and $[L - H]^-$ respectively. The dominant peak was observed at m/z 344.1, $[L + 52]^-$, but is unassigned.

When equimolar Ni^{2+} was added to the EDTA solution, the ligand peaks for $[L + Na]^+$ and $[L \pm H]^+$ completely disappeared. In positive ion detection mode, EDTA was present as $[(L - H)^{58}Ni]^+$ and $[(L - H)^{60}Ni]^+$ at m/z 349.1 and m/z 351.1 respectively, as shown in Figure 10.6(b). Peaks at m/z 347.1 and 349.1 appeared in the negative ion detection mode as shown in Figure 10.7(b). These correspond to $[(L - 3H)^{58}Ni]^-$ and $[(L - 3H)^{60}Ni]^-$ respectively.

MS/MS analysis for the Ni^{2+}:EDTA solution was carried out using the precursor ions at m/z 349.1 and 351.1 with positive ion detection mode. The collision cell voltage was set at 70 V and argon was used as the collision gas at a pressure of 3.5 mbar. Fragmentation of the Ni^{2+}:EDTA complex occurred in the collision cell and was characterised and detected by the second MS. The precursor ions of $^{349}M^+$ and $^{351}M^+$ for positive ion detection mode produced many fragments which can be difficult to identify, as shown in Figure 10.8(a) and 10.8(b). The fragments of bare $^{58}Ni^+$ and $^{60}Ni^+$ appeared in the spectra, thus confirming their presence in the $^{349}M^+$ and $^{351}M^+$ complexes. Thus positive elemental associations can be made without needing to use isotopically modified materials.
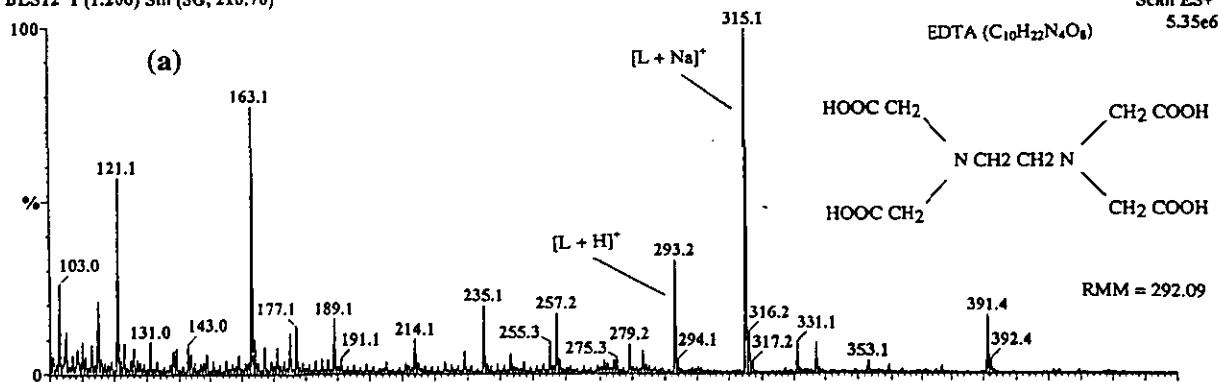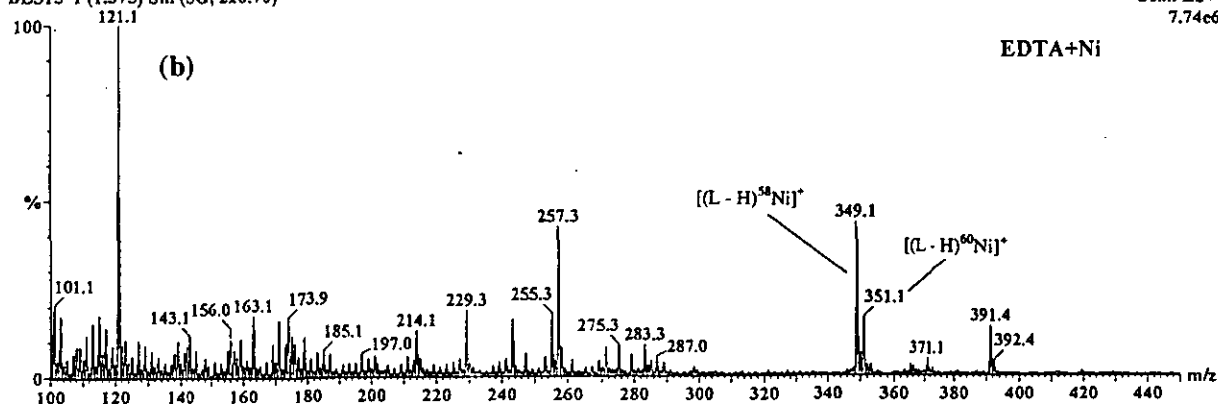
Figure 10.6: Mass spectra of: (a) 1 x 10⁻⁴ M EDTA and (b) Equimolar mixture (1 x 10⁻⁴ M) of Ni²⁺:EDTA. Acquired with positive ion detection mode and cone voltage 25 V.
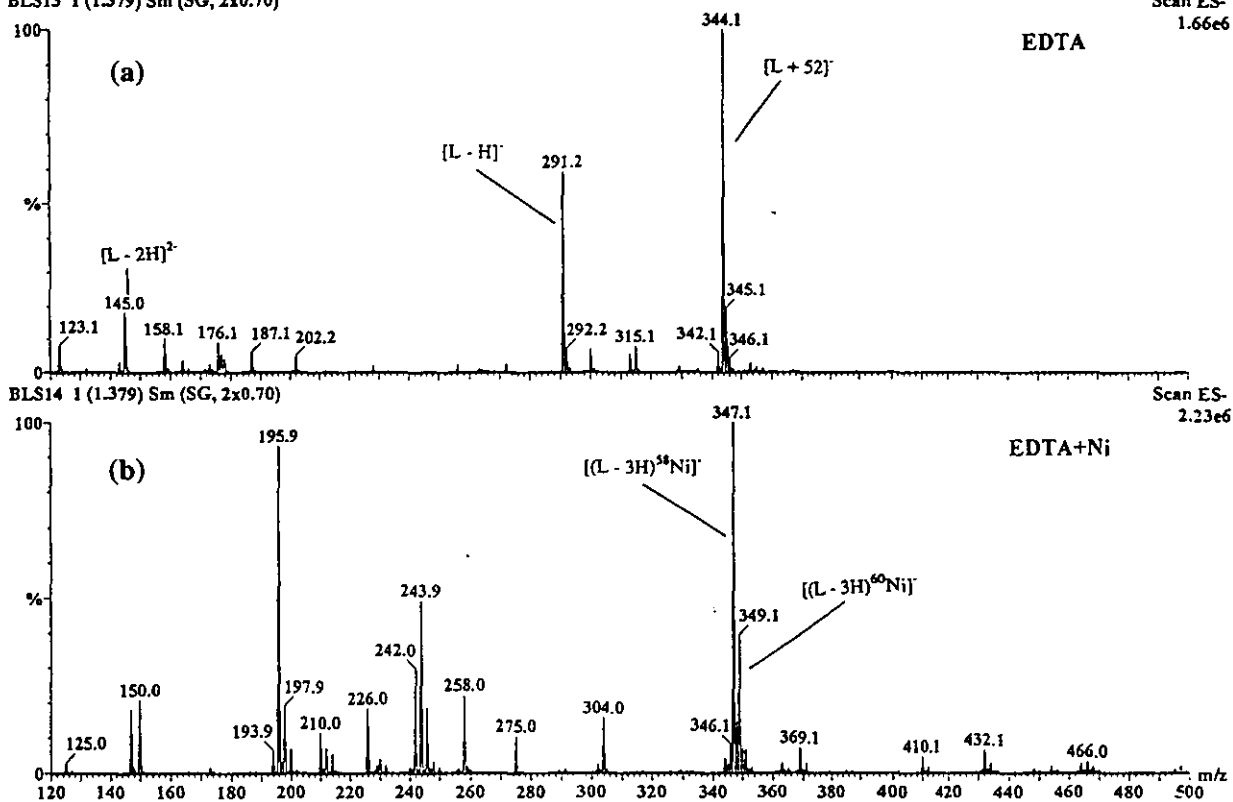
Figure 10.7:　Mass spectra of: (a) 1×10^{-4} M EDTA and (b) Equimolar mixture $(1 \times 10^{-4}$ M) of Ni^{2+}:EDTA. Acquired with negative ion detection mode and cone voltage 25 V.
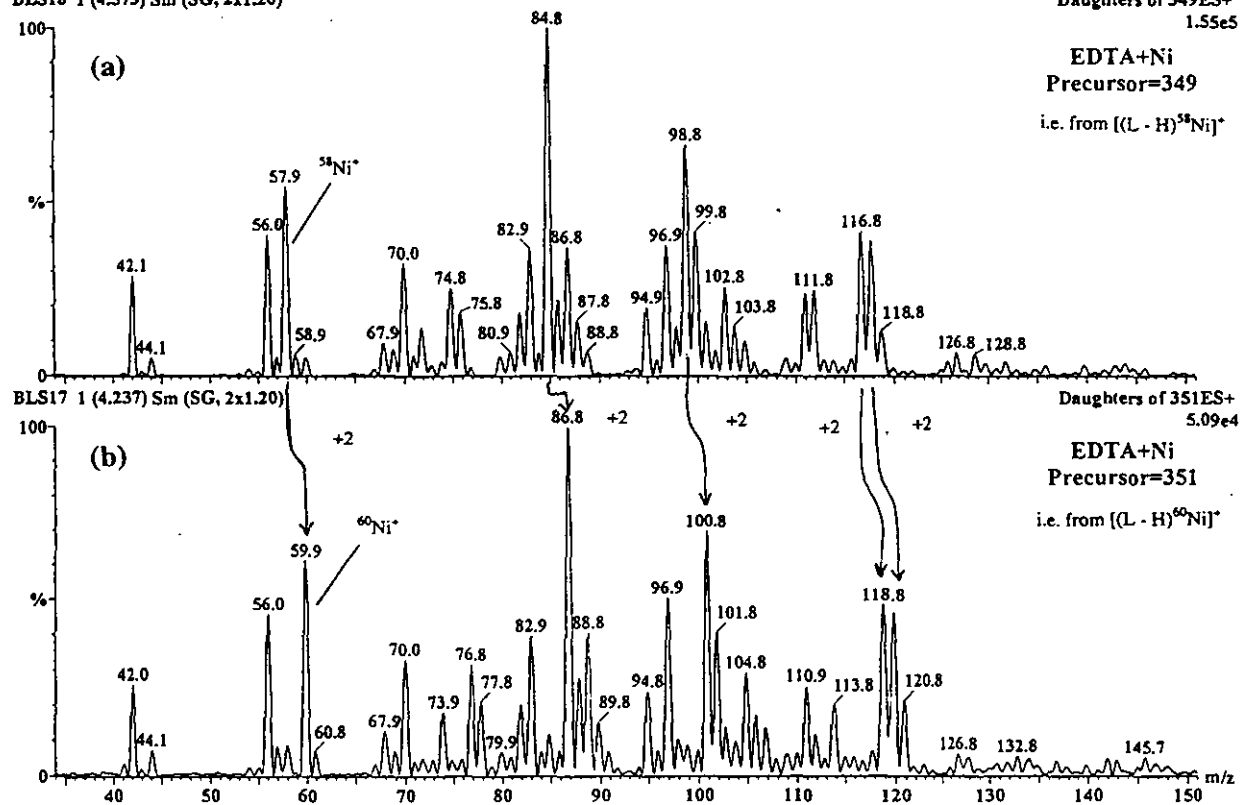
Figure 10.8:   Daughter ion mass spectra of: (a) Precursor 349, i.e. from

$[(L - H)^{58}Ni]^+$ and (b) Precursor 351, i.e. from $[(L - H)^{60}Ni]^+$.

Acquired with positive ion detection mode and cone voltage 35 V.

Other ion peaks from the precursor 349 (Figure 10.8(a)) that probably contained nickel can be assigned as: m/z 116.8 for $[^{58}Ni(CH_2COOH)]^+$, m/z 98.8 for $[^{58}Ni(CH_2COOH) - H_2O]^+$ and m/z 84.8 for $[^{58}Ni(CH_2COOH) - H_2O - CH_2]^+$. Ion peaks (showing a 2 unit mass shift between the daughters) from precursor 351 (Figure 10.8(b)) were attributed to m/z 118.8 for $[^{60}Ni(CH_2COOH)]^+$, m/z 100.8 for $[^{60}Ni(CH_2COOH) - H_2O]^+$ and m/z 86.8 for $[^{60}Ni(CH_2COOH) - H_2O - CH_2]^+$.

10.7 HUMIC ACID ANALYSIS

Mass spectra for 100 mg l^{-1} humic acid (pH ~9) in positive and negative ion detection modes are shown in Figure 10.9(a) and 10.9(b) respectively. The three most dominant peaks appeared at m/z 64.0, 162.9 and 391.1 for positive ion detection mode and at m/z 61.0 for negative ion detection mode. Attempts to assign any of these peaks were without success since the actual molecular structure of humic acid and the fragmentation of the molecule are not known.

The experiments were repeated for humic acid at pH~6 and pH~3 as shown in Figure 10.10(a)-(c). The peaks at m/z 64.0, 162.9 and 391.1 also appeared at the lower pHs with reduced intensity. For negative ion detection mode, the peak at m/z 61.0 disappeared and was replaced by a peak at m/z 45.1.

It would be interesting to run spectra of humic acid from a variety of sources to see if there were common features and finger print regions that would distinguish different forms.

10.8 FERRITIN ANALYSIS

A solution of 1 x 10^{-7} M ferritin (RMM=19 846) was analysed with the positive ion detection mode and a cone voltage of 40 V. The mass spectrum is shown in Figure 10.11.
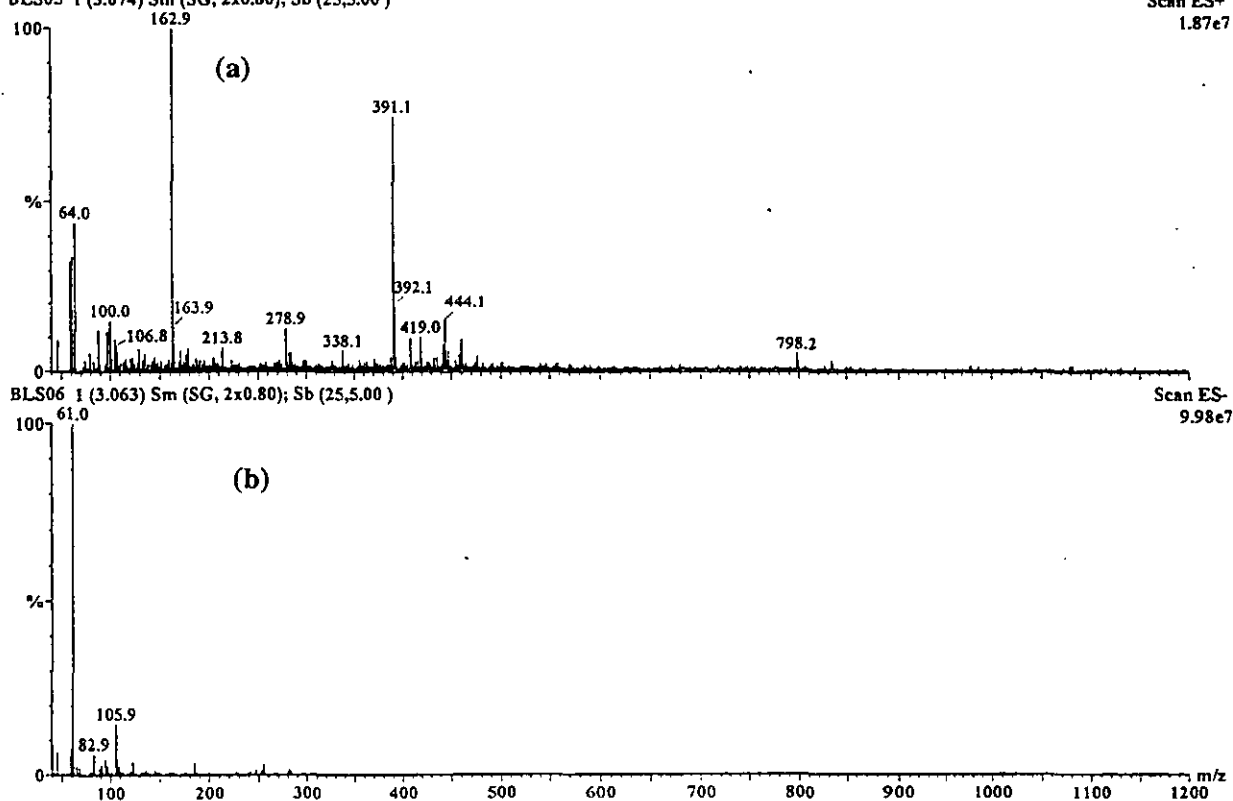
Figure 10.9: Mass spectra of 100 mg l⁻¹ humic acid, pH ~ 9 acquired at cone voltage 30 V; (a) Positive ion detection mode and (b) Negative ion detection mode.
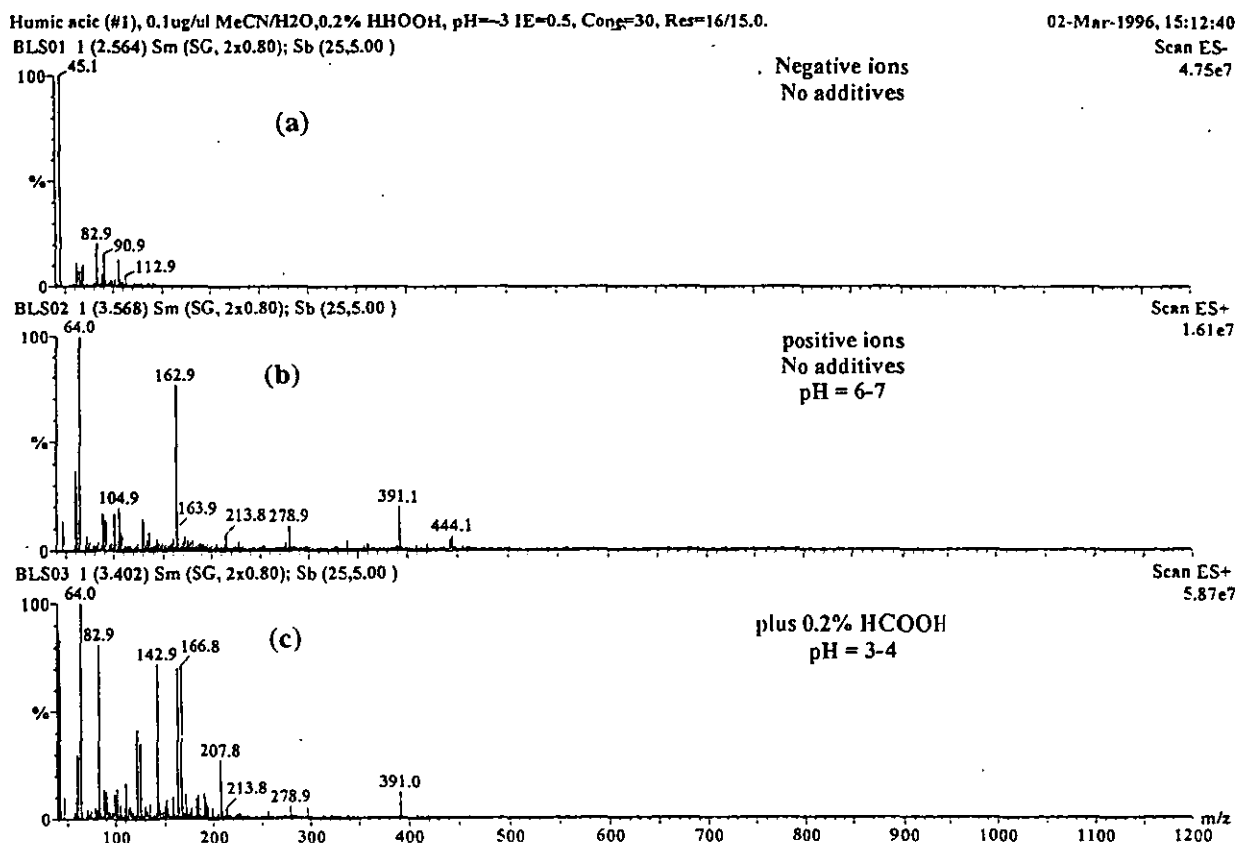
Figure 10.10:   Mass spectra of 100 mg l^{-1} humic acid; (a) pH ~ 3, acquired with

negative ion detection mode, (b) pH ~ 6, acquired with positive ion

detection mode and (c) pH ~ 3, acquired with positive ion detection

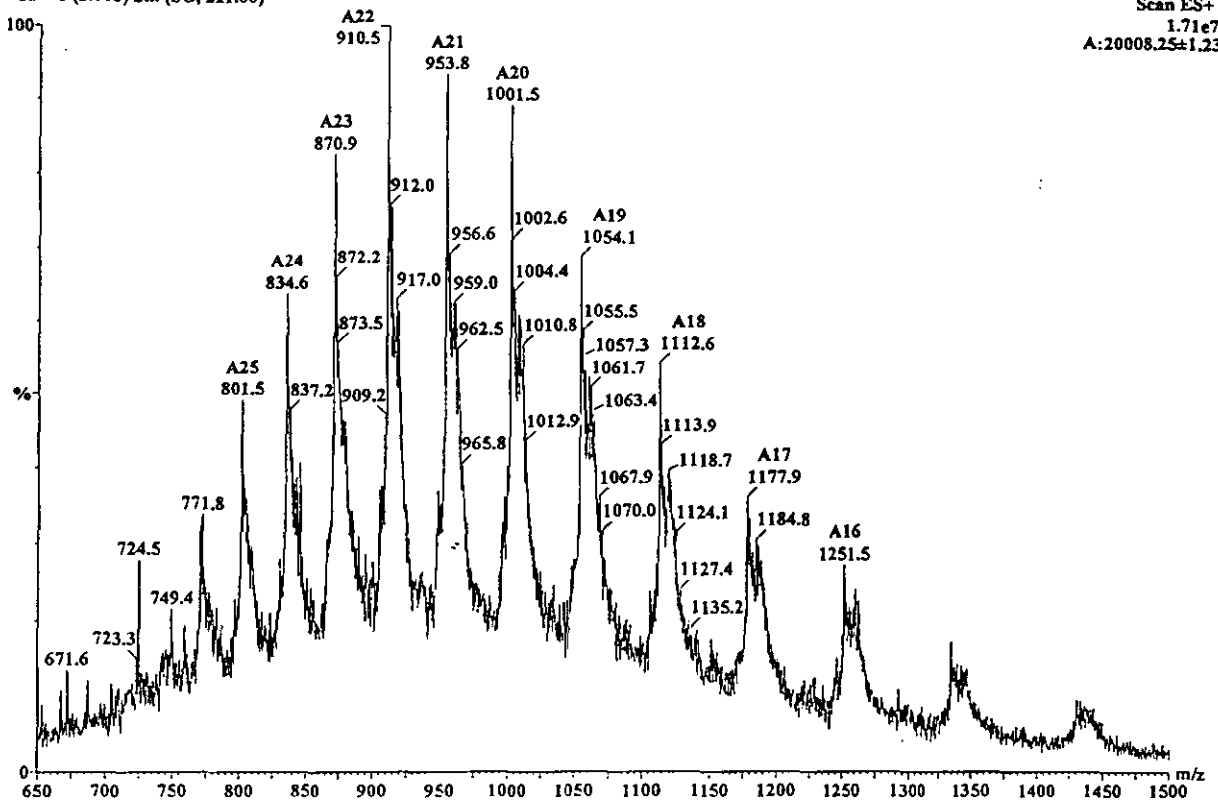mode. All measured at cone voltage 30 V.

Figure 10.11: Mass spectrum of 1×10^{-7} M ferritin acquired with positive ion detection mode and cone voltage 40 V.

A repeat pattern was observed which corresponds to the multiply charged spectra of the ferritin molecule. For example, the peaks labelled A16-A25 correspond to the molecule with 16-25 positive charges. Thus, the molecular weight of the denatured protein is e.g. 25 x 801.5 = 20037.5 which corresponds to the accepted value.

Insufficient time was available to run MS/MS spectra on the ferritin to attempt to recover Fe and Cd atoms which are associated with this molecule.

10.9   CONCLUSIONS

The use of electrospray/ion spray ionisation-mass spectrometry for these analyses produced very complex spectra, even for single component systems. The ionisation process, particularly in positive ion mode produces new species that are not necessarily present in the original aqueous solution. With typical ligands involving metal chelation by -COOH and -OH, negative ion spectra are easier to interpret. Application to multicomponent mixtures will almost certainly require the use of prior separation by chromatographic techniques. This is contrary to recent suggestions that electrospray-MS may be suitable for direct speciation of aqueous media.

However, the electrospray/ion spray ionisation source is relatively cheap and simple to build. The solution flow rates are variable from nl min^{-1} to µl min^{-1}. The conditions in the source and interface can be varied to preserve molecular information or to provide elemental information. It also has been shown that electrospray/ion spray ionisation-mass spectrometry has the capability to be applied to high molecular weight complexes such as ferritin.

Work by Horlick et al. [5] has shown that quantitation is also possible, but only by using internal standardisation.

REFERENCES

1. Agnes, G. R., Stewart, I. I., and Horlick, G., *Appl. Spectrosc.*, 1994, **48**, 1347.

2. Dean, J. A. (ed.), *Lange's Handbook of Chemistry*, 13th. edn., McGraw-Hill Book Co, New York, 1985.

3. Tang, X., Ens, W., Standing, K. G., and Westmore, J. B., *Anal. Chem.*, 1988, **60**, 1791.

4. Cheng, K. L., Ueno, K., and Imamura, T., *Handbook of Organic Analytical Reagents*, CRC Press Inc., Boca Raton, 1982.

5. Agnes, G. R., and Horlick, G., *Appl. Spectrosc.*, 1994, **48**, 649.

Chapter 11

CHAPTER ELEVEN

GENERAL CONCLUSIONS AND RECOMMENDATIONS
FOR FURTHER WORK

11.1   INTRODUCTION TO CHAPTER

This chapter contains general conclusions regarding the work presented in this thesis. Some of the problems encountered are discussed. Finally, some recommendations for further work are given.

11.2   GENERAL CONCLUSIONS

The preliminary investigation on the use of capillary electrophoresis for characterisation of humic acid has shown the potential of this technique. Under the optimum CE conditions, humic acid could be resolved into its component fractions in less than 10 minutes. Further, using ICP-MS as an elemental detector, metal cation binding to humic acid could be studied. Both CE and coupled CE-ICP-MS are complementary to the classical methods such as gel permeation and potentiometric titration.

The optimisation of the ICP-MS instrument using the HEN-170-AA and TR-30-C2 nebulisers showed that the optimum operating conditions for both nebulisers were the same except for the nebuliser gas flow rates. The comparison study on the high efficiency nebuliser and the standard concentric nebuliser showed similar performance for both in term of sensitivities, detection limits, stability and isotopic ratios. The use of the HEN allowed a significant reduction in sample consumption compared to a conventional nebuliser. This is very useful for coupling to a device with a low solution output, such as CE.

Coupling of the laboratory built CE system with ICP-MS was accomplished with a specially designed interface based on the use of both the high efficiency nebuliser and the standard concentric nebuliser. Evaluations of the CE-ICP-MS system showed that, under the optimised conditions, it performed satisfactorily.

Application of the CE-ICP-MS system to the study of metal species in various test samples showed that separations and detection could be achieved in less than 4 minutes. The natural aspiration from the nebuliser was employed to overcome the electroosmotic flow and to produce rapid migration of anionic species whilst at the same time enabling the detection of neutral and cationic species. The separation of a multielement sample, metal-ligand complexes and elemental species has been successfully achieved.

Work with the electrospray/ion spray-mass spectrometer showed that speciation in simple aqueous samples is possible. The electrospray/ion spray-mass spectrometer can also be applied for the study of high molecular weight complexes. It was shown that MS/MS is a powerful means of positively identifying elemental species without the need to resort to isotopic labelling. The use of MS/MS might, in some circumstances, remove the need for prior separation of more complex samples.

11.3 PROBLEMS AND LIMITATIONS

Concentration sensitivity was a major problem when working with the CE-ICP-MS system. This was due to the small amount of sample injected into the CE together with the use of an early generation ICP-MS instrument.

Manual operation of the CE-ICP-MS system caused some operational difficulties. The manual injection technique for sample introduction into the CE was a limitation. The protocol given in Section 8.5, Chapter 8 had to be followed for successful analyses.

The electrospray/ion spray-mass spectra produced were complex and difficult to interpret, even though only simple solutions were used. The use of prior separation by chromatographic or electrophoretic techniques is almost certainly required for real samples.

11.4 RECOMMENDATIONS FOR FURTHER WORK

The initial results suggest that CE holds great promise for the rapid separation of macromolecular polyelectrolytes and the study of metal-ligand interaction. Elements that are not well resolved in the electropherogram can still be individually detected and assigned using the ICP-MS as an element-specific detector.

The dissociation of labile complexes that can occur during separation in column chromatography might be avoided in the CE technique because there is no physical isolation of analytes into a stationary phase. Choice of buffer and counter ion might be critical, but it may nevertheless be possible to measure the stability constants for metal-ligand complexes by the CE-ICP-MS technique. A problem that cannot be addressed easily using conventional chromatography is to distinguish between covalently bonded complexes and those which exist as weak electrostatically bound complexes. The electric field used in CE might enable some distinction to be made.

Humic acids are known to possess ion-exchange and complexing properties. They bind with toxic elements and organic micro-pollutants in water. The CE electropherograms could be used as fingerprints of humic acids, reflecting their charge-to-mass ratio and their state of dispersity.

The ability of ICP-MS or coupled CE-ICP-MS to measure individual isotopes would enable metal-ligand exchange rates to be measured.

Another potential application of CE-ICP-MS is for the study of inorganic colloids, particularly the sorption of toxic metals. Colloids present in ground water can act as

a transport medium for metals and compete for them with the naturally occurring ligands.

An improvement of the CE-ICP-MS interface could be accomplished by the use of a more efficient nebuliser, with a low dead volume, such as the direct injection nebuliser (DIN). The DIN is a micro-concentric pneumatic nebuliser which is placed inside the ICP torch. The DIN has a dead volume of <2 μl and produces a mist of fine droplets (1-10 μm diameter) [1, 2]. In addition, the low dead volume and the absence of a spray chamber minimise post-column band broadening.

Electrospray/ion spray-mass spectrometry shows the presence of species in aqueous samples, but the gas phase ions are not always those that are present in the solution. It has been shown that quantitation is possible using an internal standard. Further work could involve the development of methods for simultaneously determining the metal and metal-ligand concentrations to enable estimation of equilibrium constants. Another question that requires an answer is can electrospray/ion spray-mass spectrometry ever deal with real samples, e.g. a soil extract, without prior separation by chromatography/CE to simplify the spectra. Sensitivity for low RMM molecules is also a problem.

MS-MS is valuable for interpretation and the fragmentation patterns provide information about binding strength in the metal-ligand system. It would be desirable to develop quantitative methods that allow the direct determination of total and bound metal fractions from the MS-MS experiment.

REFERENCES

1.   Shum, S. C. K., Pang, H., and Houk, R. S., *Anal. Chem.*, 1992, **64**, 2444.

2.   Wiederin, D. R., and Houk, R. S., *Appl. Spectrosc.*, 1991, **45**, 1408.

Appendix

APPENDIX A

ICP-MS OPERATION PROTOCOL

A.   TO SWITCH ON ICP

1.   Gas regulator : OPEN
2.   Gas pressure : 4 bar
3.   RF generator:
- Line - ON
- CKTS - ON
- Power - ON

(Warm-up time ~2 min)
4.   Peristaltic pump : ON, 1% HNO_3
5.   Nebuliser gas : ON (155 psi for HEN, 28 psi for TR)
6.   Auxiliary gas : ON (1.2 l min^{-1})
7.   Plasma gas : ON (16 l min^{-1})
8.   RF (red button) : ON
9.   Power : Increase (Incident power ~0.5 kW)
10.   Fine tuning : Adjust (Reflected power - minimum)
11.   Power : MIN
12.   Peristaltic pump : OFF
13.   Nebuliser gas : Reduce (0 psi)
14.   Power : Increase, Ignite ICP (Incident power ~0.7 kW, start to ignite)
15.   Incident power : 1.25 kW, Reflected power <5 W
16.   Nebuliser gas : Increase (155 psi for HEN, 28 psi for TR)
17.   Slide ICP to sample interface and lock
18.   Vacuum pump : ON (Ready RF off, if plasma goes off)
19.   Auxiliary gas : 1.0 l min^{-1}
20.   Plasma gas : 12 l min^{-1}
21.   Peristaltic pump : ON

B.   TO SWITCH ON MS

1.   Vacuum controller:Check
   #1:   ~ 0.0 x 10^{-4} mbar
   #2:   ~ 2.4 x 10^{00} mbar
   #3:   ~ 0.0 x 10^{-8} mbar
2.   Gate valve : Push (OPEN)
3.   Vacuum controller : Check
   #1:   ~ 0.0 x 10^{-4} mbar
   #2:   ~ 2.4 x 10^{00} mbar
   #3:   ~ 6.0 x 10^{-6} mbar
4.   VAC, AIR, RF indicator : None ON

5. OPERATE : Push
6. LED : ON
7. HT : ON (To the right)

(Wait ~30 min for the instrument to stabilise)

In the case of emergency: Push LARGE RED BUTTON

C.   TO SWITCH OFF MS

1. Gate valve : Pull (CLOSE)
2. STANDBY : Push
3. LED : OFF
4. HT : OFF
5. Vacuum pump : OFF

D.   TO SWITCH OFF ICP

1. RF (Blue button) : OFF
2. Peristaltic pump : OFF
3. Auxiliary gas : OFF
4. Nebuliser gas : OFF (Wait 1-2 min)
5. Plasma gas : OFF
6. Power : MIN
7. Slide ICP from sample interface, full forward and lock.

E.   TO OPTIMISE ICP-MS

1. Change to 50 ppb tuning solution
2. MANUAL : +115.4 (Tune first mass)
3. PQ Ratemeter : Reading full scale
4. To get maximum reading:
    - First Mass - Tune
    - ICP position (X, Y, Z) - Align
    - Nebuliser gas - Adjust
5. PQ LENS SUPPLY
    - Extraction ~2.5
    - Collector ~7.5
    - L1 ~8.5
    - L2 ~5.5
    - L3 ~5.0
    - L4 ~2.0
6. Switch MANUAL to AUTOMATIC
7. Start measurement

F.   TUNING

1.   PQVision software : START
2.   Select : Edit
3.   Login : CALIB
4.   Select Acquire from menu:
   - Single Sample
   - File name : Tune
   - Rpts : 1
   - Acquire mode : Scan
   - Use Element Menu : ME
   - Use Method : Default
   - Append to procedure : None
   - Add to queue
   - Stop when finish
   - Close
5.   Select Results from menu:
   - Display
   - File : Tune
   - Open
   - Spectrum
   - CPS
   - Choose mass 115 (In^+), Integrated CPS, Response for m/z 115 ~ 100,000 cps
   - Choose mass 140 (Ce^+), Integrated CPS
   - Choose mass 156 (CeO^+), Integrated CPS
   - Choose mass 70 (Ce^{2+}), Integrated CPS
6.   Calculate ratio CeO^+/Ce^+ and Ce^{2+}/Ce^+, $CeO^+/Ce^+ < 5\%$ and $Ce^{2+}/Ce^+ < 5\%$
7.   If higher than 5%:
   - Nebuliser flow rate - Reduce
   - ICP glassware - Check for leak
   - Nebuliser - Check for blockage
   - Sampler and skimmer - Check for blockage

ICP-MS CALIBRATION STRATEGY

A.   Instrument Calibration
    1.   Mass Calibration
    2.   Detector Calibration
    3.   Stability Test

B.   Analytical Calibration
    1.   Response Calibration

A1.   MASS CALIBRATION

1.   Select : Instrument form menu
2.   Click : Calib
3.   Procedure : Fine Mass Calibration
4.   Mass Calib and Fine Mass : Active
5.   Calib New Data
6.   Tuning Solution : Press OK
7.   Calibration Table : Click Cancel
8.   Show Mass
9.   Calibration Graph : Accept
10.   Save Calibration : OK
11.   Enter to Instrument Calibration window
12.   Close

A2.   DETECTOR CALIBRATION

1.   Select : Instrument from menu
2.   Click : Calib
3.   Procedure : Detector Cross Calib Proc
4.   Detector Calib : Active
5.   Yes to delete existing calibration
6.   Calib New Data
7.   Message : Cancel
8.   Tuning Solution : OK
9.   Calibration Table : Cancel
10.   Show Detector
11.   Detector Calibration : Accept
12.   Save Calibration : OK
13.   Enter to Instrument Calibration window
15.   Close

A3.   STABILITY TEST

1.   Select : Acquire from menu
2.   Choose : Procedure
3.   Analysis Procedure : Stability
4.   Queue acquisition
5.   Fully Quantitative : Active
      Print after calculating : Active
6.   Enter
7.   Tuning Solution : OK
8.   Statistic Printout : RSD ~ 0 - 2%
9.   Close

B1.   RESPONSE CALIBRATION

1.   Select : Instrument from menu
2.   Click : Calib
3.   Procedure : Response Calibration procedure
4.   Response Calib : Active
5.   Calib New Data
6.   Tuning Solution : OK
7.   Calibration Table : Cancel
8.   Show Response
9.   Response Calibration Graph : Accept
10.   Save Calibration : OK
11.   Name : Default, Enter
12.   Close